TRIBHUVAN UNIVERSITY

INSTITUTE OF ENGINEERING

PULCHOWK CAMPUS

THESIS NO.: T04/078

Spatio-Temporal Analysis of Road Traffic Crash Hotspots in Kathmandu Valley, Nepal

by

Anuradha K.C.

A THESIS

SUBMITTED TO THE DEPARTMENT OF CIVIL ENGINEERING

IN PARTIAL FULFILLMENT OF THE REQUIREMENTS FOR THE

DEGREE OF MASTER OF SCIENCE IN TRANSPORTATION ENGINEERING

DEPARTMENT OF CIVIL ENGINEERING

LALITPUR, NEPAL

JULY, 2024

COPYRIGHT

TRIBHUVAN UNIVERSITY

INSTITUTE OF ENGINEERING

PULCHOWK CAMPUS

DEPARTMENT OF CIVIL ENGINEERING

APPROVAL PAGE

The undersigned certify that they have read and recommended to Institute of Engineering for acceptance, a thesis entitled **"Spatio-Temporal Analysis of Road Traffic Crash Hotspots in Kathmandu Valley, Nepal"** submitted by Anuradha K.C. in partial fulfillment of the requirement for degree of Master of Science in Transportation Engineering.

……

Supervisor: Rojee Pradhananga
Department of Civil Engineering
Institute of Engineering

……

Co-Supervisor: Upama Koju
Forest Action Nepal

……

External Examiner: Saroj Kumar Pradhan
National Road Safety Council

……

Committee Chairperson: Anil Marsani
Coordinator: MSc in Transportation Engineering
Department of Civil Engineering

Date: ……..

ABSTRACT

Kathmandu Valley is one of the rapidly urbanizing cities in Nepal, which registers the highest incidence of road traffic crashes compared to other regions in the country. Identifying the dangerous road sections where the crashes happen frequently (or simply hotspots) is a critical initial move towards devising effective strategies for reducing the future severe incidences in the Valley. On this account, this thesis aimed to pinpoint the hotspots in the Valley by examining the spatial and temporal patterns of reported traffic crashes. The study also took an additional step by investigating relationship of hotspot occurrences with two spatial factors; population density and land use.

The study utilized three years of crash data (2019-2021) collected from Traffic Police Office, and road network polylines obtained from Survey Department. Of the total data, 23,278 (79.55%) crashes and 912.54 km of road network were analyzed. The temporal distribution reveals a notable increasing trend of crashes and their severity. The incidence of fatalities and severe injuries reaches its highest level during the month from October to April. The highest frequency of crashes is recorded during the weekday morning rush hours, from 8:00 AM to 12:00 PM, in the afternoon time, from 12.00 PM to 4:00 PM and in the evening around sunset, from 4:00 PM to 8:00 PM, but severer incidences are reported during night hours and during weekends.

A two-step methodology was adopted in this research. Firstly, a fusion of spatial autocorrelation (Global Moran's I Index), Getis-Ord Gi* statistic and Kernel Density Estimation (KDE) methods were applied to analyze the patterns and concentrations of hotspots on aggregate, severity level, crash type, year, season, day of week and time of day basis. A high positive value of Moran's I Index for all the data aggregation level indicated that the crashes were clustered spatially with high significance. The Getis-Ord Gi* measure identified the highly significant hotspot segments along the Valley roads at 90%-99% confidence level. The KDE visualization corroborated the hotspot links generated by the Getis-Ord Gi* statistics, but did not provide significance of the hotspots. From both methods, the hotspots are evident mostly along Ring Road, Tribhuwan Highway, Araniko Highway, Tripureshwor-Balaju (RingRoad), Thapathali-Ekantakuna and other feeder roads that represent high traffic movements and socio-

economic activity. The hotspot pattern on these urban roads changes more or less dramatically for severity level, crash type and crash time than other type of data classifications.

Under GIS based spatial analysis, the correlation with population density was examined using ordinary linear regression, and was found to be positively significant with (R^2=0.53) on hotspot occurrences. For interaction with land use types, a simple frequency analysis was performed, and the results show that residential, commercial, residential-commercial mix and public land uses present higher number of crashes and hotspots.

Secondly, the top ten ranking was provided to the identified hotspots from aggregate data analysis based on weightages relative to crash costs of severity level. The suggested hotspot locations have practical significance as these individually are liable to 3-5 death cases over the analysis period. Additionally, a qualitative or descriptive study, involving site visits at five hotspot locations, was also carried out to find specific causes and potential solutions for reducing crashes.

In essence, this thesis suggests a hotspot identification and prioritization methodology that can be effectively employed even with a scarcity of high-quality crash and spatial data, a common issue in Nepal. The thesis findings also equip the local transportation authorities with targeted insights not only on the hotspot areas highlighting the importance in terms of severity, collision type, days and times, but also the typical local risk factors that require rectification and enhancements to achieve desired road safety conditions.

Keywords: Traffic Crashes, GIS, Spatial Analysis, Temporal Analysis, Hotspots, Moran's I, Getis-Ord Gi*, KDE

ACKNOWLEDGEMENT

I am profoundly grateful to my supervisors; Dr. Rojee Pradhananga (Assistant Professor, IOE) and Dr. Upama Koju (Senior Researcher, Forest Action Nepal) for their consistent guidance and mentorship during my thesis. Their invaluable moral support, immense knowledge and technical advice have been instrumental in the completion of this research work. I appreciate the insightful critiques and constructive feedback they provided on my draft report, which significantly contributed to the enhancement and finalization of this mid-thesis document. I am truly unable to envision more exemplary advisors and mentors for my thesis journey other than them.

My sincere appreciation goes to the esteemed professors of the internal evaluation committee, particularly Mr. Anil Marsani (Coordinator, M.Sc. in Transportation Engineering) and Dr. Pradeep Kumar Shrestha, for imparting their wisdom and knowledge throughout the course of the study.

I am deeply thankful to Traffic Police Office, Survey Department and National Statistics Office for providing me with the required secondary data of the Kathmandu Valley, which formed the foundational basis of my research. I am equally grateful to Mr. Akhilesh Kumar Karna for his indispensable support and granting me the authorization to employ the Python program he developed for converting the traffic crash records to CSV format. I must acknowledge with thanks the contribution of Mr. Shaishav Acharya and Mr. Sanjaya Khanal in the data digitization work.

Last but not the least, I am eternally grateful to my family and friends for their cordial support and motivation during the time of difficulty.

Name: Anuradha K.C.

Roll No.: 078 /MSTrE/004

TABLE OF CONTENTS

LIST OF TABLES

LIST OF FIGURES

LIST OF ABBREVIATIONS

DOR	Department of Roads
DOS	Department of Survey
FRN	Feeder Road Network
HSM	Highway Safety Manual
IRC	Indian Road Congress
MOPID	Ministry of Physical Infrastructure Development, Province
MOPIT	Ministry of Physical Infrastructure and Transport
NSO	National Statistics Office
PDO	Property Damage Only
RTC	Road Traffic Crash
WHO	World Health Organization

CHAPTER 1: INTRODUCTION

1.1 Background

Road crashes are first and foremost the preeminent consensus of economies worldwide with the ever-soaring growth in vehicle population and the desire for efficient mobility, coupled with imbalance between user travel and activity areas. It is accountable for majority of the early deaths and physical impairments, leading to socioeconomic ordeals at national, community, and personal levels. According to latest statistics by WHO, road crash fatalities and injuries affect 1.19 million and 20-50 million people per year respectively. The safety risks are three times higher in low-income countries than the high-income countries where there are 9 deaths per 100,000 people on average (Global Status Report on Road Safety, 2023).

The majority of traffic collisions happen inside urban territories, which serve a considerable amount of traffic, usually a heterogeneous mix, and provide access to diverse land use activities alongside the busy roads. The urban traffic crashes can be attributed to the interaction of complicated spatial and temporal factors such as roadway structure, urban furniture, abutting environment, season, time of the week and hours of the day (Farmer, 2005; Shahid et al., 2015; Liu & Sharma, 2017). Without proper study of the spatial and temporal pattern of the crashes, it is impossible to state what the most significant causes are, which segments or locations pose the high crash risks and their evolution over time as well as what possible countermeasures are required to eliminate those hazards. Therefore, understanding the spatial-temporal effects in traffic crashes is essential to road safety practitioners, traffic engineers, urban planners, road agencies and all those involved in the road safety management.

Several techniques have been developed to investigate the spatial and temporal distribution of the traffic crashes at the macroscopic (e.g. state or geographical unit) and microscopic (e.g. road intersections or segments) scales. Some studies have applied the spatial analysis solely to recognize the hotspot locations (Wang et al., 2022; Yu et al., 2014; Yang et al., 2013; Troung et al., 2011). The spatial analysis approaches can be categorized into distance based and density based (Harirforoush et al, 2019). The

former method employs a range of local spatial autocorrelation techniques like nearest neighbor distance, Moran's I, Getis-Ord Gi* and K-function to measure spatial inter-dependency of crash points based on distances to the neighboring events. The latter method uses the non-parametric Kernel Density Estimation (KDE) and its improvements to measure the crash point intensity or density in the analysis region. Whereas, the temporal analysis has been performed separately to cluster the crash events according to time-series of hour, day, month and year. Recently, comap method and space time cube model are being utilized to examine the effect of spatial-temporal interplay on the traffic crashes and severity level (Brunsdon 2001; Plug et.al. 2011; Shahid et al. 2015; Harirforoush et.al. 2019; Ma et al. 2017).

The previous studies results demonstrate that spatial-temporal approaches can effectively pinpoint the specific sites with high crash density over a specific period of time (Prasannakumar et al., 2011). The spatial-temporal clustering can accurately define the probability and trend of crash occurrence across space and time. The method can aid visualize the hotspot zones, sensitive times and associated causes, particularly, for the internal and arterial roads of urbanized regions where crash level and consequences are high. The spatio-temporal analysis can guide the decision makers in prioritizing the black spots and taking the proper measures to improve the safety of hazardous sites.

To this end, such analysis can be particularly useful for Nepal, a low-income South-Asian country, which continuously grapples with traffic safety issues on highways and urban roads. The country strives to minimize at least 50% of the road crashes by implementing successful safety measures in line with the Global Plan for the Decade of Action for Road Safety 2021-2030. The road safety interventions are often centered on Kathmandu Valley, the capital city, as it alone accounts for over half of the road crash incidents. Despite this, there has been a lack of research on patterns of crash hotspots, including insights into the locations and specific causes of the crashes in the Valley. A deeper knowledge of the spatio-temporal patterns and variations in the traffic crashes can significantly enhance the identification of hotspots as well as the effectiveness of crash prevention strategies in the Valley. Consequently, this thesis aimed to examine the spatial and temporal distribution of road accidents in the Kathmandu Valley. The findings from this study are valuable for local governments,

police departments, and national agencies to ensure effective resource allocation in road safety improvement works.

1.2 Problem Statement

Given the Valley's persistent safety problem and research gap, there is an urgent need for a comprehensive evaluation of the spatial-temporal dynamics of high-risk crash locations, their contributing causes and prioritization in Kathmandu Valley to address this escalating issue effectively. The road safety situation in Kathmandu Valley is dire with an average of 10,000 traffic crashes and over 180 fatalities reported annually by the Traffic Police Directorate. Despite numerous safety interventions, the valley continues to witness a disturbingly high incidence of traffic crashes, increasing at alarming rate of 9.1 percent as per the Traffic Police record from FY73/74 to FY77/78. The complexity of this issue is further compounded by lack of sufficient studies investigating the hotspot locations, and their root causes. The available road safety studies (JICA Report, Shakya et al. 2020, Tiwari, 2015) primarily focus on statistical analysis or models, overlooking the spatial and temporal dimensions of the crashes and hotpot occurrences. To enhance identification of hotspots and safety measures, it is crucial to consider the spatial and temporal parameters like the population density, landuse, time of day etc. as these determine socio-economic activities, trip generation and distribution, which in turn influence crash patterns and hotspot occurrences.

1.3 Objective of Study

The main objective of the study is to analyze the spatial and temporal distributions of traffic crashes hotspot locations in the Kathmandu Valley. The specific objectives of the research are as follows:

1) To analyze the spatial patterns of traffic crashes within the Valley.
2) To assess the temporal clustering of observed traffic crashes within the Valley.
3) To identify the road traffic crash hotspots through geospatial approach and investigate potential casual factors for some of the identified hotspots.

1.4 Scope of Study

The present thesis provides insight into patterns and characteristics of traffic crash hotspots in the Kathmandu Valley, and identifies spatial and temporal factors that play a significant role in the occurrence of hotspots. The thesis emphasizes the usefulness of GIS based spatial analysis techniques in identification of critical hotspot segments and the 'how' and 'why' behind the occurrence of crashes in specific hotspot locations. The application of the present analysis methods provides deeper insights into the spatial and temporal dynamics of traffic crashes, as well as helps to unravel the prominent hotspots based on different attribute values.

Overall, the scope of works underpinning the research is outlined below:

1) Review existing literature to ascertain the scope of problem and pertinent research in spatio-temporal analysis;
2) Acquire traffic crash records from the Traffic Police Headquarters and geocode them with appropriate attributes;
3) Gather administrative, population, road network and land use data of the study areas as available from different Government Departments;
4) Digitize/process all obtained information in geodatabase formed using ArcGIS 10.8;
5) Carry out Global Moran's I statistical tests to detect the clustering of crash events;
6) Perform hotspots analysis using Getis–Ord Gi* Statistic and Kernel Density Estimation (KDE) at various spatial and temporal levels of interest;
7) Evaluate influence of spatial factors (population density and landuse) on hotspot occurrences;
8) Rank the top ten hotspot sites based on weighted severity index.
9) Conduct site visit to reflect the explanatory factors of traffic crashes at sample hotspot locations.

The findings from this study are expected to provide the concerned road safety agencies with the direction to focus on the identified hotspot locations, and target more actionable, specific and impactful interventions tailored to reduce the occurrences and severity of crashes in the Kathmandu Valley.

1.5 Limitation of Study

The key constraint to this research is the delineation of acceptable definition of hotspots. The deficiency of standardized definition of hotspots in Nepal introduced subjectivity into the analysis. For instance, the criteria used to define a 'hotspot' were based on the preliminary concept of crash frequency being greater than those of surrounding area. Such subjective nature of the hotspot definition could pose difficulties in achieving comparable results across different regions or time periods.

Another limitation identified in the study is relevant to quality of secondary data sources, notably the crash records. The system for collecting crash data in Nepal is faced with irregularities and gaps in the reporting of fatalities, injuries and property damage only (PDO) cases, leading to potential undermining of critical hotspots. The crash records were primarily in the Nepali language and lacked accurate geographic coordinates for each crash sites and in some cases information on tentative distance from responsible police station was missing. Manual geocoding method became necessary, which proved to be a time-consuming process. As a result, only crash records of three years from 2019 to 2021 were converted into digital format. Despite digitizing approximately 79.73% of the data with X and Y coordinates, the analysis is subject to bias as major hotspot areas nearby Boudha and Tokha Traffic Police station, remained undetected in the analysis due to data quality issues. In particular, the identified hotspot locations must be corroborated with physical site inspections and local inquiries to ensure their accuracy and outline any changes in the road safety characteristics since the reporting period.

Also, the study was restricted by the limited range of spatial and temporal variables included in the crash cluster analysis. Only the land use, population density, year, season, day and time of day were taken into account. The evaluation did not consider other possible factors that could influence crash hotspot formation, such as road surface quality, traffic volume, driver behavior and urban development pattern. This is due to unavailability of complete data relevant to crash causes, road infrastructure and environment, that hindered the comprehensive understanding of the factors contributing to crashes.

These limitations highlight the need for future research to focus on developing a comprehensive definition of hotspots that considers various factors such as collision type, crash frequency, and environment. A more comprehensive approach to data collection and analysis is required to improve the accuracy and applicability of crash hotspot identification.

1.6 Organization of Report

The thesis report is structured in a sequential manner, commencing with introduction and background in Chapter 1, and literature review in Chapter 2, and progresses through an initial description of the methodology and dataset in Chapter 3, discusses a spatial and temporal analysis finding in Chapter 4, and proposes conclusive remarks in Chapter 5. The thesis structure is as follows:

Chapter 1: Introduction briefly describes the context, problem statement, objectives, scope and limitations of the study.

Chapter 2: Literature Review provides insight into previous dissertations, articles, papers, reports, and literature relevant to methods of hotspot analysis, and significance of GIS based spatial and temporal analysis techniques in identification of road crash hotspots. Moreover, the crash analysis techniques prevalent in Nepal are discussed along with their limitations.

Chapter 3: Research Methodology proposes an organized methodology for data collection, database creation and processing, hotspot analysis and ranking method as applied in the research. The hotspot analysis process is divided into three parts including, spatial analysis (spatial autocorrelation, Getis-Ord Gi* statistics, KDE analysis), temporal analysis and site investigation.

Chapter 4: Results and Discussion presents the spatial and temporal patterns of the crashes in forms of maps and tables, and possible explanations to observed phenomena of hotspots in space and time. It lists out the top ten high-risk segments as per the severity index, elaborates on their possible causes based on spatial analysis and field visit, and suggests some safety improvement measures.

Chapter 5: Conclusion and Recommendation summarizes the major findings of the thesis work, direction for future research and final suggestions for improving safety in the Valley.

CHAPTER 2: LITERATURE REVIEW

2.1 General

This chapter covers the review of past research efforts, both local and global, in the field of road traffic crash hotspots. The literature review summarizes the state of affairs and the context of relevant studies in Kathmandu Valley. It provides a general overview of factors contributing to road crash risks, and their consideration in previous studies. It explores the definition of hotspots and current approaches to crash hotspot identification, concentrating on state-of-the-art spatial and temporal analysis techniques, and their respective strengths and weaknesses.

2.2 Definition and Concept of Road Traffic Crash Hotspots

There exist numerous definitions pertaining to crash hotspots. Cheng and Washington, 2005 defined hotspot (also known as blackspots) defined as an area where, over a prolonged period of time (usually 1-3 years), there are more and different types of traffic crashes than other normal locations, and where there may be safety risks due to the influence of the environment, climate, and road conditions. Elvik, 2007 provided a definition of hotspots as locations exhibiting a higher frequency of crashes compared to similar spots, attributed to local risk factors. This conceptualization emphasizes the significant role of geometric and traffic design risk factors in crashes at hotspots, which can be mitigated through crash engineering strategies. While, Yang et.al, 2016, characterized hotspots as the hazardous sites on road segments which demonstrate high clustering of crash events than its surrounding places. The definition incorporates spatial and temporal aspects, recognizing that hotspots can exhibit fluctuations in both severity and duration on spatial or temporal basis.

In the general context, a universally accepted and precise definition of crash hotspots remains elusive (Elvik, 2008; Anderson, 2009; Choudhary et al., 2015, Sajed et. al., 2019). The basic concept revolves around the idea that for a particular road zone to be classified as a hotspot, the crash occurrences must exceed a certain threshold in a

specific period of time. Consequently, the definition of hotspots varies among different regions and jurisdictions as evidenced below in table 2.1.

Table 2.1 Criteria of Traffic Crash / Crash Hotspots' Definition in Different Countries (Source: IRC, 2020)

Country/ Institution	Section Length (m)	Crash Threshold (nos.)	Time Period (yrs)
Australia	250	3	5
Belgium	Variable	3	3
Denmark	Detailed categorization of roadway elements	4	5
England	300	12	3
India	500 (section) or junction	Average Annual Total Crashes (AATC)	3-5
China	150 (junction) or 500 (section)	6 (pedestrian) or 9 (injuries) 2 (fatal) in 5 year	1-5
Thailand	300 or 500 or 1000	3	1
Bangladesh	30 (intersection)	Fixed by Government	3
Indonesia	500 (section) or 100 (intersection)	Recorded	2
Germany	300	3 (same type) or 5 (all types)	1 (same type) or 3 (all types)
Netherlands	Variable	10 (total) or 5 (same type)	3-5
Norway	100 (spot) or 1000 (section)	4 (spot) or 10 (section)	5
Spain	1000	5 (injury) or 2 (fatal) per year 10 (injury) or 5 (fatal) per 3 year	3
Switzerland	Variable	10 (all), 4 (injuries) or 2 (casualties) for highways 8 (all), 4 (injuries) or 2 (casualties) for rural roads 10 (all), 6 (injuries) or 2 (casualties) for intersections	2
PIARC	Map based clustering approach	5 per year or 3 pedestrian injuries per year	3-5
HSM 2010	Aggregation based on base conditions	Weighted observed and predicted values by EB method	3

It is important to set a standard for critical thresholds to target only the key locations representing high crash risks for the optimal allocation of road safety improvement funds. Evidently, the selection of an appropriate criteria will necessitate a comprehensive examination of current traffic patterns, prevalent crash frequencies,

function of road infrastructure, surrounding environments (urban or rural), and differentiation between road segments and junctions.

According to ADB SHIP Road Safety Final Report Part-A, 2021, the proposed definition of a blackspot in Nepal, is “a location or 100 m highway segment with either five crashes or five fatalities over the past three years”, which is not yet officially incorporated into laws. Given the challenges related to crash data quality and availability, identifying hotspots based on this specific definition might be merely impossible for Nepal. The blackspot improvement study suggested to estimate the hotspot length by considering the proximity of major and minor junctions. Fixing it at approximately 500 m near the identified location is a reasonable approach, and the locations are to be prioritized by suitable approach such as highest severity index value. By doing so, authorities can focus on allocating resources more effectively and address critical safety concerns promptly within the prioritized stretch of the road.

2.3 Factors Contributing to Road Traffic Crash Hotspots

The identification of crash prone location requires more robust understanding of the casual factors that are crucial in formulating effective strategies aimed at improving safety (Anderson, 2009). Various studies have identified human behavior, vehicle attributes, road conditions, and environmental factors as the key determinants influencing traffic crashes (Greibe, 2003; Cheng et al., 2005; Harirforoush et al., 2019; Seyed Mohsen Hosseinian et al., 2020). The interplay among these factors is intricate and presents challenges in being assimilated into a unified model.

Often, the human behavior is recognized as the primary factors impacting traffic collisions (Evans, 1996; Hour, 2007). It encompasses actions like speeding, usage of seatbelts, distracted driving (e.g., phone usage), driving under the influence of substances, pedestrian carelessness and non-adherence to traffic regulations. The second main factors are related to road design aspects which consist of the geometric characteristics, junctions, signage, traffic safety features and maintenance conditions. Other factors also contribute to the incidence of traffic road crashes including environmental circumstances (e.g. extreme weather conditions, poor visibility, lack of illumination, and rugged terrain) and vehicle-related aspects (e.g., type, age, brake

efficiency, maintenance conditions and any defects associated with the vehicle) (Austroads, 1994).

Besides these factors, some studies examine the impact of population, density, vehicle count, income and other socio-economic parameters on the number of crashes. As such, Liu and Sharma (2017) modelled vehicle miles travelled, population, employment rate and income as spatial factors for fatal crashes in Iowa, however, these indicators were not found significant. Machado-Leon et al. (2016) expanded the scope of their study to investigate various socio-economic variables, encompassing seven specific factors: gender, age, occupational status, qualifications, household size, net family income level, and driving experience. The variables of gender and age emerged as major determinants related to road traffic crashes.

In recent times, studies tend to consider a multitude of spatial and temporal heterogeneities in traffic crash analysis (Huang and Abdel-Aty (2010); Liu and Sharma (2018); Chen et al. (2017); Seyed Mohsen Hosseinian et al., 2020). The research by Huang and Abdel-Aty (2010) associates crash occurrences with the causal factors at macroscopic and microscopic levels. It utilizes spatial units like regions, counties, and cities at macroscopic level. Conversely, the investigation connects to the microscopic level, focusing on factors such as traffic site (location), driver-vehicle unit, traffic crashes, and occupants.

To account for unobserved heterogeneity, Liu and Sharma (2017) conducted a study examining the frequency of days where the minimum temperature exceeded 320F, as well as the levels of rainfall and snowfall using data from Iowa RTA. In a similar vein, Ma et al., 2017 formulated models that incorporated a wet surface and the presence of November as an indicator in Colorado. These investigations suggest that researchers should consider delving into a more granular time scale, such as analyzing data at a seasonal or monthly level to better explore the changing trends and impacts of climatic conditions.

Likewise, Seyed Mohsen Hosseinian et al., 2020 demonstrates that season, day of the crash, time of the crash, geometric characteristics, daylight conditions, weather conditions and other numerous variables exert an influence on the severity of road crashes in the urban area. It reveals that a considerable proportion of crashes occurred

during the summer season, at the beginning of the week, in daylight hours between 12 PM and 18 PM.

2.4 Techniques for Identifying Hotspots

There is currently no global consensus on the standardized concepts and methodology for identifying hotspots, as a result, Researchers employ different techniques. The methodologies can be broadly categorized into statistical modelling, spatial clustering and temporal analysis.

2.4.1 Statistical Methods

The conventional methods for hotspot identification rely upon analyzing historical data for metrics of crash severity, crash frequency, crash rate, or any combination of these at particular locations (Hauer, 1997, Elvik (2007, 2008)). If the statistical value associated with a specific road section exceeds the predetermined threshold, it is classified as a hotspot. However, establishment of unreasonable threshold may result in erroneous identification of hotspots, overlooking the stochastic nature of crashes across time and space, and the effects of environmental conditions (Dereli et.al., 2017). In order to address this issue, a diverse range of statistical models are used to identify high-risk locations or segments. Generalized Linear Models (GLM) and hierarchical Bayesian models are commonly used to correlate the crash occurrence and severity with various predictors, including roadway characteristics, traffic volumes, land use patterns, and environmental factors (Lord & Mannering, 2010).

Persaud et al. (1999) employed the Empirical Bayes (EB) estimates to determine the anticipated quantity of collisions occurring in signalized intersections and highway segments. The negative binomial approach was utilized to develop a crash frequency model, incorporating factors such as AADT, segment length, and lane width. Furthermore, the discrepancy between the anticipated and actual crash counts, denoting surplus crash frequency, served as the criterion for prioritizing the locations.

Ahmed and colleagues (2011) employed Bayesian hierarchical models incorporating spatial and random effects in order to forecast the occurrence of crashes on road segments in mountainous regions, considering factors such as driver behavior, traffic

patterns, geometric attributes, and adverse weather conditions. The research revealed a positive correlation between crash risk and certain variables including roadway geometry, segment downgrades, and the snow season.

Montella, 2010 compared various approaches for determining hotspots including frequency of traffic crashes, crashes rates, equivalent property damage only (EPDO) crash frequency, method of proportion, EB estimate of total-crash frequency, EB estimate of severe-crash frequency (EBs), and potential for improvement method (PFI) using four quantitative tests indicators. Consistent with the findings of Cheng and Washington (2008) and Elvik (2007, 2008), it was found that the Empirical Bayes (EB) technique exhibited superior performance over other hotspot identification methods.

Despites, the statistical methods remain pivotal for the analysis of crash patterns, trends, and relationships, they show significant limitations to account for spatial and temporal dependencies present within the crash dataset (Wang and Li, 2017; Washington et al., 2003, 2010). To add to this, failure to meet the pre-defined distribution assumptions can lead to biased and inaccurate model estimation results (Lord et.al. 2009, 2010). For instance, Poisson model can produce erroneous results for over-dispersed data.

2.4.2 Geo-Spatial (or Spatial Clustering) Techniques

Geographic Information System (GIS) aided spatial data mining and mapping techniques have been widely applied to combine crash data with spatially referenced variables in order to identify high-risk areas (Lavrac et al. 2008; Prasannakumar et al. 2011; Deshpande et al. 2011; Shafabakhsh et al., 2017; Bíl et al. 2019; Wang et al. 2022). With a capability for effective visualization and spatial assessment of crash data, GIS based spatial analysis techniques assist in identifying critical areas for Traffic Police and transportation planners to implement targeted safety interventions. The spatial analysis typically involves identifying clusters of locations with similar attribute values to assess spatial autocorrelation among those locations (Getis et al., 1992). An examination of the spatial distribution of crash data is conducted to ascertain if the observed distribution of point events is a consequence of random occurrences or if it adheres to certain systematic processes resulting in a clustered or regular pattern (Bailey et al., 1995).

Various geospatial tools such as Moran's I Index (global and local), Getis-Ord Gi* statistics, Kernel Density Estimation (KDE), nearest neighbor distance, and K-mean clustering have been extensively employed to identify crash hotspots (Nazneen et al., 2020). These approaches can be segregated into two main categories: (1) distance-based and (2) density-based (Loo & Anderson, 2016; Harirforoush et. al. 2019). The distance-based methods involve the application of spatial autocorrelation techniques such as nearest neighbor distance, Moran's I, Getis-Ord Gi*, and K-function, to assess the spatial inter-dependency of crash points based on their distances to neighboring events (Hazaymeh et.al, 2022, Shariff et al., 2018; Tola et.al, 2021; Harirforoush et al. 2019; Rahman et al., 2018; Mohaymany et al., 2013; Prasannakumar et al. 2011; Erdogan 2009). On the other hand, the density-based approaches utilize planar KDE, Network Kernel Density Estimation (NetKDE), KDE+ and other KDE extensions to evaluate the crash point intensity within the study area (Nazneen et al., 2020; Harirforoush et al. 2019; Shafabakhsh et al., 2017, Choudhary et al., 2015; Thakali et al., 2015; Mohaymany et al., 2013; Yang et at., 2013; Bil et al. 2013; Plug et al., 2011; Anderson 2009; Pulugurtha et al. 2008; Erdogan et al. 2008, Xie et al., 2008 etc.)

The above-mentioned methods were sequentially devised to address the limitations observed in the preceding approaches. The nearest neighbor method was replaced by the K-function to delineate the clustering extent across a wider range of scale, which was a constraint of the former nearest neighbor method. Unlike the K-function and Nearest Neighbor Distance methods that merely look at the general tendency of data clustering and are unable to pinpoint the crash sensitive locations, (Delmelle, 2009; Bil et al., 2013) the Kernel Density Estimation (KDE) method can actually localize the clusters. As such, Anderson (2009) identified Kernel Density Estimation (KDE) as a method with great potential in understanding the evolving trends of point patterns within a specific geographical region.

There exist two popular variations of kernel density estimation: Planar Kernel Density Estimation (PKDE) and Network Kernel Density Estimation (NetKDE) (Loo and Anderson, 2015; Yao et al., 2018). The standard PKDE involves constructing a smooth density surface within a 2D space employing the Euclidean distance that estimates the aggregated occurrences within a specified search bandwidth. The density measure

peaks at the central point and gradually decreases as the distance from the center grows (Young et al. 2014; Truong et al. 2011).

Utilizing the standard KDE technique offers specific advantages in illustrating the location and density of crash points but also leads to controversies. The planar KDE method was used in a study conducted by Flahaut et al., 2003 to examine the distribution patterns of crashes on a 59 km long Belgian road. The analysis was done for both the network and the region; however, this is deemed inaccurate method for crash hotspot identification because road crashes mostly occur on the roadway and inside the road networks (1D space) that are subsets of the 2D space (Xie et al. 2013; Okabe, 2009). So, the methodology of the 1D approach, also referred to as the Network KDE (NetKDE) is developed, which involves the partitioning of the road network into uniform segments known as lixels. Within this framework, the term "lixel" (derived from linear pixel) is utilized to denote linear entities of consistent lengths that are evenly distributed throughout the network (Xie and Yan, 2008). Okabe et al. (2006) devised a computational method and a software toolkit known as SANET (Spatial Analysis along Network) designed to be compatible with ArcGIS software. This toolkit is primarily utilized for conducting spatial analysis along road networks.

Yang et al. 2013 compared applicability of standard KDE and network KDE for traffic crash hotspot analysis and discovered that both planar and network KDE are more effective on large scales basis, however, accuracy of network KDE is more with moderate bandwidth selection. Other studies by Yamada, 2004; Xie and Yan, 2008; Kuo, 2011 and Yao et al., 2018 also proved the accuracy of NetKDE as the PKDE resulted in overestimation bias upto 20%. The key benefit of the KDE technique over traditional statistical clustering methods is that the bandwidth of the kernel indicates the uncertainty regarding the precise position of the crashes, which has the effect of dispersing the risk of a crash (Anderson, 2009). The unavoidable flaw is that it does not examine the statistical significance of the high-density regions (or clusters) and just uses spatial dimensioning as a conditioning variable (Xie et al., 2008; Anderson, 2009).

Also, the kernel (cell) and bandwidth size can influence the results significantly, thus, hit and trial method is required to define correct thresholds (Loo and Anderson, 2015; Okabe et al. 2006). The cell size and bandwidth should be predicated based on the specific attributes of the study area and the road network (Loo and Anderson, 2015).

There is no optimal bandwidth recommended by prior scholarly works due to application of the varied bandwidth values in previous studies, however, a bandwidth selection ranging from 10 meters in urban settings to 1000 meters in rural regions is considered desirable (Nazneen et al. 2020; Harirforoush et al., 2016; Anderson, 2009; Xie and Yan, 2008,). Xie and Yan (2008) suggested using smaller bandwidths (20-250m) in order to map the local hotspots at smaller scales.

To address the limitation of cluster significance, a sophisticated analysis method known as spatial autocorrelation was developed to consider the positions of individual events and their associated values simultaneously. The spatial autocorrelation is meant to categorize numerical ranges representing two spatial patterns, namely clustering and dispersion, whose statistical significance can be evaluated using the "z score" (Getis et al., 1992), a feature not present in KDE.

The spatial autocorrelation techniques viz. Moran's I Index and Getis-Ord Gi* statistics are mostly used to determine the hotspot locations. Hazaymeh et.al, 2022, Tola et.al, 2021 and Prasannakumar et.al, 2011 applied these indicators of spatial association to examine the statistical significance of crash clusters. The global Moran's I offers several advantages, including its higher level of general stability, testability, adaptability of conditional distribution, and applicability in crash analysis (Flahaut et.al, 2003). It specifically evaluates the overall spatial arrangement of a variable without providing statistical inference for identifying particular clusters or hotspots.

When considering geographic variability and spatial correlation, it is advisable to utilize local statistical measures like local Moran's I and Getis-Ord Gi* statistics over the conventional global statistical framework (Anselin, 1995). Flahaut et.al, 2003 introduced local spatial autocorrelation indices by decomposing the global Moran I index into local components, each associated with a specific length (li). The chosen length corresponds to the one that best aligns with observed reality, ensuring that for each location i, it maximizes the local Ii index. The resulting hot spot zones exhibit varying lengths, however, focus was on areas with positive autocorrelation, where contiguous neighboring locations exhibit higher co-variation than expected. Additionally, this autocorrelation method was compared with kernel methods, and it was found that both approaches yielded quite similar results under specific parameter choices.

By complementing Moran's I with these local indicators of spatial autocorrelation (LISA), the statistics allows for the identification of pattern characteristics that may remain unobserved when solely relying on global Moran's I. Particularly, the Gi and Gi* statistics are instrumental in pinpointing local clusters of interdependence that might not be evident when utilizing global statistics. The analysis is based on a local spatial autocorrelation count or index that indicate the spatial concentration of crashes. Depending on the size and location of the aggregate units utilized in this scenario, the Getis-Ord method may yield various results. A noteworthy advantage of the G statistics is their ability to neutralize the spatial distribution of data points, thus facilitating the formulation of hypotheses without the risk of data point patterns biasing the outcomes (Getis et.al. 1992). The method is established to be sufficient for quantifying the geographic link between crashes and environmental factors.

On the part of visualization, Manepalli et al. 2011 compared the KDE and Getis-Ord Gi* (d) statistics and observed that identical hotspots are outlined by both methods. In contrast, the comparative advantages of employing Gi* and KDE methods for the examination of crash data have been illustrated by Kuo, 2011. Gi* maps highlight areas of significant spatial clustering, while KDE maps present the spatial distribution of point data through a process of data smoothing to approximate a continuous density surface. KDE maps are observed to possess greater visual significance in comparison to those produced using Gi Z-scores. Plug et al. 2011 also utilized KDE to examine the spatial and temporal pattern of traffic crashes. It emphasizes the utility of KDE as a valuable instrument for analyzing the spatial distribution of crashes and identifying areas of high occurrence.

2.4.3 Temporal Analysis

Temporal analysis technique reveals dynamics of crash occurrence with time, facilitating the identification of peak period of crash incidences. Moreover, this technique enables to recognize the cyclical and seasonality patterns within the crash dataset, which is helpful towards the prediction of future crash conditions using statistical models (Lavrenz et al., 2018). The utilization of several time series models including ARMA, ARIMA, SARIMA, INAR, and GLARMA is proven to yield precise time series data in this domain (Lavrenz et al., 2018; Quddus, 2008). In this line, only a few researches (Jamal et al., 2020; Razzaghi et al., 2013; Quddus, 2008; Wen et al.,

2005; Liu et al., 2004; Meyerhoff, 1978) attempt to analyze crashes for various time-series dataset as available. These studies likely analyzed temporal variations in road traffic crashes over different time scales, such as hourly, daily, monthly, seasonal and annual patterns. The studies added that unavailability of high-quality data potentially impact the robustness of the time series model results.

Apart from these, few studies like Bačkalić, 2013; Plug et.al. 2011; Prasannakumar et al., 2011; Lavrac et al., 2008, etc. have considered using time series graphs and spider plots to visualize temporal patterns of crashes at different levels. The studies did not look into how the risk locations changed over time because of lack of sufficient length time-series data.

The timeframe of historical traffic crash data used to pinpoint crash hotspots ranges from 1 to 5 years (Elvik, 2008). However, according to study by Cheng and Washington (2005), there is no improvement in accuracy of hotspots through the utilization of a duration exceeding 3 years. Application of a timeframe exceeding 5 years is generally deemed unnecessary as accuracy is minimal and diminishes rapidly with extended period lengths.

2.4.4 Spatio-Temporal Analysis

Integrating spatial and temporal analysis methodologies has the potential to unveil intricate spatio-temporal patterns and relationships that may remain hidden when analyzed separately. Only limited studies have endeavored to combine both the spatial and temporal patterns of hotspots using geocoded traffic crash data. Brunsdon 2001; Plug et al., 2011; Shahid et al., 2015; Harirforoush et al., 2019; Wang et al., 2021; Feizizadeh et al., 2022 and others imposed comap technique to present the spatial pattern of crashes over time. The comap serves as an investigative visual method for analyzing the correlations between a pair of variables, such as the occurrence of crash incidents, and their temporal variability. The comap approach segregates datasets into time-series, allowing for the analysis and visualization of their patterns using clustering tool like the KDE (Brunsdon, 2001). The findings of this approach are depicted through a series of maps or graphs, organized sequentially to illustrate the evolution of traffic crash patterns over time.

Plug et al., 2011 investigated trends in single-vehicle collisions (SVCs) that occurred in Western Australia between 1999 and 2008. The study applied co-map technique and spider plots, and found that, on weekdays, the SVC distribution appeared to be more common in the afternoon till midnight (3 pm–midnight) and early in the morning (10 pm–2 am), respectively. In the meantime, regional analysis revealed that a hotspot region was focused around Perth Metropolitan.

A Research conducted by Shahid et al., 2015 delve into analysis of the spatial and temporal fluctuations in the frequency of road traffic incidents and deaths throughout the regions of Peninsular Malaysia. The results indicated a higher number of incidents but a lower rate of fatalities in regions that were more urbanized and developed. Regions with lower levels of urbanization and development demonstrated lower incident rates but a higher severity of fatalities. The majority of incidents were observed to occur during the festive month and the mid-year school holiday period.

Similarly, Harirforoush et al., 2019 combined the results of KDE representing crash density with local Moran's I to identify significant clusters of traffic crashes in the Sherbrooke region across distinct seasons. By utilizing the comap technique, the aggregate crash data spanning three years was categorized into four seasons. The results indicate a notable concentration of traffic crash clusters in the city center and along major roadways during the summer and autumn seasons.

The outcomes of above study demonstrate that the comap technique effectively emphasizes specific areas or regions linked to a high concentration of crashes within a specific timeframe. Notwithstanding the data at hand, certain scholars (Lord and Mannering, 2010) have developed analysis models to investigate the variables that contribute to the quantity of crashes occurring in various geographic locations throughout a specific time period. The space-time cube method is such an innovative spatiotemporal data analysis method to examine spatiotemporal evolution patterns and the space-time proximity of occurrences. (Wu et al., 2021).

Ma et al., 2017 made an effort to apply a multivariate space-time model in order to assess RTA frequency in conjunction with injury severity on a temporal scale. For Colorado's Interstate Highway 70, daily crash frequency data was utilized instead of annual crash data. The model was successful to capture the underlying unobserved

heterogeneity over different crash types and across spatial units. It was concluded that the space-time model performs better in this field than any other model, including spatial models and random parameter models.

Another study of traffic crashes by Cheng et al., 2018 used spatial autocorrelation analysis, and time-space cube analysis to visualize the crash locations' hotspots in Wujiang, China. For several kinds of crashes, the spatiotemporal evolution trends, which represent cold and hot spots were documented. The evolution time were analyzed with the consecutive hot spots in January and February observed weak due to spring festival during which law enforcement is strict.

2.5 Previous Applications of Spatial and Temporal Analysis

To date, the literatures concerning the exploration of road traffic crash hotspots using spatial and temporal analysis techniques have been consolidated in table 2.2. After performing an extensive review of these literatures, it is determined that hotspot analysis involves setting the spatial unit of analysis. Previous literatures have employed a range of spatial units for analysis, such as road segments, intersections, administrative zones (county, metropolitan, district) and country. The selection of spatial unit for the examination of traffic incidents displays variability, as different units provide distinct perspectives and require different techniques for analysis. (Mohammed et al., 2023).

Regarding analysis at the road network level, the base spatial units (BSUs) can be either an independent road segment formed by dividing the road network into equal units or a contiguous road segment (two or more) (Flahaut et al., 2003; Loo and Yao, 2013). While the length of these BSUs can vary depending on the context, a common practice in the literature is to use 100-meter segments as suggested by Elvik, 2008; Flahaut et al., 2003; Loo and Yao, 2013. The latter method of contiguity of road network considers spatial dependence, and hence, different global and local spatial techniques such as Global Moran’s I, Local Moran’s I, Getis-Ord Gi*, PKDE, NetKDE and point density are applied to determine the clustering patterns as listed in Table 2.2. These models take into account spatial autocorrelation and the multitude of factors influencing traffic collisions and road safety. Likewise, various temporal scales such as hour, day, week, month, season and year have been considered to identify temporal correlations.

The findings from multiple research studies carried out in different countries using various approaches indicate that the probability of traffic collisions varies across different regions. Additionally, these spatial and temporal analysis techniques are shown to be beneficial for identifying high crash frequency and severity areas, and directing targeted efforts to tackle road safety issues.

Table 2.2 Different Literatures on Spatial Analysis of Crash Hotspots

S.N	Author/ Year	Study Area	Years of Data	Analysis Unit	Analysis Methods	Findings
1	Kuo, 2011	College Station Police Department, USA	5	Spatial: Road network Temporal: Daily and weekly	Getis-Ord Gi* statistics, NetKDE, Spider graphs, Comap technique	Network restrictions required for same elevation road network Distance band should have more than 1 and not so large number of neighbors Gi* Maps are not visually impactful
2	Prasannakumar et al. 2011	Thiruvananthapuram city India, 141.74 sq.km	1	Spatial: educational institutions and religious places Temporal: monsoon and non-monsoon time	Global Moran's I, Getis-Ord Gi* statistics, KDE	Significant spatial variation among aggregate, monsoon/ non-monsoon and educational/ religious datasets
3	Truong et al. 2011	Adelaide metropolitan area	13	Spatial: Road Network and Bus stops	Global Moran I index, Getis–Ord Gi*, Network Analyst tool	Majority of pedestrian-vehicle crashes at intersections and more severity at mid-blocks
4	Yang et al. 2013	Hampden County, Massachusetts	3	Spatial: County and Road Network	Planar and network KDE	Both the method are suitable for large scale analysis Planar KDE is time saving and easily available tool NetKDE is more accurate with moderate bandwidth for large scale mapping
5	Mohaymany et al. 2013	60-km Arak-Khomein rural road, Iran	3	Spatial: Road Segment Temporal: Year	NetKDE, Moran's I, Pearson correlation	Crash data referenced to the number of kilometers due to absence of GPS points Comparing the estimated densities produces a more realistic picture than crash counts

S.N	Author/ Year	Study Area	Years of Data	Analysis Unit	Analysis Methods	Findings
6	Yu et al. 2014	622.2-km section of A1 highway, UK	10	Spatial: Road Segment	Local Moran's I, KDE, Crash rate, Empirical Bayes	KDE method outperforms others and is analogous to EB
7	Harirforoush et al. 2019	City of Sherbrooke, Canada, 353.5 sq.km.	3	Spatial: Road Network Temporal: Season	KDE, Local Moran's I, Comap	Iteration (trial and error) required to find the most appropriate bandwidth size in the KDE analysis Impact of a single fatal or injury crash on the pattern is distinctly demonstrated when weights based on severity are used.
8	Nazneen et al. 2020	Fort Peck Indian Reservation, US	10	Spatial: Road Network Temporal: time and days (weekend/ weekday)	Gi*, NetKDE, Crash Severity Map, Spider plots	Crash patterns are identical at weekdays, peaking at rush hour; Crashes tend to happen at midnight on weekends.
9	Ma. Et al., 2021	Wales, UK	1	Spatial: Administrative region Temporal: month, week, day, hour	Point density, line density, Local Moran I (outlier analysis), Getis–Ord Gi*	Results of the outlier analysis and hot spot analysis show similar clustering patterns in areas with both high and low severity crashes.
10	Wang et al. 2021	Harbin	3	Spatial: Districts Temporal: Seasons	Local Moran's I, Point Density, Comap	Majority of traffic crashes in the city's center are low-severity Combining density analysis and cluster analysis accurately identifies urban hostpots
11	Hazaymeh et al. 2022	Irbid Governorate, Jordan, 1571.7 km^2	5	Spatial: Road network (1km segments) Temporal: Year, Month, Day, Time	Global Moran I index, Getis–Ord Gi*	Reduction of hotspot length in temporal evolution suggest effectiveness of safety measures
12	Afolayan et al. 2022	385 km of Lokoja-Abuja-Kaduna highway in Nigeria	5	Spatial: Road segment and Intersection Temporal: Year	Global Moran I, Getis–Ord Gi (Optimized hotspot analysis: fishnet polygon and network spatial weight matrix), weighted mean center, KDE	Method is similar to the use of the SANET tool. The frequency of crash locations is associated with road intersections and curves No hotspots for 2015 and 2016 as the patterns are random

S.N	Author/ Year	Study Area	Years of Data	Analysis Unit	Analysis Methods	Findings
13	Wang et al. 2022	Liangshan Yi Autonomous Prefecture, Sichuan province, China	1	Spatial: Cities or Counties	Global Moran I, Optimized hotspot analysis, Correlation analysis	Robust correlation between the RBT index (no. of identified hotspots divided by no. of spatial units) and the frequency of crashes Unreasonable distance band produced for entire dataset, so, require to breakdown by crash types
14	Mohammed et al. 2023	Qatar, 11,571 sq.km	5	Spatial: Zones Temporal: Year, Month and Day (Weekend/Week days)	Time-Space cube analysis, GWR, Local Moran's I, and Getis-Ord Gi*	Highlighted the regions within the nation with greatest density of inhabitants as the specific areas where traffic crashes occur most frequently.
15	Munasinghe (2023)	Colombo Municipal Council, Srilanka, 37 sq.km	1	Spatial: Administrative region Temporal: Peak and Non-Peak hours	KDE, NNH Clustering, Severity Maps	NNH method more suitable for identifying traffic crash hot spots, but KDE is visually impactful.
16	Alam et al., 2023	Ohio	5	Spatial: State & Road network Temporal: Peak and Non-Peak hours	Getis-Ord Gi*, crash severity index, and Moran's I	Crash severity value can be utilized in Getis-Ord Gi* to identify hostspots

2.6 Previous Crash Related Studies of Kathmandu Valley

Albeit there is no standardized national definition of crash hotspots specific to Nepal, various methodologies are utilized by local researchers and road safety authorities in Kathmandu Valley to identify areas with high crash risks. These approaches encompass the analysis of historical crash data, the use of statistical models, the application of geographic information systems (GIS) for spatial examination, site inspections & safety audits, and engagement with stakeholders to comprehend local traffic patterns and risk elements. The efficacy and relevance of such methods are frequently limited by data availability and quality, institutional capability, resource ceiling and other similar factors. (MOPIT, 2019)

The existing researches do not explicitly concentrate on identifying hotspot locations, instead they offer valuable insights and context for grasping the characteristics of road crashes and factors influencing their severity and incidences. For instance, Shrestha et

al., 2014; Huang et al., 2016; Dhakal 2018; Kuikel et al., 2022; and Singh et al., 2023 performed a descriptive retrospective analysis utilizing the data provided by the Metropolitan Traffic Police on road traffic collisions. In these studies, the frequency and percentage distribution of the quantitative data are evaluated, and managed graphically using tables, bar charts, and pie charts. These investigations highlight that an upward trajectory is observed in road traffic crashes in Kathmandu Valley from the fiscal years 2015/16 to 2020/21, with a more pronounced escalation in crash incidents during the latter three fiscal years. The common disposition behind the crashes is driver's negligence followed by over speeding, alcohol consumption, overtaking, pedestrian recklessness, road condition, climate/weather and mechanical defects. The demographic group most susceptible to road traffic injuries and fatalities is the young population aged between 21-30 years. The morbidity and fatality rate among males is more than twice of females, with a significant portion falling within the economically active age bracket. The period between 12pm to 6pm records a higher frequency of traffic incidents. Notably, the head-on and rear-end collisions are the predominant types of crashes in Kathmandu Valley, indicating the necessity for speed regulation and lane dividers. (RAIMS Operation Report)

Although drivers are commonly held responsible for the crashes, research by Kuikel et al., 2022 suggests that other elements also play a significant role in these occurrences. Kuikel et al., 2022 linked the elevated crash rates in Kathmandu to a variety of factors, including an increase in the number of vehicles, insufficient infrastructure capacity, disregarded safety measures, neglected traffic segregation, haphazard roadside parking and weak law enforcement. The study also indicates several preventative measures that have been put in place to reduce road crashes. These include revoking licenses, penalizing offenders, conducting random and regular inspections, creating designated lanes on main roads, installing zebra crossings and overhead bridges, building sidewalks, and placing traffic lights on main thoroughfares. Despite these endeavors to monitor and reduce the number of crashes and their impact in the Valley, the problem continues to grow as the incidence and trajectory of crashes increase over time. As a result, it is imperative to conduct a detailed and direct investigation to identify the root causes, allowing the government and relevant authorities to take effective action.

Tiwari, 2015 and Shakya et al., 2017 independently conducted the statistical regression analysis of road traffic crashes in Kathmandu Valley. The paper by Tiwari, 2015 explored the dependency of major hotspot locations on traffic volume and speed in Kathmandu Valley. Nine hotspot sites are selected to be fairly straight so that volume and speed can be generalized throughout the section without being impacted by factors like parking, bus stops, and intersections. A linear regression model is developed to show the significant impact of speed, volume and percentage of two-wheeler on crashes, with a goodness of fit reaching up to 50%.

Expanding variables on analysis, Shakya et al. (2017) established a logistic regression model incorporating nine independent variables, including crash cause, vehicle type, driver's age and sex, victim's age, crash time, collision type, crash location, and injury type. Among these variables, only the driver's age, victim's age, and crash time are identified as significant contributors to crash severity outcomes. Also, the odds of a crash being fatal is highest during off-peak periods at night (0:00-4:00) and during the day (12:00-16:00).
Both the studies by Tiwari, 2015 and Shakya et al., 2017 underscore the necessity to consider additional independent variables such as road geometry, pavement state, vehicular condition, road user behavior, weather condition and locational parameters for the construction of a more realistic and accurate prediction model.

Additionally, a technical report by JICA, 2017 states that traffic collisions are frequent on Ring Road, as well as in major highways and intra urban roads primarily involving private vehicles. Conversely, crashes are less common among public transport and commercial vehicles, and mostly result from mechanical issues. The report also provides top ten ranking to blackspots in the manner of Koteshwor, Singhadurbar, Satdobato, New Buspark, Bhaktapur, Swayambhu, Maharajgunj, Jawlakhel, Sukedhara and Kalanki, through an analysis of crash frequency and interview with Traffic Police. The report suggests that priority funding allocation be made to these problematic sections included additional eight locations viz. Bouddha, Gaushala, Gatthaghar, Airport, Sanepa, Nagdhunga, Kalimati and Kamalpokhari, which account for 85% of the collisions, in order to optimize the use of limited resources.

At microscopic level, Shakya et al., 2020 presents a systematic approach to ranking hazardous road locations. The method, based on field surveys and the Analytical

Hierarchy Process (AHP), assigns weights to safety parameters for various road elements such as straight stretches, bends, bridges, and intersections. This study illuminates the significance of various road safety interventions, including road geometry, sight distance provisions, superelevation in horizontal curves, pedestrian crossing facilities, speed limit signs, road markings, and pavement maintenance conditions, in establishing the safety index. While this relatively new ranking methodology can be beneficial to prioritize the treatment of hazardous locations, the study also stresses on its applicability in other areas with limited crash information.

Furthermore, Manandhar, 2022 investigated the factors influencing road crashes in the Valley based on a user perspective study of drivers of two-wheeled and four-wheeled vehicles. The study highlights the perceived probability of crashes to particular scenarios. The highest number of severe crashes are perceived to be caused by drunk driving followed by inadequate driving skills, poor road conditions, vehicle condition, overspeed, overtaking action and bad weather. Since the study relies on self-reported data from convenient number of drivers, it may be subject to sample bias, social desirability bias and limit the generalizability of the findings.

A project report by Adhikari, 2024 provides insight into blackspot identification by means of heat map analysis based on KDE and Getis-Ord Gi* results for three zones of Bhaktapur and Kavrepalanchowk district. The analysis did not observe any significant hotspots in Bhaktapur and Suryabinayak region as these have the least number of crashes. A multiple linear regression model is also developed to predict the total number of crashes occurring in each zones using independent factors such as driver behavior, pedestrian movement, vehicle characteristics, and road geometry. The predictive model shows limitations in capturing all the complex factors contributing to frequencies and severity of crashes, especially the time-based occurrence.

It is evident that that a lack of research exists in incorporating spatial and temporal interaction elements in hotspot analysis of Kathmandu Valley, despites the alarming increase in crashes as pointed out by previous studies. To bridge this gap in the existing literature, the present study seeks to utilize Global Moran's I, Getis-Ord Gi* and KDE to detect the statistically significant hotspot locations and their change over various time intervals. The study also aims to rank the identified hotspots on the basis of severity index, and correlate them with land use characteristics, population density, and other

casual variables to guide policymakers for the prioritization of potential safety interventions.

2.7 Summary of Key Findings

Upon conducting a thorough examination of various research papers and reports outlined above, it is apparent that traditional statistical models are gradually being replaced by the cutting-edge GIS based spatial and temporal analysis techniques. The geo-spatial analysis proves to be more adept at capturing unobserved spatial variations, yielding consistent results and outperforming classical GLM and EB methods through matching with location-specific data. Essentially, the geo-spatial analysis allows to readily explore the temporal variations and cycles within the road crash domain through disintegration and visualization of subset data.

From the global perspective, spatial autocorrelation statistics, LISA and KDE method are considered promising for their ability to highlight high crash risk locations compared to surrounding locations. Despite this, the published researches in Nepal continue to rely upon the regressive techniques which cannot counteract the regression-to-the-mean bias and spatial effects, resulting in inaccurate crash estimations.

Consequently, the present investigation strives to delineate the spatial and temporal patterns of road traffic hotspots currently with the application of three methods viz. Global Moran's I Index, Getis-Ord Gi* statistics and KDE. This study will be instrumental in filling the knowledge gap regarding the spatial and temporal factors influencing the crash types and their severity, as there is dearth of studies conducted in this setting in Kathmandu Valley. Ultimately, the current study will contribute to the ongoing efforts to improve road safety and reduce the incidence of traffic crashes in Kathmandu Valley.

CHAPTER 3: METHODOLOGY

3.1 General

The chapter outlines the detailed methodology adopted to achieve the objectives of the present thesis study. The chapter consists of other six sections. Section 3.2 explains the research methodology selected for the study. The Section 3.3 describes the characteristics of the selected study area. A comprehensive elucidation is provided regarding the data collection, dataset preparation and structures in Section 3.4. The Section 3.5 outlines the data cleaning and preprocessing steps required for the analysis. The Section 3.6 provides an in-depth discussion of each of the selected data analysis methods, encompassing context of the methodology, standard equations and the tools correlated with it that are organized in subsequent sub-sections. Lastly, the chapter enlists the software and packages utilized for the spatial and temporal analysis in Section 3.7.

3.2 Research Design

The methodological steps followed in the present study is shown in figure 3.1. The research employs an integration of various analysis methods; Global Moran's I Index, Getis-Ord Gi* statistics, Kernel Density Estimation (KDE), comap and GIS spatial analysis tools to evaluate the statistically significant hotspots and their spatial-temporal interaction. The combination of these methods was chosen for this study due to numerous research findings validating the stability, reliability and precision of these methods when compared to alternative techniques and limitations associated with application of these methods alone (ESRI). Each method can fulfill the limitation of another method, reckoning on the comparative advantages as discussed in Chapter 2. The method of clustering analysis with Global Moran's I Index and Getis-Ord Gi* statistics has the capability to offer a greater amount of spatial feature information when compared to the KDE analysis method, while the KDE analysis method proves to be more advantageous than the spatial autocorrelation method in terms of the simplicity of principle and computational efficiency. The Getis-Ord Gi* statistic proves more

advantageous in pinpointing areas with significant clusters of crashes compared to the Moran's I index. Therefore, the comprehension of these methods is deemed to precisely pinpoint the hotspot location, identify the clustering patterns and provide a more nuanced understanding of spatial and temporal attributes underlying the crashes.

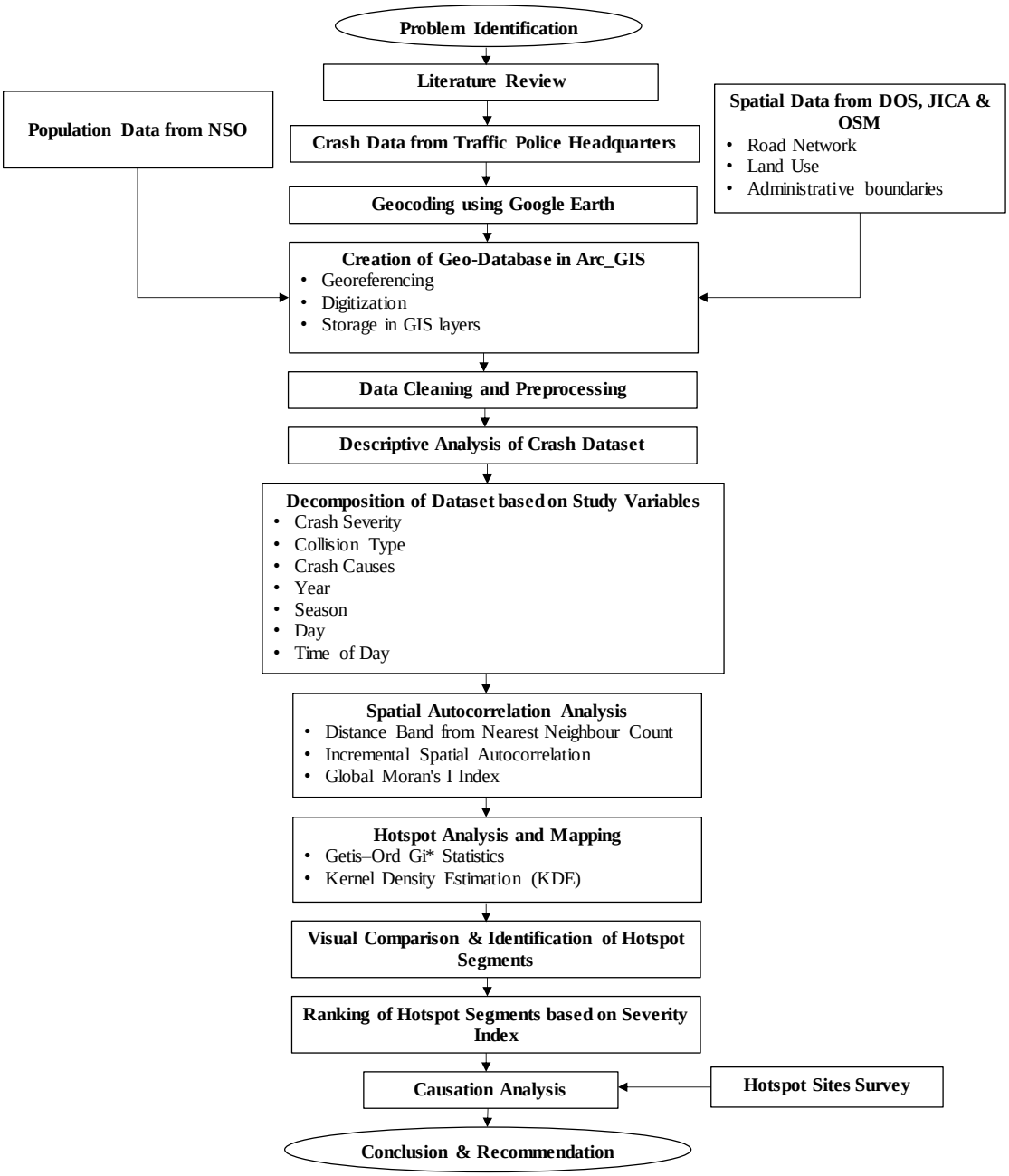

Figure 3.1 Methodological Workflow

The Getis-Ord Gi* statistics and KDE, either alone or in combination, have already been tested in Nepal by JICA, Jimme et al. 2023 and Adhikari et al. 2024, and these methods best suit the objectives and quality of data at hand. The Global Moran's I is utilized for capturing the average spatial pattern across an entire Valley. The Getis-Ord

Gi* statistic is employed for delineating statistically significant hotspots and coldspots. Planar KDE is utilized for estimating the density distribution of point events and identifying concentrations of crashes (hot spots) on a road network. While the Comap method is relatively new in Nepal, it is applied for generating hotspot maps from temporal datasets and analyzing temporal variations in crash occurrences. Spatial analysis is conducted using appropriate GIS tools to examine contributing factors, aiming to determine suitable countermeasures for enhancing road safety. The causation and solution analysis are further complemented with site observation at five sample locations selected from top ten hotspots ranked based on weighted severity index.

As such, the research matrix is presented below in table 3.1 along with the specific objectives, study variables, analysis methods/tools and expected results.

Table 3.1 Proposed Research Matrix

Specific Objectives	Study Variables	Analysis Methods/Tools	Expected Results
1. To investigate the spatial patterns of observed traffic crashes in the Valley.	• Spatial Characteristics of Clusters (Aggregate, Severity and Collision Type) • Spatial Relations (Land Use, Population)	Descriptive Analysis using MS_Excel	• Statistical tables, charts and graphs related to spatial distribution
		Spatial Analysis (Moran's I Index, Gi* Statistics and KDE) using Arc_GIS	• Hotspot maps showing spatial distribution (patterns) through comparison of Gi* and KDE results
2. To determine the temporal clustering of observed traffic crashes in the Valley.	• Temporal Characteristics of Clusters (Year, Season, Day, Time)	Descriptive Analysis using MS_Excel etc.	• Statistical tables, charts and graphs related to temporal distribution
		Temporal Disintegration of Datasets Spatial Analysis (Moran's I Index, Gi* Statistics and KDE) using Arc_GIS Comap technique	• Hotspot maps showing temporal distribution (year, season, day and hour)
3. To uncover the clustered locations (hotspots) and casual factors for some of the identified hotspots.	• Road Geometry • Environment • Safety features • Driver Factors	Descriptive Analysis using MS_Excel Severity Ranking of Hotspots	• Locations and contributing factors for the hotspots • Possible countermeasures
		Observation Checklist	
		Overlay and Spatial Analysis using Arc_GIS	

3.3 Study Area

The proposed study area is Kathmandu Valley is a bowl-shaped portion of Bagmati watershed that covers an area of 671.32 km^2 in the central hilly region of Nepal as shown in figure 3.2. Geographically, the valley extends from 321583.818811 m to 355242.516185 m latitude and from 3077966.556057 m to 3046099.937480 m longitude. The valley is made up of the Kathmandu District, Lalitpur District and Bhaktapur District covering 2 metropolitan cities and 16 Municipalities. The Kathmandu Valley, being the most developed and densely populated region in Nepal, boasts a population of 2.88 million, representing approximately 9.88% of the total populace in the country according to the National Statistics Office (NSO, 2021).

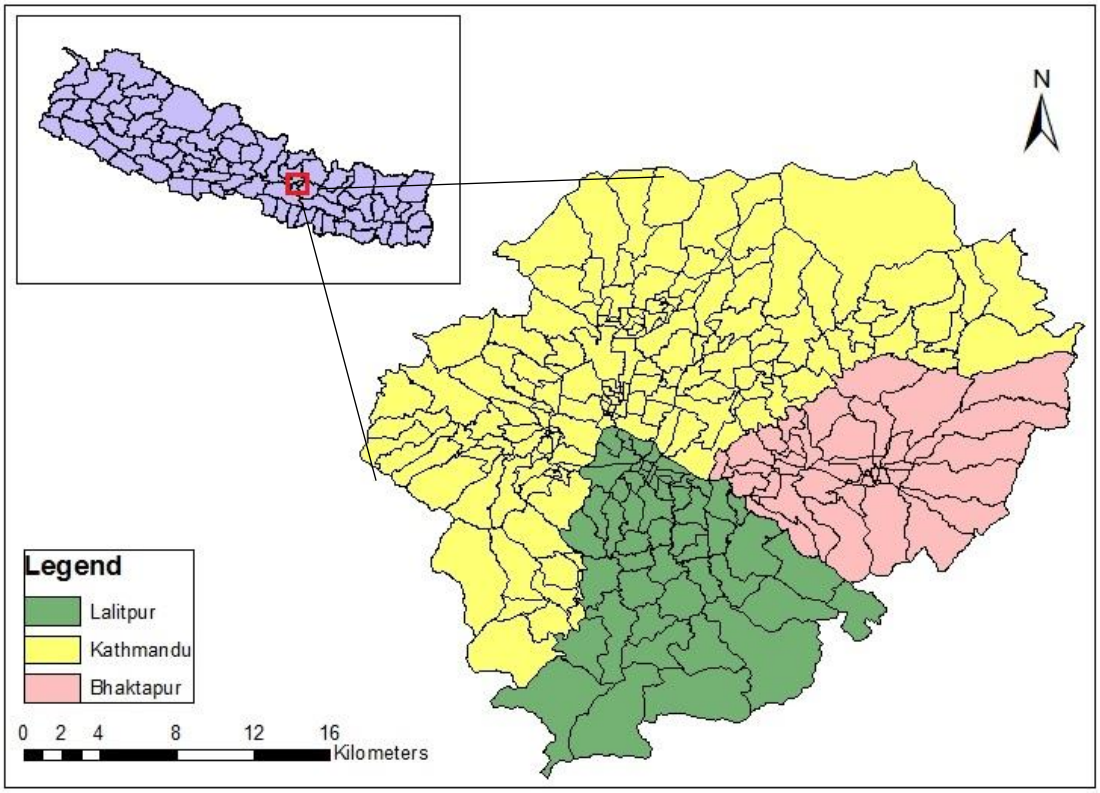

Figure 3.2 Location Map of Study Area

Over the past decade, the valley has experienced a growth rate of 11.8%, with the highest rate of expansion observed in the central urban areas. The urban growth in the valley continues to be rapid and largely uncontrolled, thereby, hampering the land-use efficiency, transport mobility, and infrastructure/service delivery inside the urban form. The haphazard development has led to an increase in vehicle usage without a corresponding rise in road infrastructures. At present, the study area is traversed by a

road network of 5724.18 km length. The quantity of officially registered automobiles within the Kathmandu valley amounts to 444,759 (Adhikari, 2014).

As a result, most of the arterial and internal roads suffer from daily congestion and traffic crashes in relation to heavy traffic flow. Moreover, the Valley roads are reported to have the highest incidences of traffic crashes than elsewhere in the country. Despite the growing tendency of crash incidents in this region, the researchers tend to rely on traditional statistical analysis to analyze or predict trends of crashes. Longitudinal studies are desired to identify the patterns of crashes, severity, causes and other variables in space and time. The spatio-temporal analysis technique has not been utilized in prior studies in Kathmandu Valley, so it was chosen for examination in the study area.

3.4 Data Collection and Preparation

The availability, quality and authenticity of data may act as a constraining element in determining the scope of crash analysis and will have an impact on the validity and precision of the outcomes. As far as possible, the data relevant to the thesis were collected from credible sources and subjected to careful scrutiny to ensure its accuracy, coverage and usability in hotspot analysis. The datasets acquired and utilized in this study are summarized in this specific section.

3.4.1 Data Collection

Data is the key element in conducting the research and achieving the study's goals. As such, secondary data for this study has been sourced from various agencies. The typical secondary data required for the study and their corresponding sources are tabulated below in table 3.2.

Table 3.2 Summary of Secondary Data Requirement

Data Category	Details	Sources
Land use	Classes, Name, Local Level, Area	Department of Survey (DoS)
Demographics	Population Density (heads/sq.km)	National Statistics Office (NSO)
Administrative	District, Local levels and Wards	Department of Survey (DoS), National Geoportal

Data Category	Details	Sources
Road Network	Road Name, Class, Length and others	Japan International Cooperation Agency (JICA), OpenStreetMap (OSM)
Traffic Crashes	Location, Date, Time, Crash Description, Type (Injury/Serious/Death), Causes, Vehicle involved, Persons injured/died	Traffic Directorate

The recent traffic crash records from 2019 to 2021 was obtained from Nepal Police Headquarters, Naxal in electronic form (MS Word format). From a statistical perspective, data of a minimum of three years are needed for any spatial analysis to obtain credible results (Elvik, 2008; Saric et.al. 2011 Cheng and Washingston, 2005).

The records provided by the Nepal Police Headquarters were actually the concise summary of crash reports recorded by 44 Traffic Police stations that include details such as the location of station, date and time of the incident, a description of the event circumstances, the vehicles and people involved, severity of the incident, the contributing factors related to the driver or pedestrian, and tentative distance from the reporting station, all written in Nepali language. Under-reporting and bias exist in the reporting of the true number of road traffic crashes, particularly minor injury, property damage, and single-vehicle crash as indications from World Health Organization data.

In the context of this study, the JICA provided the road network dataset in GIS shapefile format for the year 2021. The dataset included attribute information such as ID, surface type, road width, pavement type, link name, start and end of section, road class (district/municipal/national highway/feeder), carriageway width, construction status, length and remarks. Another road network dataset for the Kathmandu Valley was downloaded from OpenStreetMap (OSM) Project using the Geofabrik's server. The attribute features of this dataset comprised Osm ID, code, road feature class, road name, reference (highway/feeder), direction (oneway/twoway), speed limit, bridge, tunnel and length. The purpose of sourcing the road network dataset form two different sources is to compare the overall quality and merge/reclassify the required polylines and attributes to form a complete dataset for analysis.

This research also incorporates other explanatory variables like the administrative boundaries, land use, size of the population, road infrastructure data etc. Administrative area of districts/local levels/wards and landuse data, which were needed for this study, were supplied by DOS. Data population size is downloaded from census 2021 portal of NSO in Excel format.

Additionally, primary data on design, condition and safety risks of the roads (only for the hotspot segment) was gathered through field observation and administration of standard checklist.

3.4.2 Dataset Preparation

The process of digitization involves encoding the spatial characteristics into a digital format represented by x and y coordinates. The crash database, which was supplied in Word format, contained important crash details including the location of the incident, the date and time of the occurrence, the reason of crashes and so on as described previously in Section 4.4.1, however these were in Nepali language. To convert that information to CSV format, a ready python program coded specifically for the Traffic Police was applied with prior permission from the developer. The pertinent codes have not been disclosed in this report due to confidentiality issues.

The excel dataset lacks precise coordinates for crash points. To address this, each crash record was manually read and the collisions were mapped on specific routes. Then, the missing coordinates were determined by measuring distances on the paths from the specified Traffic Police station, and adding pinpoints for corresponding crash locations in the Google Earth interface. In aggregate, 29,262 crashes were reported during the study period (2019-2021), however, only 23,330 crashes (79.73%) have been plotted. The crash points were geocoded only for those records which exhibit the correctness of distance from Traffic Police station, locations of crashes and travel paths description based on crash reports. The distribution of the geocoded crash points across the project area is shown in figure 3.3.

Consistency in dataset is of utmost importance in ensuring precision and facilitating the seamless integration of additional data. In the context of utilizing the crash data in GIS, the sole aspects that necessitate uniformity and consistency were the headings of the variable columns and their values. To ensure uniformity, the CSV format crash dataset

was formatted for every record to include a unique key (I.D.), year, month, day, time, X and Y coordinates, and other descriptive variables that are pointed out in Section 3.4.3.

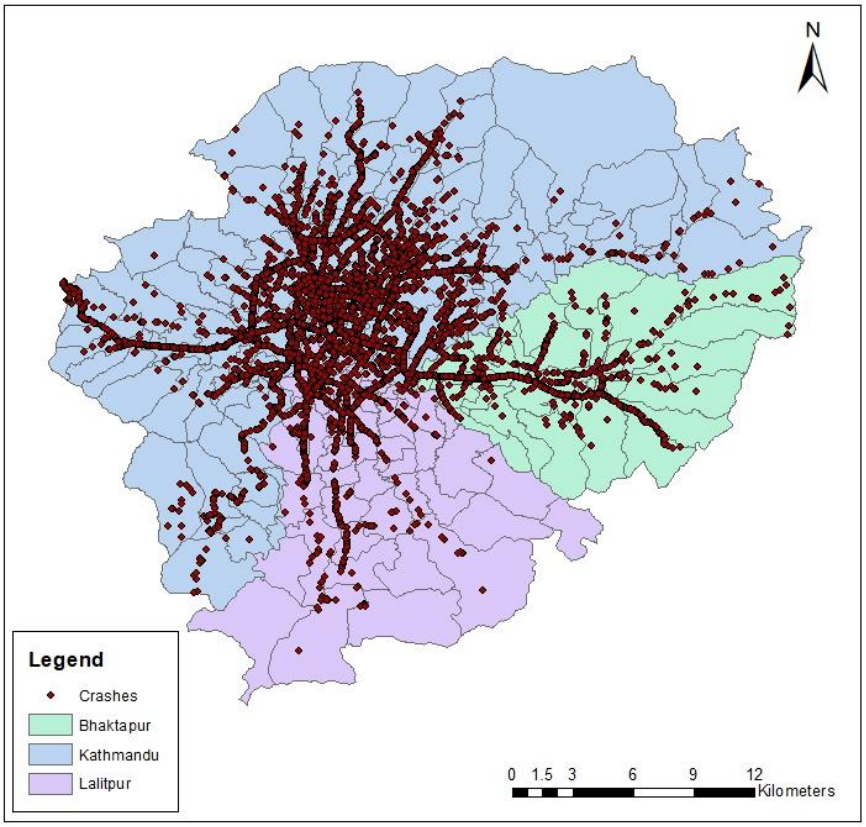

Figure 3.3 Spatial Distribution of Crash Points (2019-2021) in the Study Area

After that, the latitude and longitude of the crashes were added to ArcMap 10.8 to form point features appended with various attribute information and converted into shape files. The crash data points were plotted and dereferenced to the suitable coordinate system, specifically UTM Zone 45N, utilizing the Projections Tool. The details of the projection system are presented in the table 3.3.

Table 3.3 Standard Coordinate Reference System

Coordinate System	Parameters
Coordinate system	WGS_1984_UTM_Zone_45N
Projection	Transverse Mercator
False easting	500000 m
False northing	0.0 m
Central meridian	87° E, 0° N
Scale factor	0.9996
Latitude of origin	0.0
Linear unit	Metre

Coordinate System	Parameters
Angular unit	Degree (°)
Prime meridian	Greenwich (0.0)
Datum	D_WGS_1984
Spheroid	WGS_1984
Semi major axis	6378137.0
Semi minor axis	6356752.314245179
Inverse flattening	298.257223563

Considering the high road density and the regions of crashes, the focus was on the road sections that have experienced crash events previously. Therefore, the road network dataset for the study was meticulously developed by overlapping the crash points with road network and then extracting the relevant road segments from the shapefiles of JICA. The road network shapefile of OSM was also overlayed to identify any missing road segments or joins with intersections within the datasets of JICA. Then, the extracted study road network was modified using GIS editor tools, aligning it with the OSM road network for missing segments. The final road network produced is shown in figure 3.4.

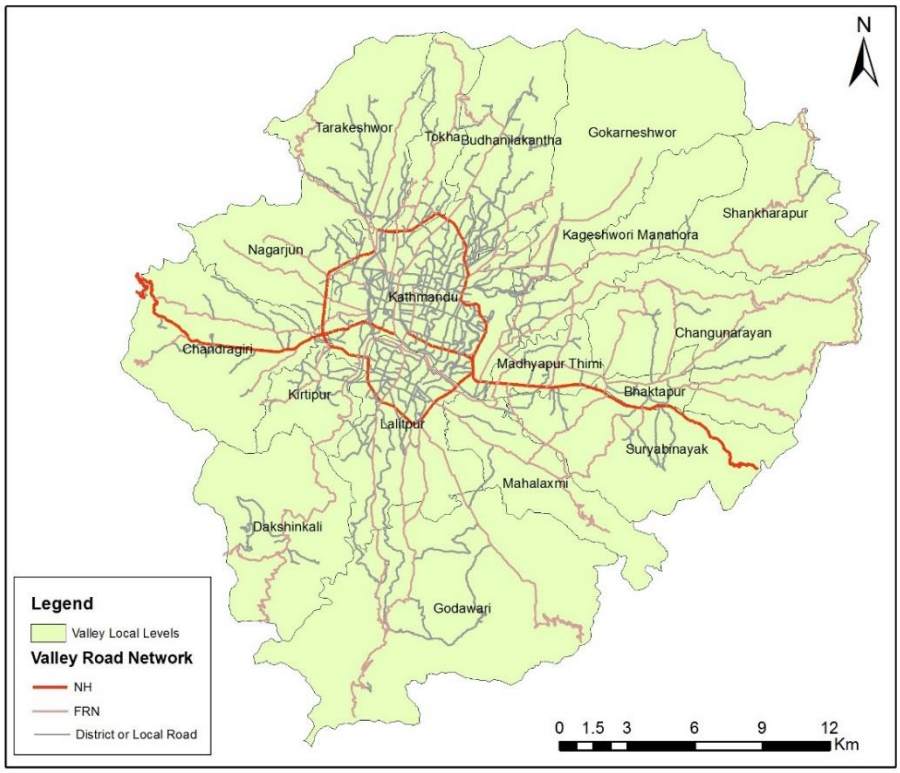

Figure 3.4 Road Network Considered in the Study Area

Besides, administrative boundaries, land-use, population and vehicle asset information were also appropriately digitized in ArcGIS 10.8 environment to the required

coordinate systems to create respective database layers. The initial land cover dataset supplied by the DOS was restricted to ward-wise data. A schema was devised to consolidate various pieces of land-use data, provided separately in the spatial layer, into a single layer.

3.4.3 Dataset Characteristics

For all vector datasets including lines (Road network), polygons (Land Use & Administrative), and point features (Crashes), separate attribute tables are maintained as elaborated in trailing sub-sections.

A. Crash Data

In this particular setting, a crash is delineated as an incident or event including the motion of at least one vehicle that leads to fatality, injury, or destruction of property. The crash dataset consists of data fields as shown in table 3.4.

The severity level of a crash is determined based on the most severe injury sustained by any participant in the crash. For example, if a crash results in at least one death, it is classified as a fatal crash. If there is at least one serious injury but no deaths, it is categorized as a serious injury crash. If no deaths or injuries are reported, it falls under the property damage only category. Drawing on the classification principle from existing literature and actual record, the crashes have been classified according to the severity levels as shown in table 3.5.

Table 3.4 Crash Dataset Attributes

Field Name	Values
I.D	Unique identification number
Year	2019, 2020, 2021
Month	January, February, March, April, May, June, July, August, September, October, November, December
Day of Week	Sunday, Monday, Tuesday, Wednesday, Thursday, Friday, Saturday
Time of Day	Actual time of crash occurrence
X	Longitude (Degree)
Y	Latitude (Degree)
Type of Severity and Numbers	Death, Major Injury, Major Injury, Property Damage Only
Type of Crash	Head on Collision, Rear End/Side Collision, Crossing Collision, Turning Collision, Hit Pedestrian Crossing, Hit

Field Name	Values
	Pedestrian, Hit Object, Hit Animal, Overturned Vehicle, Multiple Collision, Others
Contributing Reason	Driver Carelessness, Alcohol Influence, High Speed, Overtake, Bad Turning, Lane Violation, Calling on Mobile, Vehicle Defect, Road Condition, Overloading, Weather Condition, Others
Type of Vehicles Involved and Numbers	Truck, Bus, Rent Micro, Car/Jeep/Van, Motorcycle, Tempo, Tractor, Non-Motorized Vehicle (NMV)

Table 3.5 Severity Levels of Crashes

Collision Type	Description
Death	An incident that resulted in the death of one or more individuals instantly or within 30 days of intensive medication.
Serious injury	An incident where one or more individuals were seriously injured and required hospitalization for treatment lasting at least one day.
Minor injury	An incident where one or more individuals sustained injuries without need of hospitalization.
Property-damage-only (PDO)	An incident where no fatalities or injuries occurred, but there was damage to vehicles and/or other property.

The crashes are also categorized based on their collision type as Head on Collision, Rear End/Side Collision, Crossing Collision, Turning Collision, Hit Pedestrian Crossing, Hit Pedestrian, Hit Object, Hit Animal, Overturned Vehicle, Multiple Collision and Others. Table 3.6 summarizes the terminologies for various collision types adopted in this thesis based on the interpretation of existing crash records.

Table 3.6 Terminologies of Collision Types

Collision Type	Description
Head on Collision	This involves two vehicles travelling in opposite directions hit each other on the front
Rear End/Side Collision	This occurs when two vehicles moving in one direction collide with each other either on the end or sides
Crossing Collision	This occurs when two crossing vehicles collide with each other either at an angle or right angle (T shape).
Turning Collision	This occurs when one of the vehicles driving in opposing or same direction makes sudden u-turn, left-turn or right turn action
Hit Pedestrian Crossing	This occurs when a pedestrian is struck by a vehicle while crossing the road, either at a marked crosswalk (zebra-crossing) or an unmarked crosswalk
Hit Pedestrian	This happens when a pedestrian walking, standing or doing any other activities on the roadside is struck by a vehicle
Hit Object	This happens when the vehicle crashes into objects either on-road or roadside like dividers, curbs, railing, light pole, trees, house etc.

Collision Type	Description
Hit Animal	This occurs when vehicle strikes an animal in its path
Overturned Vehicle	This occurs when the vehicle loses control and rolls over
Hit Parked Vehicle	This happens when a moving vehicle strikes with parked vehicle
Multiple Collision	This symbolizes collision between two or more vehicles at a time or in series as in bus stops or red sign, or just the combination of any other collision types
Others	The collisions which are not described by types illustrated above.

B. Road Network Data

Out of total road network, only 912.54 km of roads was considered for the study to ensure convergence with crash regions. The attributes of road network dataset are categorized into 12 groups as delineated below:

- Unique Identification Number (I.D),
- Surface type (Blacktopped/PCC/Gravel/Earthen/Track),
- Road width (1-32m),
- Link name,
- Start and end of section,
- Road class (national highway/feeder/district/municipal/),
- Carriageway width (<3.5m, 3.5-5.5m, 5.5 -<13m, >13m))
- Length

C. Administrative Data

The selected study region encompasses 3 districts, 18 local levels and 227 wards, the details of which is outlined in table 3.7.

Table 3.7 Administrative Units and Their Characteristics

District	Local Level	No. of Wards	Population
Kathmandu	Budhanilkantha Municipality	13	177557
	Chandragiri Municipality	15	136860
	Dakshinkali Municipality	9	26372
	Gokarneshwor Municipality	9	149366
	Kageshwori Manahora Municipality	9	130433
	Kathmandu Metropolitan City	32	862400
	Kirtipur Municipality	10	81578
	Nagarjun Municipality	10	115437
	Shankharapur Municipality	7	24086
	Tarakeshwor Municipality	11	151479
	Tokha Municipality	11	133755

District	Local Level	No. of Wards	Population
Bhaktapur	Bhaktapur Municipality	10	79136
	Changunarayan Municipality	9	15995
	Madhyapur Thimi Municipality	9	119756
	Suryabinayak Municipality	10	140085
Lalitpur	Godawari Municipality	14	97633
	Lalitpur Metropolitan City	29	294098
	Mahalaxmi Municipality	10	123116

D. Land Use Data

The land use data is characterized by a number of feature class (polygons) including agricultural, commercial, cultural and archaeological, forest, industrial, mine and minerals, public use, residential, riverine, lake and marsh area, and others as per the standard definition of DOS and Land Use Policy, 2015 (Refer table 3.8).

Table 3.8 Land Use Categories

Class Name	Description
Agricultural	Land designated for farming and cultivation activities, including growing crops, rearing livestock and fisheries
Commercial	Areas allocated for business activities, trade, and services.
Public Use	Spaces intended for public services and amenities, health service, educational instituition, open parks, government buildings, and infrastructure.
Residential	Zones primarily used for housing and living spaces.
Industrial	Land used for manufacturing, processing, and other industrial operations.
Cultural and Archaeological	Zones that are important for historical, religious, or heritage reasons, including sites of archaeological significance.
Forest	Regions covered with trees and vegetation or managed for conservation or timber production.
Riverine, Lake, and Marsh Area	Land adjacent to rivers, lakes, and wetlands, which may include floodplains and conservation areas
Mine and Minerals	Areas designated for the extraction of natural resources such as minerals, ores, and fossil fuels.
Others	This category includes land uses not covered by the aforementioned classes, which could vary based on specific local regulations and needs

The coverage of different land use classes is depicted in figure 3.5. The primary land use in the valley is agriculture accounting for 33.93%, followed by forests comprising 27.48% and residential areas making up 25.21%. Land designated for public use represents 8.65%, while riverine, lake and marsh area cover 1.67%. Industrial and commercial uses are relatively smaller, at 1.40% and 1.29% respectively. Cultural and

archaeological sites occupy a mere 0.35%, and other miscellaneous uses constitute just 0.02%.

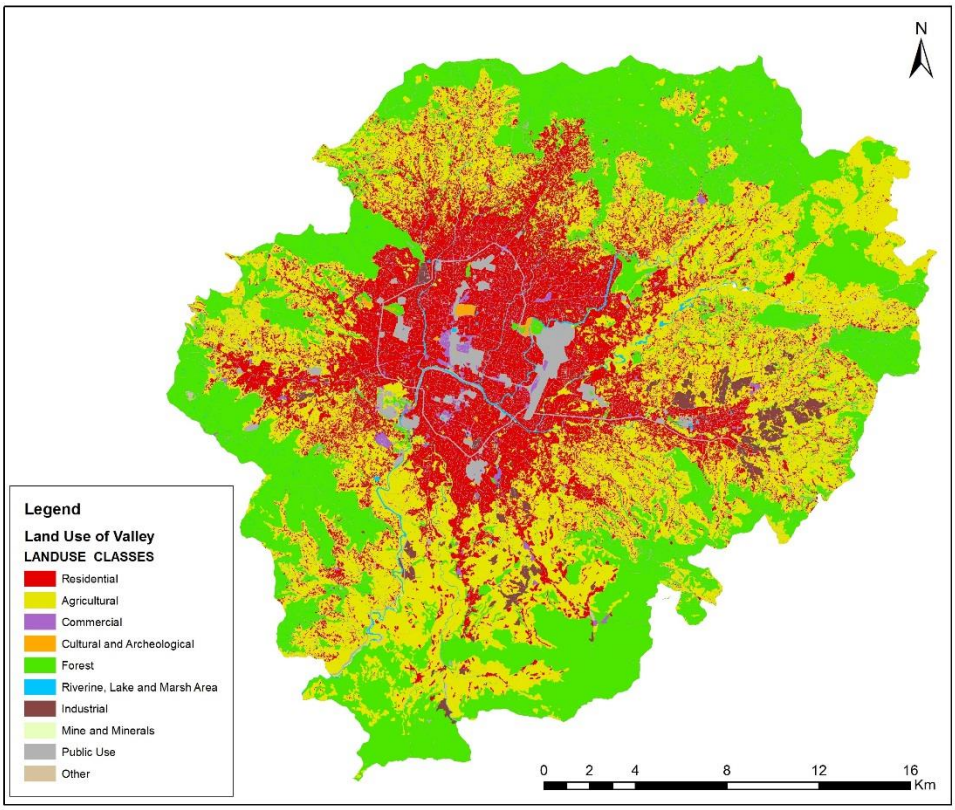

Figure 3.5 Land Use Map of Study Area

3.5 Data Cleaning and Preprocessing

Prior to the data analysis, data cleaning and pre-processing is necessary to ensure consistency and reliability of digitized datasets. This procedure comprises various steps, which proceeds as follows in order to prepare quality of dataset:

- Identification of crashes with duplicate id and same field values
- Detection of crash records with missing or null values
- Identification of crash records containing one or more empty fields.
- Addition of field values, if available in records
- Removal of identified observations if more field values are missing (reduction process)
- Editing or formatting of field values as required

Additionally, crash dataset and road network is overlaid to identify outliers and adjust crash points to intersect with nearest edge of road network using snap function. After

data purification, 23,278 (79.55%) crash records were available for the analysis. The attribute table with road crash data was also cleaned, and details for each variable were scrutinized and made uniform. All non-viable polyline segments other than the road centerlines were filtered out.

3.6 Data Analysis Methods

In the initial stage of hotspot analysis, road segmentation is required. The road segment length in the dataset varies considerably with some segments being less than 100m and some greater than 1000m. These road segments need to strike a balance: they should be long enough to identify hot spots but short enough to capture environmental changes that might impact road safety (Loo, 2009). So, the original road segments as given in the dataset were considered as spatial units of analysis.

For the spatio-temporal analysis, the hotspot is defined as a collection of adjacent spatial units characterized by a significant occurrence of crashes. Specifically, the analysis considers positive autocorrelation resulting from high values as the sole criterion (as explained in Section 2.5). The following distance-based and density-based point pattern analysis techniques was applied to identify the hotspots based on variables of aggregate crashes, severity type, collision type, year, season, day and time of crashes.

3.6.1 Spatial Autocorrelation (Global Moran's I Index)

Moran's I is one of the earliest markers of spatial autocorrelation (Moran, 1948). The global Moran's I is used to examine whether the crash locations and attributes exhibit any regularity, i.e. whether they are spatially clustered, dispersed or random. It can be computed using equation 3.1.

$$I = \frac{n}{\sum_{i=1}^{n}\sum_{i=1}^{n} w_{ij}} * \frac{\sum_{i=1}^{n}\sum_{i=1}^{n} w_{ij}(x_i - X)(x_j - X)}{\sum_{i=1}^{n}(x_i - X)^2} \quad (3.1)$$

Where, n is the total number of cases (crashes), xi is the attribute value for feature i, xj is the attribute value at another location j, X is the global mean value of the variable, and wij is a spatial weight applied to the comparison between location i and location j. All adjacent features within specified distance receive the weight of 1, whereas other features outside are assigned with weight 0.

The Z-score for the index can be obtained as shown in equations 3.2, 3.3 and 3.4.

$$Z = \frac{I - E[I]}{\sqrt{V[I]}} \quad (3.2)$$

Where,

$$E[I] = \frac{-1}{(n-1)} \quad (3.3)$$

$$V[I] = E[I^2] - E[I]^2 \quad (3.4)$$

The "Distance Band from Neighbor Count" geo-processing function generated an average distance to be used as the starting distance and the increment for the spatial autocorrelation analysis. The threshold distance that gives the scale of the analysis was assessed using Incremental Spatial Autocorrelation function. The peak distance (distance at which most of the crashes tend to cluster) respective to the maximum z-score and minimum number of neighbors required was selected. For the conceptualization of spatial relationships, both the fixed distance band method was applied.

The spatial pattern analysis tool of ArcGIS was applied to generate the Moran's I, z-score and p-value. The score indicates whether the identified spatial aggregation of high or low values is more conspicuous than what would be anticipated in a random arrangement. The Moran's I value close to -1 denotes dispersed patterns, while the value close to +1 denotes clustered patterns in the analysis regions (Prasannakumar et al. 2011). The significance of the spatial autocorrelation increases with the absolute magnitude of Moran's I. A value of 0 denotes perfect spatial randomness.

3.6.2 Hotspot Analysis and Mapping

The Getis-Ord Gi* spatial statistics is computed to differentiate the clustering features of high values from low values. The Gi*statistics analyzes each feature in the dataset within the context of neighboring features (Getis et al., 1992). By calculating the Getis-Ord G* statistic for each data point, hot spot analysis can detect whether a point belongs to the same category as nearby points. It classifies a feature as statistically significant hotspot when both the feature and its neighbors have high value (Nanzeen et al. 2020, Prasannakumar et al., 2011, Truong et al. 2011). A statistically significant Z score is produced when the local sum is significantly different from the expected local sum and that difference is too large to be the result of random chance. This comparison is made

between the local sum for a feature and its neighbors in proportion to the sum of all features. The statistic is derived from equations 3.5, 3.6 and 3.7.

$$G_i^*(d) = \frac{\sum j\ (W_{ij}\, x_j - W^*_{ij}\, \bar{x})}{s^* \sqrt{\frac{(nS^*1i) - W^*_{ij}}{n-1}}} \tag{3.5}$$

Where, Wij is a spatial weight vector with values for all features 'j' within distance d of target feature i, W*ij is the sum of weights, S* is the sum of squared weights, s* is the standard deviation of the data in the cells and n is equal to total number of features, and:

$$s = \sqrt{\frac{\sum_{j=1}^{n} x_j}{n} - \bar{x}^2} \tag{3.6}$$

$$\bar{x} = \frac{\sum_{j=1}^{n} x_j}{n} \tag{3.7}$$

To perform this, the crash data was consolidated using the Integrate and Collect Event Tool provide a new weighted point feature class that represents the sum of all crashes that occur in geographic area. When this tool is executed, features within a certain default proximity to each other converge to the same location, thereby forming a group of overlapping features with identical XY coordinates. The Hot Spot Analysis function (Getis-Ord GI*) from the Spatial Statistics toolbox of ArcMap 10.8 was then fed with this new weighted point feature (denoted as I Count) as the input for hotspot computations.

Alternative method was also utilized, in which a spatial join was executed within ArcMap 10.8 to integrate the crash points layer with the road network layer, thereby consolidating the variables pertaining to crashes and roads into a unified dataset. This integrated layer was augmented with two additional fields; the initial field enumerates the new object identity, and the next field named as joint count that quantified the number of crashes per segment. Again, the joint count was inputted in the Hot Spot Analysis function (Getis-Ord GI*) as the input for hotspot identification.

The Gi* (d) statistics returns an output feature class containing z-score (Standard Deviations), p-value, and a bin field for confidence level (Gi_Bin) for each feature within the input feature class. The Gi_Bin field accurately identifies significant hot and cold spots in a statistical manner. Features falling within the ±3 bins accurately represent statistical significance with a confidence level of 99%; whereas those within

the ±2 bins indicate a confidence level of 95%, and those within the ±1 bins indicate a confidence level of 90%. A high z-score and small p-value of a feature suggest a spatial clustering of high values, whereas a low negative z-score and small p-value indicate a spatial clustering of low values. Essentially, the intensity of the clustering of high values is directly proportional to the Z score for statistically significant positive Z scores and so is the clustering of low values. A z-score close to zero suggests an absence of apparent spatial clustering.

3.6.3 Kernel Density Estimation (KDE)

KDE technique is applied to determine the density of crashes within a given bandwidth (search radius) surrounding each point across study area. The KDE utilizes a kernel function to give the region surrounding the point event a weight based on how far away it is from the point event. To put it another way, the surface value is largest at the point location (the center) and gently decreases to zero along the circle's radius (bandwidth). Each individual kernels in the study area are summed up to smooth continuous density surface (Young et al. 2014; Truong et al. 2011; Anderson, 2009). The mathematical form of the intensity at each location can be represented as shown in equation 3.8.

$$f(x,y) = \frac{1}{nh^2}\sum_{i=1}^{n} k\left(\frac{d_i}{h}\right) \quad (3.8)$$

Where, f (x,y) is the density measured at location (x,y), h is the radius of the circle (bandwidth or kernel size), K () is the kernel which is a function of the bandwidth and distance, and di is the distance between point (x, y) and ith location. (Fotheringham et al. 2000)

With the help of the KDE calculator feature offered by the spatial analyst tool, kernel density hotspots were detected using the crash point layer and populated field as none. Using the input field, it determines the magnitude per unit area from each hotspot feature; in other word the spread of risks around crash cluster. The primary factor to consider in determining the appropriate density level is the bandwidth and cell size, which play a crucial role in defining the level of smoothing and the scope of clustering. A sensitivity analysis was conducted to ascertain the most appropriate bandwidth (also known as search radius) and cell size for the given dataset. A bandwidth of 250 m and a cell size of 10 m were found suitable. The output was a raster file illustrating the locations of high and low clusters of crash occurrence.

3.6.4 Comap Technique (Temporal Analysis)

On the part of temporal analysis, crash dataset was disaggregated into time intervals of year (2019, 2020, 2021), season (pre-monsoon, monsoon, post-monsoon, winter), day (weekdays and weekend) and time of the day (late night, early morning, morning, afternoon, evening and night) as appropriate. It is recommended by Plug et al. 2011, & Bil et al. 2013 that the class boundaries should exhibit some degree of overlap. Therefore, to address the issue of temporal boundaries, particularly in seasonal dataset, 15 days within each period were purposely aligned to overlap.

The hotspot analysis with Getis-Ord Gi* (d) and KDE is then carried out separately to investigate the effect of time on spatial distribution of crash occurrences. The outcomes from each subset of data are then visually presented in a sequential manner to illustrate the spatial-temporal relationship between crash data.

3.7 Identification and Ranking of Hotspots

The statistically significant crash hotspots in the Valley were ascertained by overlapping the high-risk maps created by KDE and Getis-Ord Gi* (d) statistics. A visual comparison was made between these two approaches to ensure that road segments identified as hotspot in Getis-Ord Gi * (d) also shows high intensity of clustering in the KDE maps. Further, severity weighted technique was utilized to pinpoint the hotspots and rank the top ten sites. The weights for each severity level were determined in proportionality to associated crash costs as suggested by Highway Safety Manual (HSM). The crash costs were excerpted from Rizal et al. 2023, and the weights were calculated by dividing the crash costs corresponding to different levels of injury severity by the PDO. The derived weights of each severity level are shown in table 3.9.

Table 3.9 Crash Cost based Weights of Crash Severity

Severity Level	Crash Cost (NRs.)	Weight
Death	7,459,501	353
Major Injury	169,706	8
Minor Injury	35,646	2
Property Damage Only	21,132	1

To assign severity index (SI) to each segment, equation 3.9 was used.

$$SI = 353 * A + 8 * B + 2 * C + D \quad (9)$$

Where, SI is severity index, A is death crashes, B is major injury crashes, C is minor injury crashes and D is property damage only crashes.

3.8 Site Reconnaissance

Five sites among the top ten hotspot segments identified based on crash severity intensity were chosen for field reconnaissance in order to supplement and/or validate the hotspot analysis results. Sample sites were selected purposively considering different severity level, type of road elements present (such as intersections, mid blocks, curves and bus stops,), situated on different highways, and where significant design changes have not been implemented since 2021. Then, field survey was conducted to determine the location specific characteristics that contribute to high number of crashes at hotspot places. A specialized data collection form is devised as shown in Appendix D to streamline the process of gathering information on road design conditions, environment factors and risky road users' behaviors from individual sites. Photographic proofs; video of site for evaluation of safe road user behavior, and photos of the observed problems were acquired from each site. The primary data obtained from field observation was analyzed using subjective method to elucidate the physical characteristics and road user behaviors at the locations that link with observed crash patterns at those sites. Additionally, the presence of over speeding incidences was confirmed by taking sample of 40 vehicles (10 each for heavy/light truck, bus, car/van/jeep/pick-up, and motorcycles/scooters).

3.9 Spatial Analysis

The dispersion of crash point patterns was related to spatial features such as landuse, population, road infrastructure (mid-block/curves/intersections etc.) etc. in order to explore the spatial association. The spatial relationships were investigated by superimposing the hotspot maps with a variety of feature types, including points, lines, and polygons, that reflect the spatial features, and conducting regression analysis with ordinary least squares where applicable. The analysis was also combined with field observations to portray realistic pattern of hotpots over the study area.

3.10 Software and Packages

The research entails digitizing, processing, and analyzing geo-referenced data containing variables and information related to both spatial and non-spatial data. Given the complexity of the current analysis, previous researchers in this field have favored utilizing software tools such as MS Excel, Python, and ESRI's ArcMap to analyze and interpret findings. Taking into account the constraints of statistical software and the appropriateness for this research, MS Excel 2016, Python, and ArcMap 10.8 were employed. Microsoft Excel 2016 was used for illustrating data, creating graphs and conducting statistical evaluations, and GIS for managing geospatial data, mapping, visualization, and analysis. Python, recognized for its adaptability and support for diverse programming paradigms, was applied to convert crash records to csv files.

CHAPTER 4: RESULTS AND DISCUSSIONS

4.1 General

This chapter presents the results of implementing the methodologies proposed in the preceding chapter. The subsequent segments of this chapter are structured as follows: a descriptive examination of the crashes, administrative, and demographic data acquired for the study in Section 4.2; the respective model parameters utilized for each methodology in Section 4.3; the spatial and temporal analysis results in Section 4.4 and Section 4.5 respectively; the list of top ten significant hotspots in Section 4.6, and an on-site evaluation of hotspot locations, specific causes of crashes and the deliberations on the interventions for safety enhancement in Section 4.7.

4.2 Descriptive Analysis of Datasets

The crash data was classified and analyzed in light of various factors such as crash severity, collision types, crash causes, vehicle types, year, season, month, day and hour. This categorization was necessary in order to identify the specific associations of these variables with the lowest and greatest frequency of crashes in the Valley. The classified datasets were statistically analyzed using MS Excel 2016 and ArcMap 10.8 to prepare illustrative graphs, charts, tables and maps for this section. The results from the descriptive analysis have been discussed as follows:

4.2.1 Yearly Distribution

In the yearly distribution of crashes for each severity types as shown in figure 4.1, the peak road traffic crashes (RTCs) occurred in 2019, decreased in 2020 and again hiked in 2021. The deaths, serious injury, minor injury and PDO type crashes also follow the similar trend. The observed reduction in crashes may be due to the nationwide lockdown and vehicle travel restrictions imposed in COVID-19 period from January, 2020 to June, 2020.

The trend of crash severity types corresponds with the assertion made by Dahal (2018), that Kathmandu with high population and traffic experience a greater frequency of

vehicular crashes, albeit with fewer casualties. Another notable point is that in 2020 and 2021, the incidences of minor injuries reported are greater than that of PDO crashes. This stems to the issue of under-reporting, particularly in cases involving minor injuries and property damage, which significantly impacts the accurate assessment of road traffic crashes in Kathmandu Valley. Indeed, there is a need for rigorous efforts to address these reporting gaps and enhance the reliability of RTC data collection and analysis (WHO).

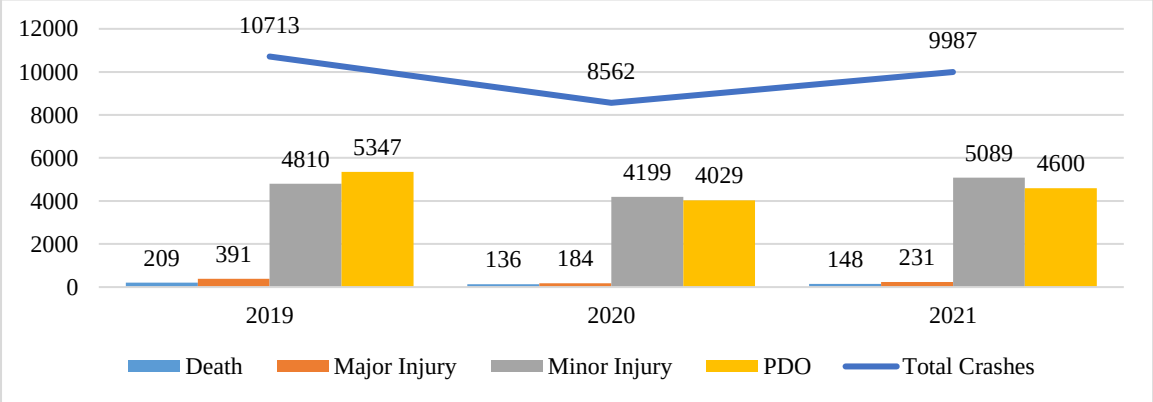

Figure 4.1 Yearly Distribution of Crashes (2019-2021)

Figure 4.1 and 4.2 clearly demonstrate a discernible relationship between RTCs and the resulting casualties as well as injuries as they follow similar trend. This illustrates a decreasing pattern in the death rate as also indicated by the Kuikel et al. (2022). The death rate has decreased to 0.4 per 100,000 population in the year 2021, which is much less than compared to death rate of 0.6 per 100,000 population in the year 2019. In terms of people injuries, 2021 emerges as the year with the most injured individuals, reaching a total of 7713 as shown in figure 4.2, which is 0.2 per 100,000 population. Consequently, an essential focal point for road safety authorities should be the mitigation of crashes specifically in areas where fatal and severe injuries are common.

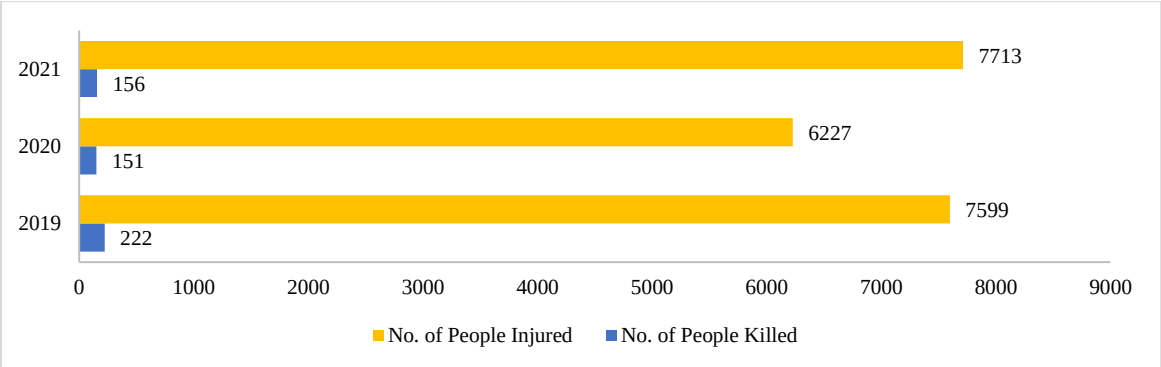

Figure 4.2 Person Involvement in Causalities and Injuries per Year (2019-2021)

4.2.2 Monthly Distribution

Figure 4.3 illustrates that the distribution of crash volumes varies steadily from 4.01 % in May to 12.02% in December. The months of November, December and January can be regarded as black months as these respectively account for 10.26%, 12.02%, and 10.29% of the total crashes. The peaks in these months can be attributed to winter season that is associated with low temperature affecting driver and vehicle performance, and fogs limiting visibility.

As per monthly classification (figure 4.3), a similar trend is observed in the case of minor injuries and PDO crashes, whereas, the trend of death and major injury type crashes is quite uniform throughout the year. The cases of deaths and major injuries are at their peak during the months of October to April, which contrasts with findings of Shrestha, 2014 indicating that the peak occurs in the summer months between April and July.

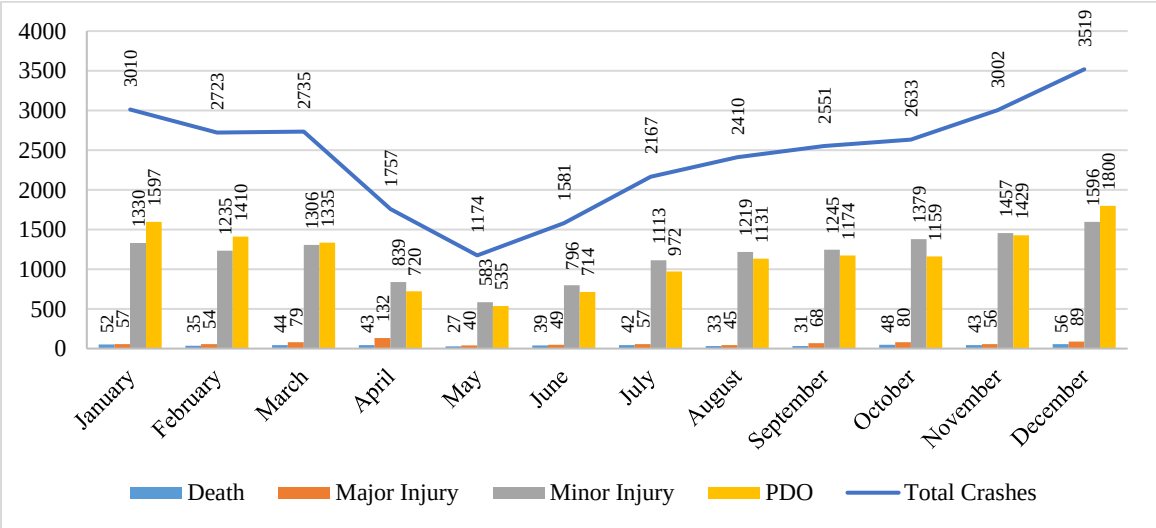

Figure 4.3: Monthly Distribution of Crashes

4.2.3 Daily Distribution

On weekly basis, the trends of total crashes and severity types display a relatively uniform distribution across weekdays (i.e. Sunday to Friday), and witness a sudden decrease on weekend (i.e. Saturday) as depicted by figure 4.4. Most likely, this phenomenon is due to socio-economic activities active during the weekdays, whereas during Saturdays there is reduced travel and less commercial activities in the Valley. Nonetheless, it is observed that crashes resulting in fatalities and serious injuries are

highest on Saturdays, possibly as a consequence of vehicles traveling at greater speeds over the weekend.

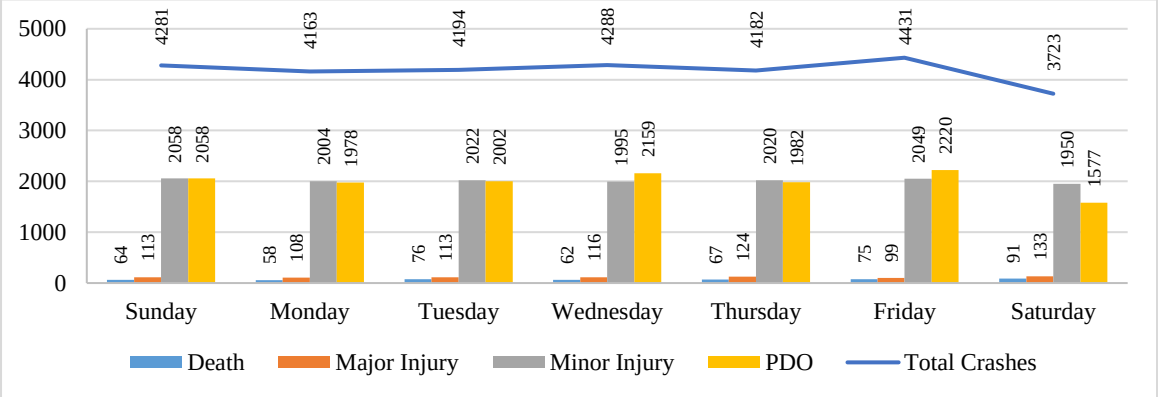

Figure 4.4: Weekly Distribution of Crashes

4.2.4 Hourly Distribution

Figure 4.5 depicts the daily fluctuations in the time of crashes. The findings indicate steady rise from 6:00 am to 12:00 pm, followed by constant frequency till 4:00 pm and subsequent escalation until 8:00 pm. The crashes tend to be more prevalent during the morning time (8:00-12:00), afternoon hour (12:00-16:00) and evening time (16:00-20:00). Approximately 22.14% of all crashes are recorded during morning peak hour, 25.32% suing the afternoon time and 28.96% during the evening time. The trend is probably due to higher travel activities as government offices, private companies, educational institutions, and commercial establishments operate during the day. Similarly, evenings witness increased activity as these facilities close and people head home.

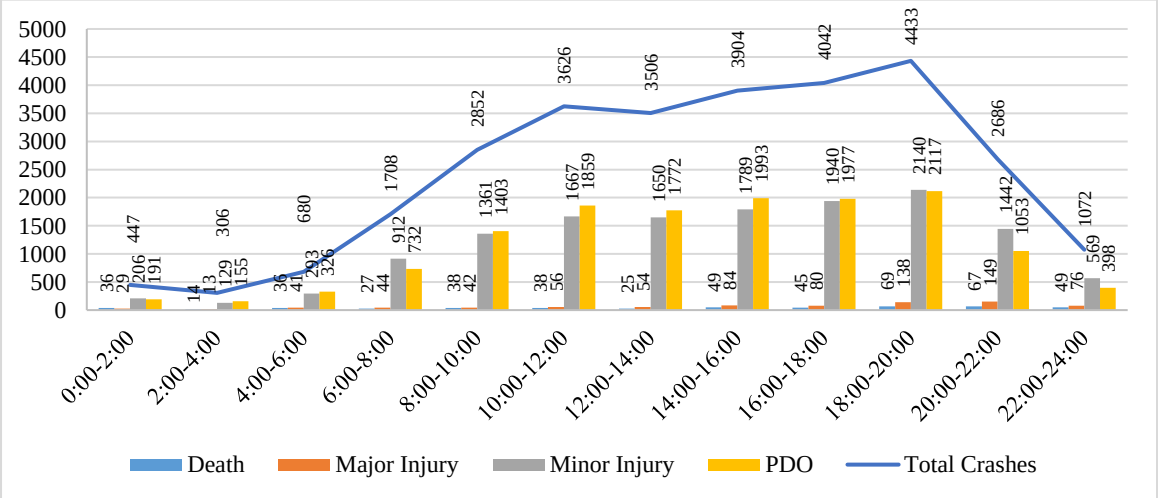

Figure 4.5: Time of Day Distribution of Crashes

In terms of crash severity, the night time between 18:00 and 24:00, is most perilous as opposed to the decreasing trend in total crashes during this time. This trend is predominantly discernible due to high speed, drink and drive, and movement of heavy vehicles.

4.2.5 Collision Types and Severity

Figure 4.6 outlines the incidences of crash severity categorized by the types of collisions. The data shows that the rear end/side and head-on impacts are frequently observed in the Valley with respective total occurrences of 10,774 and 6,000 recorded in three consecutive years. These are trailed by turning collision, hit pedestrian crossing, hit pedestrian, hit object, overturned vehicle, multiple collision, hit parked vehicle, others, crossing collision and hit animal cases with recorded incidences of 1919, 1765, 1753, 1560, 1496, 1350, 1045, 860, 607 and 69 respectively.

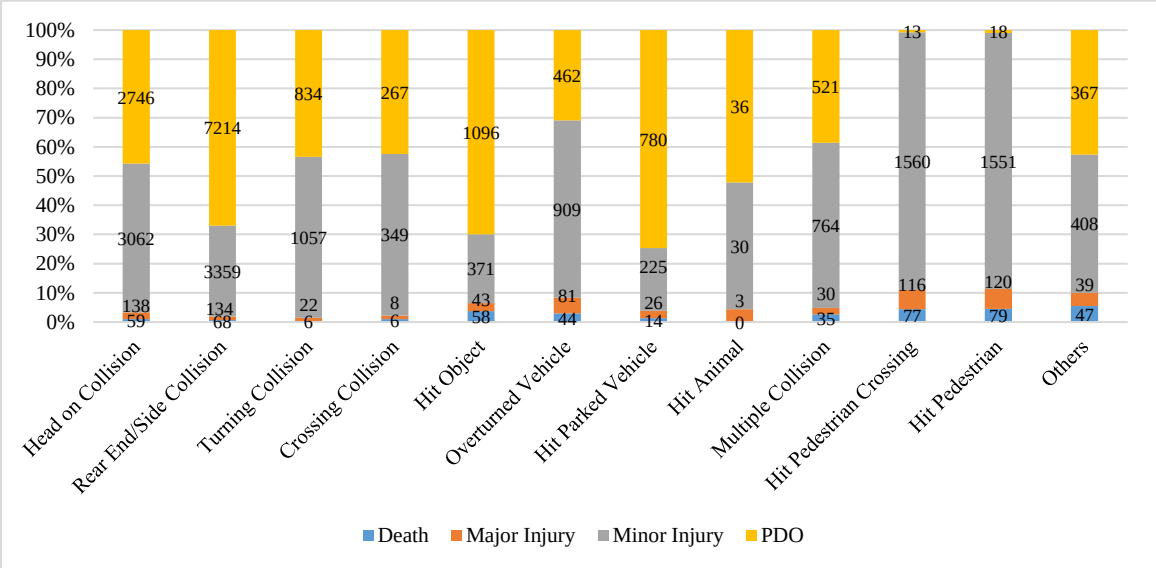

Figure 4.6 Collision Types and Resulting Severity

The hit pedestrian crossing and hit pedestrian type collisions, along with rear end/side collision, head-on collision, hit object and overturned vehicle are the primary contributors of fatalities and major injuries. These collectively represent 78.09% of death crashes and 83.16% of major injuries crashes. The figure 4.6 further indicates that when pedestrians are struck by vehicles while crossing the road or engaging in roadside activities, the impact tends to have a higher death rate at 4.43% compared to overturned vehicle at 3.71% and hit parked vehicle at 2.94% of the total incidents. These predominant types of collisions are followed by the hit object, head on and rear end/side

impact collisions resulting in the death rates of 0.99%, 0.98% and 0.63% respectively. From this, it is clear that pedestrians remain the most at-risk demographic of road users in the Kathmandu valley.

4.2.6 Vehicle Involvement and Severity

When examining the distribution of crash severity across various vehicle types (figure 4.7), it is noted that motorcycle is the dominant category of vehicle involved in crashes, representing 38.7% of crashes. The crashes due to motorcycles account for 6.36% of deaths and 10.90% major injuries. This highlights that motorcyclists are among the vulnerable road users of Kathmandu Valley.

Following the death shares of motorcycle, the crashes involving trucks and buses result fatalities at rate of 3.02%, and 1.31% of total crashes, while, car/jeep/van exhibit low fatality rate at 1.95%, but disproportionately high severe injuries at 4.2% of total crashes.

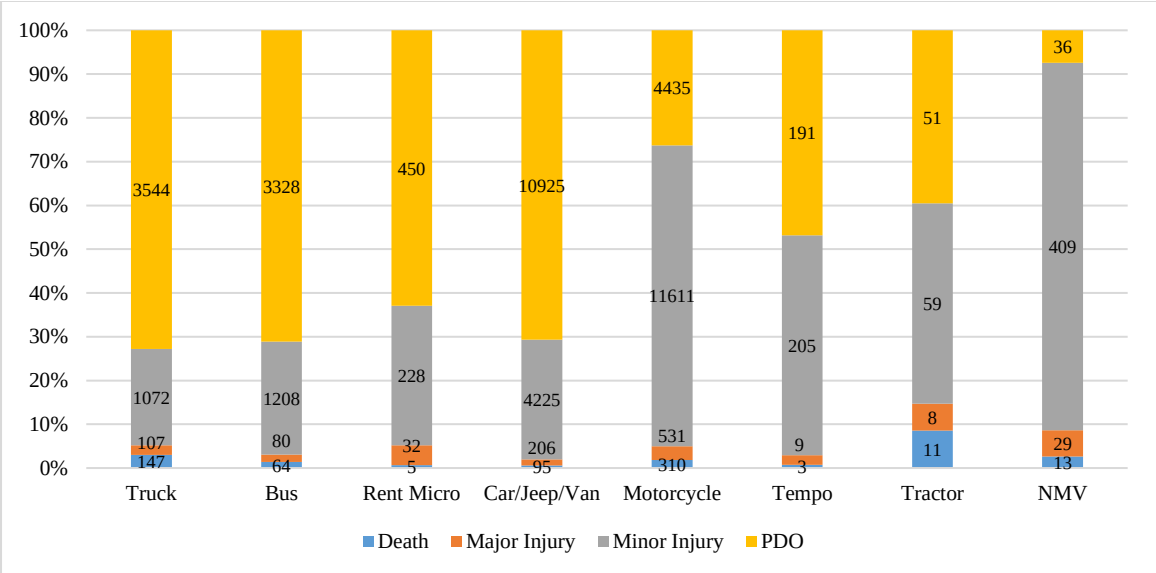

Figure 4.7 Vehicle Involvement and Resulting Severity

4.2.7 Contributory Causes and Severity

According to figure 4.8, a significant proportion (79.13%) of the crashes are caused by driver's carelessness, followed by high speed at 11.52% and driving under alcohol influence at 5.70% of total crashes. However, these factors do not emerge as primary reasons for fatalities, contributing to only 1.35%, 3.00%, and 2.10% of deaths. In contrast, lane violation, road conditions, vehicle defects, and overtaking play a minor

role in crashes, with shares of 0.08%, 0.28%, 0.84%, and 0.94% respectively, but they result in significantly higher fatality rates at 8.33%, 3.66%, 3.24%, and 2.5% respectively.

From these speculations, it is clear that, in order to enhance the general safety measures in the Valley, the government must lay emphasis on the education of drivers, implementation of speed restrictions, enforcement of penalties on offenders (drink & drive, lane violation, high speed etc.), and maintenance of the quality of roads.

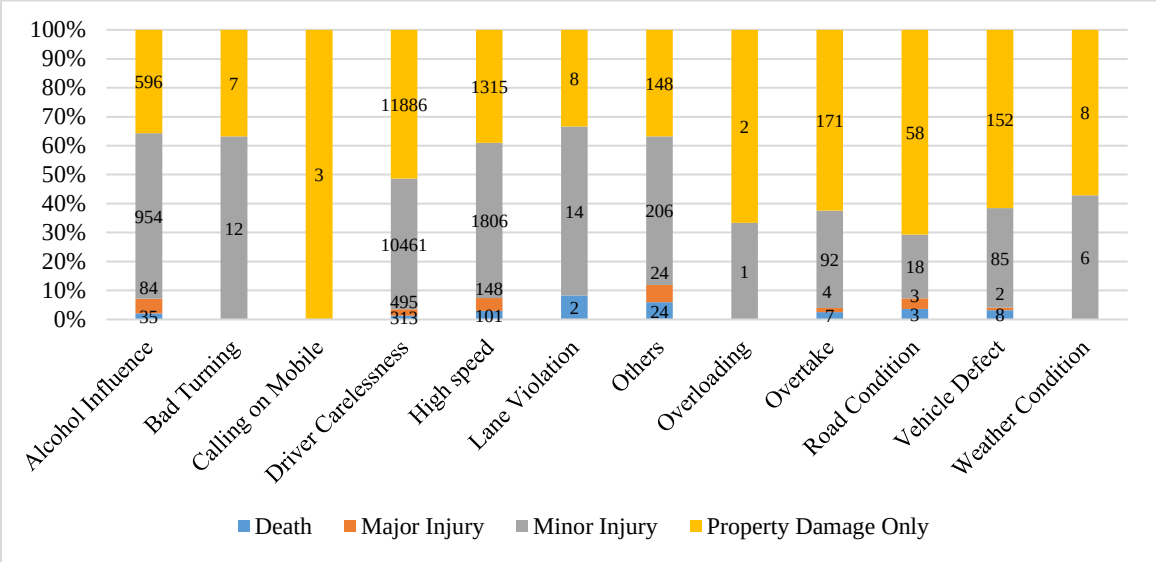

Figure 4.8 Causes and Resulting Severity

4.2.8 Regional Distribution

The population density pattern of the Valley exhibits a significant concentration towards central area encircled by the Ring Road. The local administrative units, namely Kathmandu Metropolitan City, Tokha Municipality, Kritipur Municipality, Madhyapur Thimi Municipality, Bhaktapur Municipality, and Lalitpur Metropolitan City, represent the most densely populated areas, each exceeding a density threshold of 5500 individuals per square kilometer. These regions are distinguished by elevated levels of socio-economic engagement, extensive road infrastructure, and extreme traffic flow.

Figure 4.9 reveals that the Kathmandu Metropolitan City alone observed crashes in excess of 13,000 numbers within the specified timeframe (2019-2021). Adjacent to this area, the Lalitpur Metropolitan City to the south, and Madhyapur Thimi Municipality and Bhaktapur Municipality to the east, were also registered with substantial vehicular crashes in excess of 3800, 1300 and 1100 counts respectively along their principal

highways and feeder routes. In contrast, the Chandragiri, Nagarjun and Suryabinayak municipalities, despite their lower population density and level of urban development, experienced a notable frequency of RTCs i.e. over 1600, 1500 and 1100 respectively. These less urbanized areas are intersected by heavily trafficked highways, which are known for difficult alignment and high-speed vehicular movement.

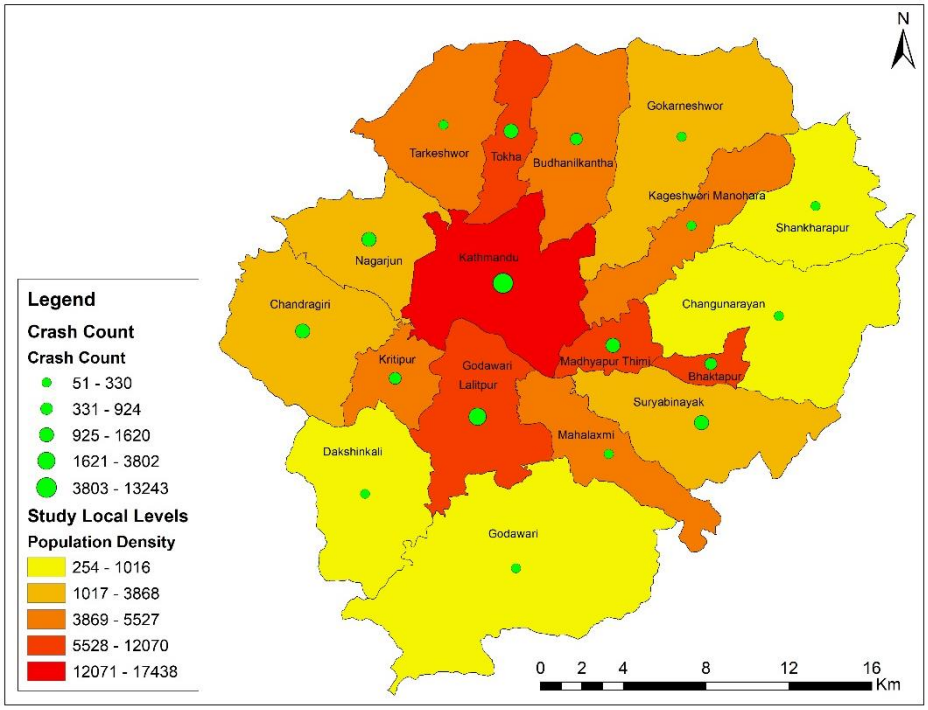

Figure 4.9: Population Density vs. Crash Frequency Distribution

4.3 Model Parameters

The parameters utilized in the estimation of spatial models viz. Global Moran's I, Getis-Ord Gi*, and Kernel Density Estimation (KDE) are presented separately in this section. The parameter fixation is based on the assumption that the entire crash dataset and its subsets are randomly distributed. Owing to the nature of the data, the parameters were decided through an iterative process of trial and error to align optimally with the study objectives.

4.3.1 Global Moran's I Index

The Global Moran's I index is computed for various classifications of RTC datasets, including the total number, severity, collision type, and temporal factors such as year, season, day, and time. This calculation aims to identify the maximum distance over

which significant clustering within the crash data is evident. To begin, an average distance to at least 2 number of nearest neighbors is arrived at by using the Calculate Distance Band from Neighbor Count Tool, unlike for death crash dataset only 1 neighbor was considered. The average distance ranged from 39 m to 540 m depending upon the dataset as given in table 4.1.

Table 4.1 Dataset wise Average Distance Calculation

Variables	Dataset Category	No. of Crashes	Average Distance (m)
Aggregate	Total	23,300	39
Severity Level	Death	385	280
	Major Injury	611	70
	Minor Injury	10,920	70
	Property Damage Only (PDO)	11,384	60
Collision Type	Head On Collision	4,634	143
	Rear End/Side Collision	8,928	65
	Crossing Collision	574	286
	Turning Collision	1,600	174
	Overturned Vehicle	1,126	415
	Hit Parked Vehicle	738	393
	Hit Pedestrian Crossing	1,499	250
	Hit Pedestrian	1,324	334
	Hit Object	1,128	370
	Multiple Collision	1,085	310
	Others	664	540
Year	2019	8514	79
	2020	6652	92
	2021	8134	86
Season	Pre-Monsoon (February 15 – June 30)	7,009	95
	Monsoon (June 15 – September 30)	6,382	101
	Post-Monsoon (September 15 – December 31)	8,422	80
	Winter (December 15 – February 28)	5,949	107
Day of Week	Weekdays (Sunday-Friday)	20,341	44
	Weekend (Saturday)	2,959	180
Time of Day	Late Night (0 AM to 4 AM)	608	470
	Early Morning (4 AM to 8 AM)	1,917	231
	Morning (8 AM to 12 PM)	5,090	124
	Afternoon (12 PM to 4 PM)	5,861	111
	Evening (4 PM to 8 PM)	6,823	97
	Night (8 PM to 0 AM)	3,001	164

This average distance is input for the Incremental Spatial Autocorrelation tool along with fixed distance method applied for the conceptualization of spatial association. In the incremental analysis, a peak distance that yielded the highest z-score was identified.

To determine the most appropriate threshold distance for total crashes, the analysis methodically increased the distance from 250 m to 2500 m in 500 m increments for ICount field input using collect event tool, and the distance from 50 m to 400 m in 50 m increments for the Joint_Count field input using Spatial Join tool, as demonstrated in the results of the incremental spatial autocorrelation test (presented in figure 4.10). The result of incremental spatial autocorrelation for total crashes shows one peak at 1060 m (z-score of 31.28) for collect event input, and single peak at 351 m (z-score of 67.27) for join count input.

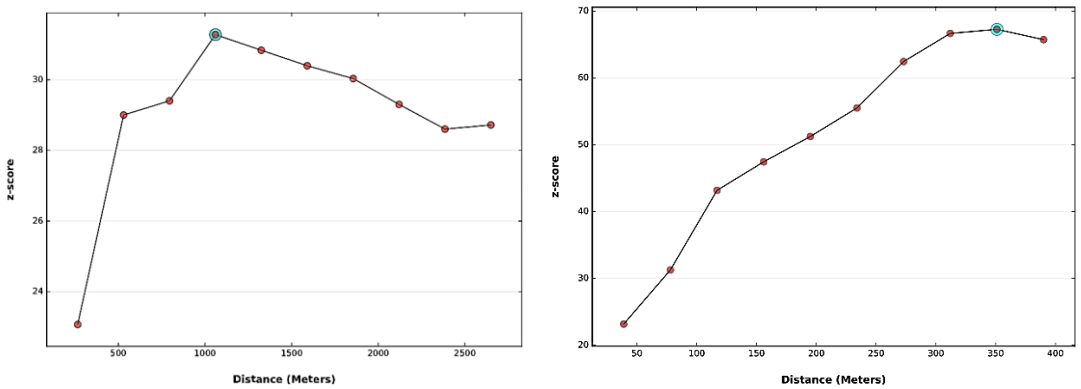

(a) Collect Event as Input **(b) Spatial Join with Road Network as Input**

Figure 4.10 Results of Incremental Spatial Autocorrelation for Aggregate Data

Wang et al. (2022) cautioned that merely inputting the entire crash dataset into the model without considering its classification can lead to the establishment of impractical distance bands. This, in turn, may result in the identification of irrelevant features or a disruption in the continuity of data. So, in this study the incremental spatial autocorrelation was tested for each dataset.

The findings (figure 4.11) indicate that the threshold distance range varies across distinct categories of crash severity. For death crashes, the scale distance range is between 250 m to 3000 m with one peak evident at 560 m for a z-score of 20.63. In contrast, an optimum scalar distance between 50 m and 700 m with existence of at least one peak point is observed for the rest of the classified datasets. The maximum z scores of 22.17, 64.76 and 69.55 are observed at distances of 560m, 350 m and 360 m respectively for major, minor and PDO crashes. The coincidence of peak distances for death and major injury crashes suggests that there is presence of a common spatial pattern across these two datasets.

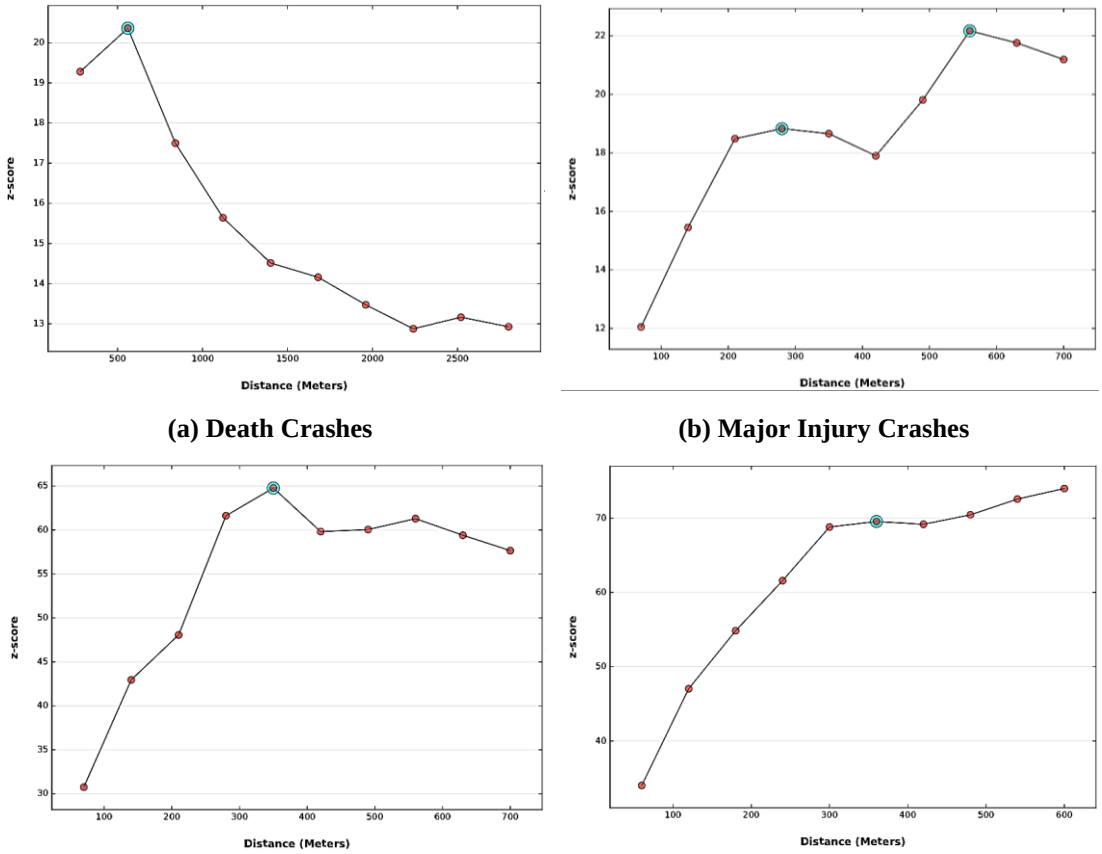

(a) Death Crashes **(b) Major Injury Crashes**

(c) Minor Injury Crashes **(d) PDO Crashes**

Figure 4.11 Results of Incremental Spatial Autocorrelation for Severity Types

According to figure 4.12, the threshold distance range varies across distinct categories of collisions. For head-on collisions, there are two evident peaks at distances of 572 m (with a z-score of 47.76) and 1144 m (with a z-score of 49.11). The rest of the classified datasets have only one peak point at the following distances and maximum z-scores:

- Rear end/side collision: 585 m (z-score of 70.29)
- Crossing collision: 2288 m (z-score of 18.84)
- Turning collision: 348 m (z-score of 43.82)
- Overturned vehicle: 3320 m (z-score of 25.70)
- Hit parked vehicle: 588 m (z-score of 23.94)
- Hit pedestrian crossing: 500 m (z-score of 39.63)
- Hit pedestrian: 2672 m (z-score of 25.08)
- Hit object: 1110 m (z-score of 26.49)
- Multiple collision: 1550 m (z-score of 35.90)
- Others: 4320 m (z-score of 15.64)

These distinct peaks imply that spatial processes affecting crashes vary among the collision types.

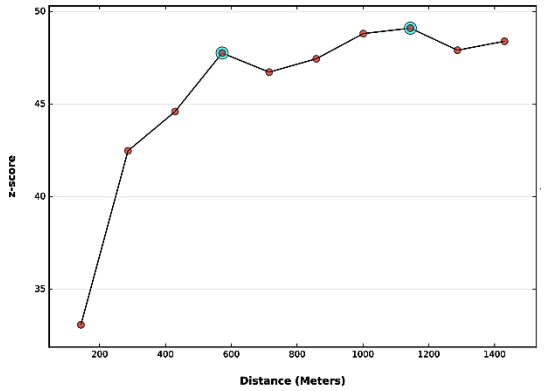

(a) Head-on Collision

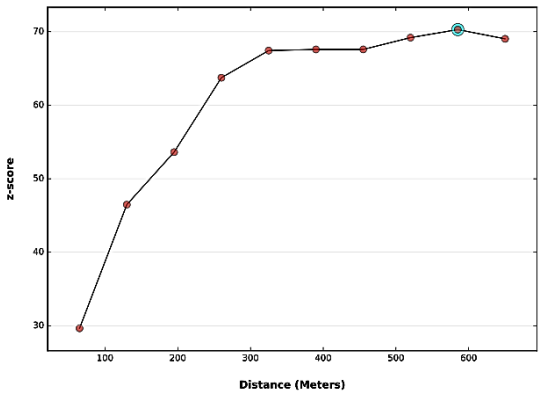

(b) Rear End/Side Collision

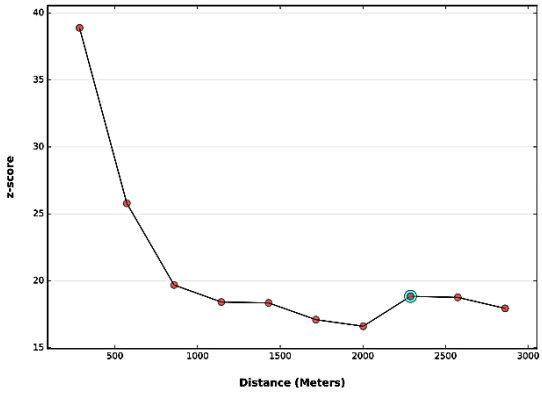

(c) Crossing Collision

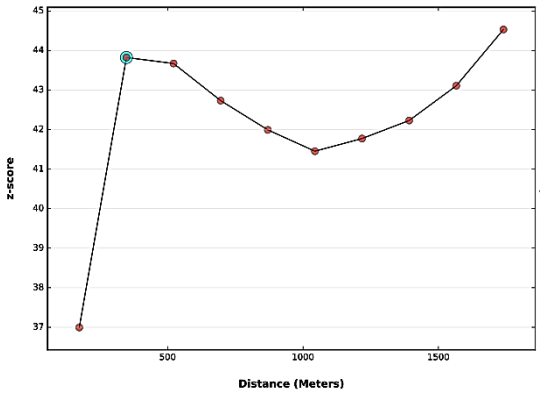

(d) Turning Collision

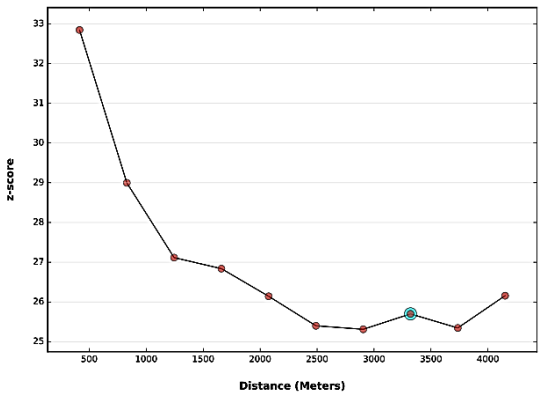

(e) Overturned Vehicle

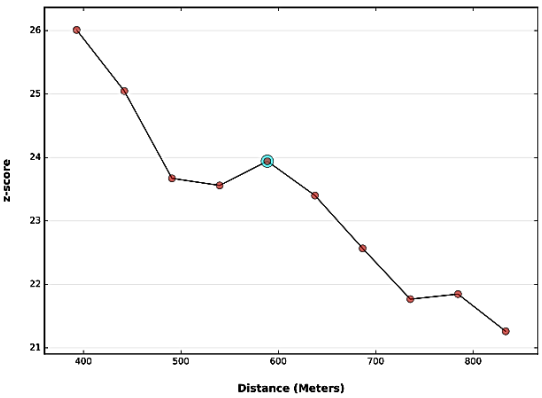

(f) Hit Parked Vehicle

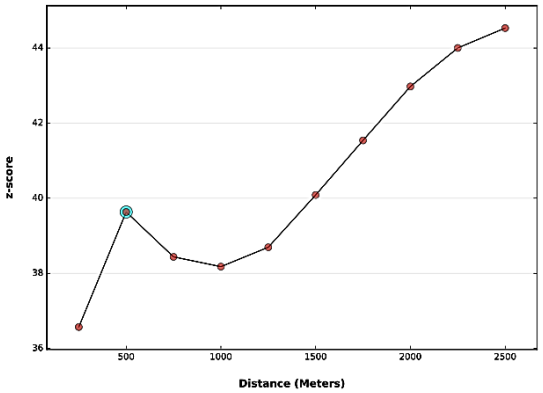

(g) Hit Pedestrian Crossing

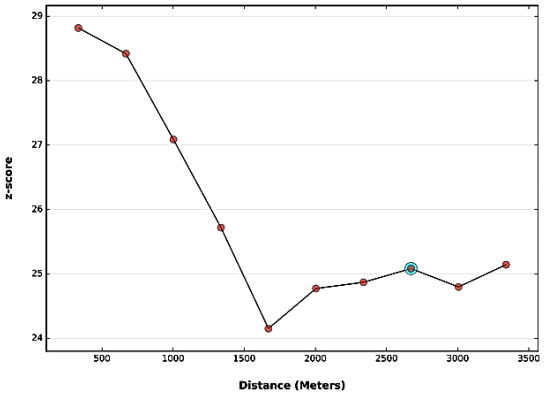

(h) Hit Pedestrian

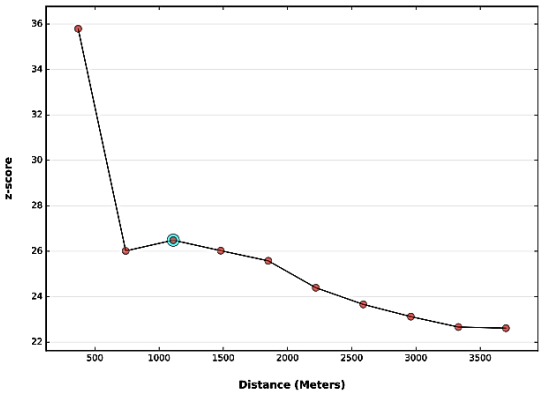

(i) Hit Object

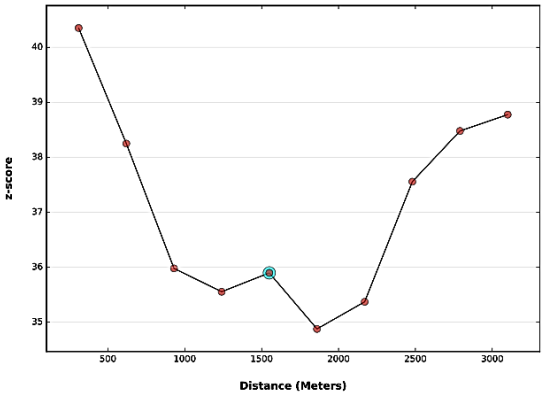

(j) Multiple Collision

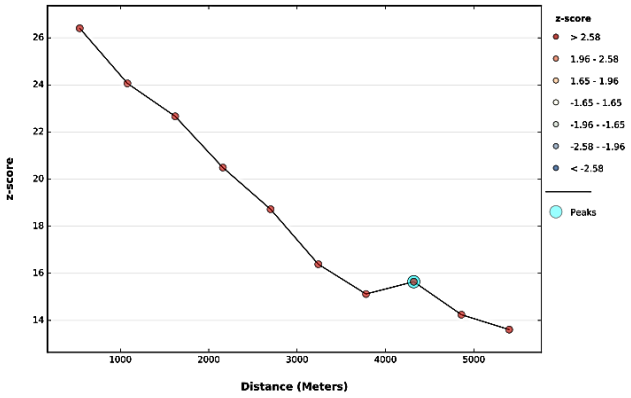

(k) Others

Figure 4.12 Results of Incremental Spatial Autocorrelation for Collision Types

Regarding yearly classification, maximum peaks are observed at distances of 553 m (with a z-score of 71.16), 552 m (with a z-score of 47.40), and 343 m (with a z-score of 60.79) for year 2019, 2020 and 2021 respectively.

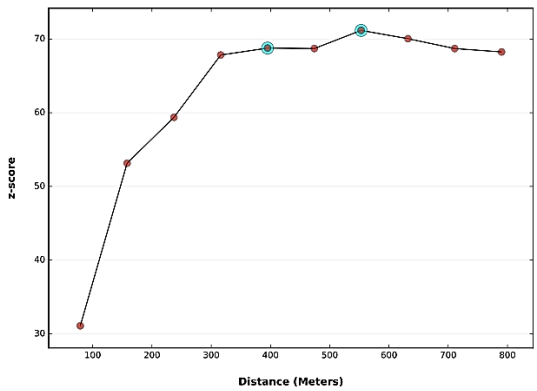

(a) 2019

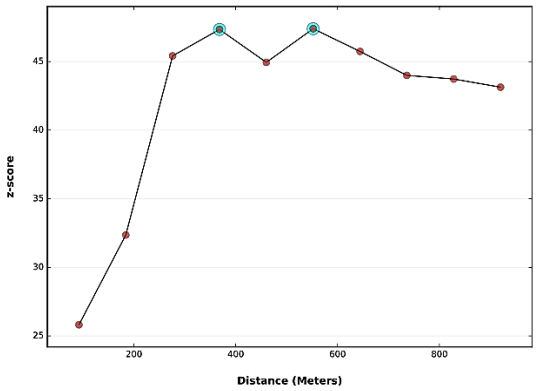

(b) 2020

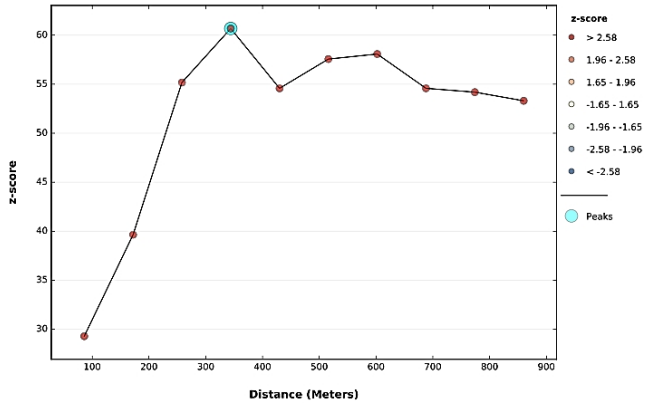

(c) 2021

Figure 4.13 Results of Incremental Spatial Autocorrelation for Years

For four seasons, the spatial incremental results show similar nature of curve as scale distance spans from 100 m to 1000 m. The maximum peak points for pre-monsoon, monsoon, post-monsoon and winter seasons are visible at 570 m, 606 m, 560 m and 321 m for z-scores 59.13, 56.89, 60.01 and 57.45 respectively.

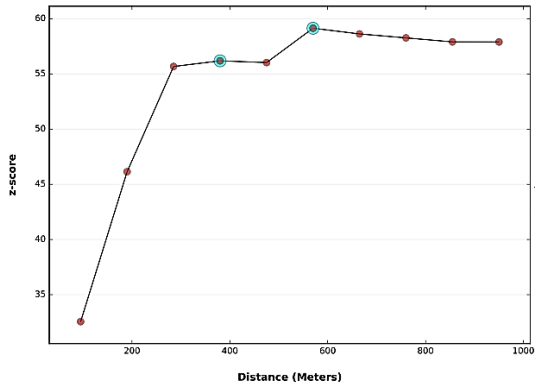

(a) Pre-Monsoon

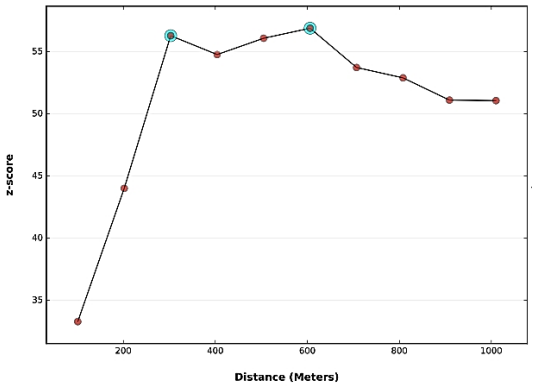

(b) Monsoon

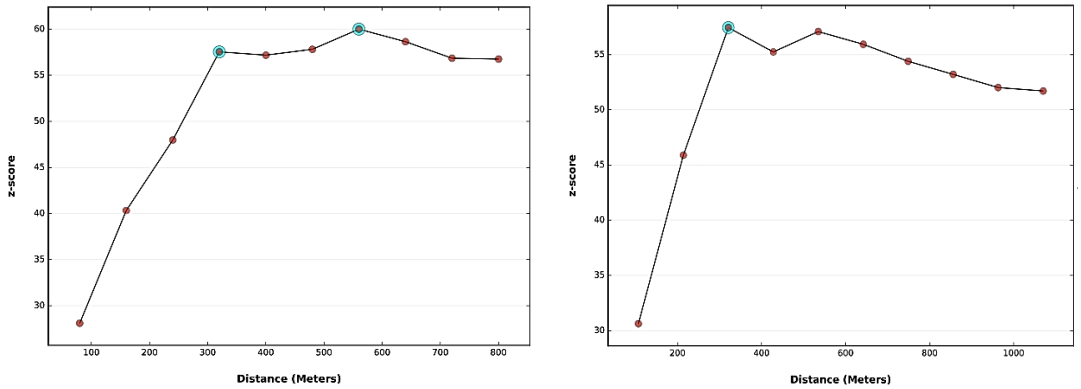

(c) Post-Monsoon **(d) Winter**

Figure 4.14 Results of Incremental Spatial Autocorrelation for Seasons

For weekdays, the z-score peaks around 308 m with value of 66.28 (figure 4.15a), and for weekend, the peak distance is found at distance of 540 m for corresponding z-score of 54.03 (figure 4.15b), indicating the optimal spatial scale for their clustering.

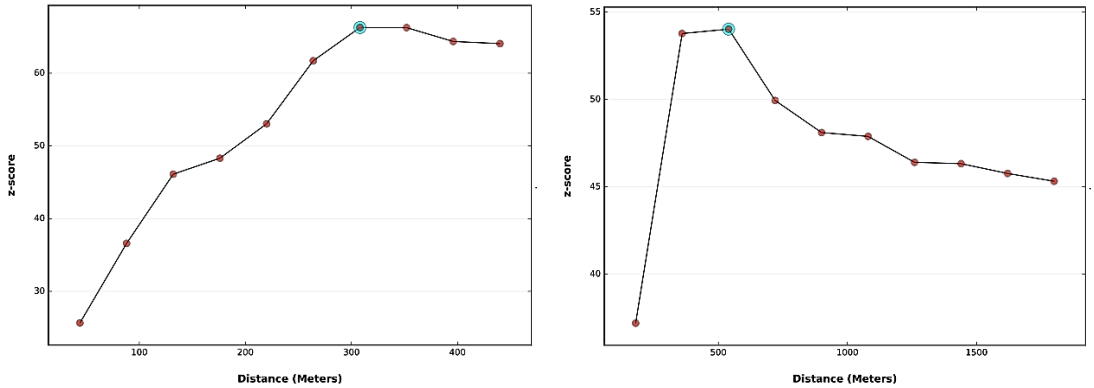

(a) Weekday **(b) Weekend**

Figure 4.15 Results of Incremental Spatial Autocorrelation for Day of Week

For crash data categorized by different time intervals, the peak distance is measured at 1412 m, 462 m, 620m, 335 m, 586 m and 656 m with z-score of 34.31, 42.84, 58.78, 56.94, 63.78 and 55.95 for late night, early morning, morning, afternoon, evening and night crashes respectively, as depicted in figure 4.16. These peak measurements indicate the spatial extent to which crashes are correlated within each time frame.

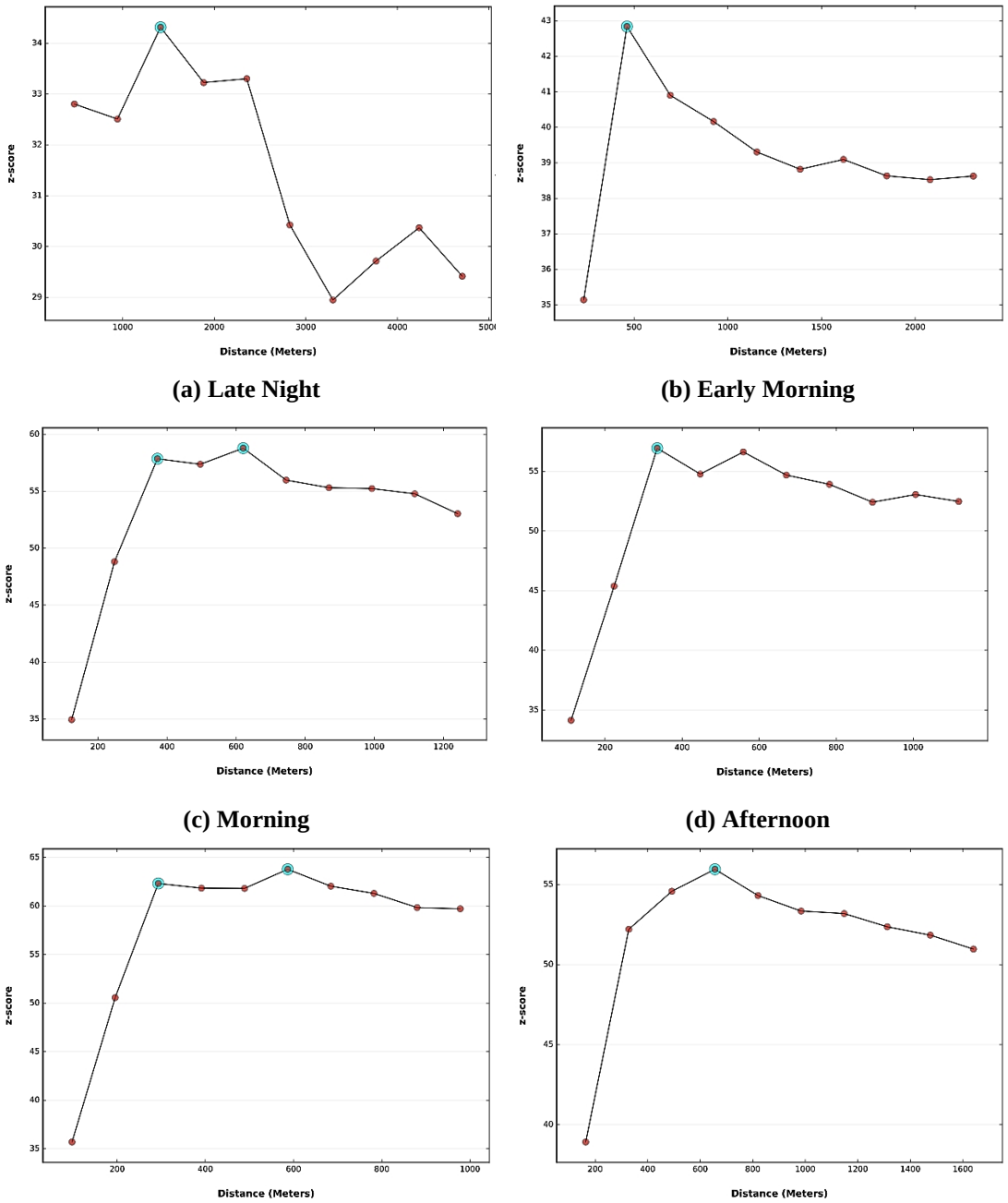

(a) Late Night **(b) Early Morning**

(c) Morning **(d) Afternoon**

(e) Evening **(f) Night**

Figure 4.16 Results of Incremental Spatial Autocorrelation for Time of Crash

For most of the datasets, peak distances led to instances where hotspot features were overestimated as compared to number of crashes that actually occurred, potentially undermining the validity of the associated findings. To address this problem, a reduced threshold distance that matches scale of the analysis was employed in the hotspot analysis rather than the peak distance.

4.3.2 Getis-Ord Gi* Statistics

The threshold distance derived from the Incremental Spatial Autocorrelation Test serves as the foundational input for the Getis-Ord Gi* Statistics tool. For this analysis, two spatial relationship conceptualization methods were employed: the fixed distance band and the inverse distance. Normalization was accomplished via. row standardization, which guarantees that the aggregate of weights assigned to each road segment and its proximate neighbors is unity. Subsequent reductions to the threshold distances and a reiteration of the hotspot analysis were conducted to identify the most effective combination of distance and conceptualization method that resonates with the local context.

A threshold distance of 100 meters was deemed optimal for the fixed distance approach. In contrast, the inverse distance method, whether applied with or without a threshold distance, consistently outperformed the fixed distance approach. The analysis revealed that the inverse distance method, which assigns diminishing weight to increasingly distant locations, produced favorable outcomes in the study. Whereas, the fixed distance approach tended to overestimate hotspot presence, even in segments with minimal crash occurrences. The outcomes of the hotspot analyses, utilizing both the collect event input and spatial join input, indicated comparable spatial crash patterns. However, the hotspot map generated from the spatial join input revealed a greater number of hotspots, aligning more closely with the crash distribution data, thereby justifying its selection for subsequent analysis of the disaggregated datasets. Therefore, only the results of spatial join method using inverse distance approach are presented in this chapter.

4.3.3 KDE Method

A kernel function calculates traffic crash density within a specified bandwidth or search radius, and within proximity to each grid cell, with the cell's density being the product of the crash count and a weight, divided by the area. There are no definitive standards for cell width and bandwidth, so, an experimental approach (hit and trial) was taken to ascertain the ideal bandwidth and cell size for the dataset. It was determined that a bandwidth of 250 m and a cell size of 10 sq. km. provided the best kernel density estimates for the datasets, considering the desired smoothness and clustering extent.

4.4 Spatial Analysis

The spatial analysis was oriented towards finding the patterns in the aggregate crashes, the four levels of crash severity and the 11 types of collision. The spatial analysis also delved into exploring potential correlations with spatial impact factors such as land use, and population density. The results and discussions of the spatial analysis are elaborated below, and the sample output maps are attached to Appendix A (Getis-Ord Gi* Maps) and Appendix B (KDE Maps).

4.4.1 Aggregate Crashes

The spatial autocorrelation analysis (figure 4.17) indicates a significant clustering of high-value crashes as evidenced by a Moran's Index of 0.11, a z-score of 8.29, and a p-value of 0.00 at a 99% confidence interval for join count case. These results suggest the rejection of the null hypothesis and that the observed pattern is not due to random chance.

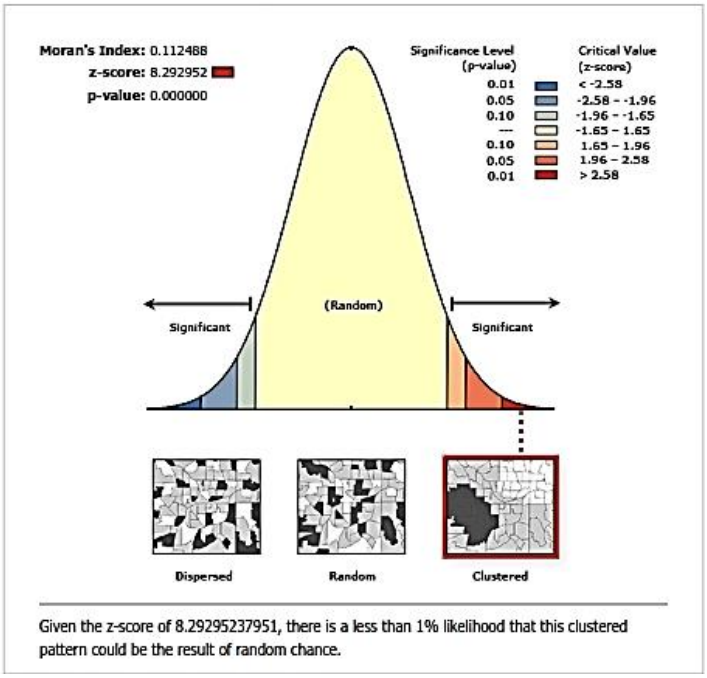

Figure 4.17 Spatial Autocorrelation Report for Aggregate Data

The Getis-Ord Gi* statistics was applied to identify road sections that are significantly more hazardous than adjacent features. The GiZ-score ranged from -0.60 to 19.76 and GiP value ranged from 0 to 0.999976. The statistics has categorized the spatial units into seven distinct classifications. These include spatial hotspots with a 99% confidence

interval (+3 bins), 95% confidence interval (+2 bins), and 90% confidence interval (+1 bins), spatial units of no significant pattern (0 bins) and spatial coldspots with a 99% confidence interval (-3 bins), a 95% confidence interval (-2 bins), and 90% confidence interval (-1 bins). There were 302 segments with +3 bins, 89 segments with +2 bins and 95 segments with +1 bins.

The hotspot analysis further reveals that 23,300 collisions took place across 4,188 distinct segments, with multiple incidents occurring at 2,398 locations. While 1,790 segments experienced a single collision, one segment is reported with as many as 134 crash incidents. Among these, the thesis prioritizes 302 spatial hotspots at the 99% confidence level for further examination. The details of the high significant hotspots at 99% confidence in terms of road links are shown in table 4.2.

Table 4.2 Significant Hotspot Links at 99% Confidence

S.N.	Link Name	Crash Count	Locations	Length	Hotspot (%)
1	Manohara-Sallaghari-Hanumante Culvert	1375	28	6152.73	0.09
2	Thapathali-Tikabhairab (KVRR)	1012	19	3849.52	0.06
3	Nagdhunga-Kalanki (Ring road)	826	19	2522.73	0.06
4	Maitighar-Tinkune	664	15	1744.94	0.05
5	Koteshwar-Manohara bridge	558	9	920.64	0.03
6	Tinkune - Sinamangal - Gaushala (KTM Ringroad)	537	18	1985.83	0.06
7	Maharajganj - Balaju Bypass Junction (KTM Ringroad)	500	14	1706.40	0.05
8	Kalanki - Balkhu (KTM Ringroad)	476	12	1062.96	0.04
9	Chabahil - Sankhapark (KTM Ringroad)	394	12	1420.97	0.04
10	Manohara River - Koteshwor (H03) KTM Ringroad)	357	11	855.17	0.04
11	Tripureshwar-Ring road	354	11	1638.10	0.04
12	Satdobato- Gwarko (KTM Ringroad)	330	8	823.39	0.03
13	Ekantakuna- Kusanti - Satdobato (KTMRingroad)	318	10	1051.01	0.03
14	Ring road-Balaju Bypass	268	4	666.76	0.01
15	Kalanki (Ring road)-Tripureswor	241	8	883.78	0.03
16	Swoyambhu - Kalanki (KTM Ringroad)	240	9	1013.00	0.03
17	Balkhu - Ekantakuna (KTMRingroad)	221	6	674.71	0.02
18	Tinkune-Koteshwar	185	5	407.36	0.02
19	Peepalmod-Nagdhunga	184	5	1586.15	0.02
20	Jadibuti (ARM)-Sinamangal	153	4	741.12	0.01
21	Balaju Junction - Banasthali - Swoyambhu (KTM Ringroad)	149	5	372.76	0.02
22	Lainchaur-Maharajgunj	143	6	824.37	0.02
23	Nakhudobato-Nakhu Chowk	125	3	693.41	0.01

S.N.	Link Name	Crash Count	Locations	Length	Hotspot (%)
24	Sankhapark - Maharajganj (KTM Ringroad)	125	5	502.82	0.02
25	Balkhu-Kuleswor-Kalimati	121	4	486.48	0.01
26	Gwarko-Manohara River(Balkumari)(KTMRingroad)	118	5	440.55	0.02
27	Narayanhiti palace southgate- Durbarmarg-Ghantaghar-Bhadrakali	106	4	693.19	0.01
28	Hanumante Culvert-Sanga	104	4	589.78	0.01
29	Mitrapark - Chabahil (KTM Ringroad)	97	3	181.08	0.01
30	Jayanepal-Thapathali(KVRR)	91	3	408.16	0.01
31	Thapathali-Tripureswor	72	3	421.68	0.01
32	Satdobato-Karmanas bridge	71	2	579.62	0.01
33	Kalopul-Nagpokhari-Kesharmahal-Tridevimarg (Sanchayakosh)	68	3	333.75	0.01
34	Chabahil (Ktm Ring road)-Pipalbot	63	2	158.54	0.01
35	Satdobato-Jawalakhel	61	2	572.01	0.01
36	Balkhu-Chovar	54	2	298.37	0.01
37	Gaushala - Mitrapark (KTM Ringroad)	52	2	173.50	0.01
38	Jawlakhel-St.Mary's West	52	1	262.58	0.00
39	Purano Baneswor-Naya Baneswor (BICC)	45	2	281.76	0.01
40	Gwarko-Lubhu-Lankuri Bhanjyang	31	1	283.66	0.00
41	Golphutar-Pipalbot-Sankhapark	29	1	177.24	0.00
42	Shantinagar - Bhimsengola	28	1	191.45	0.00
43	Bijulibazar-Anamnagar	27	1	224.46	0.00
44	Chardobato-Balkot	27	1	105.56	0.00
45	Jadibuti-Narephant	26	1	193.17	0.00
46	Satdobato (Ring Road)-Dhapakhel - Thecho(KVRR)	24	1	255.34	0.00
47	Sundhara-Singhadarbar (Prithivi path)	24	1	231.50	0.00
48	Samakhushi Chok-Tokhagaun-Chandeshwarigaun(KVRR)	22	1	206.59	0.00
49	New Buspark Road (Inside)	21	1	301.63	0.00
50	Satdobato-Sunakothi	21	1	82.83	0.00
51	Bansbari-Budhanilkantha	20	1	116.45	0.00
52	New Buspark- Mahepi	20	1	124.85	0.00
53	Pipal Bot-Sankhu	20	1	81.07	0.00
54	Darbarmarg-Jamal	19	1	138.12	0.00
55	Tinkune north	19	1	115.41	0.00
56	Maharajgunj-Bansbari	18	1	69.41	0.00

As shown in Getis-Ord Gi* map (figure 4.18), the prevalence of red segment is readily apparent, whereas the orange and yellow segments are less conspicuous. This observation suggests that the spatial hotspots established with 99% confidence ($p < 0.01$) cover a substantial portion of the spatial units with statistical significance, even

though the not significant cases (grey segments) is dominant in the overall spatial network.

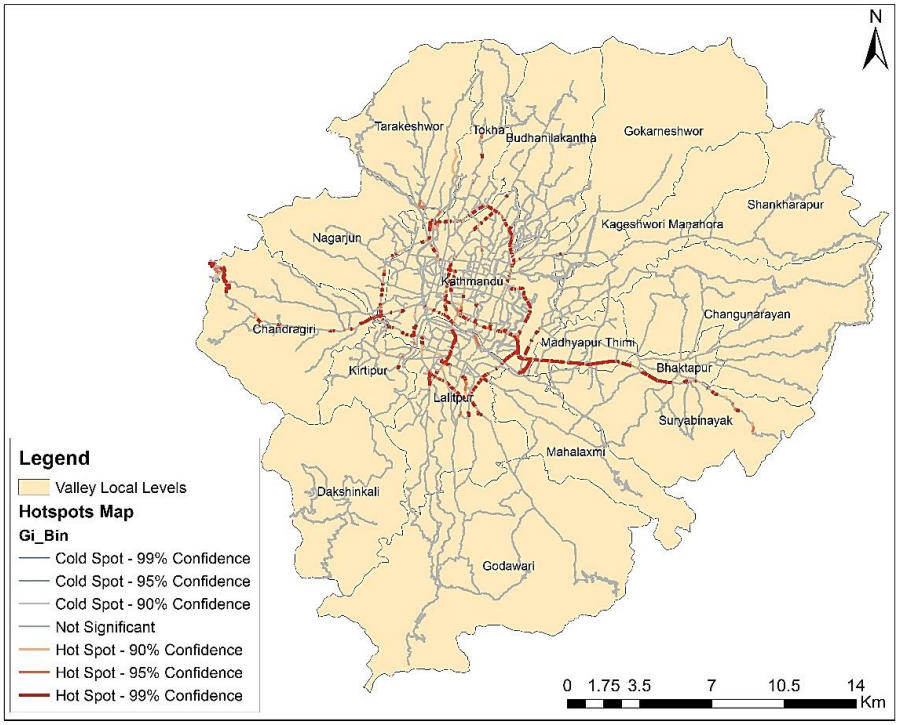

Figure 4.18 Results of Hotspots Analysis for Aggregate Crashes

The above map illustrates a significant concentration of high value crash clusters around the Ring Road, Araniko Highway, Tribhuwan Highway and central core areas of the Valley. The hotspots are more persistent where there is presence of intersections, curves, bridge approaches, access roads, median barrier openings, entrances from side road (or outer divider openings), bus stops, roadside objects, pedestrian crossings, fuel stations and other features. This cluster is closely linked with traffic volume, pedestrian volume, population density, residential developments and commercial/institutional activities (hospitals, schools, shopping complex, markets etc.). Additionally, the slope extremity and sharp bends may contribute to the higher RTC frequency observed in the eastern Araniko Highway and western Tribhuwan Highway. Supplementary maps to clear such judgments for the hotspots are provided in Appendix A.

Another method using KDE visualization also illustrates the spatial distribution of hotspots. In figure 4.19, the results of the estimated kernel density are displayed in color gradient symbolizing the intensity of hot spots, ranging from 778 points/sq.km to 5436 points/sq.km. White color denotes absence of hot spots, yellow indicate mild concentration, and finally red color represents significant concentrations of hotspots.

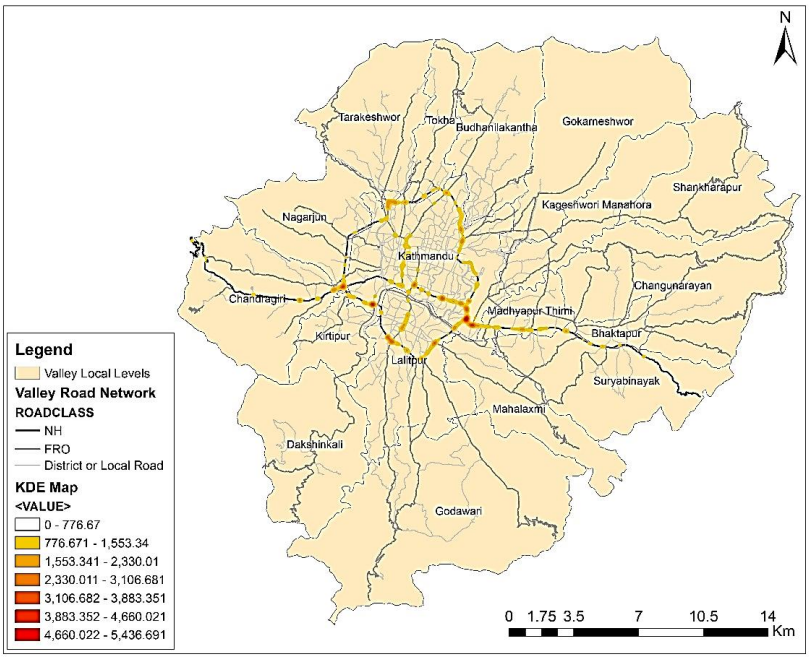

Figure 4.19 Results of KDE Analysis for Aggregate Crashes

Based on the visual interpretation of figure 4.19, the prevalence of hotspots is higher on the Ring Road compared to other highways. On the Ring Road, hotspots were observed in Koteshwor, Tinkune, Chabahil, Sukedhara, Narayan Gopal Chowk, Samkhusi, New Buspark, Kalanki, Balkhu, Nakhu Dobato, Ekantakuna, Satdobato and Gwarko areas, especially at intersections.

By overlaying the maps created from Getis-Ord Gi* and KDE methods, it is evident that similar hotspots are identified by these approaches. Though KDE visualization technique effectively detected spatial hotspots, it is essential to acknowledge that this visual representation is subjective as it fails to provide insights into the statistical significance of high or low crash frequencies at various locations. On the other hand, the Getis-Ord Gi* analysis revealed some hotspots along additional urban roads in northern and southern area of the Valley. However, a limitation raised in this Gi* hotspot analysis method due to application of segment lengths as the analytical unit. In cases where a small portion of a segment exhibits a high concentration of crashes, the entire segment is flagged as a hotspot, irrespective of its overall length. Nevertheless, this approach offers the advantage of precisely delineating the significant hotspot segments for subsequent investigative purposes.

Thus, in the study, the collective potency of both methodologies is used to identify the consistent hotspots. Only the hotspots which were observed to be present in both maps,

are taken into consideration for further ranking. Among the 302 segments identified as significant hotspots at 99% confidence level, 275 of them were determined to be actual hotspot segments. The detailed list of hotspot locations is presented in Appendix-C.

4.4.2 Crash Severity Types

All the crash severity type dataset displayed a clustered pattern, as illustrated in figure 4.20, with positive Moran's I value of 0.05, 0.08, 0.19 and 0.24 respectively for death, major injury, minor injury and PDO crashes. The statistical significance of the spatial distribution of the crashes is evident with positive z-values of 15.93, 9.86, 22.87 and 25.61 respectively. Consequently, the null hypothesis can be confidently rejected and it can be concluded that the severity type dataset manifests a discernible clustering tendency rather than a purely random dispersion.

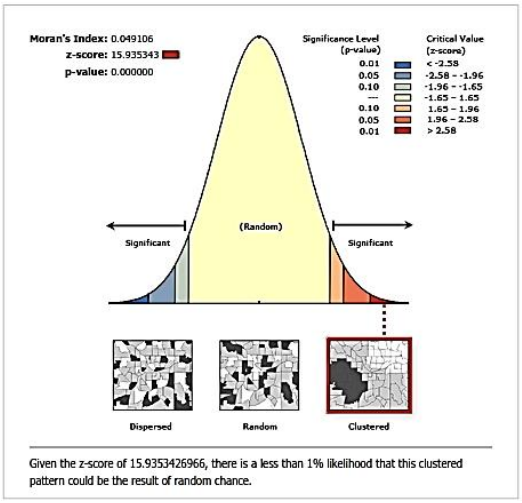

(a) Death

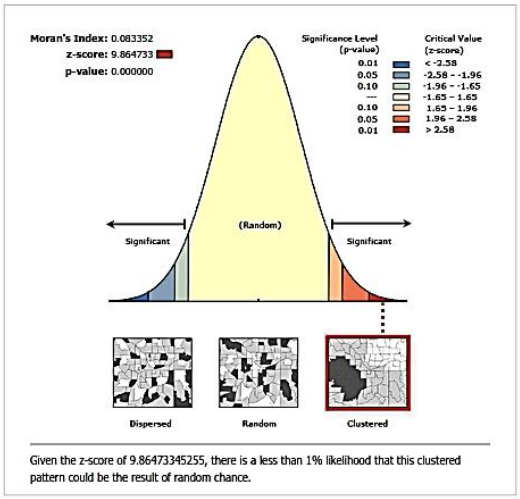

(b) Major Injury

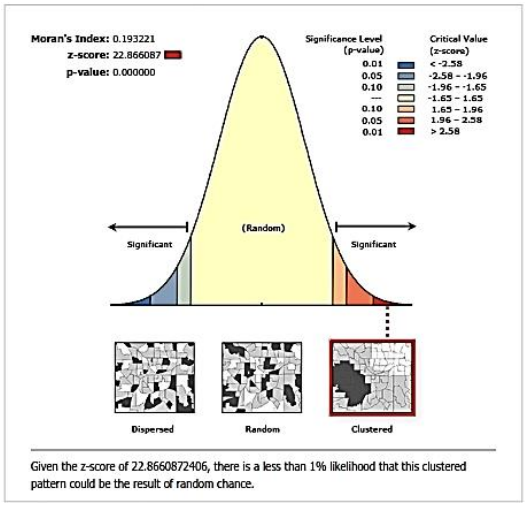

(c) Minor Injury

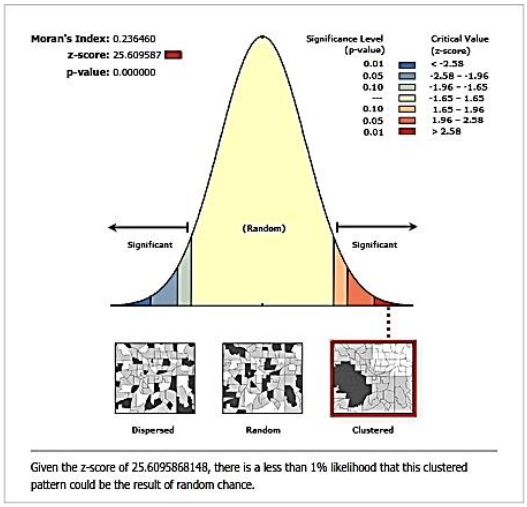

(d) PDO

Figure 4.20 Spatial Autocorrelation Report for Severity Type Dataset

A statistically significant map of clusters across different levels of crash severity was generated through the application of Getis-Ord Gi* statistics as depicted in figure 4.21. The analysis shows a variation of GiZ-score from -0.33 to 23.35 and GiP value from 0 to 0.9998 for death crashes. In case of major injury crashes, GiZ-score varies from -0.40 to 17.71 and GiP value varies from 0 to 0.9961. The crashes with minor injury are distinguished by GiZ-score of -0.596 to 21.17 and GiP value of 0 to 0.99999. Likewise, the crashes with property damage only have GiZ-score in the range of -0.55 to 23.66 and GiP value the range of 0 to 0.99997. The positive GiZ-score and small GiP value indicates statistically significant clustering of high values, while the negative GiZ-score and high GiP values means intense clustering of low values.

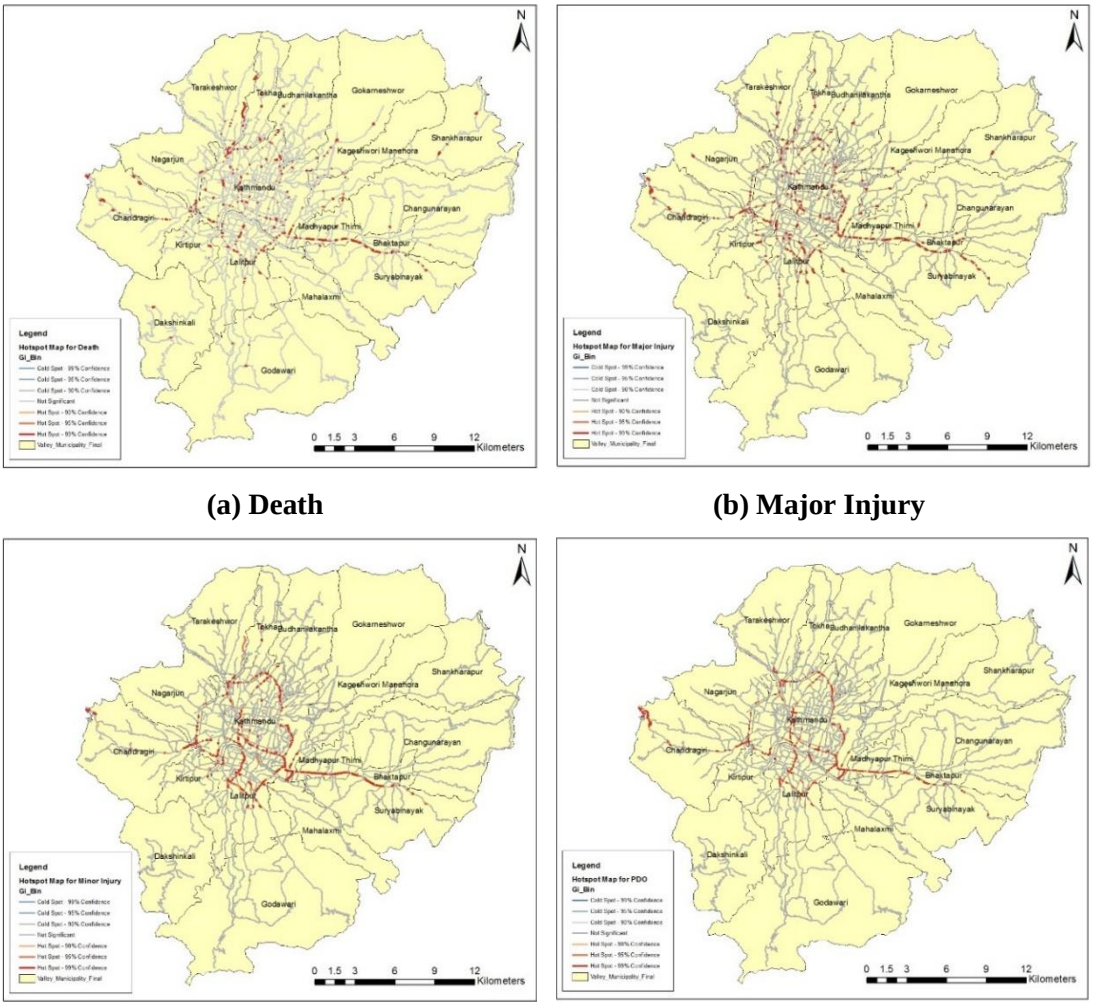

(a) Death **(b) Major Injury**

(c) Minor Injury **(d) PDO**

Figure 4.21 Hotspots Analysis Maps for Crash Severity Types

The clustering tendency of severity-classified crashes closely resembles with the distribution pattern of total crashes (figure 4.18), as they occur on the same roadways. A total of 332 segments were identified as significant hotspots for fatal crashes, 499

segments for major injuries, 311 segments for minor injuries, and 278 segments for PDO crashes at 99% confidence level. Tables 4.3 to 4.6 detail the information of road segments that are most susceptible to different severity level of crashes.

Table 4.3 Significant Hotspot Links for Deaths

S.N.	Link Name	Crash Count	Length (m)	Locations
1	Manohara-Sallaghari-Hanumante Culvert	48	5349.168	30
2	Nagdhunga-Kalanki (Ring road)	18	1372.05	16
3	Kalanki - Balkhu (KTM Ringroad)	17	871.9657	11
4	Ekantakuna- Kusanti - Satdobato (KTMRingroad)	13	704.3727	10
5	Maharajganj - Balaju Bypass Junction (KTM Ringroad)	13	894.0617	9
6	Maitighar-Tinkune	11	659.3687	10
7	Tripureshwar-Ring road	10	1055.485	7
8	Gwarko-Manohara River(Balkumari)(KTMRingroad)	9	509.1296	7
9	Jadibuti (ARM)-Sinamangal	9	741.7782	6
10	Balaju Junction - Banasthali - Swoyambhu (KTM Ringroad)	8	472.4895	6
11	Balkhu - Ekantakuna (KTMRingroad)	8	678.9489	6
12	Bansbari-Budhanilkantha	8	472.1909	6
13	Satdobato- Gwarko (KTM Ringroad)	8	485.9513	6
14	Thapathali-Tikabhairab(KVRR)	8	1233.441	7
15	Tinkune - Sinamangal - Gaushala (KTM Ringroad)	8	360.3259	6
16	Balaju-Nepaltar-Sangla Bazar	6	601.4753	6
17	Hanumante Culvert-Sanga	6	638.2298	6
18	Koteshwar-Manohara bridge	6	320.2318	4
19	Ring road-Balaju Bypass	6	561.421	3
20	Swoyambhu - Kalanki (KTM Ringroad)	6	476.7834	5
21	Jorpati-Sundarijal	5	630.9013	5
22	Karkigaun-Mulpani-Gokarna(KVRR)	5	680.9414	5
23	Manohara River - Koteshwor (H03) KTM Ringroad)	5	352.4205	4
24	Pipal Bot-Sankhu	5	383.5384	4
25	Balkhu-Chovar	4	493.8361	3
26	Chabahil - Sankhapark (KTM Ringroad)	4	643.6229	4
27	Kalanki (Ring road)-Tripureswor	4	261.3143	4
28	Nagdhunga(TRP)-Tankeswor(KVRR)	4	311.974	4
29	Samakhushi Chok-Tokhagaun-Chandeshwarigaun(KVRR)	4	402.1833	3
30	Satdobato-Sunakothi	4	488.0943	4
31	Newbuspark- Baniyatar (Manohar Marg)	4	517.8712	3
32	Gokarna-Jorpati-Gothatar(KVRR)	3	132.1139	3
33	Lainchaur-Maharajgunj	3	155.5959	3
34	Sakhu-Lapsephedi-Bhotechaur	3	745.2857	3
35	Sankhapark - Maharajganj (KTM Ringroad)	3	225.3359	3

S.N.	Link Name	Crash Count	Length (m)	Locations
36	Shantinagar - Bhimsengola	3	284.2455	3
37	Sunakothi-Junction, road to Lele	3	140.5647	3
38	Chuchchepati-Mahankal-Kapan-Dandagaun(KVRR)	2	186.1071	2
39	Gaushala-Purano Baneswor	2	79.74021	2
40	Gaushala-Rato pul-Kamalpokhari-Kamaladi	2	166.9352	2
41	Gwarko-Lubhu-Lankuri Bhanjyang	2	323.137	2
42	Jayanepal-Thapathali(KVRR)	2	238.4845	2
43	Karmanas bridge-Godavari	2	171.5197	2
44	Mitrapark - Chabahil (KTM Ringroad)	2	53.82226	2
45	Narayanhiti palace southgate- Durbarmarg-Ghantaghar-Bhadrakali)	2	194.9502	2
46	Peepalmod-Nagdhunga	2	579.4909	1
47	Pepsicola-Karkigaun(KVRR)	2	274.8001	2
48	Satdobato-Karmanas bridge	2	313.344	1
49	Shital Niwas-Tangal-Dillibazar	2	198.3532	2
50	Sinamangal-Manohara-Thimi-Sallaghari	2	199.2154	2
51	Sundhara-Singhadarbar (Prithivi path)	2	389.7659	2
52	Swoyambhu roads	2	92.5487	2
53	Nakkhu Dobato-Nakkhu Chowk	2	180.2631	1

Table 4.4 Significant Hotspot Links for Major Injuries

S.N.	Link Name	Crash Count	Length (m)	Locations
1	Manohara-Sallaghari-Hanumante Culvert	52	4970.126	25
2	Nagdhunga-Kalanki (Ring road)	36	3062.178	28
3	Maitighar-Tinkune	30	1173.391	16
4	Maharajganj - Balaju Bypass Junction (KTM Ringroad)	22	1195.48	13
5	Kalanki - Balkhu (KTM Ringroad)	20	1150.404	13
6	Tinkune - Sinamangal - Gaushala (KTM Ringroad)	19	1439.508	12
7	Balkhu - Ekantakuna (KTMRingroad)	18	1094.1	13
8	Hanumante Culvert-Sanga	18	1515.024	13
9	Swoyambhu - Kalanki (KTM Ringroad)	16	868.0697	11
10	Ekantakuna- Kusanti - Satdobato (KTMRingroad)	15	1076.708	10
11	Satdobato- Gwarko (KTM Ringroad)	15	828.5574	10
12	Kalanki (Ring road)-Tripureswor	13	769.6834	12
13	Tripureshwar-Ring road	13	920.6686	11
14	Pipal Bot-Sankhu	11	717.5064	10
15	Thapathali-Tikabhairab(KVRR)	11	914.493	8
16	Balaju Junction - Banasthali - Swoyambhu (KTM Ringroad)	10	600.0268	8
17	Balkhu-Chovar	10	659.5667	6
18	Jadibuti (ARM)-Sinamangal	10	854.2417	7
19	Koteshwar-Manohara bridge	10	496.8373	5

S.N.	Link Name	Crash Count	Length (m)	Locations
20	Chabahil (Ktm Ring road)-Pipalbot	8	321.2952	7
21	Lainchaur-Maharajgunj	8	622.355	8
22	Manohara River - Koteshwor (H03) KTM Ringroad)	8	291.3471	4
23	Ring road-Balaju Bypass	8	699.5021	6
24	Pepsicola-Karkigaun(KVRR)	6	462.641	6
25	Balkhu-Kuleswor-Kalimati	5	271.1382	4
26	Jayanepal-Thapathali(KVRR)	5	464.6688	5
27	Samakhushi Chok-Tokhagaun-Chandeshwarigaun(KVRR)	5	395.8856	4
28	Satdobato (Ring Road)-Dhapakhel -Thecho(KVRR)	5	629.3704	3
29	Sinamangal (Ring road) -Dillibazar-Bhotahiti	5	323.3024	5
30	Bansbari-Budhanilkantha	4	318.4863	4
31	Chabahil - Sankhapark (KTM Ringroad)	4	492.838	4
32	Gaushala-Rato pul-Kamalpokhari-Kamaladi	4	286.6179	4
33	Gwarko-Manohara River(Balkumari)(KTMRingroad)	4	197.3379	3
34	Narayanhiti palace southgate- Durbarmarg-Ghantaghar-Bhadrakali)	4	441.7683	3
35	Pulchowk-St. Marys-Thadodhunga_Balkhu (ring road)	4	511.6029	2
36	Sallaghari (Bhaktapur)-Duwakot(KVRR)	4	553.7348	4
37	Sankhapark-Handigaun	4	186.4874	3
38	Satdobato-Jawalakhel	4	859.3226	3
39	Tinkune-Koteshwar	4	334.7763	3
40	Gwarko-Lubhu-Lankuri Bhanjyang	3	561.6491	3
41	Jagati(ARM)-Chyamasingh -Kamalbinayak	3	288.9317	3
42	Mahankal-Atterkhel	3	127.4191	3
43	Satdobato-Karmanas bridge	3	483.0336	2
44	Satdobato-Sunakothi	3	462.1293	2
45	Sundhara-Singhadarbar (Prithivi path)	3	389.7659	2

Table 4.5 Significant Hotspot Links for Minor Injuries

S.N.	Link Name	Crash Count	Length (m)	Locations
1	Manohara-Sallaghari-Hanumante Culvert	795	6412.015	32
2	Maitighar-Tinkune	405	1935.77	20
3	Tinkune - Sinamangal - Gaushala (KTM Ringroad)	272	1922.262	18
4	Thapathali-Tikabhairab(KVRR)	255	2240.909	12
5	Kalanki - Balkhu (KTM Ringroad)	229	944.0443	11
6	Nagdhunga-Kalanki (Ring road)	223	1435.83	13
7	Maharajganj - Balaju Bypass Junction (KTM Ringroad)	217	1708.099	13
8	Satdobato- Gwarko (KTM Ringroad)	217	1092.628	12
9	Manohara River - Koteshwor (H03) KTM Ringroad)	189	686.3091	9

S.N.	Link Name	Crash Count	Length (m)	Locations
10	Chabahil - Sankhapark (KTM Ringroad)	182	1320.331	11
11	Koteshwar-Manohara bridge	180	920.6392	9
12	Ekantakuna- Kusanti - Satdobato (KTMRingroad)	169	1001.849	11
13	Tripureshwar-Ring road	149	1416.375	8
14	Kalanki (Ring road)-Tripureswor	142	1110.479	10
15	Balkhu - Ekantakuna (KTMRingroad)	122	889.8836	8
16	Swoyambhu - Kalanki (KTM Ringroad)	118	1045.958	10
17	Ring road-Balaju Bypass	109	666.7581	4
18	Gwarko-Manohara River(Balkumari)(KTMRingroad)	93	516.6752	6
19	Lainchaur-Maharajgunj	81	860.8838	6
20	Jadibuti (ARM)-Sinamangal	78	741.1221	4
21	Balaju Junction - Banasthali - Swoyambhu (KTM Ringroad)	69	437.6266	5
22	Balkhu-Kuleswor-Kalimati	63	665.1514	5
23	Tinkune-Koteshwar	61	407.3564	5
24	Jayanepal-Thapathali(KVRR)	57	480.3197	4
25	Sankhapark - Maharajganj (KTM Ringroad)	57	589.7143	5
26	Nakhu Dobato-Nakhu Chowk	51	432.9519	2
27	Balkhu-Chovar	49	591.4969	4
28	Hanumante Culvert-Sanga	49	341.9372	4
29	Satdobato-Karmanas bridge	39	579.6191	2
30	Samakhushi Chok-Tokhagaun-Chandeshwarigaun(KVRR)-Jhor	35	559.7301	3
31	Satdobato-Jawalakhel	34	572.0063	2
32	Thapathali-Tripureswor	33	421.6761	3
33	Narayanhiti palace southgate- Durbarmarg-Ghantaghar-Bhadrakali	30	411.2363	2
34	Jawlakhel-Bhanimandal-Nakhu Dobato	29	340.3333	2
35	Peepalmod-Nagdhunga	25	968.3661	2
36	Chardobato (Araniko Highway)-Balkot	25	105.5602	1
37	Kalopul--Nagpokhari-Kesharmahal-Tridevimarg (Sanchayakosh)	22	232.9956	2
38	Chabahil (Ktm Ring road)-Pipalbot	20	76.59107	1
39	Mitrapark - Chabahil (KTM Ringroad)	18	122.8102	2
40	Golphutar-Pipalbot-Sankhapark	17	177.2406	1
41	Gwarko-Lubhu-Lankuri Bhanjyang	16	283.6645	1
42	Purano Baneswor-Naya Baneswor (BICC)	14	224.3445	1
43	Shantinagar - Bhimsengola	14	191.4515	1
44	Bijuli Bazaar-Anamnagar	14	224.4634	1
45	Satdobato (Ring Road)-Dhapakhel -Thecho(KVRR)	13	255.3403	1
46	Sundhara-Singhadarbar (Prithivi path)	13	231.4986	1
47	Satdobato-Sunakothi	12	281.0684	1
48	TU Gate-Kirtipur	12	73.53748	1
49	Jadibuti-Narephant	12	176.4909	1

S.N.	Link Name	Crash Count	Length (m)	Locations
50	Bansbari-Budhanilkantha	11	116.4461	1
51	Roads circumscribing the Sinhadurbar	11	156.5055	1
52	Gaushala - Mitrapark (KTM Ringroad)	10	41.90703	1
53	Shital Niwas-Tangal-Dillibazar	10	139.6562	1
54	Tridevimarg (Sanchayakosh)-Chhetrapati-Sobhabagawati	10	58.89481	1
55	New Buspark-Baniyatar	10	292.7493	1
56	Khahare-Karkigaun	10	96.66514	1
57	Maharajgunj-Bansbari	9	51.55558	1
58	Nagdhunga(TRP)-Tankeswor(KVRR)	9	28.17174	1
59	Chardobato-Purano Thimi	9	80.8482	1
60	Maitighar-Bhadrakali	9	15.20923	1
61	Tinkune north	8	115.4077	1

Table 4.6 Significant Hotspot Links for PDO Crashes

S.N.	Link Name	Crash Count	Length (m)	Locations
1	Nagdhunga-Kalanki (Ring road)	613	2880.077	24
2	Manohara-Sallaghari-Hanumante Culvert	547	5304.165	25
3	Koteshwar-Manohara bridge	381	920.6392	9
4	Thapathali-Tikabhairab(KVRR)	303	1878.862	10
5	Maitighar-Tinkune	287	1127.663	12
6	Manohara River - Koteshwor (H03) KTM Ringroad)	254	795.4138	11
7	Maharajganj - Balaju Bypass Junction (KTM Ringroad)	252	1315.101	12
8	Tinkune - Sinamangal - Gaushala (KTM Ringroad)	240	1478.54	14
9	Chabahil - Sankhapark (KTM Ringroad)	211	1325.362	11
10	Kalanki - Balkhu (KTM Ringroad)	211	856.0024	9
11	Tripureshwar-Ring road	202	1736.604	13
12	Peepalmod-Nagdhunga	186	2377.38	8
13	Ring road-Balaju Bypass	161	691.4366	5
14	Ekantakuna- Kusanti - Satdobato (KTMRingroad)	147	822.0608	9
15	Tinkune-Koteshwar	127	407.3564	5
16	Satdobato- Gwarko (KTM Ringroad)	117	603.3132	5
17	Swoyambhu - Kalanki (KTM Ringroad)	117	879.0449	8
18	Balkhu - Ekantakuna (KTMRingroad)	106	398.668	5
19	Mitrapark - Chabahil (KTM Ringroad)	97	295.0834	5
20	Balaju Junction - Banasthali - Swoyambhu (KTM Ringroad)	81	372.7627	5
21	Kalanki (Ring road)-Tripureswor	79	412.3555	4
22	Balkhu-Kuleswor-Kalimati	72	486.4811	4
23	Jayanepal-Thapathali(KVRR)	71	600.6936	5
24	Nakkhu Dobato-Nakkhu Chowk	67	693.4099	3
25	Sankhapark - Maharajganj (KTM Ringroad)	65	352.8987	4

S.N.	Link Name	Crash Count	Length (m)	Locations
26	Narayanhiti palace southgate- Durbarmarg-Ghantaghar-Bhadrakali	61	693.1858	4
27	Gaushala - Mitrapark (KTM Ringroad)	58	360.2372	4
28	Jadibuti (ARM)-Sinamangal	58	476.708	3
29	Kalopul-Nagpokhari-Kesharmahal-Tridevimarg (Sanchayakosh)	52	489.631	4
30	Hanumante Culvert-Sanga	50	599.0823	3
31	Lainchaur-Maharajgunj	34	355.7221	3
32	Jawlakhel-Bhanimandal	31	262.5781	1
33	Thapathali-Tripureswor	30	337.1298	2
34	Chabahil (Ktm Ring road)-Pipalbot	27	81.94601	1
35	Purano Baneswor-Naya Baneswor (BICC)	23	281.7595	2
36	Balkhu-Chovar	18	93.39242	1
37	Satdobato-Karmanas bridge	18	313.344	1
38	Gwarko-Lubhu-Lankuri Bhanjyang	16	283.6645	1
39	Satdobato-Jawalakhel	16	250.6404	1
40	Tinkune north	15	115.4077	1
41	Jadibuti-Narephant	15	176.4909	1
42	Darbarmarg-Jamal	14	138.1249	1
43	Satdobato-Sunakothi	14	82.8303	1
44	Bijuli Bazaar-Anamnagar	13	224.4634	1
45	Golphutar-Pipalbot-Sankhapark	12	177.2406	1
46	Pipal Bot-Sankhu	12	81.06632	1
47	Shantinagar - Bhimsengola	12	191.4515	1
48	Nepaltar-Jarankhu	12	628.1047	1
49	Gathhaghar (ARM) -Thimi	11	76.67598	1
50	Gwarko-Manohara River(Balkumari)(KTMRingroad)	11	97.4701	1
51	Kopundole-Sankhamul	11	607.6407	1
52	Maharajgunj-Bansbari	11	69.40839	1
53	Nagdhunga(TRP)-Tankeswor (KVRR)	11	28.17174	1
54	Sundhara-Singhadarbar (Prithivi path)	11	231.4986	1

The kernel density ranges from 776.67 points/sq.km to 5,436.69 points/sq.km for total crashes, 13.88 points/sq.km to 97.17 points/sq.km for death, 20.89 points/sq.km to 146.25 points/sq.km for major injury, 248.83 points/sq.km to 1,741.82 points/sq.km for minor injury and 550.15 points/sq.km to 3,851.02 points/sq.km for PDO (figure 4.22). It is important to recognize that hotspots as identified by Getis-Ord Gi* method were also consistently present in KDE maps for all levels of severity. The Getis-Ord Gi* hotspot maps corroborate with the locations of the hotspots as indicated by the KDE analysis.

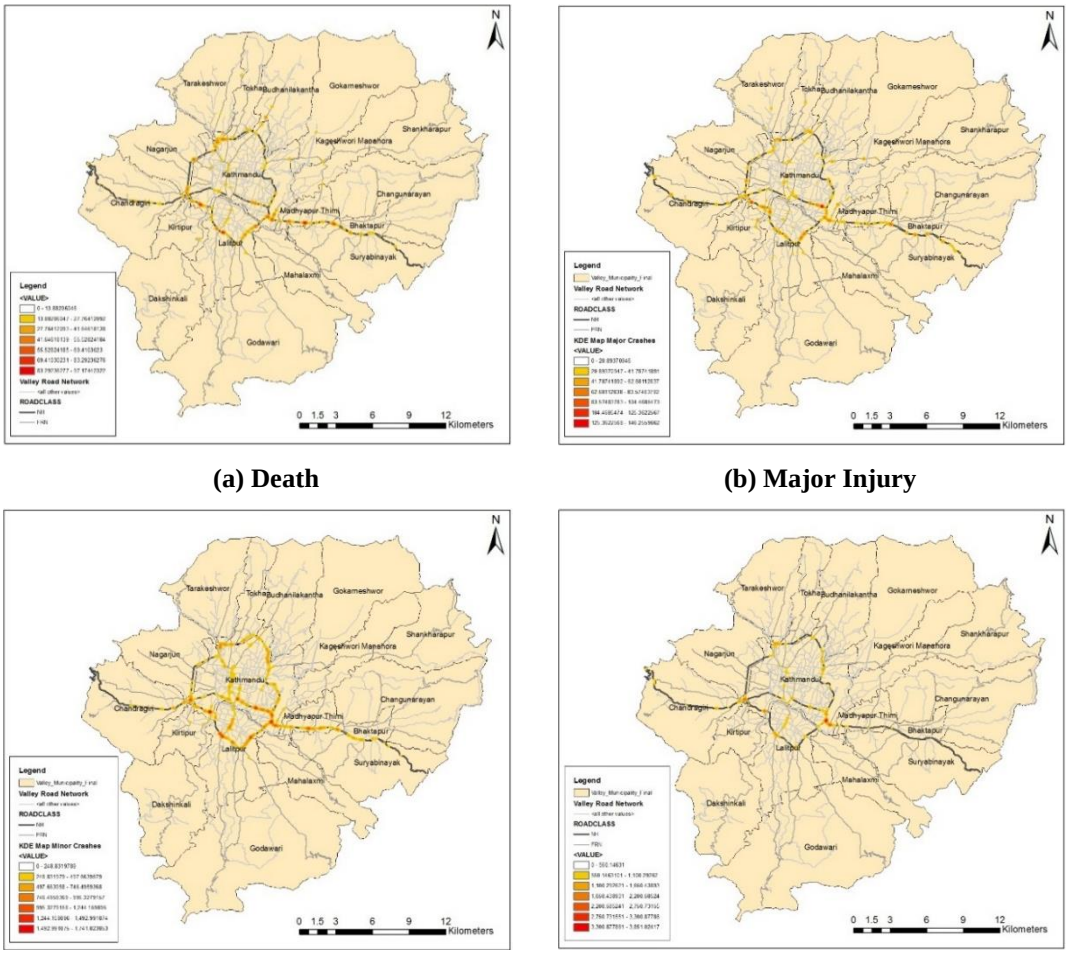

(a) Death **(b) Major Injury**

(c) Minor Injury **(d) PDO**

Figure 4.22 KDE Maps for Crash Severity Types

As per the comparison of the KDE maps, the distinct patterns of hotspots are observed for the severity categories, as detailed below:

i) Death: High-intensity traffic hotspots are located along key routes such as the Ring Road (Koteshwor, Kharibot, Balkumari, Gwarko, B&B Hospital, Bodigram, Chapagaun Dobato, Thasikhel, Kusunti, NakkhuDobato, Harihar Bhawan, Dhobighat, Nayabato, Balkhu, Kalanki, Thulobharyang, Balaju, Machhapokhari, Newbuspark, Samakhusi, Basundhara, Sinamangal, Gairigaun), Araniko Highway (New Baneshwor, Koteshwor, Jadibuti, Kaushaltar, Chardobato, SS Chowk, Radheradhe, Srijananagar, Katunje, Chundevi, Doleshwor Chowk, Adarsha Chowk, Jagate, Nalinchowk), Tribhuwan Highway (Teku, Kalanki, Dhungeadda, Sipradi Trading, Satungal-CG Park), Jadibuti-Pepsicola, Tripureshwor-Balaju (Sundhara, Bhotahiti, Lainchaur) and other major connections. Additionally, these are prevalent in lower intensity along feeder routes and urban roads connecting the core city with other districts, religious

pilgrimages and recreational sites like Bhakatapur Hospital-Byasi, Dekocha-Changunarayan, Sallaghari-Duwakot, Chyamasingh-Nala, Pepsicola-Karigaun, Madhyapur Thimi-Mulpani, Chabahil-Peepalbot-Mulpani-Sankhu, Mahankal-Atterkhel, Jorpati-Sundarijal, Maharajgunj-Bansbari-Budhanilkantha, Samakhusi-Tokha-Jhor, Balaju-Nepaltar-Sanglabazar, Bishnumati corridor, Nepaltar-Jarankhu, Purano Nikap-Dahachowk, Kritipur Ringroad, Balkhu-Dakshinkali, Ekantakuna-Tikabhairab, Satdobato-Sunakoti-Tikabhairab and Satdobato-Pulchowki. Such occurrences of death hotspots in suburban areas may be attributed to challenging road sections, high speeds and distances to nearest trauma centers.

ii) Major Injury: The clusters of major injury crashes overlap with the traffic hotspots mentioned for the death. While the major highways and core network show a heightened intensity and number of hotspots, some feeder and local roads connecting to outer suburban areas, namely Pepsicola-Karkigaun, Maharajgunj-Bansbari-Budhanilkantha, Samakhusi-Tokha-Jhor see reduction in hotspots. In contrast, other feeder and local roads, including Chabahil-Sankhu (Chucchepati, Naryantar Bridge, Grand Norling), Nepaltar-Jarankhu (Jarankhu), Balkhu-Chobhar (TU Gate, Sundarighat), Ekantakuna-Tikabhairab (Sainbu), Satdobato-Sunakoti (Loktantrik Chowk), Bhaktapur-Duwakot (KMC, Duwakot), and Trishuli Highway (Mudkhu, Nepaltar Ward-4 Office) experience an increase in intensity or location.

iii) Minor Injury: The clusters of minor injury hotspots are more continuous on the principal roadways viz. Ring Road, Araniko Highway, Tripureshwor-Balaju (Ring Road), Jaynepal- Thapathali, Thapathali-Ekantakuna, among others. Unlike death and major injury crashes, the hotspots are less evident in suburban roads outside of the Ring Road or that intersecting the Tribhuwan and Araniko Highway.

iv) PDO: The concentration of PDO clusters is considerably lower compared to other severeity level, with clusters present at New Baneshwor, Tinkune, Koteshwor, Jadibuti, Balkumari Bridge, Gwarko, Satdobato, Ekantakuna, Nakkhudobato, Jawlakhel-Hariharbhawan, Balkhu, Kalanki, Dhungedeadda, Naikap, Sipradi trading, Balaju, Macchapokhari, Samakhusi, Maharajgunj, Sukedhara and Chabahil. The limited presence of damage only hotspots may suggest a substantial underreporting of incidents within the Valley.

4.4.3 Collision Types

To examine the spatial patterns within the crash dataset, it was categorized into eleven key groups, including head-on collision, rear end/side collision, crossing collision, turning collision, overturned vehicle, hit parked vehicle, hit pedestrian crossing, hit pedestrian, hit object, multiple collision and others. The spatial autocorrelation test of all the collision type dataset reveals a clear pattern of clustering, as shown in table 4.7. This is supported by positive Moran's I values, large z-scores and small p values, which allows to confidently reject the null hypothesis.

Table 4.7 Spatial Autocorrelation Results for Various Collision

S.N	Dataset	Crashes	Moran's I	Z-score	P value	Pattern
1	Head-on Collision	4634	0.182982	35.718836	0.000000	Clustered
2	Rear End/Side Collision	8928	0.212265	23.803493	0.000000	Clustered
3	Crossing Collision	574	0.119236	42.510970	0.000000	Clustered
4	Turning Collision	1600	0.198015	44.629725	0.000000	Clustered
5	Overturned Vehicle	1126	0.064465	29.003037	0.000000	Clustered
6	Hit Parked Vehicle	738	0.051298	24.814087	0.000000	Clustered
7	Hit Pedestrian Crossing	1499	0.144678	42.717910	0.000000	Clustered
8	Hit Pedestrian	1324	0.076106	28.513250	0.000000	Clustered
9	Hit Object	1128	0.060796	24.949713	0.000000	Clustered
10	Multiple Collision	1085	0.109467	38.441150	0.000000	Clustered
11	Others	664	0.046670	26.450819	0.000000	Clustered

For each collision type, the Getis-Ord Gi* statistics delineated high-priority road segments exhibiting significant crash occurrences at 99% confidence (bin 3), 95% confidence (bin 2) and 90% confidence (bin 1). The details of the GiZ scores, GiP values and number of segments in three bins are described in table 4.8.

Table 4.8 Getis-Ord Gi* Results for Various Collision

S.N	Dataset	GiZ score		GiP value		Hotspots in Bin 3	Hotspots in Bin 2	Hotspots in Bin 1
		Low	High	Low	High			
1	Head-on Collision	-0.635711	24.486544	0	0.998151	309	194	9
2	Rear End/Side Collision	-0.48202	25.902282	0	0.9999854	268	91	51
3	Crossing Collision	-0.217684	68.63501	0	0.999609	103	207	0
4	Turning Collision	-0.42684	34.548436	0	0.999786	321	8	27
5	Overturned Vehicle	-0.465139	30.557957	0	0.999809	200	594	5

S.N	Dataset	GiZ score		GiP value		Hotspots in Bin 3	Hotspots in Bin 2	Hotspots in Bin 1
		Low	High	Low	High			
6	Hit Parked Vehicle	-0.41149	34.463724	0	0.999866	586	0	1
7	Hit Pedestrian Crossing	-0.458615	19.381708	0	0.999874	292	21	153
8	Hit Pedestrian	-0.498864	21.721789	0	0.999879	244	257	416
9	Hit Object	-0.404836	31.51923	0	0.999518	172	174	438
10	Multiple Collision	-0.44744	21.02702	0	0.999845	217	512	0
11	Others	-0.392189	19.914737	0	0.999759	507	1	0

The examination of spatial clusters for different types of collision utilizing the Getis-Ord Gi* statistical method reveals significant aggregations, as depicted in figure 4.23. An analysis of this figure reveals that the hotspots of head-on impacts, rear-end/side collisions, turning collisions, stationary/parked vehicle impacts, vehicle-pedestrian crashes, and multiple collisions are characterized by higher density, and these emerge as continuous segments along Ring Road, Araniko Highway, Tribhuwan Highway, Thapathali-Ekantakuna Road, and other principal urban roadways. The spatial distribution of hotspots pertaining to crossing collisions, vehicle overturns, and hit object impacts is comparatively sparse than other types of collisions, appearing as isolated segments on these roadways.

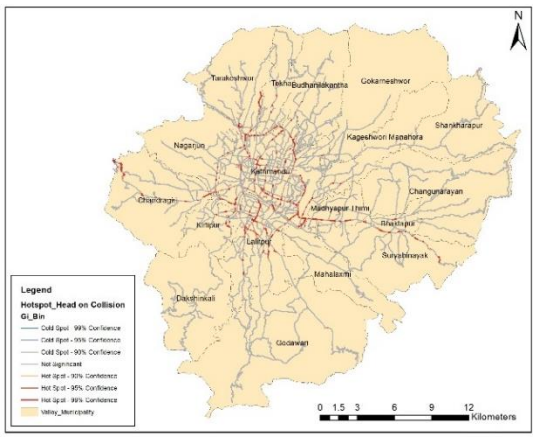

(a) Head On Collision

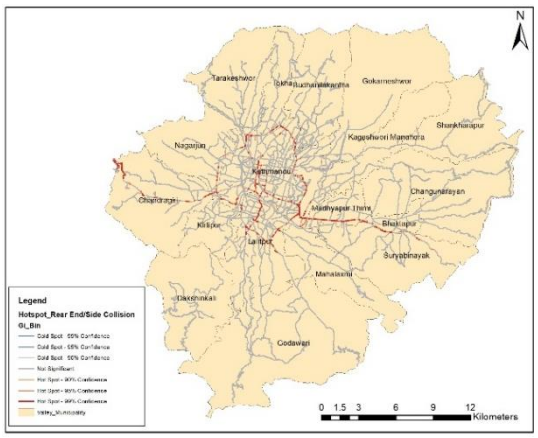

(b) Rear End/Side Collision

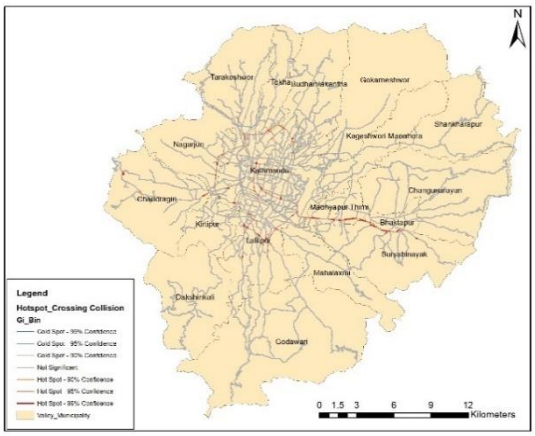

(c) Crossing Collision

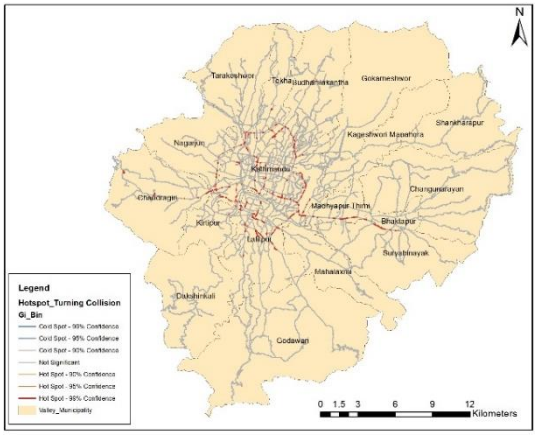

(d) Turning Collision

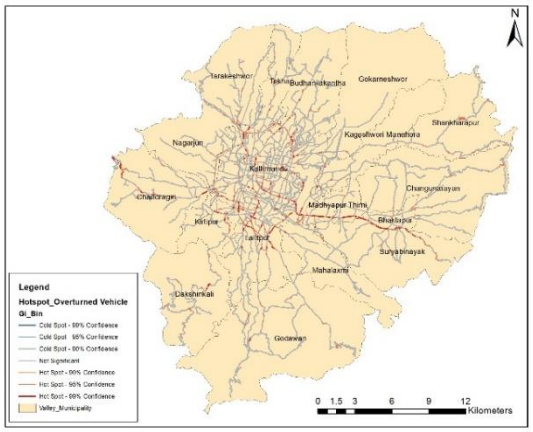

(e) Overturned Vehicle

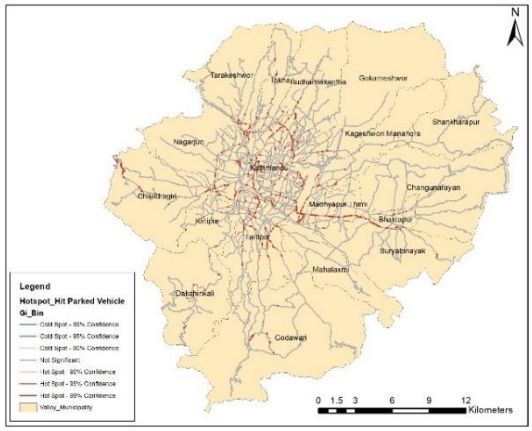

(f) Hit Parked Vehicle

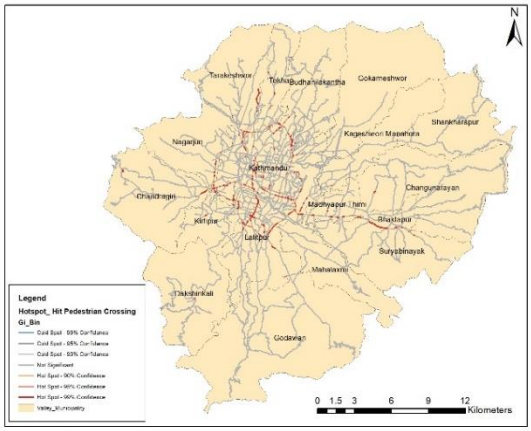

(g) Hit Pedestrian Crossing

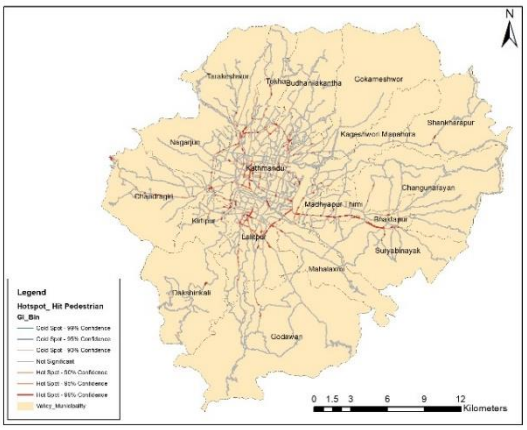

(h) Hit Pedestrian

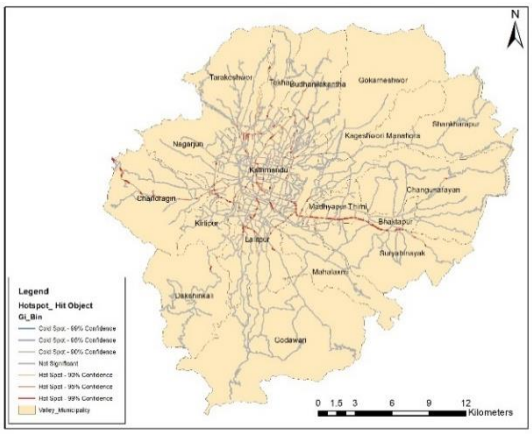

(i) Hit Object

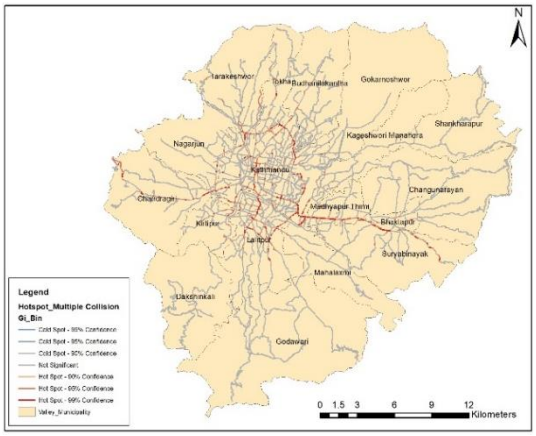

(j) Multiple Collision

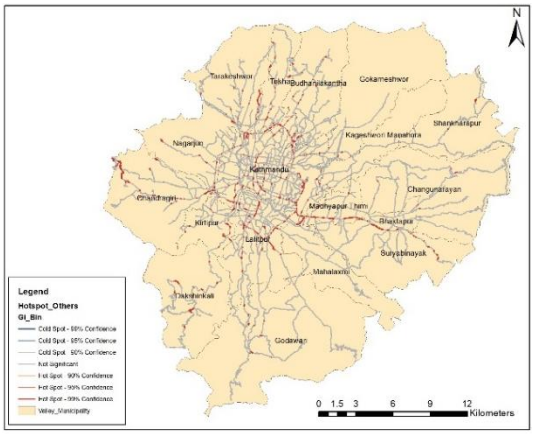

(k) Others

Figure 4.23 Hotspots Analysis Maps for Collision Types

The highest risk segments for various types of collisions are outlined in table 4.9 to table 4.19.

Table 4.9 Significant Hotspot Links for Head on Collision

S.N.	Link Name	Crash Count	Length (m)	Locations
1	Manohara-Sallaghari-Hanumante Culvert	124	3454.774	16
2	Thapathali-Tikabhairab(KVRR)	113	2517.621	14
3	Maharajganj - Balaju Bypass Junction (KTM Ringroad)	110	1739.197	15
4	Maitighar-Tinkune	96	1410.174	14
5	Chabahil - Sankhapark (KTM Ringroad)	92	1170	10
6	Kalanki - Balkhu (KTM Ringroad)	88	982.145	12
7	Nagdhunga-Kalanki (Ring road)	78	1812.228	12
8	Tinkune - Sinamangal - Gaushala (KTM Ringroad)	74	1357.075	12
9	Tripureshwar-Ring road	64	1517.788	11
10	Ring road-Balaju Bypass	53	680.394	4
11	Koteshwar-Manohara bridge	52	832.866	7
12	Manohara River - Koteshwor (H03) KTM Ringroad)	51	640.314	8

S.N.	Link Name	Crash Count	Length (m)	Locations
13	Kalanki (Ring road)-Tripureswor	47	700.760	6
14	Lainchaur-Maharajgunj	47	1118.61	9
15	Peepalmod-Nagdhunga	40	1455.086	4
16	Balaju Junction - Banasthali - Swoyambhu (KTM Ringroad)	38	511.127	6
17	Balkhu-Chovar	37	883.784	5
18	Ekantakuna- Kusanti - Satdobato (KTMRingroad)	35	497.104	6
19	Hanumante Culvert-Sanga	34	1012.459	7
20	Satdobato-Jawalakhel	34	920.459	4
21	Jadibuti (ARM)-Sinamangal	32	684.478	4
22	Jayanepal-Thapathali(KVRR)	28	594.370	4
23	Balkhu-Kuleswor-Kalimati	26	486.481	4
24	Balkhu - Ekantakuna (KTMRingroad)	25	429.447	4
25	Satdobato- Gwarko (KTM Ringroad)	25	499.722	4
26	Nakhudobato-Nakhu Chowk	23	693.409	3
27	Bansbari-Budhanilkantha	22	303.943	5
28	Kalopul--Nagpokhari-Kesharmahal-Tridevimarg (Sanchayakosh)	22	566.279	5
29	Sankhapark - Maharajganj (KTM Ringroad)	21	398.947	4
30	TU Gate-Kirtipur	20	527.707	4
31	Mitrapark - Chabahil (KTM Ringroad)	19	181.081	3
32	Swoyambhu - Kalanki (KTM Ringroad)	16	469.042	3
33	Samakhushi Chok-Tokhagaun-Chandeshwarigaun(KVRR)	15	375.360	3
34	Satdobato (Ring Road)-Dhapakhel -Thecho(KVRR)	15	758.822	3
35	Tinkune-Koteshwar	15	220.779	3
36	Satdobato-Karmanas bridge	14	313.344	1
37	Jawlakhel-Bhanimandal	14	262.578	1
38	Bhaktapur-Army camp	13	338.637	2
39	Gaushala-Rato pul-Kamalpokhari-Kamaladi	13	224.802	3
40	Gaushala - Mitrapark (KTM Ringroad)	12	173.495	2
41	Shital Niwas-Tangal-Dillibazar	11	161.813	2
42	Gwarko-Lubhu-Lankuri Bhanjyang	10	336.345	2

Table 4.10 Significant Hotspot Links for Rear End/Side Collision

S.N.	Linkname	Crash Count	Length (m)	Locations
1	Manohara-Sallaghari-Hanumante Culvert	554	5257.2635	25
2	Nagdhunga-Kalanki (Ring road)	495	2781.4064	22
3	Koteshwar-Manohara bridge	362	920.63918	9
4	Maitighar-Tinkune	280	1305.1922	11
5	Thapathali-Tikabhairab (KVRR)	277	2082.7372	11
6	Tinkune - Sinamangal - Gaushala (KTM Ringroad)	258	2010.8393	18

S.N.	Linkname	Crash Count	Length (m)	Locations
7	Maharajganj - Balaju Bypass Junction (KTM Ringroad)	243	1672.3172	15
8	Manohara River - Koteshwor (H03) KTM Ringroad)	184	732.19466	10
9	Kalanki - Balkhu (KTM Ringroad)	178	998.41667	11
10	Tripureshwar-Ring road	167	1643.3235	11
11	Satdobato- Gwarko (KTM Ringroad)	150	801.7391	8
12	Ekantakuna- Kusanti - Satdobato (KTM Ringroad)	126	834.67113	8
13	Peepalmod-Nagdhunga	121	2306.6568	7
14	Chabahil - Sankhapark (KTM Ringroad)	119	996.78592	9
15	Swoyambhu - Kalanki (KTM Ringroad)	119	1045.9578	10
16	Tinkune-Koteshwar	118	407.35644	5
17	Ring road-Balaju Bypass	115	666.7581	4
18	Balkhu - Ekantakuna (KTMRingroad)	82	627.93309	5
19	Kalanki (Ring road)-Tripureswor	72	341.17779	4
20	Narayanhiti palace southgate- Durbarmarg-Ghantaghar-Bhadrakali	63	693.18579	4
21	Sankhapark - Maharajganj (KTM Ringroad)	59	478.33493	5
22	Jayanepal-Thapathali(KVRR)	55	683.41816	5
23	Jadibuti (ARM)-Sinamangal	54	621.99447	3
24	Mitrapark - Chabahil (KTM Ringroad)	52	220.79572	3
25	Balkhu-Kuleswor-Kalimati	51	486.48106	4
26	Balaju Junction - Banasthali - Swoyambhu (KTM Ringroad)	50	289.86049	4
27	Gaushala - Mitrapark (KTM Ringroad)	44	360.23718	4
28	Sundhara-Singhadarbar (Prithivi path)	33	488.1767	2
29	Nakkhu Dobato-Nakhu Chowk	32	432.9518	2
30	Chabahil (Ktm Ring road)-Pipalbot	29	158.53708	2
31	Thapathali-Tripureswor	28	337.1298	2
32	Hanumante Culvert-Sanga	27	335.29935	2
33	Kalopul--Nagpokhari-Kesharmahal-Tridevimarg (Sanchayakosh)	23	193.3139	2
34	Satdobato-Karmanas bridge	22	579.61909	2
35	Jawlakhel-Bhanimandal	21	262.578	1
36	Lainchaur-Maharajgunj	19	293.33487	2
37	Gwarko-Manohara River (Balkumari) (KTM Ringroad)	18	200.38066	2
38	Balkhu-Chovar	14	93.392417	1
39	Gwarko-Lubhu-Lankuri Bhanjyang	14	283.66447	1
40	Satdobato-Jawalakhel	11	250.64039	1
41	Darbarmarg-Jamal	10	138.12493	1
42	Bijulibazar-Anamnagar	10	224.46341	1
43	Satdobato-Sunakothi	9	82.830302	1

S.N.	Linkname	Crash Count	Length (m)	Locations
44	Shantinagar - Bhimsengola	9	191.4515	1
45	Tinkune north	9	115.40767	1
46	Maharajgunj-Bansbari	8	69.408386	1

Table 4.11 Significant Hotspot Links for Crossing Collision

S.N.	Linkname	Crash Count	Length (m)	Locations
1	Manohara-Sallaghari-Hanumante Culvert	100	3856.234	19
2	Nakkhu Dobato-Nakhu Chowk	38	258.0183	1
3	Kalanki - Balkhu (KTM Ringroad)	25	324.8476	4
4	Ekantakuna- Kusanti - Satdobato (KTMRingroad)	23	411.0318	6
5	Balkhu - Ekantakuna (KTMRingroad)	19	251.0252	5
6	Kalopul--Nagpokhari-Kesharmahal-Tridevimarg (Sanchayakosh)	11	267.2464	3
7	Satdobato- Gwarko (KTM Ringroad)	11	254.2404	2
8	Thapathali-Tikabhairab(KVRR)	11	348.6542	4
9	Jayanepal-Thapathali(KVRR)	9	195.4299	2
10	Maitighar-Tinkune	9	183.7051	3
11	Ring road-Balaju Bypass	7	529.2456	3
12	Tripureshwar-Ring road	7	243.1737	3
13	Maharajganj - Balaju Bypass Junction (KTM Ringroad)	6	164.9695	2
14	Nagdhunga-Kalanki (Ring road)	6	626.7438	3
15	Satdobato-Jawalakhel	6	249.0204	2
16	Swoyambhu - Kalanki (KTM Ringroad)	6	358.9433	3
17	Gaushala-Rato pul-Kamalpokhari-Kamaladi	5	68.91998	2
18	Gwarko-Mangal Bazar-Pulchowk	5	50.61389	2
19	Tinkune - Sinamangal - Gaushala (KTM Ringroad)	5	113.7062	2
20	Balaju Junction - Banasthali - Swoyambhu (KTM Ringroad)	4	182.7147	2
21	Kalanki (Ring road)-Tripureswor	4	264.0357	2
22	Maharajgunj-Bansbari	3	69.40839	1
23	Manohara River - Koteshwor (H03) KTM Ringroad)	3	129.5771	1
24	Naya Baneswor (BICC)-Sankhamul	3	30.63558	1
25	Tinkune-Koteshwar	3	27.71012	1

Table 4.12 Significant Hotspot Links for Turning Collision

S.N.	Linkname	Crash Count	Length (m)	Locations
1	Maitighar-Tinkune	103	1300.687	16
2	Kalanki - Balkhu (KTM Ringroad)	67	1229.4	15
3	Tinkune - Sinamangal - Gaushala (KTM Ringroad)	67	2202.789	24
4	Manohara River - Koteshwor (H03) KTM Ringroad)	59	661.2416	9
5	Manohara-Sallaghari-Hanumante Culvert	54	3429.993	17

S.N.	Linkname	Crash Count	Length (m)	Locations
6	Nagdhunga-Kalanki (Ring road)	44	1475.32	12
7	Chabahil - Sankhapark (KTM Ringroad)	39	1311.1	11
8	Tripureshwar-Ring road	39	1563.023	13
9	Swoyambhu - Kalanki (KTM Ringroad)	38	1085.514	14
10	Balkhu - Ekantakuna (KTMRingroad)	36	584.2412	6
11	Kalanki (Ring road)-Tripureswor	32	1038.122	12
12	Lainchaur-Maharajgunj	31	1087.922	8
13	Jayanepal-Thapathali(KVRR)	28	1039.937	9
14	Thapathali-Tikabhairab(KVRR)	28	1072.459	7
15	Maharajganj - Balaju Bypass Junction (KTM Ringroad)	27	1048.492	9
16	Balaju Junction - Banasthali - Swoyambhu (KTM Ringroad)	24	601.6874	9
17	Koteshwar-Manohara bridge	24	791.9067	7
18	Satdobato- Gwarko (KTM Ringroad)	24	670.5778	7
19	Ekantakuna- Kusanti - Satdobato (KTMRingroad)	22	728.1682	6
20	Ring road-Balaju Bypass	19	723.7883	5
21	Jadibuti (ARM)-Sinamangal	16	650.2558	5
22	Balkhu-Kuleswor-Kalimati	15	703.63	6
23	Sankhapark - Maharajganj (KTM Ringroad)	14	550.4868	6
24	Gwarko-Manohara River(Balkumari)(KTMRingroad)	10	260	4
25	Chabahil (Ktm Ring road)-Pipalbot	9	289.5058	3
26	Gaushala-Rato pul-Kamalpokhari-Kamaladi	9	68.29439	2
27	Bijuli Bazaar - Anamnagar	9	315.0792	2
28	Gaushala - Mitrapark (KTM Ringroad)	8	134.5865	3
29	Kalopul--Nagpokhari-Kesharmahal-Tridevimarg (Sanchayakosh)	8	378.938	4
30	Satdobato-Jawalakhel	8	866.8852	4
31	Satdobato-Karmanas bridge	8	579.6191	2
32	Nakkhu Dobato-Nakkhu Chowk	8	432.9519	2
33	Pulchowk (Narayani Hotel)- Jhamsikhel-Sanepa-Amarawati-Kandeba	6	513.41	2
34	Purano Baneswor-Naya Baneswor (BICC)	6	393.6668	3
35	Thapathali-Tripureswor	6	337.1298	2
36	Maharajgunj-Bansbari	5	68.49659	2
37	Samakhushi Chok-Tokhagaun-Chandeshwarigaun(KVRR)	5	152.8526	2
38	Shantinagar - Bhimsengola	5	191.4515	1
39	Tinkune-Koteshwar	5	27.71012	1
40	Jawlakhel-Bhanimandal	5	262.5781	1
41	Balkhu-Chovar	4	293.1223	2
42	Baniyatar-Samakhusi Chok-Lainchaur (Ascol) (KVRR)	4	122.5536	2
43	Bansbari-Budhanilkantha	4	173.657	2
44	Gwarko-Lubhu-Lankuri Bhanjyang	4	283.6645	1

S.N.	Linkname	Crash Count	Length (m)	Locations
45	Kamaladi-Darbarmarg	4	91.51925	2
46	Mitrapark - Chabahil (KTM Ringroad)	4	33.22856	1
47	Pulchowk-St. Marys-Thadodhunga_Balkhu (ring road)	4	365.9337	2

Table 4.13 Significant Hotspot Links for Overturned Vehicle

S.N.	Link Name	Crash Count	Length (m)	Locations
1	Manohara-Sallaghari-Hanumante Culvert	25	5198.527	90
2	Nagdhunga-Kalanki (Ring road)	11	1515.108	23
3	Satdobato- Gwarko (KTM Ringroad)	10	882.9063	28
4	Maitighar-Tinkune	10	942.5031	17
5	Thapathali-Tikabhairab(KVRR)	9	1280.177	23
6	Kalanki - Balkhu (KTM Ringroad)	8	763.3117	26
7	Ekantakuna- Kusanti - Satdobato (KTMRingroad)	6	438.7171	14
8	Hanumante Culvert-Sanga	6	819.4897	20
9	Tinkune - Sinamangal - Gaushala (KTM Ringroad)	6	827.203	17
10	Tripureshwar-Ring road	6	757.814	14
11	Koteshwar-Manohara bridge	5	523.6035	15
12	Balkhu - Ekantakuna (KTMRingroad)	4	696.9532	14
13	Jayanepal-Thapathali(KVRR)	4	508.4515	8
14	Manohara River - Koteshwor (H03) KTM Ringroad)	4	296.7463	8
15	Peepalmod-Nagdhunga	4	1136.933	10
16	Balkhu-Chovar	3	612.9016	7
17	Bansbari-Budhanilkantha	3	268.7202	7
18	Chabahil - Sankhapark (KTM Ringroad)	3	599.6162	8
19	Kalanki (Ring road)-Tripureswor	3	285.7755	6
20	Lainchaur-Maharajgunj	3	438.9332	7
21	Ring road-Balaju Bypass	3	655.7162	12
22	Tinkune-Koteshwar	3	277.5831	10

Table 4.14 Significant Hotspot Links for Hit Parked Vehicle

S.N.	Linkname	Crash Count	Length (m)	Locations
1	Nagdhunga-Kalanki (Ring road)	48	2557.756	25
2	Manohara-Sallaghari-Hanumante Culvert	44	5030.511	29
3	Thapathali-Tikabhairab(KVRR)	26	2519.866	18
4	Chabahil - Sankhapark (KTM Ringroad)	22	1406.479	13
5	Tripureshwar-Ring road	22	1840.514	18
6	Maitighar-Tinkune	16	1216.019	12
7	Swoyambhu - Kalanki (KTM Ringroad)	16	915.1201	11
8	Tinkune - Sinamangal - Gaushala (KTM Ringroad)	16	1279.229	14
9	Jadibuti (ARM)-Sinamangal	15	1220.452	12

S.N.	Linkname	Crash Count	Length (m)	Locations
10	Maharajganj - Balaju Bypass Junction (KTM Ringroad)	15	1029.859	10
11	New Buspark	13	525.7236	1
12	Bansbari-Budhanilkantha	12	795.9551	11
13	Ekantakuna- Kusanti - Satdobato (KTMRingroad)	12	611.5008	9
14	Kalanki - Balkhu (KTM Ringroad)	12	793.2137	9
15	Chovar-Chhaimale	11	1575.657	11
16	Samakhushi Chok-Tokhagaun-Chandeshwarigaun(KVRR)	11	740.0052	10
17	Kalanki (Ring road)-Tripureswor	10	811.0538	9
18	Sankhapark - Maharajganj (KTM Ringroad)	10	664.8026	7
19	Satdobato- Gwarko (KTM Ringroad)	10	678.0851	7
20	Sinamangal (Ring road) -Dillibazar-Bhotahiti	10	681.2974	9
21	Balaju Junction - Banasthali - Swoyambhu (KTM Ringroad)	9	565.2576	8
22	Balkhu-Kuleswor-Kalimati	9	527.2723	5
23	Golphutar-Pipalbot-Sankhapark	9	887.1464	5
24	Koteshwar-Manohara bridge	9	794.7484	7
25	Manohara River - Koteshwor (H03) KTM Ringroad)	9	402.7955	7
26	Lainchaur-Maharajgunj	8	1053.742	8
27	Bhaktapur-Army camp	7	669.9966	6
28	Chabahil (Ktm Ring road)-Pipalbot	7	251.5844	5
29	Narayanhiti palace southgate- Durbarmarg-Ghantaghar-Bhadrakali	7	831.0673	6
30	Pipal Bot-Sankhu	7	608.9576	7
31	Satdobato (Ring Road)-Dhapakhel -Thecho(KVRR)	7	1111.189	5
32	Jayanepal-Thapathali(KVRR)	6	283.7436	5
33	Ring road-Balaju Bypass	6	265.287	2
34	Saleek-Indrachowk	6	442.5264	4
35	Satdobato-Sunakothi	6	651.6623	5
36	Nepaltar-Jarankhu	6	790.4637	3
37	Kalopul--Nagpokhari-Kesharmahal-Tridevimarg (Sanchayakosh)	5	576.6149	5
38	Maharajgunj-Bansbari	5	316.7068	5
39	Peepalmod-Nagdhunga	5	1043.012	4
40	Pepsicola-Karkigaun(KVRR)	5	489.8111	3
41	Satdobato-Karmanas bridge	5	1074.996	4
42	Sunakothi-Junction, road to Lele	5	178.8158	4
43	Balkhu - Ekantakuna (KTMRingroad)	4	287.8956	4
44	Gaushala-Purano Baneswor	4	199.6489	3
45	Hanumante Culvert-Sanga	4	446.3346	4
46	Kashibazar-Kirtipur-Machhegaun-Tinthana(KVRR)	4	333.8932	3
47	TU Gate-Kirtipur	4	246.877	3

Table 4.15 Significant Hotspot Links for Hit Pedestrian Crossing

S.N.	Link Name	Crash Count	Length (m)	Locations
1	Maitighar-Tinkune	79	1615.215	18
2	Manohara-Sallaghari-Hanumante Culvert	53	3571.843	17
3	Maharajganj - Balaju Bypass Junction (KTM Ringroad)	47	1507.84	14
4	Nagdhunga-Kalanki (Ring road)	47	1715.724	14
5	Thapathali-Tikabhairab(KVRR)	45	2421.896	13
6	Kalanki - Balkhu (KTM Ringroad)	43	1107.299	13
7	Kalanki (Ring road)-Tripureswor	43	1320.126	14
8	Tinkune - Sinamangal - Gaushala (KTM Ringroad)	40	1254.6	14
9	Manohara River - Koteshwor (H03) KTM Ringroad)	35	559.6742	6
10	Satdobato- Gwarko (KTM Ringroad)	35	794.974	9
11	Swoyambhu - Kalanki (KTM Ringroad)	30	911.6285	8
12	Ekantakuna- Kusanti - Satdobato (KTMRingroad)	29	684.8199	9
13	Balkhu - Ekantakuna (KTMRingroad)	28	1003.124	10
14	Chabahil - Sankhapark (KTM Ringroad)	25	1059.441	8
15	Ring road-Balaju Bypass	25	723.7883	5
16	Tripureshwar-Ring road	25	1589.419	10
17	Gwarko-Manohara River(Balkumari)(KTMRingroad)	21	343.0809	4
18	Sankhapark - Maharajganj (KTM Ringroad)	15	414.3746	6
19	Balkhu-Kuleswor-Kalimati	14	568.9419	6
20	Jadibuti (ARM)-Sinamangal	14	741.1221	4
21	Lainchaur-Maharajgunj	13	576.0227	4
22	Satdobato-Jawalakhel	13	913.4457	4
23	Jayanepal-Thapathali(KVRR)	12	290.1482	3
24	Koteshwar-Manohara bridge	11	571.836	5
25	Narayanhiti palace southgate- Durbarmarg-Ghantaghar-Bhadrakali	10	610.4449	5
26	Samakhushi Chok-Tokhagaun-Chandeshwarigaun(KVRR)	10	405.1038	4
27	Bansbari-Budhanilkantha	7	182.1447	3
28	Maharajgunj-Bansbari	7	144.8247	3
29	Satdobato-Karmanas bridge	5	446.6303	2
30	Thapathali-Tripureswor	5	228.6833	1
31	Nakkhu Dobato- Nakkhu Chowk	5	432.9519	2
32	Balaju Junction - Banasthali - Swoyambhu (KTM Ringroad)	4	118.926	2
33	Balkhu-Chovar	4	138.6242	1
34	Chovar-Chhaimale	4	153.8017	2
35	Gaushala-Purano Baneswor	4	147.6695	2
36	Gaushala-Rato pul-Kamalpokhari-Kamaladi	4	69.43931	2
37	Hanumante Culvert-Sanga	4	241.4607	2

S.N.	Link Name	Crash Count	Length (m)	Locations
38	Mitrapark - Chabahil (KTM Ringroad)	4	187.5672	2
39	Nagdhunga(TRP)-Tankeswor(KVRR)	4	65.34955	2
40	Roads circumscribing the Sinhadurbar	4	347.2491	2
41	Shantinagar - Bhimsengola	4	191.4515	1
42	Tinkune-Koteshwar	4	186.5765	2
43	Chabahil (Ktm Ring road)-Pipalbot	3	76.59107	1
44	Purano Baneswor-Naya Baneswor (BICC)	3	57.415	1
45	Shital Niwas-Tangal-Dillibazar	3	139.6562	1
46	Sinamangal (Ring road) -Dillibazar-Bhotahiti	3	224.0564	1

Table 4.16 Significant Hotspot Links for Hit Pedestrian

S.N.	Link Name	Crash Count	Length (m)	Locations
1	Manohara-Sallaghari-Hanumante Culvert	82	4767.282	24
2	Nagdhunga-Kalanki (Ring road)	33	882.7811	12
3	Tripureshwar-Ring road	30	1427.279	12
4	Satdobato- Gwarko (KTM Ringroad)	29	645.2182	7
5	Maharajganj - Balaju Bypass Junction (KTM Ringroad)	24	970.5017	8
6	Thapathali-Tikabhairab(KVRR)	24	1600.547	11
7	Gwarko-Manohara River(Balkumari)(KTMRingroad)	21	499.3175	7
8	Manohara River - Koteshwor (H03) KTM Ringroad)	20	632.4047	7
9	Ring road-Balaju Bypass	17	515.4327	3
10	Maitighar-Tinkune	16	444.037	5
11	Ekantakuna- Kusanti - Satdobato (KTMRingroad)	15	516.3112	5
12	Tinkune - Sinamangal - Gaushala (KTM Ringroad)	14	591.4471	5
13	Balaju Junction - Banasthali - Swoyambhu (KTM Ringroad)	13	560.0657	5
14	Chabahil - Sankhapark (KTM Ringroad)	13	545.9832	4
15	Samakhushi Chok-Tokhagaun-Chandeshwarigaun(KVRR)	13	502.5311	5
16	Balkhu-Chovar	12	738.756	5
17	Balkhu - Ekantakuna (KTMRingroad)	11	507.4632	4
18	Kalanki - Balkhu (KTM Ringroad)	11	428.715	4
19	Kalanki (Ring road)-Tripureswor	11	566.8719	5
20	Sunakothi-Junction, road to Lele	11	359.9798	3
21	Koteshwar-Manohara bridge	10	401.5974	3
22	Swoyambhu - Kalanki (KTM Ringroad)	8	393.9931	4
23	New Buspark -Baniyatar (Manohar Marga)	8	681.9783	3
24	Balkhu-Kuleswor-Kalimati	7	271.5932	3
25	Jadibuti (ARM)-Sinamangal	7	414.7328	3
26	Pipal Bot-Sankhu	7	253.9898	3
27	Chabahil (Ktm Ring road)-Pipalbot	6	122.0256	2

S.N.	Link Name	Crash Count	Length (m)	Locations
28	Gaushala-Rato pul-Kamalpokhari-Kamaladi	6	297.7474	3
29	Jayanepal-Thapathali(KVRR)	6	384.3161	3
30	Satdobato-Karmanas bridge	6	457.0031	2
31	Sinamangal (Ring road) -Dillibazar-Bhotahiti	6	137.5522	3
32	Nepaltar-Jarankhu	6	247.2465	2
33	Pepsicola-Karkigaun(KVRR)	5	293.9764	2
34	Sallaghari (Bhaktapur)-Duwakot(KVRR)	5	254.3296	2
35	Satdobato-Jawalakhel	5	506.7778	2
36	Gaushala - Mitrapark (KTM Ringroad)	4	175.0974	2
37	Gwarko-Lubhu-Lankuri Bhanjyang	4	525.5881	2
38	Lainchaur-Maharajgunj	4	205.5512	2
39	Sankhapark - Maharajganj (KTM Ringroad)	4	157.1023	2
40	Satdobato-Sunakothi	4	281.0684	1
41	Tridevimarg (Sanchayakosh)-Chhetrapati-Sobhabagawati	4	158.1343	2
42	TU Gate-Kirtipur	4	226.2987	2
43	Bhaktapur-Army camp	3	175.4009	1
44	Kausaltar-Balkot-Sirutar-Biruwa(KVRR)	3	72.57963	1
45	Peepalmod-Nagdhunga	3	579.4909	1
46	Saleek-Indrachowk	3	161.8857	1
47	Ratopul-Kalopul (Rudramati Marga)	3	254.133	1

Table 4.17 Significant Hotspot Links for Hit Object

S.N.	Link Name	Crash Count	Length (m)	Locations
1	Manohara-Sallaghari-Hanumante Culvert	147	5667.318	29
2	Nagdhunga-Kalanki (Ring road)	43	1787.582	16
3	Maitighar-Tinkune	24	719.9144	7
4	Ekantakuna- Kusanti - Satdobato (KTM Ringroad)	23	656.117	8
5	Kalanki - Balkhu (KTM Ringroad)	21	806.8739	7
6	Tripureshwar-Ring road	17	488.244	5
7	Koteshwar-Manohara bridge	16	473.5028	4
8	Thapathali-Tikabhairab(KVRR)	15	1225.437	6
9	Maharajganj - Balaju Bypass Junction (KTM Ringroad)	14	576.0582	5
10	Manohara River - Koteshwor (H03) KTM Ringroad)	12	308.1549	4
11	Lainchaur-Maharajgunj	10	475.6856	4
12	Peepalmod-Nagdhunga	10	899.989	3
13	Balkhu - Ekantakuna (KTMRingroad)	9	105.5351	1
14	Hanumante Culvert-Sanga	9	321.2482	2
15	Kalanki (Ring road)-Tripureswor	9	377.0649	4
16	Ring road-Balaju Bypass	9	515.4327	3
17	Swoyambhu - Kalanki (KTM Ringroad)	9	366.2811	3
18	Bansbari-Budhanilkantha	8	204.2672	4

S.N.	Link Name	Crash Count	Length (m)	Locations
19	Gwarko-Manohara River(Balkumari)(KTMRingroad)	6	233.3788	3
20	Jadibuti (ARM)-Sinamangal	6	413.7655	3
21	Narayanhiti palace southgate- Durbarmarg-Ghantaghar-Bhadrakali	6	311.1456	2
22	Mitrapark - Chabahil (KTM Ringroad)	5	49.24474	2
23	Satdobato-Karmanas bridge	5	313.344	1
24	Sundhara-Singhadarbar (Prithivi path)	5	184.2131	2
25	Balaju Junction - Banasthali - Swoyambhu (KTM Ringroad)	4	110.7635	2
26	Gaushala-Purano Baneswor	4	195.4795	2
27	Golphutar-Pipalbot-Sankhapark	4	248.9758	2
28	Jayanepal-Thapathali(KVRR)	4	204.7798	2
29	Kalopul--Nagpokhari-Kesharmahal-Tridevimarg (Sanchayakosh)	4	211.3921	2
30	Samakhushi Chok-Tokhagaun-Chandeshwarigaun (KVRR)	4	196.9953	2
31	Nakkhu Dobato-Nakkhu Chowk	4	513.1469	2
32	Kopundole-Sankhamul	3	607.6407	1

Table 4.18 Significant Hotspot Links for Multiple Collisions

S.N.	Link Name	Crash Count	Length (m)	Locations
1	Manohara-Sallaghari-Hanumante Culvert	86	4568.193	25
2	Tinkune - Sinamangal - Gaushala (KTM Ringroad)	34	1278.19	12
3	Nagdhunga-Kalanki (Ring road)	31	1745.451	14
4	Hanumante Culvert-Sanga	26	1058.687	8
5	Koteshwar-Manohara bridge	26	882.9669	8
6	Thapathali-Tikabhairab(KVRR)	24	1384.264	6
7	Chabahil - Sankhapark (KTM Ringroad)	22	1153.809	9
8	Maharajganj - Balaju Bypass Junction (Ringroad)	22	1019.75	8
9	Satdobato- Gwarko (KTM Ringroad)	20	568.7648	6
10	Maitighar-Tinkune	19	808.7575	7
11	Tripureshwar-Ring road	18	935.1891	7
12	Ekantakuna- Kusanti - Satdobato (KTMRingroad)	17	571.9786	8
13	Manohara River - Koteshwor (H03) KTM Ringroad)	17	459.7278	5
14	Balaju Junction - Banasthali - Swoyambhu (KTM Ringroad)	14	207.8267	4
15	Kalanki - Balkhu (KTM Ringroad)	12	497.0954	4
16	Kalanki (Ring road)-Tripureswor	12	673.757	5
17	Gwarko-Manohara River(Balkumari)(Ringroad)	9	386.2069	4
18	Sankhapark - Maharajganj (KTM Ringroad)	9	436.6332	4
19	Tinkune-Koteshwar	8	334.7763	3
20	Balkhu - Ekantakuna (KTMRingroad)	7	133.8463	3
21	Jadibuti (ARM)-Sinamangal	7	563.5937	3
22	Jayanepal-Thapathali(KVRR)	7	289.1576	3

S.N.	Link Name	Crash Count	Length (m)	Locations
23	Kalopul--Nagpokhari-Kesharmahal-Tridevimarg (Sanchayakosh)	7	333.7522	3
24	Lainchaur-Maharajgunj	7	189.2501	3
25	Mitrapark - Chabahil (KTM Ringroad)	7	160.888	3
26	Gaushala-Rato pul-Kamalpokhari-Kamaladi	6	266.114	3
27	Narayanhiti palace southgate- Durbarmarg-Ghantaghar-Bhadrakali	5	382.0402	2
28	Ring road-Balaju Bypass	5	504.3908	2
29	Sinamangal (Ring road) -Dillibazar-Bhotahiti	5	184.7231	2
30	Swoyambhu - Kalanki (KTM Ringroad)	5	300.8627	2
31	Nagarjun Thulo Khola	4	111.1507	2
32	Purano Baneswor-Naya Baneswor (BICC)	4	281.7595	2
33	Satdobato (Ring Road)-Dhapakhel -Thecho(KVRR)	4	529.5883	2
34	Satdobato-Jawalakhel	4	406.668	2
35	Thapathali-Tripureswor	4	127.8978	2
36	Bansbari-Budhanilkantha	3	116.4461	1
37	Chabahil (Ktm Ring road)-Pipalbot	3	81.94601	1
38	Gwarko-Mangal Bazar-Pulchowk	3	50.61389	2
39	Kausaltar-Balkot-Sirutar-Biruwa(KVRR)	3	73.03954	1
40	TU Gate-Kirtipur	3	73.53748	1
41	Jawlakhel-Bhanimandal	3	262.5781	1

Table 4.19 Significant Hotspot Links for Others

S.N.	Link Name	Crash Count	Length (m)	Locations
1	Manohara-Sallaghari-Hanumante Culvert	55	4936.988	25
2	Nagdhunga-Kalanki (Ring road)	37	2962.805	24
3	Thapathali-Tikabhairab(KVRR)	26	2740.313	18
4	Maharajganj - Balaju Bypass Junction (KTM Ringroad)	23	1771.97	17
5	Tinkune - Sinamangal - Gaushala (KTM Ringroad)	22	1869.078	19
6	Chovar-Chhaimale	20	2214.985	15
7	Chabahil - Sankhapark (KTM Ringroad)	17	927.8744	9
8	Koteshwar-Manohara bridge	17	696.8053	7
9	Peepalmod-Nagdhunga	17	1952.148	7
10	Kalanki - Balkhu (KTM Ringroad)	16	967.0537	12
11	Maitighar-Tinkune	15	1161.156	11
12	Hanumante Culvert-Sanga	14	1353.322	11
13	Tripureshwar-Ring road	13	1207.601	9
14	Balkhu - Ekantakuna (KTMRingroad)	12	631.3525	10
15	Samakhushi Chok-Tokhagaun-Chandeshwarigaun(KVRR)	12	897.386	12
16	Swoyambhu - Kalanki (KTM Ringroad)	12	682.1872	8
17	Ekantakuna- Kusanti - Satdobato (KTMRingroad)	11	932.0825	9
18	Satdobato- Gwarko (KTM Ringroad)	10	694.1135	8

S.N.	Link Name	Crash Count	Length (m)	Locations
19	Jayanepal-Thapathali(KVRR)	9	730.1194	9
20	Balkhu-Chovar	8	1386.077	8
21	Balkhu-Kuleswor-Kalimati	8	554.1638	5
22	Kalanki (Ring road)-Tripureswor	8	401.0815	6
23	Manohara River - Koteshwor (H03) KTM Ringroad)	8	360.9592	5
24	Balaju Junction - Banasthali - Swoyambhu (KTM Ringroad)	7	366.3039	6
25	Bansbari-Budhanilkantha	7	620.9631	6
26	Chabahil (Ktm Ring road)-Pipalbot	7	459.739	7
27	Gwarko-Manohara River(Balkumari)(KTMRingroad)	7	390.9875	5
28	Lainchaur-Maharajgunj	7	576.1523	6
29	Sankhapark - Maharajganj (KTM Ringroad)	7	444.3383	4
30	Golphutar-Pipalbot-Sankhapark	6	414.6565	6
31	Jadibuti (ARM)-Sinamangal	6	521.3726	4
32	Pipal Bot-Sankhu	5	443.3626	5
33	Ring road-Balaju Bypass	5	504.3908	2
34	Army camp-Nagarkot	4	682.8096	4
35	Maharajgunj-Bansbari	4	304.336	4
36	Satdobato-Karmanas bridge	4	892.9677	4
37	Tinkune-Koteshwar	4	250.263	2
38	TU Gate-Kirtipur	4	121.7737	3
39	Bahiti-Sitapaila	3	522.6554	3
40	Balaju-Nepaltar-Sangla Bazar	3	122.5325	3
41	Gaushala - Mitrapark (KTM Ringroad)	3	156.0576	2
42	Gaushala-Rato pul-Kamalpokhari-Kamaladi	3	205.0328	3
43	Kausaltar-Balkot-Sirutar-Biruwa(KVRR)	3	145.6192	2
44	Mitrapark - Chabahil (KTM Ringroad)	3	71.30631	2
45	Nagarjun Thulo Khola	3	372.6241	2
46	Pepsicola-Karkigaun(KVRR)	3	200.6128	2
47	Satdobato-Jawalakhel	3	329.2152	2
48	Sunakothi-Junction, road to Lele	3	99.83237	3
49	Budhanagar-Bijuli Bazaar	3	173.5347	1

Figure 4.24 presents a spatial distribution of hotspots for various types of collisions as produced using the KDE technique. The crash density maps identified the same critical hotspot areas as those detected using Getis-Ord Gi* Statistics. However, they resulted in fewer segments compared to figure 4.23.

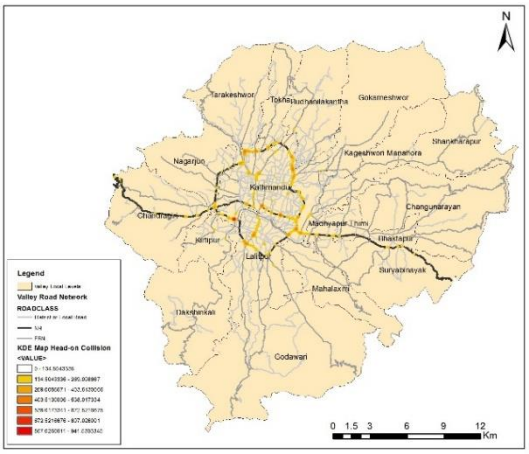

(a) Head On Collision

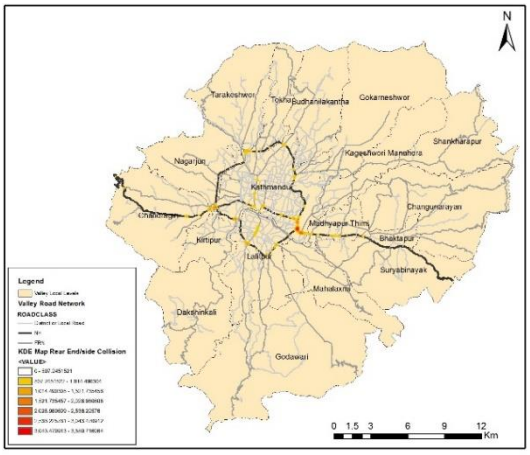

(b) Rear End/Side Collision

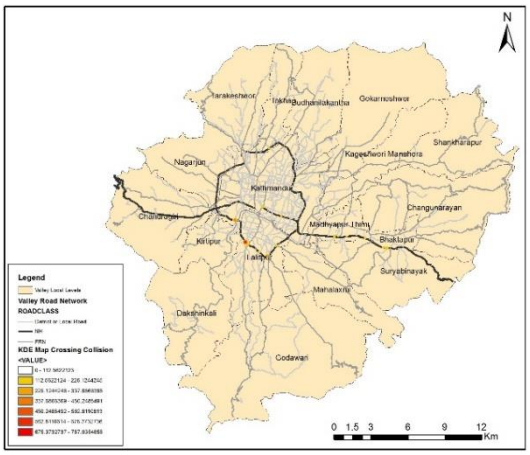

(c) Crossing Collision

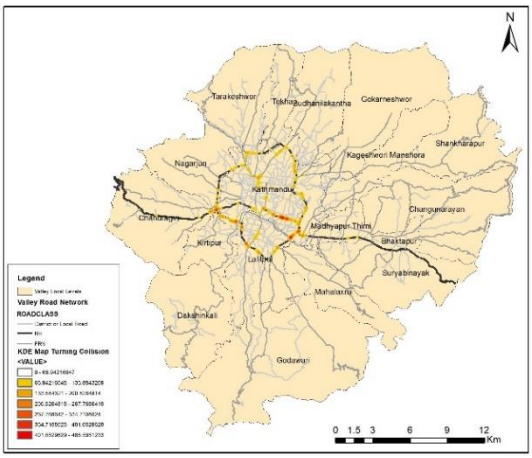

(d) Turning Collision

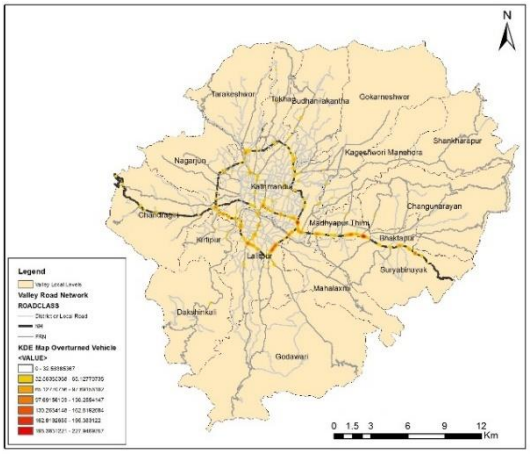

(e) Overturned Vehicle

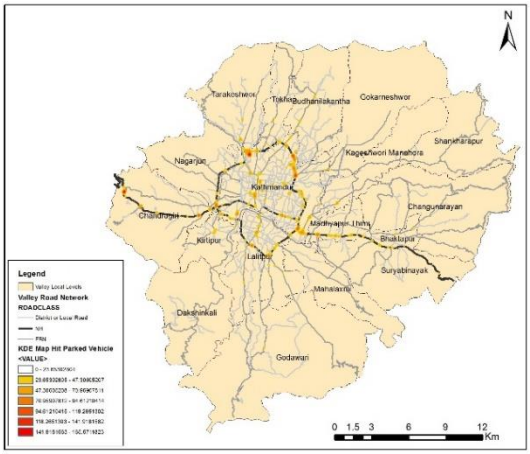

(f) Hit Parked Vehicle

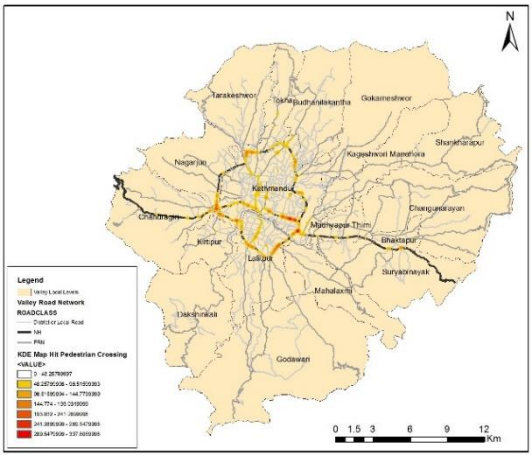

(g) Hit Pedestrian Crossing

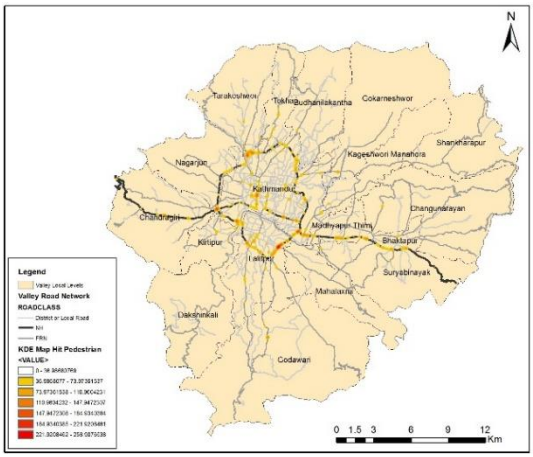

(h) Hit Pedestrian

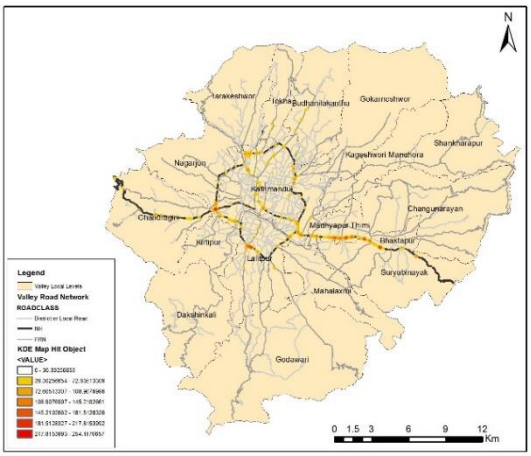

(i) Hit Object

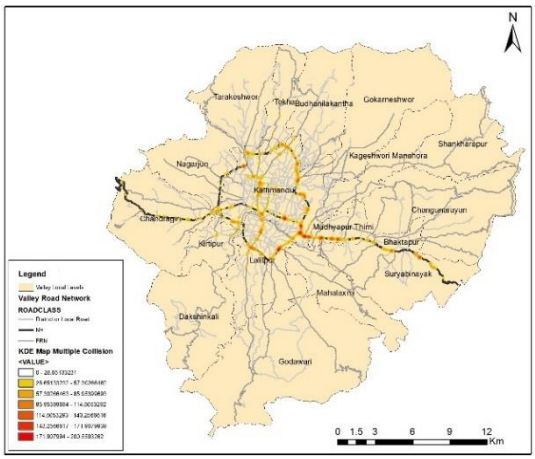

(j) Multiple Collision

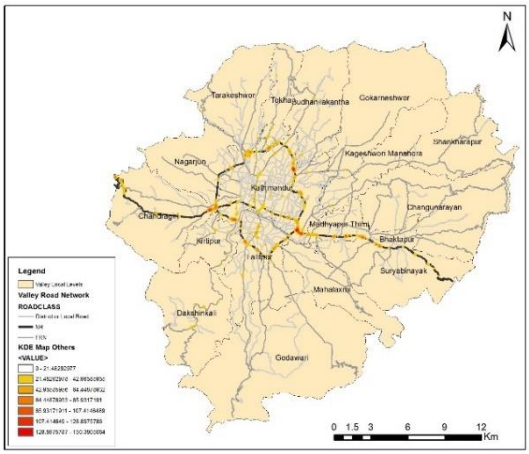

(k) Others

Figure 4.24 KDE Maps for Collision Types

As illustrated in figure 4.24, the crash density surface related to the head-on and rear end/side collisions vary from 134.504 to 941.530 points/sq.km and 507.245 to 3550.71 points/sq.km respectively. This crash frequency value is quite larger when compared to density ranges of the remaining collision types, which pertains to the fact that the

incidences of head on and rear end/side impacts are predominant in the analysis dataset. The concentrations of high-density segments for both the head on and rear end/side collisions are located along the major highways and internal feeder roads enveloped by the central Ring Road. The head on collision hotspots appears more continuous along some sections of Ring Road (Sinamnagal- Koteshwor-Balkumari, Gwarko-Stadobato, Balkhu-Kalanki, Gaushala-Chabahil-Sankhapark and Samakhusi-Machhapokari-Balaju), and Thapathali-Ekantakuna road than that of rear end/side collisions. The clusters of head-on collision also appear as isolated patches along Araniko Highway, Tribhuwan Highway, Tripureshwor- Balaju, TU Gate-Kritipur, Balkhu-Chovar, Satdobato-Godawari, Jadibuti-Pepsicola, Chabahil-Pipalbot and Maharajgunj-Budhanilkantha road sections. Head-on collisions typically happen at crossroads, on roads without a median (undivided road segments), and at mid-block locations where U-turns are allowed. Rear end/side collisions tend to occur at intersections with or without traffic signals when a vehicle doesn't recognize the slowed or halted traffic in front, and at mid-blocks when a driver fails to maintain a safe following or passing (overtaking) distance or make sudden lane changes.

The KDE map of crossing collision displayed a limited number of areas posing the highest level of risk with density range of 112.562 to 787.935 points/sq.km. These collisions tend to cluster at major intersections, junctions with minor roads, mid blocks with divider openings or broken barrier line sections where crossing is allowed, such as in Pandubazar, Srijanagar, Gatthaghar, Gwarko, Satdobato, Thasikhel, Ekantakuna, Nakkhudobato, Balkhu, Newbaneshwor, Jamal and Maitighar areas. On the other hand, turning collisions have a lower density range of 66.942 to 468.595 points/sq.km, but show sprawling nature likely due to numerous access roads in the Valley. These are more pronounced at Maitighar-Tinkune-Koteshwor, Koteshwor-Balkumari, Koteshwor-Jadibuti, Gwarko-Satdobato, Ekantakuna-Nakkhudobato, Hariharbhawan-Jawlakhel, Sanepa-Dhobighat, Balkhu-Kalanki, Jamal-Lajimpat, Machhapokhari-Balaju-Sanobharyang, Maharajgunj-Lazimpat, Dhumbahari-Chabahil and Sinamangal-Gaushala road sections. The turning collisions are frequent at intersections with major roads or access roads, undivided roads as well as at mid blocks with divider openings often resulting from abrupt u-turns and turning maneuvers.

Unlike the collisions mentioned earlier, the vehicle overturn, hit parked vehicle, hit pedestrian crossing, hit pedestrian, hit object, multiple and others categories of crashes appear to exhibit lower density in the ranges of 32.564 to 227.947 points/sq.km, 23.653 to 165.571 points/sq.km, 48.258 to 337.806 points/sq.km, 36.987 to 258.908 points/sq.km, 36.302 to 254.118 points/sq.km, 28.651 to 200.559 points/sq.km and 21.483 to 150.380 points/sq.km respectively, indicating they are less frequent. The hotspots for overturned vehicle seem to cluster predominantly along the southern Ring Road section, Araniko highway and feeder roads such as Bakhu-Chobhar Dakshinkali, Ekantakuna-Bhaisepati, Satdobato-Godawari, Jadibuti-Pepsicola, Chabahil-Pipalbot, Sankahusi-Tokha-Jhor and Maharajgunj-Budhanilkantha road sections which may have strong relation with loss of vehicular control due to excessive speeds on these roadways or mechanical failure due to neglected maintenance, road conditions and long-distance travel.

The hit parked vehicle hotspots are quite pronounced along major and minor roadways where there is presence of busparks, busstops, fuel pumps, checkposts, bridges and other segments where parking provisions are not regulated. High intensity of such hotspots are seen at Nagdhunga, Thankot, Kalanki, Panga, Nayabazar, Balkhu, Ekantakuna, Satdobato, Gwarko, Koteshwor, Tilganga, Chabahil, Sukedhara, Dhumbarahi, Maharajgunj, Samakhusi, New Buspark, Sorakhutte, Nepaltar, Pulchowk, Kupondole, New Baneshwor, Sundhara, Jamal, Durbarmarg, Jadibuti, Pepsicola, Harhar mahadev, Manohara Bridge, Gatthaghar, New Thimi and Chundevi areas. The clusters of hit object collision are observed more continuous along Tinkune-Koteshwor, Koteshwor-Jadibuti, Manohara-Kaushaltar, and Gatthaghar-Sallaghari-Pandubajar road sections of Araniko Highway than Ringroad, Tribhuwan highway and other urban roads. This is particularly due to presence of on-road or roadside obstacles like dividers, traffic island, railing, trees, poles etc. resulting in severe vehicle damage and injuries. The high risks of hit object type collisions persists due to indiscriminate encroachment of right of way and mixed land use setting in the Valley.

Likewise, the critical hotspots for the pedestrian related crashes appear to be more continuous along Ring Road, Araniko Highway, Tripureshwor-Kalimati-Kalanki, Tripureshwor-Lainchaur-Balaju, Thapathali-Ekantakuna and Maitighar-Putalisadak road sections. These particular stretches experience a significant volume of both

vehicular and pedestrian traffic, and show proximity to markets, residential, institutional (hospital, schools, colleges etc.), and commercial establishments. In these roadways, the most frequent places of occurrences are at intersections, bus stops and parts of streets that have pedestrian crossings and narrow walkways. Additionally, the absence of pedestrian sidewalks, zebra-crossings, overhead bridge and other essential pedestrian safety requisites like guardrails contributes to the pedestrian collision risks.

In the case of multiple collisions, the high intensity clusters are observed to be contiguous segments of the principal highways and urban roads mentioned earlier. The high risks zones for this type of collision are marketed by heavily congested traffic, including both vehicular and pedestrian movements. In heavy traffic conditions, a single vehicle collision can produce domino effect leading to series of crashes.

4.4.4 Spatial Factors

The spatial distribution of traffic crashes in the Valley might be influenced by certain spatial factors, including population density, and patterns of urban land use. Tables 4.20 through 4.22 represent the variation of crashes and hotspots according to these three spatial determinants.

A. Hotspots by Population Density

The study area is divided into local administrative zones to explore the connection between crash incidents, hotspot occurrences and population density. From table 4.20, it is evident that administrative regions with a significant population density experience intensive traffic crash. Consequently, Kathmandu Metropolitan City and Lalitpur Metropolitan City are the most vulnerable local levels with greatest number of high crash risk clusters at 54.63% and 17.57% respectively. The Chandragiri Muncipality, Suryabinayak Municipality, Madhyapur Thimi Municipality, Nagarjun Municipality and Tokha Municipality circumscribing these critical zones, also represent a significant present of hotspot segments at 6.18 %, 4.63 %, 4.63 %, 4.25 % and 4.05 % respectively.

Table 4.20 Hotspot Clusters and Population Density

Local Level	Population Density	Crash Count	Crash (%)	Hotspot Clusters	Hotspot Length (m)	Hotspots (%)
Kathmandu	17440.51	11981	51.00	283	30269.31	54.63
Lalitpur	8143.12	3580	15.24	91	12488.48	17.57
Chandragiri	3116.35	1541	6.56	32	5374.87	6.18

Local Level	Population Density	Crash Count	Crash (%)	Hotspot Clusters	Hotspot Length (m)	Hotspots (%)
Suryabinayak	3300.26	918	3.91	24	3828.94	4.63
Madhyapur Thimi	10779.45	1216	5.18	24	4570.19	4.63
Nagarjun	3867.66	892	3.80	22	2120.94	4.25
Tokha	7816.52	899	3.83	21	2570.33	4.05
Kirtipur	5527.32	543	2.31	9	798.60	1.74
Bhaktapur	12072.89	361	1.54	6	943.75	1.16
Budhanilakantha	5103.15	428	1.82	2	131.38	0.39
Tarakeshwor	4334.62	276	1.17	2	2671.29	0.39
Kageshwori Manahora	4765.48	147	0.63	1	96.67	0.19
Mahalaxmi	4645.86	70	0.30	1	1000.64	0.19
Changunarayan	254.05	132	0.56	0	0	0
Dakshinkali	617.90	136	0.58	0	0	0
Godawari	1015.90	184	0.78	0	0	0
Gokarneshwor	2554.49	138	0.59	0	0	0
Shankharapur	667.71	51	0.22	0	0	0

The linear regression model depicted in figure 4.25 indicates that the frequency of hotspots rises as population density increases, as evidenced by the positive slope coefficient. The model demonstrates moderate representativeness of hotspot occurrences based on population density. The R^2 statistic reveals a moderate goodness of fit, with 53.17% of the variation in hotspots explained by population density. This result is quite rational as local levels with higher population density tend to have a greater concentration of road networks and more frequent trips to socio-economic facilities.

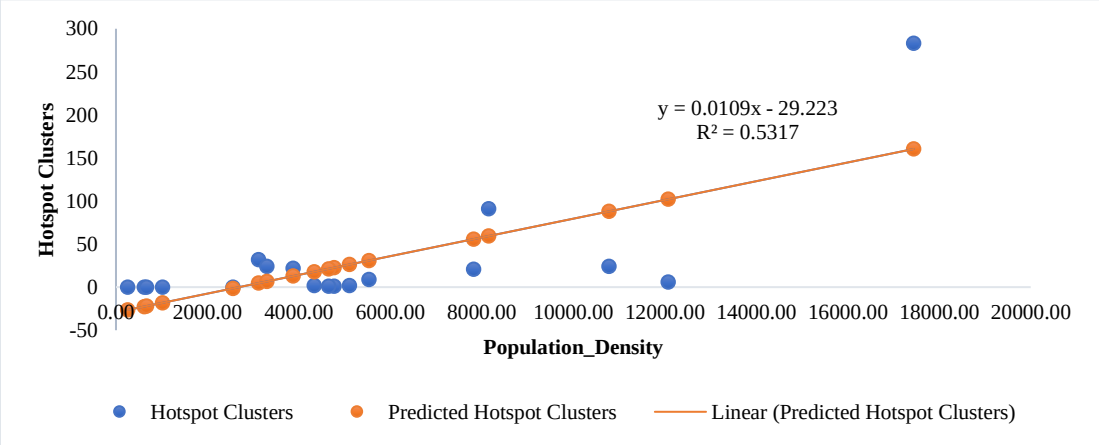

Figure 4.25 Correlation of Hotspots and Population Density

B. Hotspots by Land Use

Landuse is a critical environmental factor that determines the distribution of socio-economic activity, traffic flow pattern and likelihood of crashes. The connection between the type of adjacent land use, the frequency of crashes, and the prevalence of hotspots is illustrated in table 4.21. The data presented in the table suggests that areas of residential and commercial uses, which naturally attracts higher traffic movement, are more prone to crash incidents. About 90% of the total crashes are evident in the residential, commercial or residential-commercial mix neighborhoods. This positions residential and commercial uses as significant contributors to the number of hotspot locations at 80.79% and 70.20% respectively. The public space that incorporates governmental, educational, health, recreational and other service-related areas, is also identified with higher occurrences of crashes at 15.14% and hotspots at 24.17%. On the other hand, the emergence of hotspots are quite low in cultural and archeological, riverine, lake and marsh area, agricultural forest and industrial landuse zones with numbers ranging from 2% to 7%.

Table 4.21 Hotspot Clusters and Land Use Classes

Land Use Class	Area sq.km	Crash Count	Crash (%)	Crash/ Area	Hotspot Cluster	Length (m)	Hotsp-ot (%)	Hotspot /Area
Residential	142.71	22022	94.52	154.31	244	33377.54	80.79	1.71
Commercial	7.10	5412	23.23	761.89	212	28007.89	70.20	29.84
Public Use	48.26	3527	15.14	73.09	73	10085.17	24.17	1.51
Cultural and Archeological	1.29	526	2.26	408.02	20	2851.48	6.62	15.51
Riverine, Lake and Marsh Area	9.74	629	2.70	64.58	20	3835.17	6.62	2.05
Agricultural	242.52	1538	6.60	6.34	15	3957.01	4.97	0.06
Forest	211.74	470	2.02	2.22	8	1737.03	2.65	0.04
Industrial	9.46	268	1.15	28.34	7	815.92	2.32	0.74
Mine and Minerals	0.01	0	0.00	0	0	0	0.00	0
Others	0.29	0	0.00	0	0	0	0.00	0

To facilitate the cross-comparison across land use categories, the crashes and hotspots per sq.km of the area are also estimated in the table 4.21. The commercial landuse category has the highest frequency with 761.89 crashes per sq.km and 29.84 hotspots per sq.km. The business areas experience crashes more than 4 times, and high-risk clusters more than 17 times than those produced by residential uses. The cultural and archeological zones also report a considerable crash rate and hotspot occurrences with

408.02 and 15.51 counts per area respectively. This zone encounters crashes over 3 times as frequently, and hotspots more than 9 times compared to residential regions. Lands used for residential and public services show similar frequencies of hotspots per area, with 1.71 and 1.51 per sq.km respectively. The area surrounding the water bodies has comparatively higher hotspot occurrence than residential and public land uses. As with the presence of agricultural, forest, industrial and mining lands, these have a lower effect on per area calculations of crash and hotspot counts because these land types are less likely to have frequent traffic. They contribute to a lower number of crashes per sq.km when compared to previously mentioned land use areas which are more densely populated or trafficked.

4.5 Temporal Analysis

The analysis focused on finding the patterns of hotspot occurrences from the temporal classifications of year, season, day and hour. The detailed findings and discussions of the temporal analysis are presented in sub-sections below, and the sample output maps are attached in Appendix A (Getis-Ord Gi* Maps) and Appendix B (KDE Maps):

4.5.1 Yearly Aggregation

As depicted in figure 4.26, the yearly aggregated crash datasets showed a pattern of clustering with Moran's I values indicating positive autocorrelation: 0.22 for year 2019, 0.15 for year 2020, and 0.18 for year 2021. The spatial arrangement of the crashes is statistically significant, as demonstrated by the positive z-scores: 29.75 for year 2019, 22.15 for year 2020, and 25.48 year for 2021. These findings allow to confidently reject the null hypothesis, leading to the conclusion that the yearly datasets exhibit a clear pattern of clustering.

The significant clusters of hotspots as produced using the Getis-Ord Gi* statistics technique over various years are shown in figure 4.27. From the figure, it is apparent that the hotspots emerge at junctions, curves and straight stretches along Ring Road, Araniko Highway, Tribhuwan Highway, Kalanki-Tripureshwor road, Balkhu-Kalimati road, Balkhu-Chobhar road, TU gate-Kritipur Ringroad, Thapathali-Tripureshwor-Sorakhutte-Balaju (Ringroad) road, Lainchaur-Maharajgunj road, Samakhusi-Tokha road, Maharajgunj-Budhanilkantha road, Chabahil-Pipalbot road, Thapathali-

Jawlakhel-Ekantakuna-Tikabhairab road, Nakhudobato-Nakhu Chowk road, Satdobato-Godawari road, Jadibuti-Pepsicola road, and Satdobato-Sunakoti-Lele road throughout three years. The annual hotspot maps reveal fluctuations in both the location and extent of these hazardous road segments, with 279 segments totaling 36,735.53 m in 2019, 278 segments totaling 38,359.22 m in 2020, and 297 segments totaling 41,783.12 m in 2021, all identified as hotspots with a 99% confidence level. There are 124 number of persistent hotspots across three years' analysis period with total length of 20390.59 m. In the consecutive years of 2019 and 2020, 170 consistent hotspots are recognized, spanning 25,255.19 m, and from year 2020 to 2021, 169 common hotspots are observed, extending 26,515.54 m.

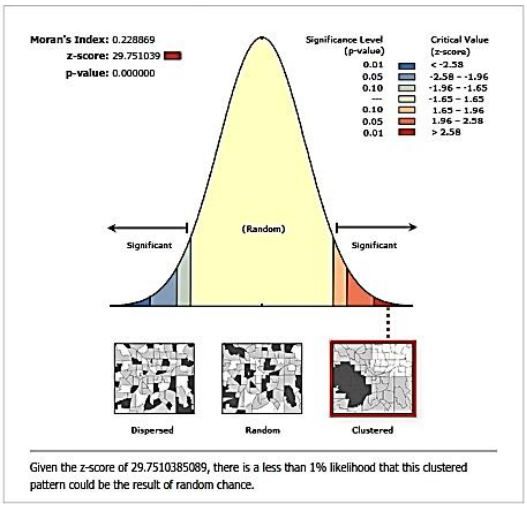

(a) 2019

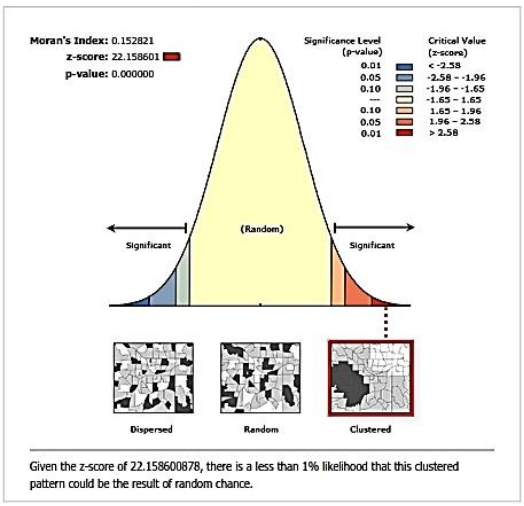

(b) 2020

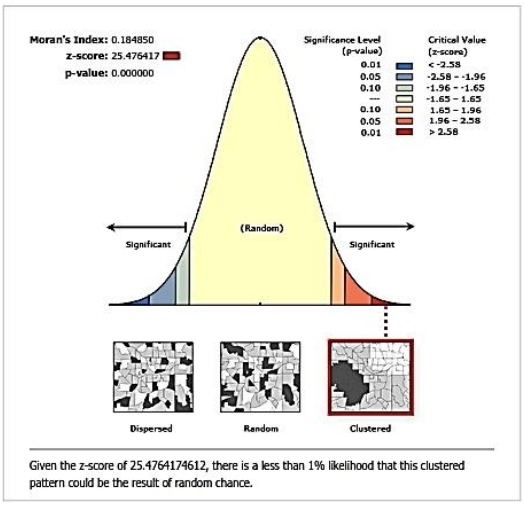

(c) 2021

Figure 4.26 Spatial Autocorrelation Report for Yearly Datasets

Remarkably, there is increase in the extent of hotspot segments with a high level of statistical significance over the three years. This may be credited to the major road

infrastructure upgradation works during that period, namely Tripureshwor, Teku, Maharajgunj, Kalanki underpass, Baluwatar, Bhadrakali, Ratnapark, Singhadurbar, Babarmahal, New Baneshwor, Koteshwor, New BusPark to Kuleshwor (Bishnumati Corridor), and many road section improvement projects were completed in 2021 except Kalanki-Maharajgunj-Chabahil (Dhobikhola).

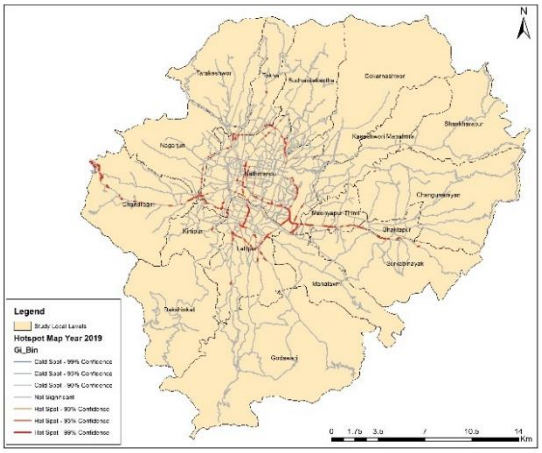

(a) 2019

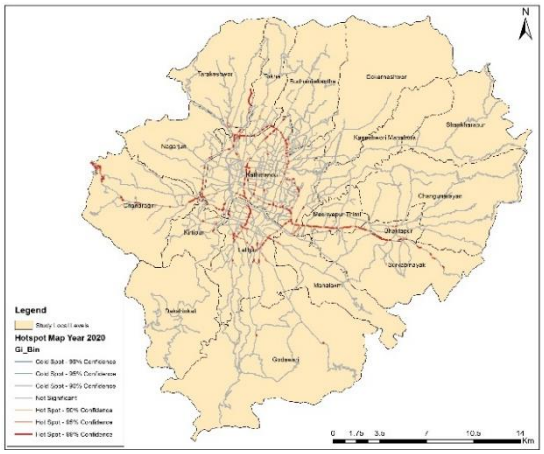

(b) 2020

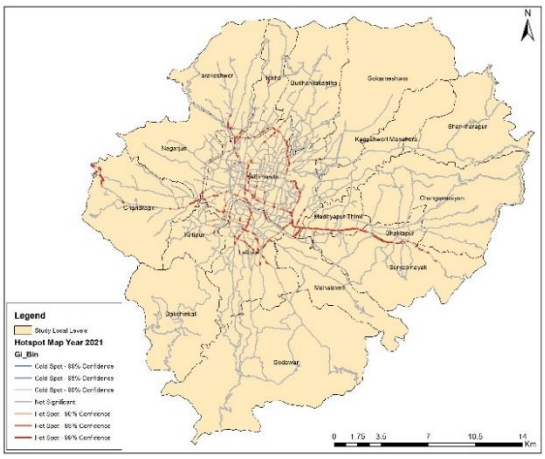

(c) 2021

Figure 4.27 Hotspots Analysis Maps for Yearly Datasets

In figure 4.28, a spatial distribution of hotspots for the analysis years is depicted using the KDE technique. Specifically, the crash density surface related to year 2019 varies from 453.042 to 3171.299 points per sq.km, the density for year 2020 ranges from 151.192 to 1058.341 points per sq.km and the density for year 2021 spans from 201.584 to 1410.946 points per sq.km. These density values provide insights into the concentration pattern of hotspots in different years.

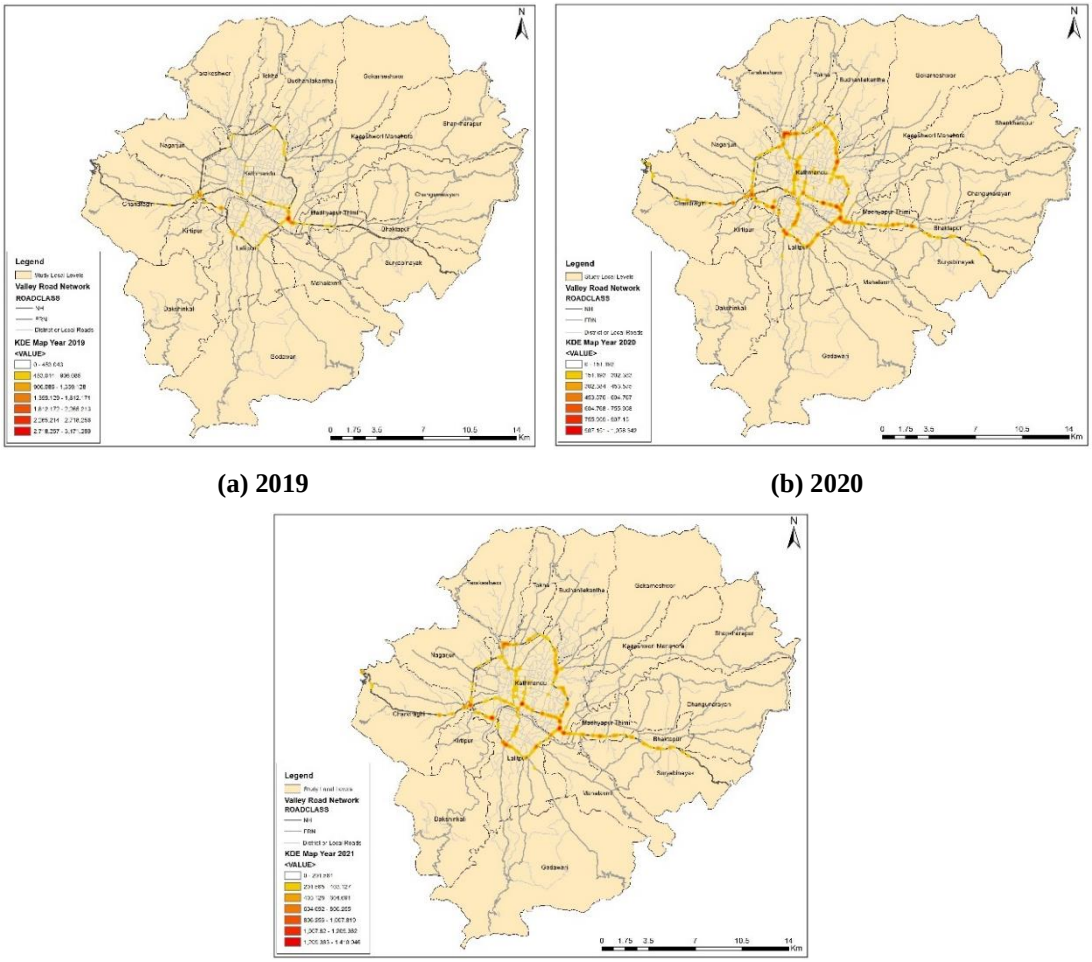

(a) 2019 **(b) 2020**

(c) 2021

Figure 4.28 KDE Maps for Yearly Datasets

The crash density maps from this method identified critical hotspot areas similar to those detected using Getis-Ord Gi* Statistics, however, the KDE approach resulted in fewer hotspot segments compared to figure 4.27. From a comparative analysis of all Getis-Ord Gi* and KDE hotspot maps, the following differential patterns are identified for yearly datasets.

i) 2019: In the year 2019, less clusters are evident across the Kathmandu Valley at New Baneshwor-Tinkune, Tinkune-Koteshwor, Koteshwor-Jadibuti, Chabahil-Sukedhara, Koteshwor-Balkumari, Gwarko-Satdobato, Ekantakuna-Nakkhudobato, Balkhu-Kalanki, Thapathali-Jawlakhel and Kaushaltar-Chardobato road sections. The Kalanki-Thankot and Sallaghari-Hanumante road sections also show isolated patches of hotspots. During this period, the widened Koteshwor-Kalanki section (10.5 km) was newly opened to traffic and is observed to witness high crashes which may be due to lack of dividers, traffic lights, and pedestrian/cyclist friendly facilities.

ii) 2020: The concentration of crash hotspots increased in the year 2020, and clusters appeared as more continuous segments than that of the year 2019 along the Ring Road, Araniko Highway, Thapathali-Ekantakuna road and Tripureshwor- Balaju road. The crash hotspots peaked in the year 2020 probably due to many undergoing constructions or upgradations in various roads of the Valley. The patches of hotspots seem to be increasing towards the northern valley roads mainly along the Ring Road section of Gausala-Sukedhara-Basundhara-Machhapokhari-Balaju area and feeder roads connecting to this core road section such as Maharajgunj-Budhanilkantha and Maharajgunj-Lazimpat roads.

iii) 2021: The intensity of hotspots decreased slightly in the year 2021 as many upgradation projects were completed and safety enhancements operations were carried out during that period. The concentration of hotspot locations is more discontinuous along Balkhu-Kalanki, Dhumbarahi-Basundhara-Machhapokhari-Balaju, Thapathali-Jawlakhel-Ekantakuna, Nagdhunga-Kalanki and Sallaghari-Hanumate Culvert road sections than that of the year 2020. The results also coincide with the traffic crash heat map analysis performed by JICA Project for Introduction of Urban Transport Management in Kathmandu Valley, 2023. In contrast to the analysis by JICA, the intensity of crashes is more pronounced along Sinamangal-Gairigaon, Ekantakuna-Nakkhu Dobato, Chappro- Jadibuti, Dhungeadda, Naikap and Sallaghari-Jagate areas. This discrepancy may be due to consideration of larger road network and calendar year-based analysis in this thesis. These additional areas highlight the need for targeted safety measures in those specific regions.

4.5.2 Seasonal Aggregation

Based on reference to previous articles on temporal analysis and the classification defined by the Department of Hydrology and Meteorology, the crash data is disaggregated into four seasonal bases as Pre-Monsoon (February 15 – June 30), Monsoon (June 15 – September 30), Post-Monsoon (September 15 – December 31) and Winter (December 15 – February 28). Every seasonal dataset shares a transitional period of 15 days that overlap with the preceding season.

The results of spatial autocorrelation test for each seasons showed a pattern of clustering, as depicted in figure 4.29. The Moran's I values are positive across all

seasons: 0.21 for Pre-monsoon, 0.21 for Monsoon, 0.19 for Post-monsoon, and 0.19 for Winter crashes. The z-values, which test the statistical significance of the spatial distribution, are also highly positive: 26.28 for Pre-monsoon, 26.96 for Monsoon, 21.47 for Post-monsoon, and 26.20 for Winter crashes. These results allow us to confidently reject the null hypothesis, affirming that the seasonal crash dataset is not randomly dispersed but rather exhibits a clear pattern of clustering.

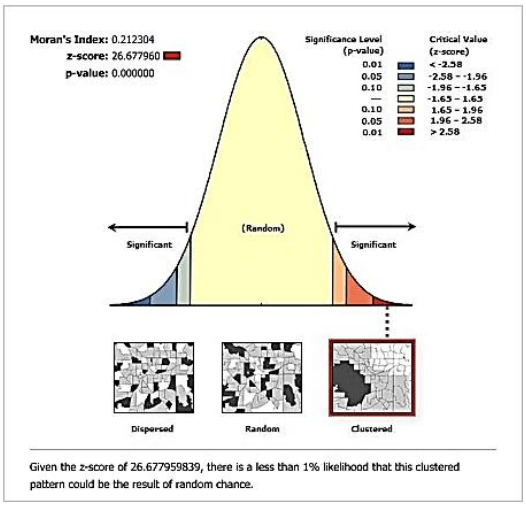

(a) Pre-Monsoon

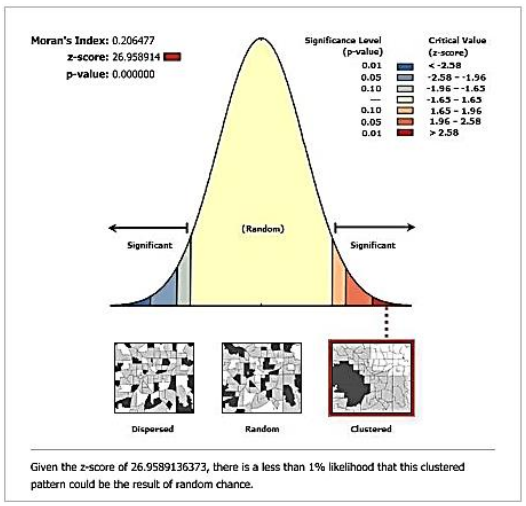

(b) Monsoon

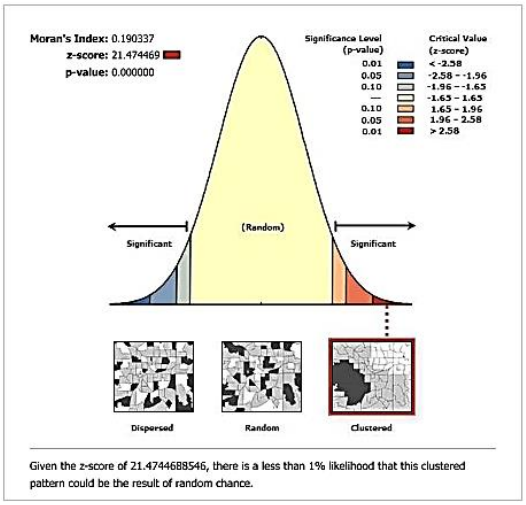

(c) Post-Monsoon

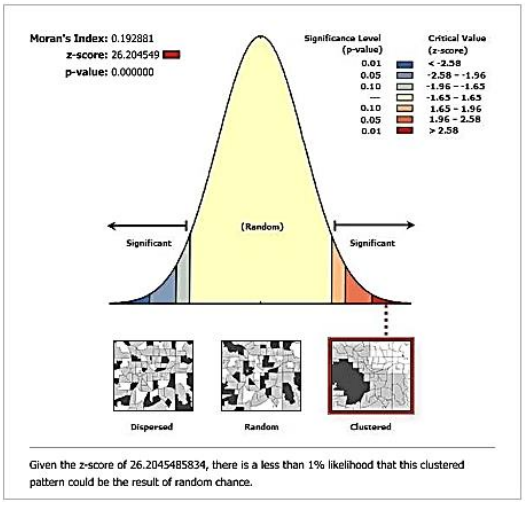

(d) Winter

Figure 4.29 Spatial Autocorrelation Report for Seasonal Datasets

Figure 4.30 showcases significant clusters of crashes for different seasons, as determined by Getis-Ord Gi* statistics. Pre-monsoon dataset exhibits a GiZ-score variation from −0.58 to 22.42 and a GiP value range of 0 to 0.99966. Monsoon crashes display a GiZ-score range from −0.54 to 21.82 and GiP values from 0 to 0.99971. Post-monsoon dataset is characterized by a GiZ-score from −0.56 to 20.37 and GiP values between 0 and 0.99983. Winter season has a GiZ-score ranging from −0.55 to 24.30

and GiP values from 0 to 0.999907. These high positive GiZ-scores coupled with a low GiP value indicate a significant cluster of crashes in all seasons.

The analysis identified 300 segments as significant hotspots during pre-monsoon period, 295 segments for monsoon period, 275 segments for post-monsoon period, and 282 segments for winter period, all at a 99% confidence level (i.e. Bin 3). The analysis resulted in hotspot road segment lengths of 39359.18 m, 39780.17 m, 41352.60 m and 38116.14 m, respectively, for these seasons. The number and length of hotspots correspond to the recorded traffic crash figures (table 4.1) meaning that a rise in crashes correlates to an expansion of hotspot lengths, and conversely, a decrease in crashes leads to a reduction in hotspot lengths. The hotspots are similarly distributed in all the seasons, as depicted in figure 4.30, with no discernible trend in the clustering of hotspots over the seasons (i.e., no clear increase or decrease). In totality, 132 number of common segments are recognized across all seasonal datasets with the concentration primarily in the Ring Road, Araniko Highway, Tribhuwan Highway, Kalanki-Tripureshwor road, Balkhu-Kalimati road, Balkhu-Chobhar road, Thapathali-Tripureshwor-Sorakhutte-Balaju road, Lainchaur-Maharajgunj road, Samakhusi-Tokha road, Maharajgunj-Budhanilkantha road, Thapathali-Jawlakhel-Ekantakuna-Tikabhairab road, Nakhudobato-Nakhu Chowk road, Satdobato-Godawari road, and Jadibuti-Pepsicola road.

Some exclusive segments for monsoon period are identified along Maharajgunj-Budhanilkantha, Nepaltar-Jarankhu, Satdobato-Dhapakhel, Satdobato-Tikabhairab, Tripureshwor-Kalanki, Maitighar-Bhadrakali, Gyaneshwor-SanoGaucharan, and Lazimpat-Maharajgunj road sections. Some exclusive segments have also been identified for different seasons. For instance, KMC Hospital (Sinamangal road), Nagdhunga busstop (Thankot-Nagdhunga road), and Patan Industrial Estate busstop (Lagankhel-Satdobato) are observed as unique hotspots in Pre-Monsoon. Monsoon period shows seasonal hotspot occurrences in Jarankhu, Padmodaya School, Loktantrik chowk (Satdobati-Khumaltar road), Chapali (Maharajgunj-Budhanilkantha road), National Agronomy Research Center (Satdobato-dhapakhel), Maitighar-Bhadrakali road and Gyaneshwor chowk. The seasonal hotspots for Post-Monsoon period lies in Sankhamul-unpark road, Bhatbhateni-Baluwatar road, and Tokha-Jhor road. Winter

exclusive hotspots at Sanepa chowk, Singhadurbar Chowk and Boudha stupa (Chabahil-Pipalbot road).

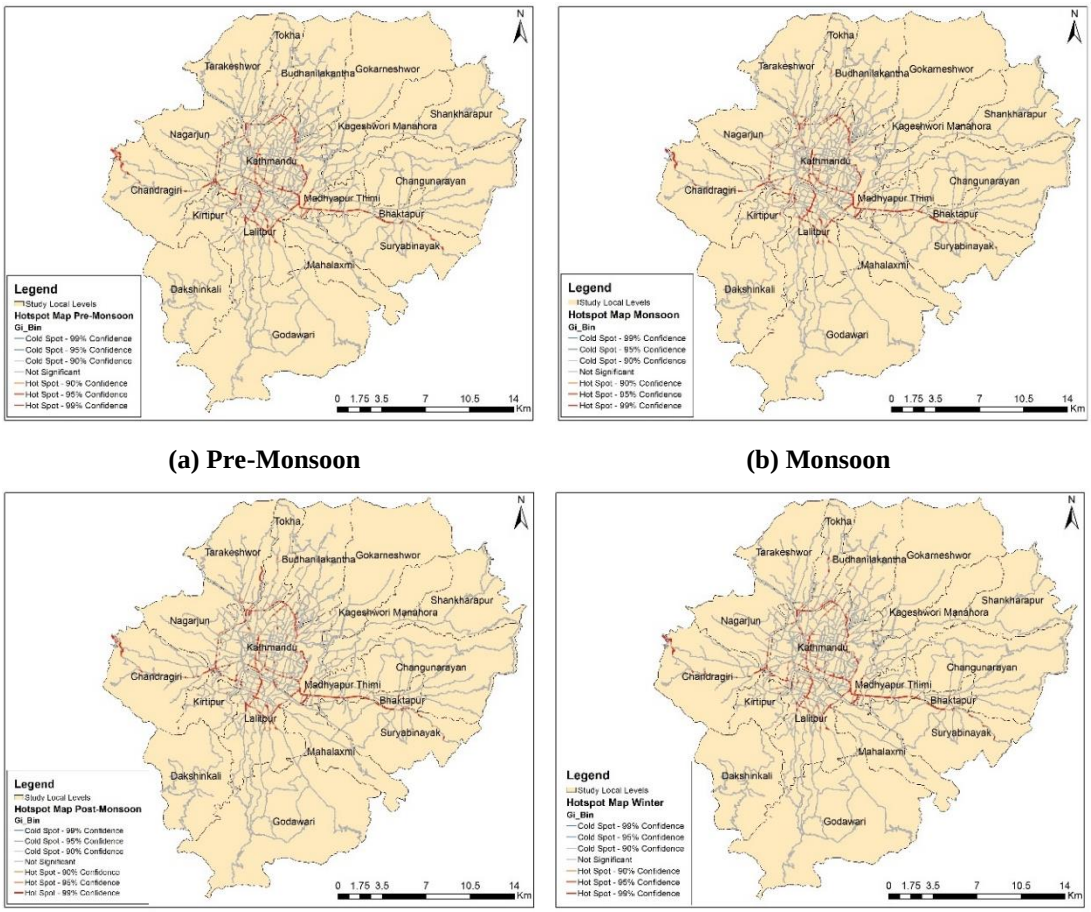

(a) Pre-Monsoon **(b) Monsoon**

(c) Post-Monsoon **(d) Winter**

Figure 4.30 Hotspots Analysis Maps for Seasonal Datasets

Figure 4.31 illustrates the spatial distribution of hotspots over the analysis seasons using the KDE method. The crash density surface for the Pre-Monsoon fluctuates between 230.231 and 1611.618 points per sq.km, for the Monsoon, the density ranges from 196.706 to 1376.94 points per sq.km, for Post-Monsoon, it extends from 251.788 to 1762.511 points per sq.km, and for Winter, it varies from 216.256 to 1513.789 points per sq.km. From observation of KDE maps of all seasons, there is less variation in hotspot locations due to seasonal changes, directly leading to conclusion that season is much less of a concern in occurrence of hotspots in Kathmandu Valley.

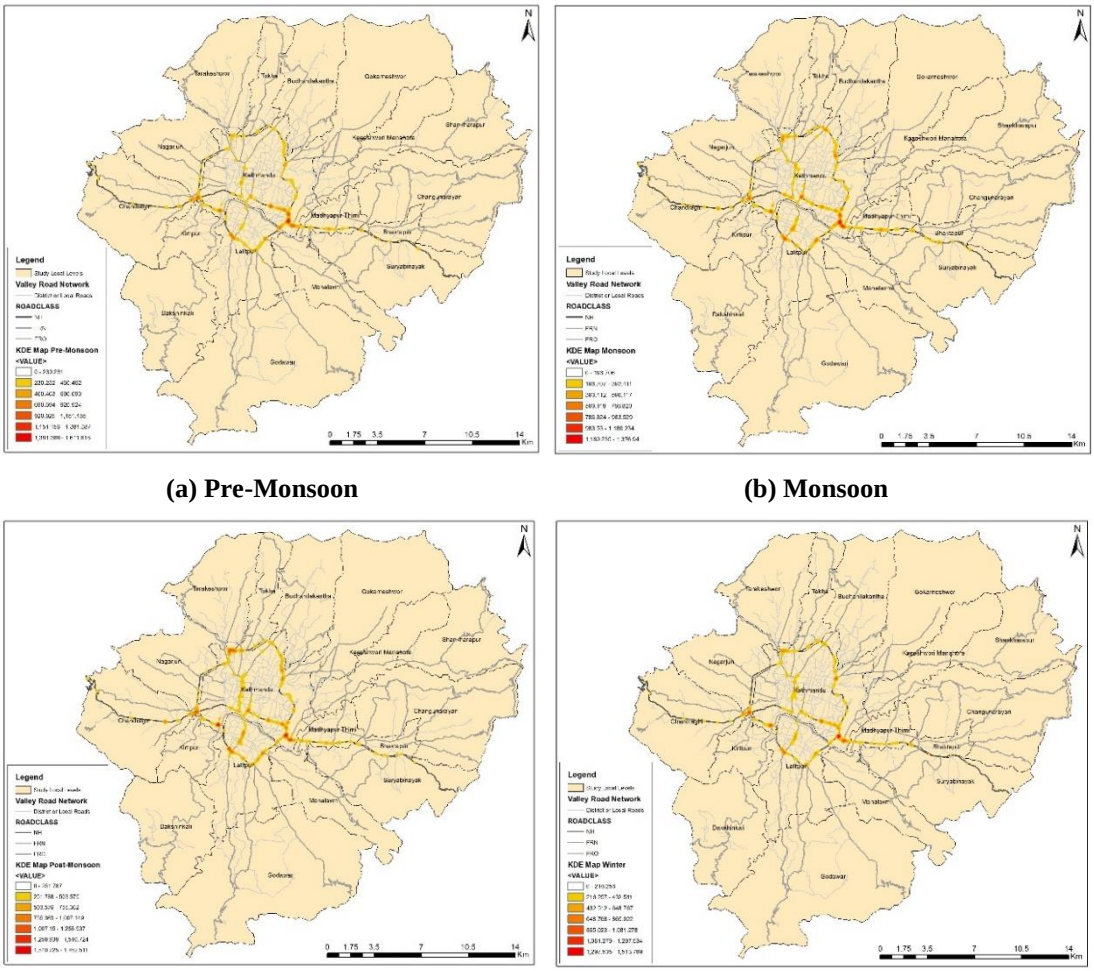

(a) Pre-Monsoon **(b) Monsoon**

(c) Post-Monsoon **(d) Winter**

Figure 4.31 KDE Maps for Seasonal Datasets

From the comparative evaluation of KDE maps, the following distinct patterns are identified with subtle change according to seasons of the year.

i) Pre-monsoon: There is a considerable number of hotspots in premonsoon season at many sections throughout the Ring Road, Araniko Highway, Tribhuwan Highway and major roadway links. The concentration in more dominant at New Baneshwor, Koteshwor, Tinkune, Balkumari, Jadibuti, Kaushaltar, Chardobato, Radheradhe, Gwarko, Satdobato, Ekantakuna, Balkhu, Kalanki, Dhudgeadda, Macchapokhari, Sukedhara, Chabahil, Maitighar and Newroad areas. As the premonsoon season is the season with no seasonal disturbances like fog or mist of winter, slipper roads and potholes of monsoon regions, such crashes can be attributed to reckless driving, crashes due to driver behavior or any other similar non-road element causes.

ii) Monsoon: During the monsoon season, there is a notable number of hotspots on various segments of the major roadways stated earlier in pre-monsoon season. For instance, there is a decrease in hotspots at the Koteshwor-NewBaneshwor junction, but an increase in the Kupondole-Ekantakuna, Maitighar-Singhadurbar and Macchapokhari-Balaju section areas. Additionally, significant hotspots are observed at Tripureshwor, Teku, Maharajgunj, Samakhusi, Naikap area and Thankot Pass. The monsoon season brings challenges such as slippery roads, heavy rainfall, and potholes, which can lead to vehicular crashes primarily due to these adverse driving conditions (visibility), potholes, slippage and flooding.

iii) Post-monsoon: The post-monsoon season sees a significant number of hotspots across various sections of major roadways, with some fluctuations such as continuous hotspots at Gaushala-Sinamangal, Sundhara-Durbarmarg and Maitighar-Thapathali-Kupondole sections. Given that this season coincides with festivals and vacations, it is often considered the most picturesque time of the year, and consequently, there is an expectation of an increase in crashes involving non-motorized vehicles and pedestrian crashes. The festive atmosphere, coupled with heightened street activity and instances of late-night drinking and driving, could contribute to the higher incidences of s single-vehicle crashes.

iv)Winter: A substantial number of hotspots are observed across various sections of major roadways during winter season, which coincides with post-monsoon pattern. This season is characterized by disturbances such as fog or mist during late nights and early mornings. These conditions further necessitate a disintegrated analysis on the time-of-day crashes and crashes related to driver behavior or any other similar non-road element causes.

4.5.3 Weekly Aggregation

In the weekly analysis, the crash data of six days from Sunday to Friday were categorized into weekdays and Saturday grouped into weekends. Both the weekday and weekend type datasets revealed a clustered pattern, as illustrated in figure 4.32, with positive Moran's I value of 0.13, and 0.18 respectively for weekdays, and weekend crashes. The respective positive Z-scores of 11.12, and 41.48 confirm the statistical significance of the spatial pattern of the weekday and weekend crashes. The null

hypothesis can be confidently dismissed, affirming that the weekly datasets show a clear pattern of clustering.

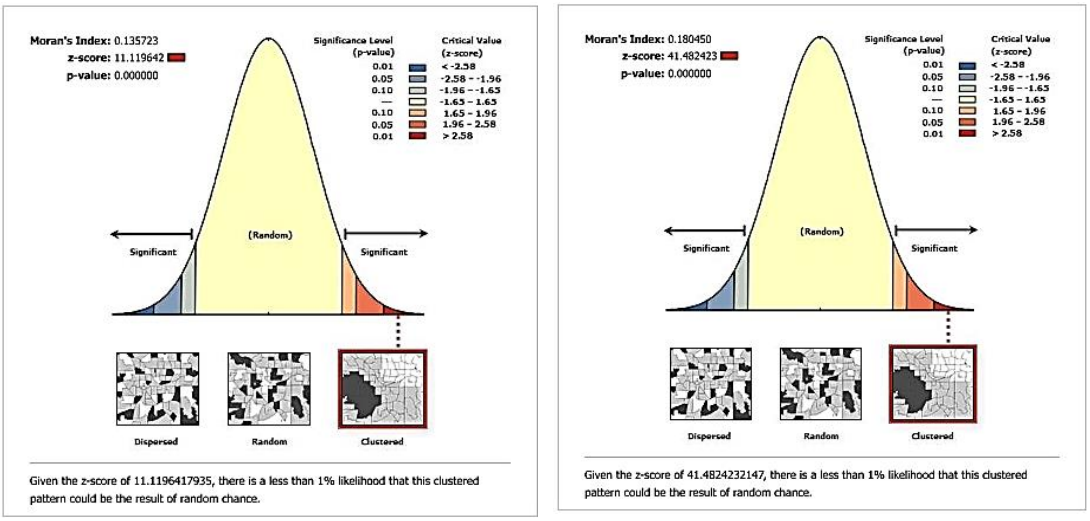

(a) Weekdays **(b) Weekend**

Figure 4.32 Spatial Autocorrelation Report for Day of Week Datasets

Figure 4.33 illustrates the significant clusters of crashes identified through the application of Getis-Ord Gi* statistics for the weekly analysis. The dataset for weekdays shows a range of Gi*Z-scores from −0.597 to 19.59 and Gi*p-values from 0 to 0.999928. For weekend incidents, the Gi*Z-scores vary from −0.54 to 18.16 with Gi*p-values spanning 0 to 0.999524. The presence of high positive Gi*Z-scores in conjunction with low Gi*p-values signifies substantial clusters of crashes throughout in weekdays and weekend.

The Getis-Ord Gi* analysis pinpointed equal number of segments (299) as significant hotspots during the weekdays and the weekend period, both at a 99% confidence level (i.e., Bin 3). The lengths of the hotspot road segments are determined to be 40,377.26 m for weekdays and 40,253.07 m for weekends. Of these, 206 segments with collective length of 30,255.47 m are identified as common hotspots between the two datasets. These common segments are predominantly located along major roadways such as the Ring Road, Araniko Highway, Tribhuwan Highway, Shahidgate-Lainchaur, Lainchaur-Maharajgunj, Tripureshwor-Kalanki, Thapathali-Jawlakhel, Jadibuti-Pepsicola, Chabahil-Peepalbot, Satdobato-Hattiban, Satdobato-Dhapakhel, Kuleshwor-Balkhu, Durbarmarg-Ghantaghar-Bhadrakali and several other key road sections within the Valley.

The analysis revealed that certain areas showed specific occurrences on weekdays and weekend. For instance, the clusters of weekday crashes are prominent on Maitighar-Tinkune-Koteshwor-Jadibuti-Sallaghari-Jagate section of Araniko Highway, Kalanki-Dhungeadda section of Tribhuwan Highway and Thapathali-Tripureshwor-Sundhara road. The weekends show additional clustering along the roads connecting the core city with cultural and recreational spaces, as in road sections of Dhungeadda-Nagdhunga (Tribhuwan Highway), Jagate-Sanga (Araniko Highway), TU Gate-Kritipur (Nayabazar), Sankhamul-UN Park, Lainchaur-Sorakhutte-Balaju bypass, Satadobato-Godawari-Pulchowki, Balkhu-Chobhar-Dakshinkali, Pepsicola Chowk-Kadaghari, Bhaktapur-ArmyCamp, Samakhusi-Tokha, Maharajgunj-Budhanilkantha and Nepaltar-Dharmasthali.

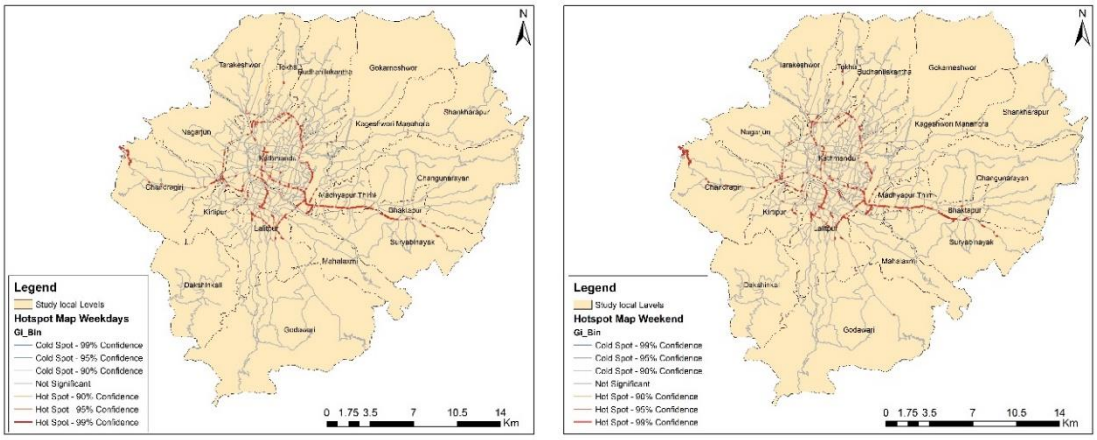

(a) Weekdays **(b) Weekend**

Figure 4.33 Hotspots Analysis Maps for Day of Week Datasets

Figure 4.34 depicts the geographical spread of hotspots throughout the weekdays and weekend, employing the KDE technique.

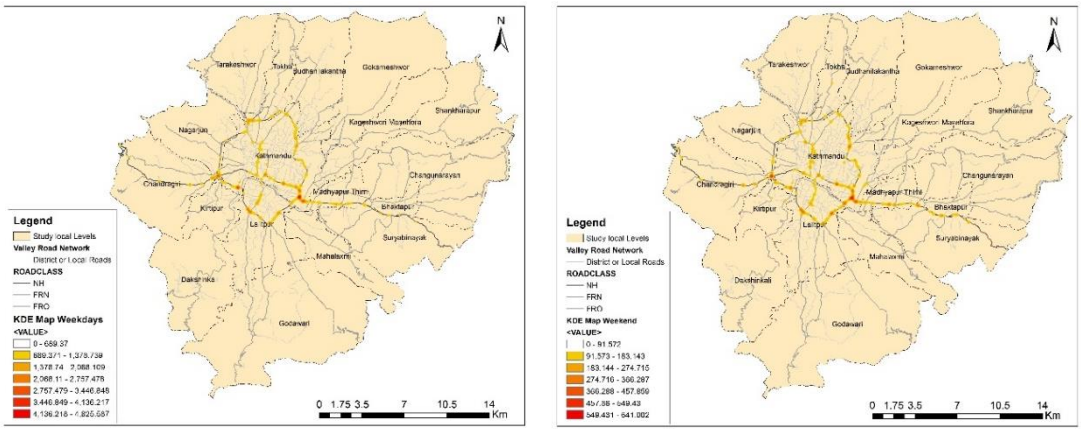

(a) Weekdays **(b) Weekend**

Figure 4.34 KDE Maps for Day of Week Datasets

The crash density surface during the weekdays varies from 689.37 to 4825.587 points per sq.km., and, during the weekend, the density spans from 91.572 to 641.002 points per sq. km. The KDE analysis revealed that certain areas consistently showed a higher number of crashes on specific days.

i) Weekdays: Weekdays have increased crash density around Kalanki, Dhungeadda, Balkhu, Ekantakuna, Kawlakhel, Pulchowk, Thasikhel, Satdobato, Gwarko, Balkumari, Koteshwor, Tinkune, Chabahil, Sukedhara, New Baneshwor, Maitighar, Tripureshwor, Jadibuti, Gatthaghar, Radheradhe, Maharajgunj, Samakhusi and Newbuspark areas. This clustering tendency may be due to heavy commuter traffic on these gateways to major employment and commercial areas during the workdays.

ii) Weekend: On weekend, the hotspots are also located in the areas of weekday crash clusters with some fluctuations such as higher concentrations along Araniko Highway (Lokanthali, Suryabinayak, Jagati), Tribhuwan Highway (Naikap, Gurjudhara, Thankot), Kantipath (Shahidgate, Newroad, Thamel) and Samkhusi-Tokha road (Bhutkhel), TU-Kritipur (Nayabazaar) and Balkhu-Chobhar (Sundarighat) roads. A significant spike in crash density is likely related to weekend activities near junctions or roads near to temples, parks, restaurants and open places.

4.5.4 Time of Day Aggregation

The crash data has been segmented into six distinct time periods throughout the day as Late Night (Midnight to 4 AM), Early Morning (4 AM to 8 AM), Morning (8 AM to Noon), Afternoon (Noon to 4 PM), Evening (4 PM to 8 PM) and Night (8 PM to Midnight). The spatial autocorrelation analysis conducted on these time-specific datasets reveals a strong clustering trend, which is illustrated in figure 4.35. The Moran's I index indicates positive values for all time slots, suggesting a non-random and structured pattern. Specifically, the Moran's I values are 0.08 for late night, 0.13 for early morning, 0.19 for morning, 0.21 for afternoon, 0.22 for evening and 0.19 for night. The z-values are significantly high; 40.68 for late night, 38.09 for early morning, 35.07 for morning, 34.84 for afternoon, 33.29 for evening and 42.56 for night crashes. With these high values the null-hypothesis is rejected, and the clustering pattern is observable, suggesting that there are some factors influencing the crash occurrences and clustering effect across the time of day.

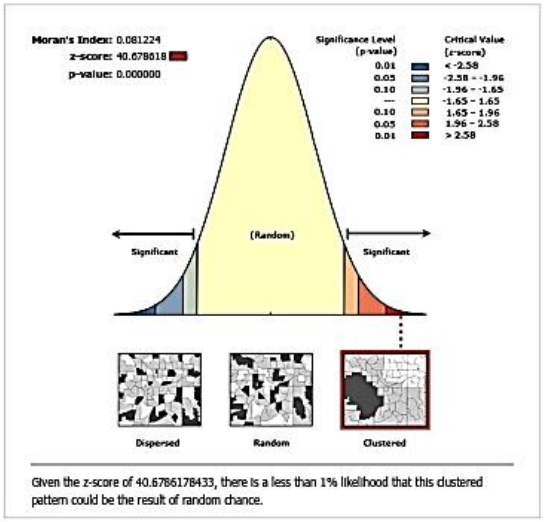

(a) Late Night

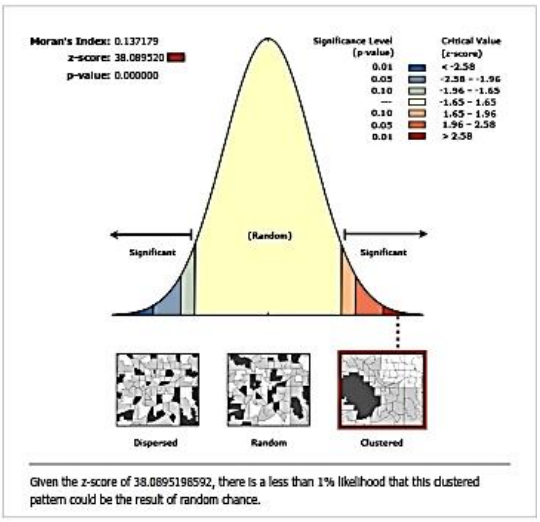

(b) Early Morning

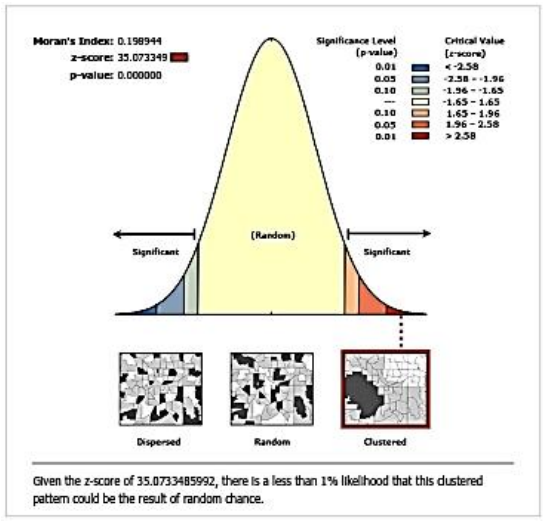

(c) Morning

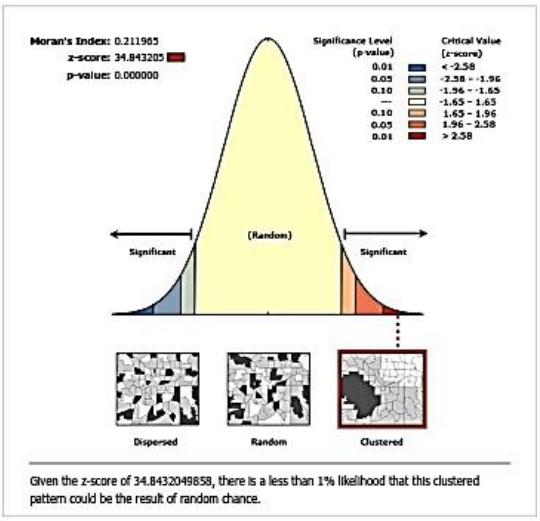

(d) Afternoon

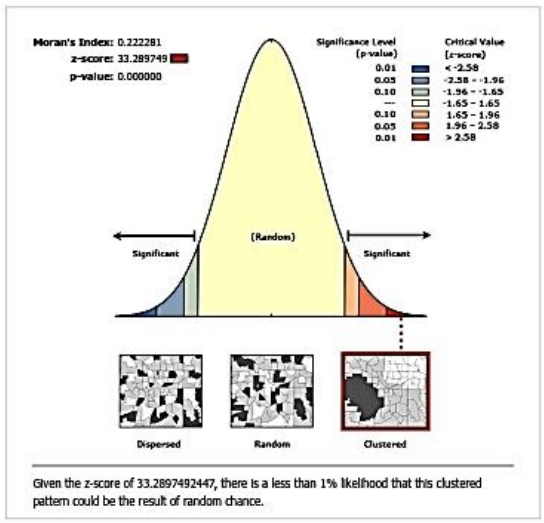

(e) Evening

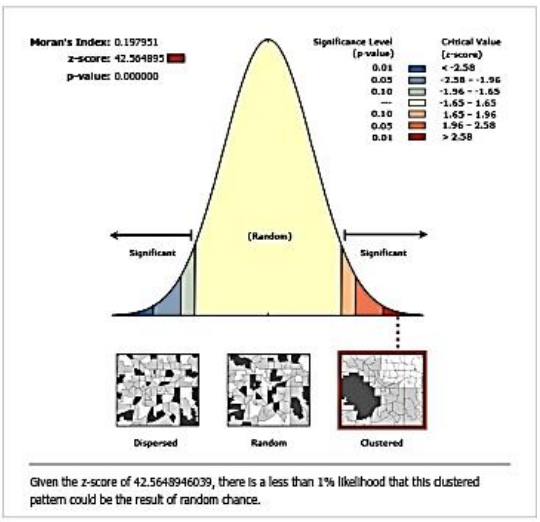

(f) Night

Figure 4.35 Spatial Autocorrelation Report for Time of the Day Dataset

The application of Getis-Ord Gi* statistics produced a statistically significant map (figure 4.36) that highlights clusters of traffic crashes at different time periods. These clusters are identified as high-priority areas with significant spatial distribution at confidence levels of 99%, 95%, and 90%. The analysis has determined the following count and length of significant hotspots at a 99% confidence level (Bin 3) for each time period:

- **Late Night:** 475 segments identified, totaling 51,497.79 m in length.
- **Early Morning:** 344 segments identified, totaling 43,439.97 m in length.
- **Morning:** 288 segments identified, totaling 38,178.70 m in length.
- **Afternoon:** 269 segments identified, totaling 37,060.15 m in length.
- **Evening:** 330 segments identified, totaling 43,896.51 m in length.
- **Night:** 322 segments identified, totaling 42,709.09 m in length.

Figure 4.36 illustrates the discernible trend in the clustering of hotspots over the time of the day, however, there is a noticeable consistency in the distribution of some common hotspots. 76 segments with a combined length of 13,049.12m are common across all the time intervals, and these segments are predominantly located in key roadways like Ring Road (Koteshwor, Kharibot, Gwarko, JRC Chowk, Thasikhel, Kusunti, Ekantakuna, Balkhu, Kalanki, Machhapokhari, Mitranagar, Samakhusi, Basundhara, Chabahil, Sukhedhara,), Araniko Highway (New Baneshwor, Bijuli Bazaar, Tinkune, Koteshwor, Jadibuti, Manohara Bridge, Lokanthali, Kaushaltar, Gatthaghar, Chardobato, NayaThimi, Radheradhe, Srijananagar, Chundevi, Pandubajaar, Bhatedikoor), Tribhuwan Highway (Nagdhunga, Naikap, Dungeadda, Kalanki), Kuleswor-Kalimati (Kuleshwor Ganeshthan), JaiNepal-Thapathali (Putalisadak), Jadibuti-Pepsicola (Pepsicola), Kalanki-Tripureshwor Road (Teku, Tripureshwor), Durbarmarg-Badhadrakali (Jamal/Trichandra Campus), Tripureshwor-Balaju Bypass (Civil Mall, Bhotahiti, Nayabazaar), and Thapathali-Jawlakhel (Kupondole, Pulchowk, Hariharbhawan, Damkal Chowk). Overall, these locations are consistently prone to crashes regardless of the time of day, suggesting that these areas may require targeted safety measures or infrastructure improvements to reduce the frequency of traffic crashes.

The distribution of hotspots is presumed to shift in accordance with the Valley's daily traffic pattern, with variations in both the number and locations of these hotspots

throughout the day. The Valley witnesses a concentration of hotspots along the Ring Road, Araniko Highway and Tribhuwan Highway, and in the urban core road roads encircled by the Ring Road during the morning and afternoon hours. These times are bustling with commuters beginning their travel routines and daily work activities. The hotspots again tend to sprawl along feeder roads and other major roads during the evening rush hour when residents conclude their workday and head home from their places of employment. The traffic congestion and public transportation crowding are at their peak during these time slots. As of night, and late night hours, there is influx of heavy vehicles through vital links between the outer suburban districts and towards the urban core roads of the Valley. The movement of heavy vehicles, coupled with poor lighting and driver fatigue, results in significant collisions during these times.

The late night and early morning hours, typically from 0:00 AM to 4:00 AM and 4:00 AM to 8:00 AM, have the high-risk segments particularly in the suburban areas outside the central Ring Road. The hotspots are noticed in Balkhu-Chobhar-Dakshinkali (Dakshinkali, Pharping, Chovar, Sundarighat), Kritipur-Machegaun (Nagaun), Kritipur RingRoad (Nayabazar), TU road, Ekantakuna-Tikabhairab (Khokana Dobato), Satdobato-Tikabhairab (Thecho), Balkot-Sirutar (Sirutar), Bagmati Corridor (Khahare), Boudha-Narayantar-Sankhu (Grand Norling Resort, Mulpani Tiwari Tol), Mahankal Marg (Arubari), Dhobikhola Road (Gopikrishna, Rudramati Chowk, Baluwakhani), Maharajgunj-Budhanilkantha (Italitar, Rudreshwor) Samakhusi-Tokha-Jhor (Grande Hospital, Bhutkhel, Tokha), Tarkeshwor road (Nepaltar, Dharmasthali) and Nagarkot-Army Camp (Thulo Byasi, Bansbari).

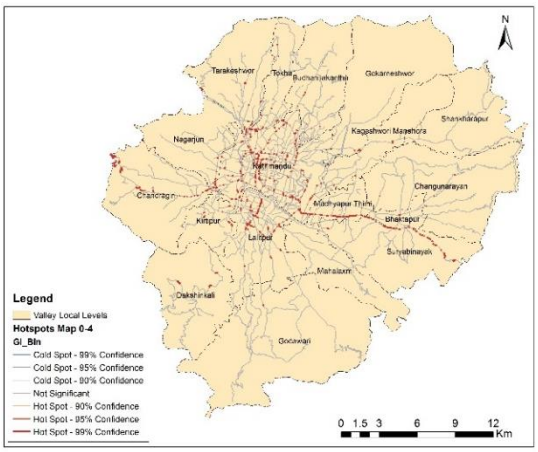

(a) Late Night

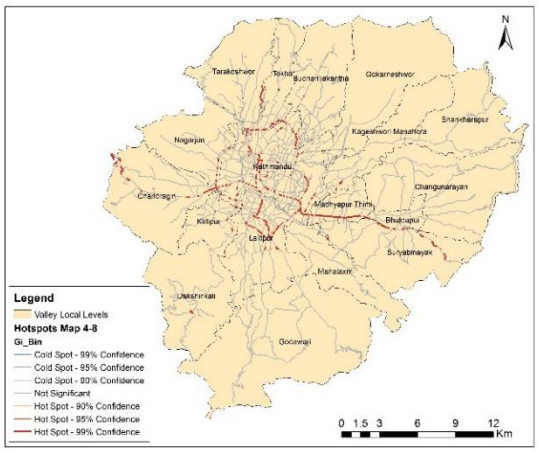

(b) Early Morning

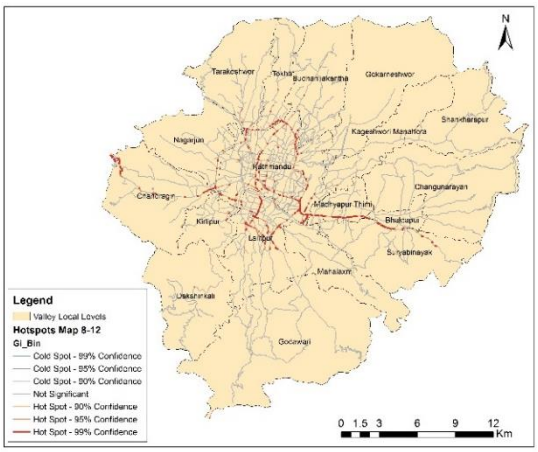

(c) Morning

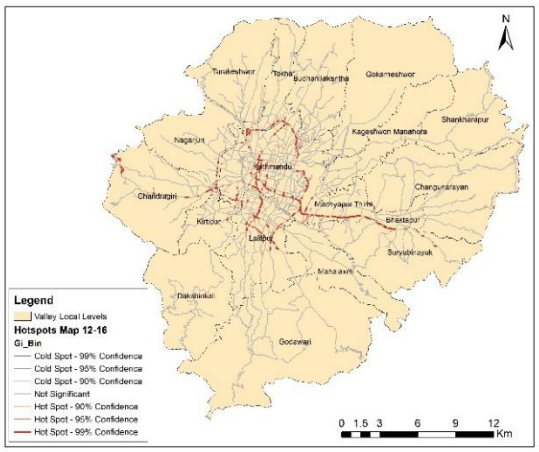

(d) Afternoon

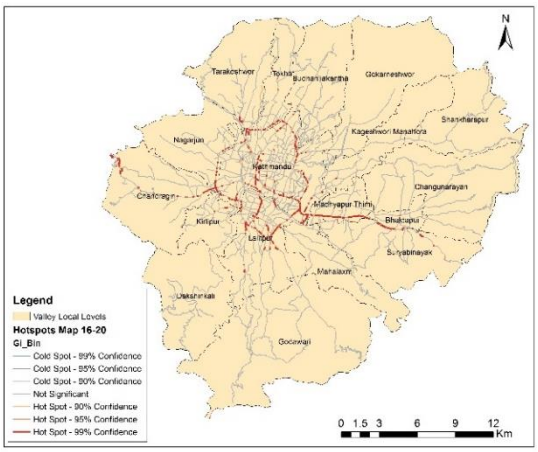

(e) Evening

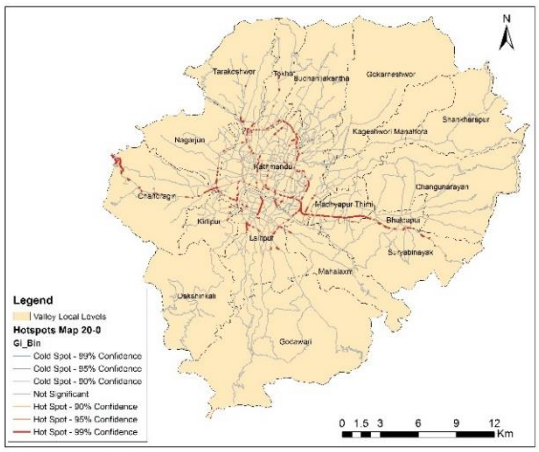

(f) Night

Figure 4.36 Hotspots Analysis Maps for Time of the Day Dataset

Figure 4.37 presents the crash density patterns across various time intervals, as determined by the KDE technique. The crash density surface shows variability across different times of the day with following values:

- **Late Night:** Ranges from 18.057 to 126.402 points per sq.km.
- **Early Morning:** Varies between 65.471 and 458.294 points per sq.km.
- **Morning:** Spans from 149.501 to 1046.504 points per sq.km.
- **Afternoon:** Extends from 175.76 to 1230.318 points per sq.km.
- **Evening:** Ranges from 232.289 to 1626.024 points per sq.km.
- **Night:** Fluctuates between 143.229 and 1002.606 points per sq.km.

The KDE maps analysis throughout the day reveals significant variations in hotspot locations, which fluctuate with the hours of the crashes. This observation leads to the

conclusion that the time of day significantly influences the emergence of hotspots in the Kathmandu Valley.

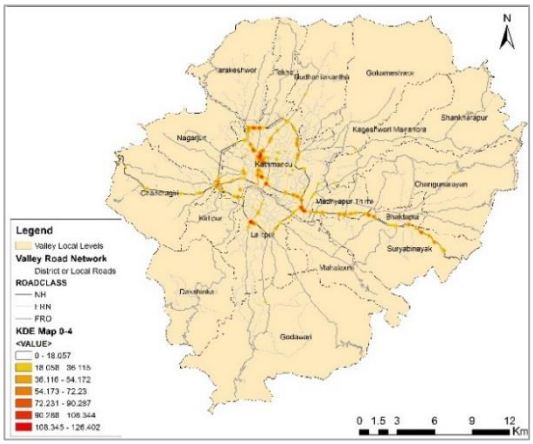

(a) Late Night

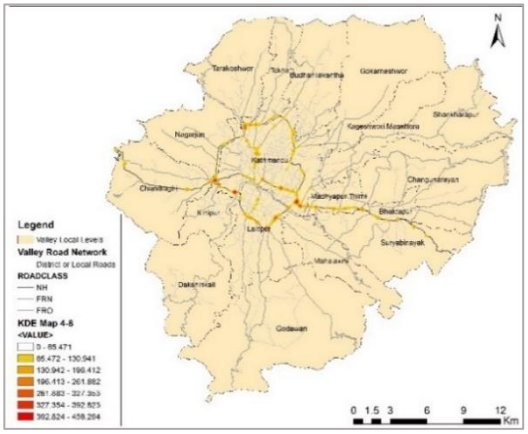

(b) Early Morning

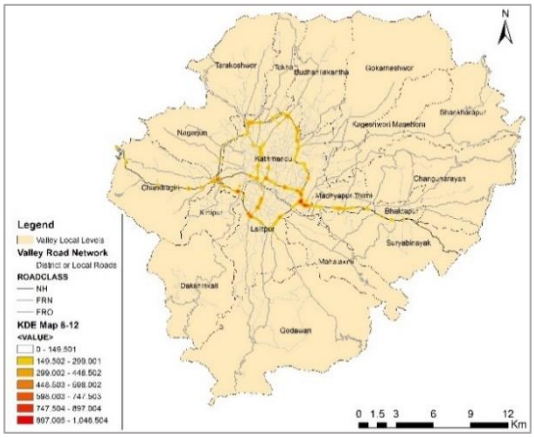

(c) Morning

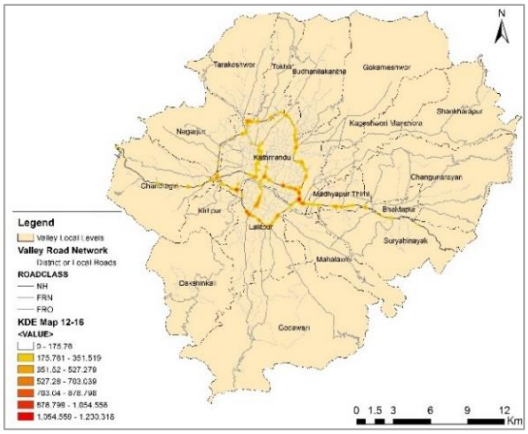

(d) Afternoon

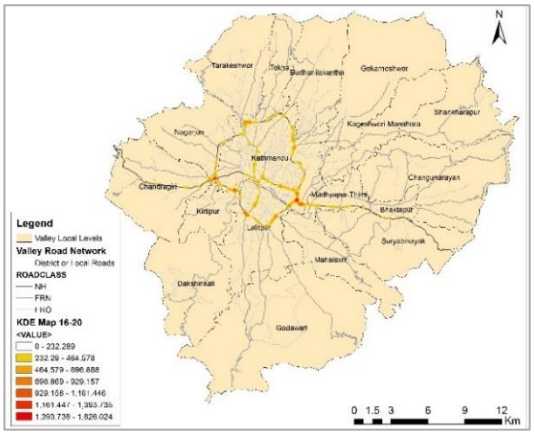

(e) Evening

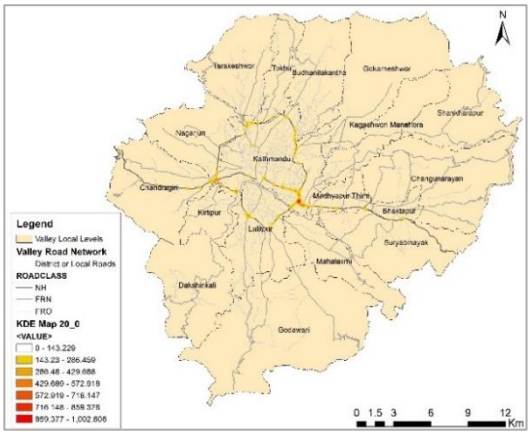

(f) Night

Figure 4.37 KDE Maps for Time of the Day Dataset

The comparative analysis of KDE Maps reveal the following distinct patterns according to the time of day:

i) Late Night (Midnight to 4 AM): KDE maps show greater intensity of late-night crashes in areas with nightlife establishments (bars, restaurants, hotels, party venues etc.) and bus parks as witnessed in Thamel-Durbarmarg-Lainchaur, Sundhara, Sorakhute and Balaju-New Buspark-Samakhusi areas. Notable hotspots are also present in Tribhuvan Rajpath, Ring Road, and Araniko Highway as these are commonly used by heavy vehicles during these hours. The scarcity of vehicles at night leads to a predominance of single-vehicle crashes or crashes involving heavy vehicles, which tend to result in significant property damage and fatalities. Contributing factors to these crashes may include overspeeding, driving under the influence, inadequate street lighting, and driver fatigue or drowsiness.

ii) Early Morning (4 AM to 8 AM): There are comparatively more hotspots of moderate intensity than that of late-night crashes at almost all road sections throughout the major roadway links. The time frame coincides with the early morning commute heading to workplace, college or vegetable market, leading to rise in crashes in Machhapokhari, Dhumbarahi, Chabahil, New Baneshwor, Koteshwor, Jadibuti, Gwarko, Satdobato, Balkhu and Kalanki areas. The intensity gets reduced for highways entering the Valley in this time possibly due to less vehicle density. The low traffic volume during these hours does not necessarily implies safer driving conditions, in fact, the presence of heavy vehicles, which often travel during off-peak hours to enter or exit the Valley, coupled with over speeding of other vehicles on empty roads, contributes to the severity of crashes. Additionally, the early morning fog, lower temperatures, and inadequate street lighting exacerbate the risks for vulnerable road users such as motorcyclists and pedestrians, leading to a higher incidence of crashes involving these groups.

iii) Morning (8 AM to Noon): The morning peak hour endures substantial traffic volume and congestion because of movement of both light and heavy vehicles on the limited roadways. Due to this, there are considerable number of hotspots in many sections of the major highways and urban links mentioned earlier. The spatial patterns of crash clusters are more intense at intersections and around areas of offices, schools, hospitals, restaurants, markets, companies and trade centers. This is demonstrated along Kalanki, Sitapaila, Balkhu, Gwarko-Ekantakuna, Jawlakhel-Kupondole, Tripureshwor-Lainchaur, Gaushala-Chabahil-Dhumbarahi, Sinamangal, Nayabaneshwor-Koteshwor-

Balkumari, Koteshwor-Jadibuti-Kaushaltar, and Gatthaghar-Thimi areas. As there are too many vehicles and pedestrian activity on these roads during the morning rush hour, most collisions are between two vehicles (fewer heavy vehicles) or pedestrian crashes. These crashes can be attributed to the urgency to reach destinations in dense traffic resulting in non-compliance with traffic rules.

iv)Afternoon (Noon to 4 PM): In the afternoon period, there is a marginal reduction in traffic volume compared to the morning and evening rush hour. This reduction in vehicular and pedestrian traffic, along with adequate lighting conditions, would typically suggest a lower frequency of traffic hotspots, however, the results do not confirm with this expectation. The intensity is slightly less than the morning hour and slightly more than the evening hour. The spatial concentration of afternoon crashes is consistent with the high-risk segments of morning and afternoon hours. While the overall risk of crashes remains same, these incidents tend to be less severe in nature, possibly due to the lower congestion levels and better visibility.

v) Evening (4 PM to 8 PM): The pattern of hotspots during the evening rush hour continues to mirror the high-risk areas identified during the morning and afternoon hours, but with less intensity (red color), despites it records a higher number of crashes compared to the morning rush and afternoon period. The crash clusters are observed around intersections and road segments with areas of offices, schools, restaurants, and markets as in the previous time slots as the commuters return home. Koteshwor, Balkumari, Gwarko, Ekantakuna, Balkhu, Kalanki, Newbuspark, Putalisadak, etc. are some of the discernable hotspots at this time. These observations suggest that the overall traffic congestion and driving patterns is similar with morning peak periods, however, the intensity of hotspots vary possibly due to differences in lighting conditions, traffic volume or driver tiredness.

iv) Night (8 PM to Midnight): Considerably less hotspots as seen in KDE maps can be expected at night hours considering police checks, less vehicle movement and pedestrian activity, and the policy of closing bars and restaurants early. A greater chunk of those crashes occurs on Tribhuvan Rajpath mostly Thankot area from where vehicles enter Kathmandu, and sections of Araniko Highway as vehicles do enter or go out more at that time. Areas like Koteshwor, Sorakhutte, Thamel, Sundhara, Bijulibazar, Baneshwor, and Maitighar have significant night crashes as they have areas of bars,

palaces, and venues. Overspeeding, drinking and driving, poor street lighting, fatigue, or drowsiness could be attributed as major causes of those crashes. Since there are less traffic at night, single vehicle crashes or collision with heavy vehicles on the road lead to fatalities and severe crashes at night.

4.6 Ranking of Top Ten Hotspots

The relative ranking of hotspots at 99% confidence was assessed in relation to severity of crashes using the Equation (9). The ranking results are presented in table 4.22.

Table 4.22 Top Ten Significant Hotspots

S.N.	Link Name	Location	Length (m)	Crash Count	Severity Index	Rank
1	Kalanki - Balkhu (Ringroad)	Balkhu (TU)	188.38	81	2017	**1**
2	Nagdhunga-Kalanki (Ringroad)	Dhungeadda	544.25	191	1862	**2**
3	Manohara-Sallaghari-Hanumante Culvert	Kaushaltar Chowk	407.25	123	1751	**3**
4	Manohara-Sallaghari-Hanumante Culvert	Chardobato Chowk	251.04	82	1723	**4**
5	Manohara-Sallaghari-Hanumante Culvert	Chundevi Bus Stop	282.24	74	1705	**5**
6	Maharajganj - Balaju Bypass Junction (Ringroad)	New Buspark (Mitranagar)	164.77	79	1634	**6**
7	Manohara-Sallaghari-Hanumante Culvert	Srijananagar Chowk	202.77	48	1561	**7**
8	Ekantakuna- Kusunti - Satdobato (Ringroad)	Thasikhel	232.45	84	1331	**8**
9	Chabahil - Sankhapark (Ringroad)	Chabahil Chowk	168.06	29	1305	**9**
10	Nagdhunga-Peepalmod	Nagdhunga	805.23	85	1203	**10**

The hotspots with the higher incidence of crashes did not occupy higher positions in terms of severity score, as detailed in table 4.22. The top ten hotspots exhibit high number of deaths and major injury crashes in comparison to other hotspots identified at 99% confidence. As a result, these specific locations were assigned with relatively high weights of severity score, despites the fact that other locations had high number of crash incidences.

At these locations, mixed cases of crashes are evident as shown in table 4.23 with the dominance of vehicle-to-vehicle collision such as rear end/side impact, head on

collision, turning collision and multiple collision. There are fewer instances of single-vehicle accidents striking an object or overturning, and vehicle-pedestrian crashes. Of these, rear end/side collision, head on collision, hit object, overturned vehicle, multiple collision and pedestrian collision are the major contributors to the severity of crashes at the identified top ten hotspots. Collision of car/jeep and motorcycles with heavy vehicles, especially trucks are considerably severe causing greater loss of life and property (table 4.24). It is critical for transportation agencies to prioritize the prevention of fatalities and severe injuries at these identified hotspots, due to their profound effects on people, families, and economic fabric.

Table 4.23 Collision Type and Severity at Top Ten Significant Hotspots

Collision Type	Death	Major Injury	Minor Injury	PDO
Rear End/Side Collision	10	1	125	257
Hit Object	8	5	24	23
Overturned Vehicle	6	5	88	7
Multiple Collision	5	3	42	33
Hit Pedestrian	3	1	34	0
Hit Pedestrian Crossing	2	2	31	0
Head on Collision	1	3	67	63
Others	1	0	18	5
Crossing Collision	1	1	23	8
Hit Parked Vehicle	1	1	8	7
Turning Collision	0	1	43	22
Hit Animal	0	0	2	2

Table 4.24 Vehicle Type and Severity at Top Ten Significant Hotspots

Vehicle Type	Death	Major Injury	Minor Injury	PDO
Car or Jeep or Van	30	12	280	296
Motorcycle	26	10	312	77
Truck	11	2	33	148
Bus	5	1	21	82
Tractor	1	0	1	0
Rent or Micro	0	1	7	6
Tempo	0	0	5	1
Non-Motorized	0	0	11	0

4.7 Site Observations and Suggestions for Safety Improvement

The specific observations at the five sample hotspot sites, which potentially relate with the crash patterns identified through spatio-temporal analysis, and the corresponding countermeasures required to enhance the safety are subjectively described under table 4.25. The observational checklist administered at one of the sample sites is attached in Appendix D.

Table 4.25 Observations and Suggestions for Sample Hotspots

Site	Crash Pattern*	Site Findings	Recommendation
Dhungeadda	Rear End/Side Collision (120)	• Steep grade surpassing 12% lead to reduced vehicle control and long stopping distance	• Fill embankment or cutting to make gradient less steep • Apply speed limit • Provide no overtaking sign
	Head on Collision (17)	• Barrier line as means to separate opposing traffic	• Provide median or crash barriers • Improve delineation with road studs
	Turning Collision (16)	• Traffic cross barrier line for making u-turn	• Provide no u-turn sign
	Hit Pedestrian Crossing (10)	• Absence of pedestrian crossings	• Provide zebra-crossing with appropriate warning sign or overhead bridge
	Hit Parked Vehicle (6)	• Illegal parking on road edges	• Install no park zone sign • Provide separate parking area or layby
	Night Time (28)	• Lighting facilities installed recently	• Install road studs along centreline and edges • Use retroreflective markings and signs
Balkhu	Rear End/Side Collision (40)	• Lane marking faded	• Apply no overtaking sign • Improve markings and arrows
	Head on Collision (27)	• Barrier line as means to separate opposing traffic	• Provide median or crash barriers • Improve delineation with road studs
	Turning Collision (20)	• Outer divider openings on either side are located too close	• Close out existing openings and provide new ones in staggered manner at specified distances as per relevant code
	Hit Pedestrian Crossing (7)	• Zebra crossing with stop line present	• Install raised pedestrian crossing with warning sign or overhead bridge
	Overturned Vehicle (6)	• Overspeeding (1 in 10 trucks/tippers, 5 in 10 buses, 3 in 10 four wheelers and 4 in 10 two wheelers)	• Use of rumble strips at overspeeding zone
	Hit Object (5)	• Presence of guide posts near service roads and	• Add reflector tapes on guide posts

Site	Crash Pattern*	Site Findings	Recommendation
		electric poles on side roads	• Provide hazard marking for roadside poles
	Night Time (16)	• No lighting facilities	• Install streetlights, road studs along centreline and edges. • Use retroreflective markings and signs.
Thasikhel	Rear End/Side Collision (38)	• Lane marking faded	• Apply no overtaking sign • Improve markings and arrows
	Head on Collision (13)	• Barrier line as means to separate opposing traffic	• Provide median or crash barriers • Improve delineation with road studs
	Turning Collision (10)	• Outer divider openings on either side are located too close • Visibility obstructed at access points	• Close out existing openings and provide new ones in staggered manner at specified distances as per relevant code • Improve access geometry, markings and delineation
	Hit Pedestrian Crossing (5)	• No crossing facilities	• Install signalized zebra crossing with warning sign or overhead bridge
	Overturned Vehicle (6)	• Overspeeding (2 in 10 trucks, 3 in 10 buses, 2 in 10 four-wheelers, and 3 in 10 two-wheelers)	• Use of rumble strips at overspeeding area
	Hit Object (5)	• Presence of electric poles on side roads	• Add reflector tapes or hazard marking for roadside poles
	Night Time (8)	• No lighting facilities	• Install streetlights, road studs along centreline and edges. • Use retroreflective markings and signs.
Kaushaltar	Rear End/Side Collision (76)	• Overspeeding (1 in 10 trucks, 1 in 10 buses, 4 in 10 four-wheelers, and 3 in 10 two-wheelers)	• Check stopping sight distance at intersection • Reduce speed limit at intersection
	Head on Collision (21)	• No separation along side roads •	• Apply centreline marking with road studs along side roads
	Hit Parked Vehicle (8)	• Parking designated near intersection	• Declare no parking zone with signs near intersection
	Hit Pedestrian Crossing (9)	• Zebra-crossing at intersection despites presence of overhead bridge	• Remove pedestrian zebra-crossing, and make overhead bridge disabled friendly
	Overturned Vehicle (14)	• Overspeeding (1 in 10 trucks, 1 in 10 buses, 4 in 10 four-wheelers, and 3 in 10 two-wheelers)	• Use of rumble strips at overspeeding area

Site	Crash Pattern*	Site Findings	Recommendation
	Crossing Collision (6)	• Common phase for right turning and crossing traffic	• Provide optimized phase for crossing traffic
	Hit Object (11)	• Presence of guide posts on main road • Presence of electric poles on service roads • Road encroachment	• Add reflector tapes for guide posts • Removal of or hazard marking for poles • Remove street vendors and structures from clear zone
	Night Time (22)	• Visibility of marking and signs poor	• Use retroreflective studs, markings and signs.
Chundevi	Rear End/Side Collision (46)	• Overspeeding (3 in 10 truck, 2 in 10 bus, 3 in 10 four-wheeler and 5 in 10 motorcycle)	• Reduce speed limit near bus stop • Add no overtaking zone sign near bus stop
	Hit Pedestrian (22)	• Discontinuous sidewalks along service roads, and • encroached for parking	• Provide guarded sidewalks • Provide suitable parking zone or laybys
	Hit Object (19)	• Presence of guide posts on main road • Presence of electric poles on service roads	• Add reflector tapes for guide posts • Removal of or hazard marking of poles
	Head on Collision (11)	• No separation along service roads •	• Apply centreline marking with road studs along side roads
	Turning Collision (8)	• Visibility obstructed at access points	• Improve access geometry, markings and delineation
	Hit Pedestrian Crossing (7)	• No pedestrian crossing along service roads	• Provide raised zebra crossing with warning sign on service roads
	Overturned Vehicle (7)	• Overspeeding (3 in 10 truck, 2 in 10 bus, 3 in 10 four-wheeler and 5 in 10 motorcycle) • Large open drainage on side road	• Provide rumble strips at overspeeding areas • Provide drain covers
	Night Time (14)	• No lighting facilities	• Install streetlights, road studs along centreline and edges. • Use retroreflective markings and signs.

*Note: Crash pattern represents type of hotspot that the site belongs to, and figure in bracket is the number of particular crash type recorded.

CHAPTER 5: CONCLUSION AND RECOMMENDATION

5.1 General

This study introduced a hotspot analysis technique based on GIS spatial tools to facilitate the effective visualization of high crash risk areas and their possible causes in the Kathmandu Valley. The outcomes have highlighted the perilous locations in both spatial and temporal dimension, as well as key spatial elements that might influence the hotspot occurrences. This part of report synthesizes the final conclusions of the study by reflecting on the findings from Chapter 4, and also outlines recommendations for essential measures, present limitations and prospects for future research.

5.2 Conclusion

The current thesis capitalized on the advantages integrating three methodologies viz. Global Moran's I, Getis-Ord Gi* and KDE, each with distinct yet complementary objectives, to explore the geographical clusters of the traffic crashes, and the variation in distribution of the highly significant hotspot segments for different analysis datasets. The combined methodology is applicable to complex datasets and is capable of producing meaningful outcomes for a variety of attribute parameters. Based on the findings, the following conclusions were drawn:

- The positive Moran's I statistic, high z-score and low p value indicate that the patterns of hotspots for all the dataset tested in the analysis are clustered in nature due to road condition or other local factors.
- Both the Getis-Ord Gi* and KDE technique highlight similar locations of hotspots (275 nos.), and hence, their collective potential can be utilized to quickly visualize the statistically significant hotspots. In most cases, Getis-Ord Gi* method outperformed the KDE analysis, enhancing the precision of dangerous spots on outer roads extending from central highway, essentially Ring Road.
- The analysis found that spatial heterogeneity exists in crash patterns of aggregate crashes, severity levels and collision types, howbeit, the concentration of all types of crashes and severity is significant along Ring Road, Araniko Highway,

Tribhuwan Highway, Tripureshwor-Ring Road, Thapathali-Ekantakuna Road and other main urban roads for all types of crash dataset. Specific hotspot locations include Koteshwor, Tinkune, Chabahil, Sukedhara, Balaju Bypass, Balkhu, Ekantakuna, Satdobato, Gatthaghar and more.

- The temporal analysis showed that incidence of hotspots is increasing over the analysis period with minimal seasonal and day of week fluctuations. The time of the day clustering data is a critical temporal parameter as it shows different pattern in relation to other temporal datasets. The 76 common hotspot segments identified across each time interval indicate the sites with persistent problems. These should be the focal points for traffic safety interventions.
- The results indicate that densely populated areas and roads in proximity with residential, commercial and residential-commercial mix land uses are more likely to experience a larger number of crashes and hotspots compared to other regions.
- The ranking strategy proved that hotspots with the higher incidence of crashes do not necessarily correlate with higher severity score, and hence, they do not occupy higher position in ranking. Top ten hotspot sections show almost fixed nature of occurrence across different spatial and temporal analysis parameters. This highlights the need for immediate mitigative action due to high incidences of deaths and major injuries associated with these sites.

5.3 Recommendations

In light of conclusions and limitations of the study, the following recommendations are offered:

- **Safety Assessment:** The native transportation management agencies (MOPIT, MOPID, Local Government) should prioritize the identified hotspot locations (Appendix C) based on the weighted severity ranking as applied in this thesis to ensure optimum allocation for financial resources. They should conduct detailed investigation of local dynamics at hotspot sites, and devise countermeasures to reduce both the frequency of crashes and severity of impacts. Considering the major collision types and times of severe crashes in Kathmandu Valley, the authorities should focus on countermeasures such as intersection improvement with optimized signalization, improved geometry and visibility at access points, segregation of

opposing traffic, providing pelican crossings or overhead bridges, removing or marking hazards in clear zones, adequate provision of road furniture and their timely maintenance, installation of streetlights, applying traffic calming measures and controlling illegal parking by designating no-park and parking areas.

- **Crash Data Management and Monitoring:** Traffic Directorate continues to face challenges in maintaining a high quality and comprehensive Road Accident Information Management System (RAIMS), for example, crashes due to illegal pedestrian crossing, illegal parking, adverse road conditions etc. are missing. It is crucial that Traffic Directorate allocate funds towards upskilling of personnel on effective reporting of crash incidences and use of developed RAIMS software. Along with these, the use of GIS and spatio-temporal analysis should be encouraged in daily operations to decipher and track crash trends, and monitor effectiveness of implemented countermeasures on reducing particular types of crashes.
- **Standardization of Hotspot Definition:** A key hurdle in this process is the precise definition of hotspots. Therefore, the study advocates policy makers to establish a clear and quantifiable criterion for hotspot identification in Nepal, ensuring its appropriateness to road facility category, crash type, traffic patterns, land use, and other relevant considerations.
- **Future Hotspot Research:** The present study establishes a foundation for future research and encourages further exploration and refinement of proposed spatial-temporal techniques for analyzing high-risk hotspots and improving road safety across other areas in Nepal. To gain a comprehensive insight into the effectiveness of applied method, it would be advantageous to validate the hotspot results through on-site visits. Future research directions may involve suitable segmentation approach to facilitate cross-comparison among different road network and regions. It is advisable that future researchers be focused around examining the dependency of hotspot occurrences on the other important determinants of crashes like road geometry (such as length, sight distance and gradient), road condition, weather, traffic volume, travel speed, distance to hospital etc. A further step to categorizing the data to reflect crash patterns due to involvement of different road users such as pedestrians, drivers, motorcyclists and NMV users, will provide more nuanced insights into the changes required in road design or traffic control measures or safety laws.

REFERENCES

Afolayan, A., Easa, S.M., Abiola, O.S., Alayaki, F.M. & Folorunso, O. (2022). GIS-Based Spatial Analysis of Crash Hotspots: A Nigerian Case Study. Infrastructures, 7, 103. https://doi.org/10.3390/infrastructures7080103

Adhikari, K. (2024). A Project Report on Identification of Crash-Prone Areas and Development of Prediction Model Using Multiple Linear Regression Model, Department of Geomatics Engineering, School of Engineering, Kathmandu University, DOI:10.13140/RG.2.2.19505.15208

Adhikari, S. (2014). City report: Kathmandu metropolitan city, Nepal. Kathmandu. Retrieved from https://www.uncrd.or.jp/content/documents/20488EST-City-Report-Nepal-Kathmandu.pdf

Alam M. S., & Tabassum N. J. (2023). Spatial pattern identification and crash severity analysis of road traffic crash hot spots in Ohio. Heliyon. https://doi.org/10.1016/j.heliyon.2023.e16303

Afolayan, A., Easa, S. M., Abiola, O. S., Alayaki, F. M., & Folorunso, O. (2022). GIS-Based Spatial Analysis of Crash Hotspots: A Nigerian Case Study. Infrastructures 2022, 7, 103.

Aghasi, N.H.M. (2018) Spatio-Temporal Analysis on Urban Traffic Crashes: A Case Study of Tehran City, Iran. Journal of Geographic Information System, 10, 603-642. https://doi.org/10.4236/jgis.2018.105032

Ahmed, M., Huang, H., Abdel-Aty, M., & Guevara, B. (2011). Exploring a Bayesian hierarchical approach for developing safety performance functions for a mountainous freeway. Crash Analysis & Prevention, 43(4), 1581-1589.

Anderson, T.K. (2009). Kernel density estimation and K-means clustering to profile road crash hotspots. Crash Analysis and Prevention 41 (3), 359-364

Anselin, L. (1995). Local Indicators of Spatial Association-LISA. Geographical Analysis. https://doi.org/10.1111/j.1538-4632.1995.tb00338.x

Asian Development Bank (ADB). (2021). ADB TA9604 - Institutional strengthening and capacity building for road safety and gender Equality, Part A - Blackspot Improvement Study Report, Deliverable #8 - Road Safety Final Report (Part I)

Austroads. Road safety audits, Australia, 1994

Bačkalić, S. (2013). Temporal analysis of the traffic crashes occurrence in province of Vojvodina. Transport Problems, 8(1), 87-93.

Bailey, T. and Gatrell, T. (1995). Interactive Spatial Data Analysis, Longman Scientific & Technical, Harlow Essex, UK.

Bíl, M., Andrášik, R., & Sedoník, J. (2019). A detailed spatiotemporal analysis of traffic crash hotspots. Applied Geography, 107, 82-90.

Bíl, M.; Andrášik, R.; & Janoška, Z. (2013). Identification of hazardous road locations of traffic crashes by means of kernel density estimation and cluster significance evaluation. Crash Analysis & Prevention, Vol 55, pp. 265-273.

Brunsdon, C. (2001). The comap: exploring spatial pattern via conditional distributions. Computers, environment and urban systems, 25(1), pp.53-68.

Chen, F., Zhang, G., & Yang, X. (2017). A temporal and spatial analysis of traffic crashes using geographic information systems: A case study in Wuhan, China. Sustainability, 9(3), 341.

Cheng, Z., Zu, Z., & Lu, J. (2018). Traffic crash evolution characteristic analysis and spatiotemporal hotspot identification of urban road intersections. Sustainability (Switzerland), 11(1). https://www.mdpi.com/2071-1050/11/1/160/pdf

Cheng, W., & Washington, S.P. (2005). Experimental Evaluation of Hotspot Identification Methods. Crash Analysis & Prevention, Vol 37, pp. 870-881.

Choudhary, J., Ohri, A. and Kumar, B. (2015). Spatial and statistical analysis of road crashes hot spots using GIS. In 3rd Conference of Transportation Research Group of India (3rd CTRG).

Delmelle, E. (2009). Point pattern analysis. In Kitchen R, Thrift N (eds) International Encyclopedia of Human Geography, 8, 204-211

Dereli, M.A.; Erdogan, S. (2017). A New Model for Determining the Traffic Crash Black Spots Using GIS-aided Spatial Statistical Methods. Transp. Res. Part A Policy Pract, 103, 106-117.

Deshpande, N., Chanda, I. & Arkatkar, S.S. (2011). Crash mapping and analysis using geographical information systems. International Journal of Earth Sciences and Engineering, 4(6), pp.342-345.

Elvik, R. (2008). A survey of operational definitions of hazardous road locations in some European countries. Crash Analysis & Prevention, 40(6), pp.1830-1835

Elvik, R. (2007). State-of-the-art approaches to road crash black spot management and safety analysis of road networks. Report 883, Institute of Transport Economics, Norwegian Centre for Transport Research.

Erdogan, S. (2009). Explorative spatial analysis of traffic crash statistics and road mortality among the provinces of Turkey. Journal of safety research, 40(5), pp.341-351.

Erdogan, S.; Yilmaz, I.; Baybura, T.; Gullu, M. (2008). Geographical information systems aided traffic crash analysis system case study: City of Afyonkarahisar. Accid. Anal. Prev., 40, 174-181.

Evans, L. (1996). The Dominant Role of Driver Behavior in Traffic Safety. American Journal of Public Health, 86(6), 784-786

Farmer, C. M. (2005). Temporal factors in motor vehicle crash deaths. Injury Prevention, 11 (1), 18-23. https://doi.org/10.1136/ip.2004.005439

Feizizadeh, B., Omarzadeh, D., Sharifi, A., Rahmani, A., Lakes, T., & Blaschke, T. (2022). A GIS-Based Spatiotemporal Modelling of Urban Traffic Crashes in Tabriz City during the COVID-19 Pandemic. Sustainability (Basel). https://doi.org/10.3390/su14127468

Flahaut, B., Mouchart, M., San Martin, M., Thomas, I. (2003). The local spatial autocorrelation and the kernel method for identifying black zones: A comparative approach, Crash Analysis and Prevention, 35(6), pp.991-1004

Fotheringham, A. S., Brunsdon, C., & Charlton, M. (2000). Quantitative geography: perspectives on spatial data analysis. Sage.

Getis, A. and Ord, J.K. (1992). The Analysis of Spatial Association by Use of Distance Statistics. Geographical Analysis, Vol. 24, no. 3, pp. 189-207. https://doi.org/10.1111/j.1538-4632.1992.tb00261.x

Greibe, Paul. (2003). Crash prediction models for urban roads. Crash Analysis & Prevention, 35 (2), pp 273-285

Hammas, M. A. M. (2023). Spatial analysis of traffic crashes in the city of Medina by using GIS (Doctoral dissertation, KING ABDULAZIZ UNIVERSITY).

Hauer, E., 1997. Observational before-after studies in road safety. Pergamon, Oxford.

Harirforoush, H., Bellalite, L., Bénié, B.B. (2019). Spatial and Temporal Analysis of Seasonal Traffic Crashes. American Journal of Traffic and Transportation Engineering, Vol. 4, No. 1, pp. 7-16.

Hazaymeh, K., Almagbile, A., & Alomari, A.H. (2022). Spatiotemporal Analysis of Traffic Crashes Hotspots Based on Geospatial Techniques. ISPRS Int. J.Geo-Inf., 11, 260.

Hour, U. C. (2007). Country Report on Road Safety in Cambodia. Royal Government of Cambodia, Ministry of Public Works and Transport, Phnom Penh, Cambodia.

How kernel density works—ArCGIS Pro | Documentation. (n.d.). https://pro.arcgis.com/en/pro-app/latest/tool-reference/spatial-analyst/how-kernel-density-works.htm

How Hot Spot Analysis (Getis-Ord GI*) works—ArCGIS Pro | Documentation. (n.d.). https://pro.arcgis.com/en/pro-app/latest/tool-reference/spatial-statistics/h-how-hotspotanalysis-getis-ord-gi-spatial-stati.htm

Huang, H. and Abdel-Aty, M. (2010). Multilevel data and bayesian analysis in traffic safety, Crash Analysis & Prevention, 42(6), pp. 1556-1565.

Huang, L., Adhikary, K.P., Choulagai, B.P., Wang, N., Poudyal, A.K. & Onta S.R. (2016). Road Traffic Crash and its Characteristics in Kathmandu Valley. Journal of the Nepal Medical Association, 55(1),1-6

Indian Roads Congress. (2022). IRC:131-2022, Guidelines for Identifying and Treating Blackspots. New Delhi: Indian Roads Congress

Jamal, A., Rahman, M. T., Al-Ahmadi, H. M. and Mansoor, U. (2020). The dilemma of road safety in the eastern province of saudi arabia: consequences and prevention strategies, International journal of environmental research and public health 17(1): 157.

Kazmi, S. S. A., Ahmed, M., Mumtaz, R., & Anwar, Z. (2020). Spatiotemporal Clustering and Analysis of Road Crash Hotspots by Exploiting GIS Technology and Kernel Density Estimation. The Computer Journal.

Khadka, A., Parkin, J., Pilkington, P., Joshi, S. K., & Mytton, J. (2022). Completeness of police reporting of traffic crashes in Nepal: Evaluation using a community crash recording system. Traffic injury prevention, 23(2), 79-84.

Kuikel, J., Aryal, B., Bogati, T., & Sedain, B. (2022). Road traffic deaths and injuries in Kathmandu. Journal of Health Promotion, Vol. 10 (1), pp: 73-88

Kuo, P. (2011). Guidelines for choosing hot-spot analysis tools based on data characteristics, network restrictions, and time distributions. Presented at 91st Annual Meeting of the Transportation Research Board. Washington, D.C.

Lavrac, N., Jesenovec, D., Trdin, N. and Kosta, N. M. (2008). Mining spatio-temporal data of traffic crashes and spatial pattern visualization. Metodoloski zvezki, 5(1), p.45.

Lavrenz, S. M., Vlahogianni, E. I., Gkritza, K. and Ke, Y. (2018). Time series modeling in traffic safety research, Crash Analysis & Prevention 117: 36

Liu, C. & Chen, C.L. (2004). Time Series Analysis and Forecast of Crash Fatalities During Six Holiday Periods. Washington, D.C. National Center for Statistics and Analysis.

Liu, C. & Sharma, A. (2017). Exploring spatio-temporal effects in traffic crash trend analysis. Analytic Methods in Crash Research, 16, 104-116. https://doi.org/10.1016/j.amar.2017.09.002

Loo, B. P. (2009). The identification of hazardous road locations: a comparison of the blacksite and hot zone methodologies in Hong Kong. International Journal of Sustainable Transportation, 3(3), 187-202.

Loo, B.P.Y., Cheung, W., and Yao, S. (2011). The Rural-Urban Divide in Road Safety: The Case of China. Open Transportation Journal, 5(1), 9-20

Loo, B. P. Y., & Anderson, T. K. (2016). Cluster Identifications in Networks. In Taylor & Francis Group (Ed.), Spatial Analysis Methods of Road Traffic Collisions (pp. 161-175). New York: CRC Press.

Lord, D., & Mannering, F. (2010). The statistical analysis of crash-frequency data: A review and assessment of methodological alternatives. Transportation Research Part A: Policy and Practice, 44(5), 291-305.

Ma, Q., Huang, G. & Tang, X. (2021). GIS-based analysis of spatial-temporal correlations of urban traffic crashes. Eur. Transp. Res. Rev. 13, 50

Ma X., Chen S., Chen F. (2017). Multivariate space-time modeling of crash frequencies by injury severity levels. Anal. Methods Accid. Res., 15 (2017), pp. 29-40, 10.1016/j.amar.2017.06.001

Machado-Leon, J. L., de Ona, J., de Ona, R., Eboli, L. and Mazzulla, G. (2016). Socio-economic and driving experience factors affecting drivers? perceptions of traffic crash risk, Transportation research part F: traffic psychology and behavior, 37, pp 41-51

Manandhar, R. B. (2022). Factors Affecting Road Traffic Crashes in the Kathmandu valley. International Research Journal of MMC, 3(3), 82-90. https://doi.org/10.3126/irjmmc.v3i3.48639

Manikandan, M., Prasad, V., Mishra, A. K., Konduru, R. K. and Newtonraj, A. (2018). Forecasting road traffic crash deaths in india using seasonal autoregressive integrated moving average model, International Journal of Community Medicine and Public Health 5(9): 3962-3968.

Manepalli, U., Bham, G. and Kandada, S. (2011). Evaluation of hotspots identification using kernel density estimation (k) and getis-ord (gi*) on I-630. Indianapolis, USA.

Meyerhoff, N. J. (1978). The influence of daylight saving time on motor vehicle fatal traffic crashes, Crash Analysis & Prevention 10(3): 207-221.

Ministry of Physical Infrastructure and Transport (MOPIT), Department of Transport Management (DoTM), Nepal India Regional Trade and Transport Project (NIRTTP), A Report on Establishment and Operation of Road Crash Information Management System (RA-IMS), 2020

Ministry of Physical Infrastructure and Transport (MOPIT), Department of Roads (DOR). (2019). Road Safety Annual Report 2019. Nepal.

Ministry of Physical Infrastructure and Transport (MOPIT), Department of Roads (DOR), Traffic Engineering and Safety Unit. (1997). Road Safety Note 8: Identifying and Treating Accidents. Nepal

Mohammed, S., Alkhereibi, A.H., Abulibdeh, A., Jawarneh, R.N. & Balakrishnan, P. (2023). GIS-based spatiotemporal analysis for road traffic crashes; in support of sustainable transportation Planning. Transportation Research Interdisciplinary Perspectives 20 https://doi.org/10.1016/j.trip.2023.100836

Mohaymany, A.S., Shahri, M., & Mirbagheri, B. (2013). GIS-based method for detecting high-crash-risk road segments using network kernel density estimation. Geo-spatial Information Science, DOI:10.1080/10095020.2013.766396.

Montella, A. (2010), A comparative analysis of hotspot identification methods. Crash Analysis & Prevention. https://doi.org/10.1016/j.aap.2014.01.017

Moran, P.A. (1948). The interpretation of statistical maps. J Royal Stat Soc Series B (Methodological), 10(2):243-251

Munasinghe D.S. (2023) Spatial Analysis of Urban Road Traffic Crashes Using GIS, British Journal of Multidisciplinary and Advanced Studies: Engineering and Technology, 4(6),70-83

National Statistical Office (NSO), National Population and Housing Census 2021, Final Report. https://censusnepal.cbs.gov.np/Home/Index/EN

Nazneen, S., Rezapour, M. & Ksaibati, K. (2020). Application of Geographical Information System Techniques to Determine High Crash-Prone Areas in the Fort Peck Indian Reservation. The Open Transportation Journal, Vol. 14, 174.

Nepal Road Safety Action Plan 2013-20, Ministry of Physical Infrastructure and Transport, 2013

Niessner, C.W. (2010). Highway Safety Manual. American Association of State Highway and Transportation Officials, Washington, DC

Okabe, A., Satoh, T. & Sugihara, K. (2009). A kernel density estimation method for networks, its computational method and a GIS-based tool. Int J Geogr Inf Sci. 23(1):7-32. doi:10.1080/13658810802475491.

Okabe A, Okunuki K.I. & Shiode S. (2006). The SANET toolbox: new methods for network spatial analysis. Trans GIS. 10(4):535-550. doi:10.1111/j.1467-9671.2006.01011.x.

Pei, J., Ding, J. (2005). Improvement in the Quality Control Method to Distinguish the Black Spots of the Road, Proceedings of the Eastern Asia Society for Transportation Studies, Vol. 5, pp. 2106- 2113.

Persaud, B., Lyon, C., & Nguyen, T. (1999). Empirical Bayes procedure for ranking sites for safety investigation by potential for safety improvement. Transportation Research Record: Journal of the Transportation Research Board, (1665), 7-12.

Plug, C., Xia, J., & Caulfield, C. (2011). Spatial and temporal visualisation techniques for crash analysis. Crash Analysis and Prevention, 43, 1937-1946.

Prasannakumar, V., Vijith, H., Charutha, R. and Geetha, N. (2011). Spatio-temporal clustering of road crashes: GIS based analysis and assessment. Procedia-Social and Behavioral Sciences, 21, pp.317-325.

Project on Urban Transport Improvement for Kathmandu Valley in Federal Democratic Republic of Nepal. (2017). Final Report.

Pulugurtha, S., Varma, S., & Sambhara, V. R. (2014). Spatial and temporal variations in the characteristics of traffic crashes at signalized intersections. Crash Analysis & Prevention, 70, 113-124.

Pulugurtha, S. & Vanapalli, V. (2008). Hazardous bus stops identification: an illustration using GIS. Journal of Public Transportation, vol. 11, no. 2, pp. 65-83, 2008.

Quddus, M. A. (2008). Time series count data models: an empirical application to traffic crashes, Crash Analysis & Prevention 40(5): 1732-1741.

Rahman, M.K., Crawford, T., & Schmidlin, T.W. (2018) Spatio-temporal analysis of road traffic crash fatality in Bangladesh integrating newspaper accounts and gridded population data. GeoJournal 83(4):645-661. https://doi.org/10.1007/s1070i8-017-9791-x

Razzaghi, A., Bahrampour, A., Baneshi, M.R., & Zolala, F. (2013). Assessment of trend and seasonality in road crash Data: An Iranian case study. International Journal of Health Policy and Management; 1: 51-55.

Rizal, S. & Tiwari, H. (2023). Analysis of Road Traffic Crash Cost in Kathmandu Valley. 2nd International Conference on Integrated Transport for Sustainable Mobility

Sajed, Y., Shafabakhsh, G., & Bagheri, M. (2019). Hotspot Location Identification Using Crash Data, Traffic and Geometric Characteristics. Engineering Journal, Vol. 23, Issue 6

Šarić, Ž. B.Eng., Zovak, G. Ph.D & Koronc, N. mag.ing.traff (2011). Comparison of Methods for Determining Crash Hotspots in the Road Traffic. Scientific Proceedings xix International Scientific-Technical Conference "trans & MOTAUTO '11", vol. 3, pp. 131-135.

Sedain, B., & Pant, P.R. (2021). Road traffic injuries in Nepal during COVID-19 lockdown. F1000Research 2021, 9:1209 (https://doi.org/10.12688/f1000research.26281.3)

Seyed Mohsen Hosseinian, Vahid Najafi Moghaddam Gilani (2020). Analysis of Factors Affecting Urban Road Crashes in Rasht Metropolis. ENG Transactions, Journal homepage: http://www.engtransactions.com

Shafabakhsh, G. A., Famili, A., & Bahadori, M. S. (2017). GIS-based spatial analysis of urban traffic crashes: Case study in Mashhad, Iran. Journal of Traffic and Transportation Engineering (English Edition), 4(3), 290-299. doi:10.1016/j.jtte.2017.05.005

Shahid, S., Minhans, A., Puan, O. C., Hasan, S. A. & Ismail, T. (2015). Spatial and temporal pattern of road crashes and casualties in peninsular malaysia. Jurnal Teknologi, 76 (14). https://doi.org/10.11113/jt.v76.5843

Shakya, S. & Marsani, A. (2020). Ranking Road Safety Hazardous Locations in Nepal (A Case Study of Kalanki Ch.10+600 km to Koteshwor Ch.20+994 km Road Section). Proceedings of IOE Graduate Conference, Vol 8, 1004-1011

Shakya, R. & Marsani, A. (2017). Using Logistic Regression to Estimate the Influence of Crash Factors on Road Crash Severity in Kathmandu Valley. Proceedings of IOE Graduate Conference, Vol 5, 311-324

Shariff, S. S. R., Maad, H. A., Halim, N. N. A., & Derasit, Z. (2018). Determining Hotspots of Road Crashes using Spatial Analysis. Indonesian Journal of Electrical Engineering and Computer Science. https://doi.org/10.11591/ijeecs.v9.i1.pp146-151

Shrestha, B. K. (2014). Road Traffic Crashes in Kathmandu Valley. The Third Pole Journal of Geography Education. https://doi.org/10.3126/ttp.v13i0.11547

Singh, S., Thapa, S.K., Shrestha, S. & Dawadi, U. (2023). A Review Paper on Road Traffic Crashes (RTA) Trends in Kathmandu Valley. International Conference on Engineering & Technology, Vol V

Thakali, L., Kwon T.J., & Fu L. (2015) Identification of crash hotspots using kernel density estimation and kriging methods: a comparison. J Mod Transp 23(2):93-106. https://doi.org/10.1007/s40534-015-0068-0

Tiwari, H. (2015). Dependency of Road Crashes with Volume and Speed (A Case Study of Major Black Spot Location within Kathmandu Valley). Proceedings of IOE Graduate Conference, pp. 339-343

Tola, A.M.; Demissie, T.A.; Saathoff, F.; Gebissa, A. (2021). Spatial Pattern and Statistical Analysis of Road Traffic Crash Hot Spots in Ethiopia. Applied Science, 11, 8828.

Truong, L. T. & Somenahalli, S. V. (2011). Using GIS to identify pedestrian-vehicle crash hotspots and unsafe bus stops. Journal of Public Transportation, vol. 14, no. 1, p. 6, 2011.

Turner, S., Subramanian, R., & Kadiyala, A. K. (2019). Hotspot identification methods for traffic crash data: A review. Crash Analysis & Prevention, 123, 201-222.

Wang, W. and Li, D. (2017). Structure identification and variable selection in geographically weighted regression models, Journal of Statistical Computation and Simulation 87(10), 2050-2068.

Wang, M., Yi, J., Chen, X., Zhang, W., & Qiang, T. (2021). Spatial and Temporal Distribution Analysis of Traffic Crashes Using GIS-Based Data in Harbin. Journal of Advanced Transportation. https://doi.org/10.1155/2021/9207500

Wang, Z.-Z., Lu, Y.N., Zou, Z.H., Ma, Y.H., & Wang, T. (2022). Applying OHSA to Detect Road Crash Blackspots. Int. J. Environ. Res. Public Health 2022, 19, 16970. https://doi.org/10.3390/ijerph192416970

Washington, S.P., Karlaftis, M.G., Mannering, F.L. (2003). Statistical and Econometric Methods for Transportation Data Analysis. Chapman Hall/CRC, Boca Raton, FL.

Washington, S.P., Karlaftis, M.G., Mannering, F.L. (2010). Statistical and Econometric Methods for Transportation Data Analysis. Second Edition, Chapman Hall/CRC, Boca Raton, FL.

Wen, J., Yuan, P., Deng, Z.H., Liu, K.L., Zhang, Y.K., & Liu L.K. (2005). Time-series analysis on road traffic injury in China. Sichuan Da Xue Xue Bao Yi Xue Ban 2005; 36: 866-9

World Health Organization. (2022). Global status report on road safety 2022.

Wu, P., Meng, X., & Song, L. (2021). Identification and spatiotemporal evolution analysis of high-risk crash spots in urban roads at the microzone-level: Using the space-time cube method. Journal of Transportation Safety & Security, DOI:10.1080/19439962.2021.1938323

Xie, Z., & Yan, J. (2008). Kernel density estimation of traffic crashes in a network space. Computers, Environment and Urban Systems 32, 396-406

Xie, Z. and Yan, J. (2013). Detecting traffic crash clusters with network kernel density estimation and local spatial statistics: an integrated approach. Journal of Transport Geography, vol. 31, pp. 64-71.

Yaacob, W. F. W., Ibrahim, S. B., Afizan, A. S., Azran, N. A. F., Nasir, S. A. M., & Harun, N. C. (2021). Spatio-Temporal Clustering of Road Crashes in Kelantan, Malaysia. International Journal of Academic Research in Business and Social Sciences, 11(9), 522-534.

APPENDIX A: Hotspot Maps

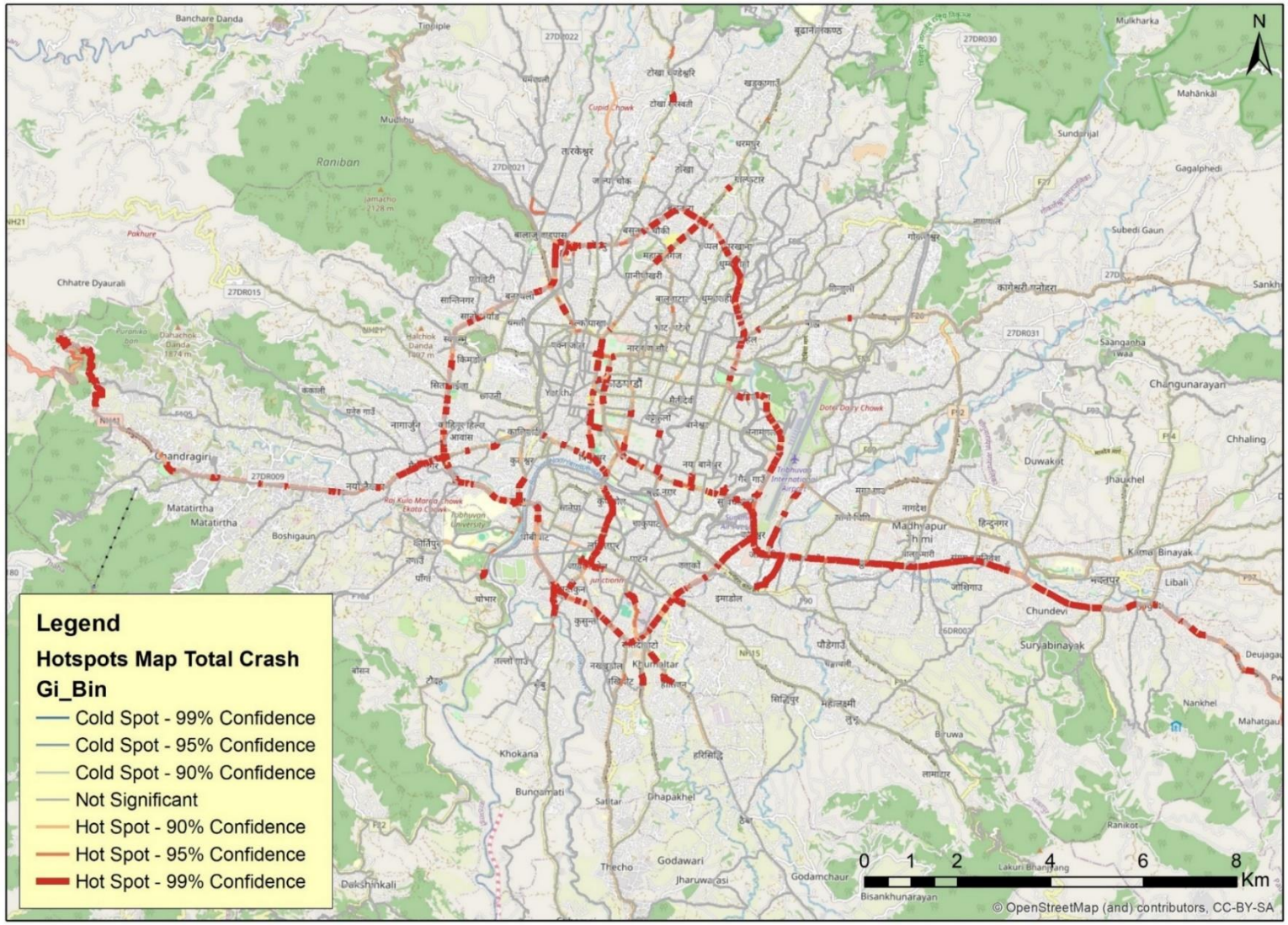
Legend
Hotspots Map Total Crash Gi_Bin
Cold Spot - 99% Confidence
Cold Spot - 95% Confidence
Cold Spot - 90% Confidence
Not Significant
Hot Spot - 90% Confidence
Hot Spot - 95% Confidence
Hot Spot - 99% Confidence
N
0 1 2 4 6 8
Km
© OpenStreetMap (and) contributors, CC-BY-SA


Legend
Hotspot Map for Death
Gi_Bin
Cold Spot - 99% Confidence
Cold Spot - 95% Confidence
Cold Spot - 90% Confidence
Not Significant
Hot Spot - 90% Confidence
Hot Spot - 95% Confidence
Hot Spot - 99% Confidence
N
0 0.75 1.5 3 4.5 6
Km
© OpenStreetMap (and) contributors, CC-BY-SA
Chatredeurali
Banchare Danda
Tinpiple
Mudkhu
Raniban
Chhatre Dyaurali
NH21
Chandragiri
Matatirtha
Boshiga
Khokana
Bungamati
Dhapakhel
Godawari
Dakshinkali
Mulkharka
Mahankal
Sundarijal
Gagalphedi
Subedi Gaun
Sankhu
Saangapha
Changunarayan
Chhaling
Jhaukhel
Dadagau
Madhyapur Thimi
Kamal Binayak
Sudal
Libali
Chundevi
Suryabinayak
Nankhel
Nasikasthan
Sanga
Biruwa
Ranikot
Lakuri Bhanjyang
Bisankhunarayan
Khumaltar

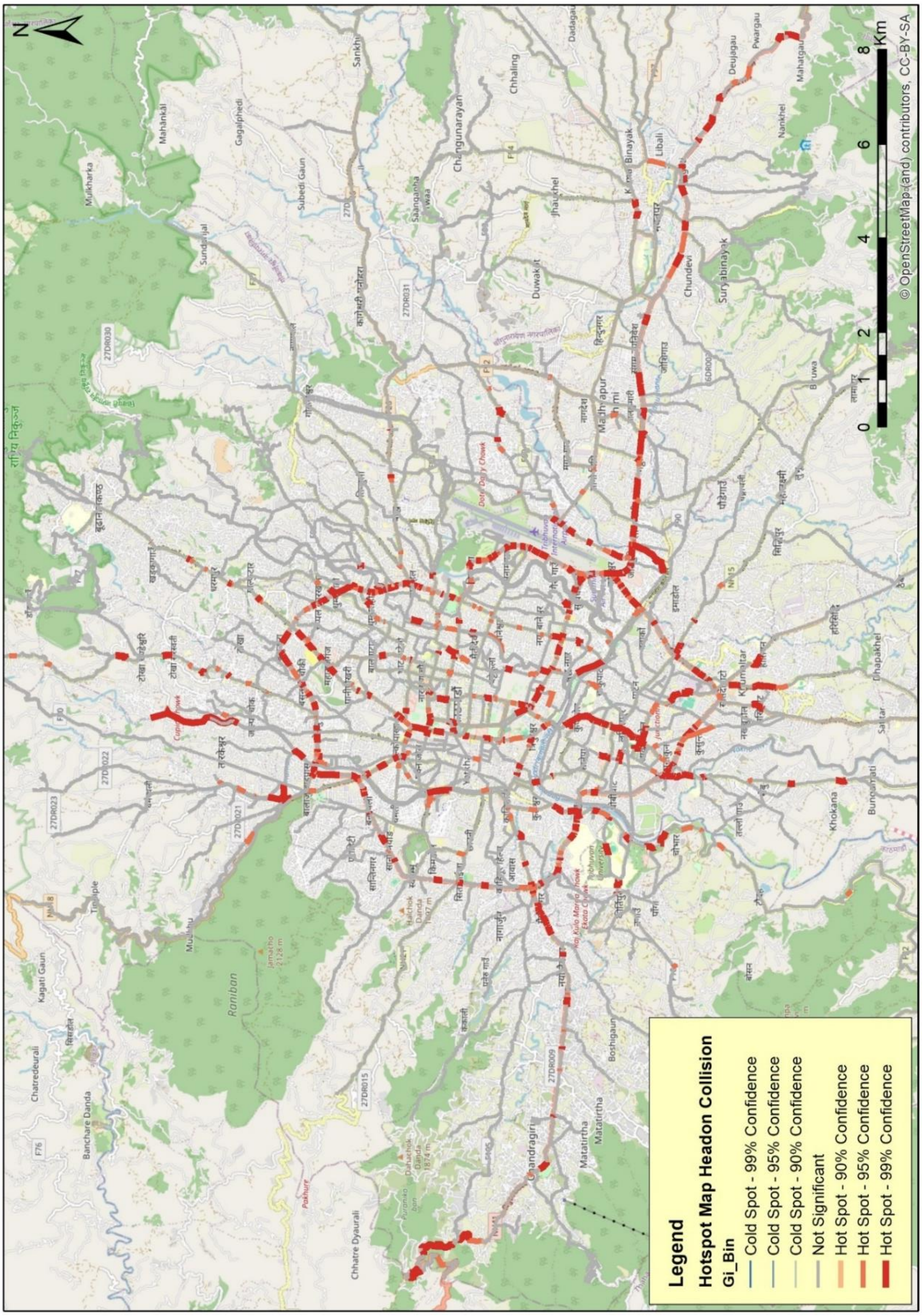
Legend
Hotspot Map Headon Collision
Gi_Bin
Cold Spot - 99% Confidence
Cold Spot - 95% Confidence
Cold Spot - 90% Confidence
Not Significant
Hot Spot - 90% Confidence
Hot Spot - 95% Confidence
Hot Spot - 99% Confidence
0 1 2 4 6 8 Km
© OpenStreetMap (and) contributors, CC-BY-SA

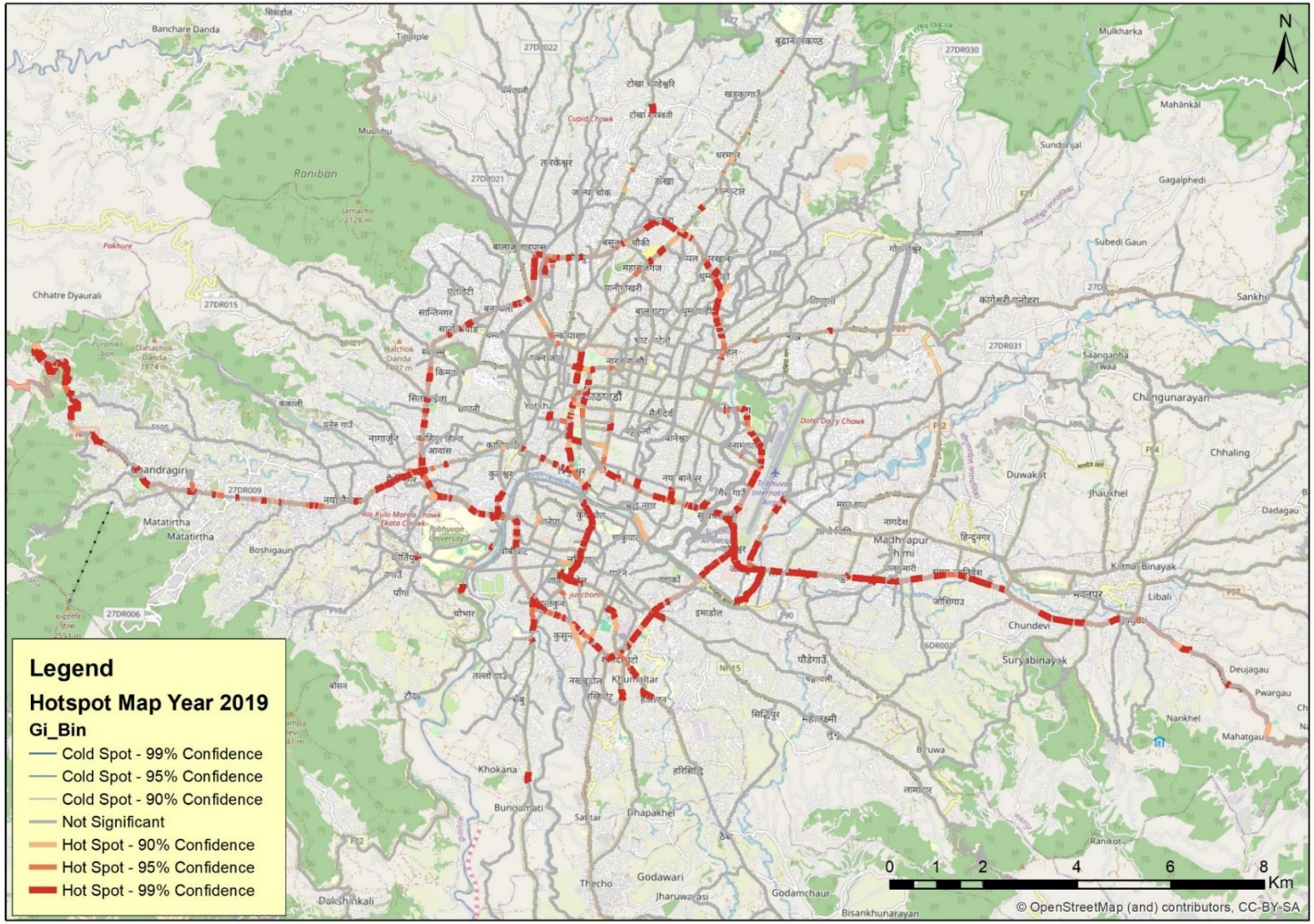
Legend
Hotspot Map Year 2019
Gi_Bin
Cold Spot - 99% Confidence
Cold Spot - 95% Confidence
Cold Spot - 90% Confidence
Not Significant
Hot Spot - 90% Confidence
Hot Spot - 95% Confidence
Hot Spot - 99% Confidence
N
0 1 2 4 6 8
Km
© OpenStreetMap (and) contributors, CC-BY-SA
Banchare Danda
Tinjuple
Raniban
Mulkharka
Mahankal
Gagalphedi
Subedi Gaun
Sankhu
Chhatre Dyaurali
Changunarayan
Chhaling
Duwakot
Jhaukhel
Dadagau
Bhandragiri
Matatirtha
Boshigaun
Tribhuvan University
Tribhuvan International Airport
Madhyapur Thimi
Kirna Binayak
Libali
Chundevi
Suryabinayak
Deujagau
Pwargau
Nankhel
Mahatgau
Khokana
Bungamati
Sattar
Dhapakhel
Ranikot
Thecho
Godawari
Jharuwarasi
Godamchaur
Bisankhunarayan
Dakshinkali

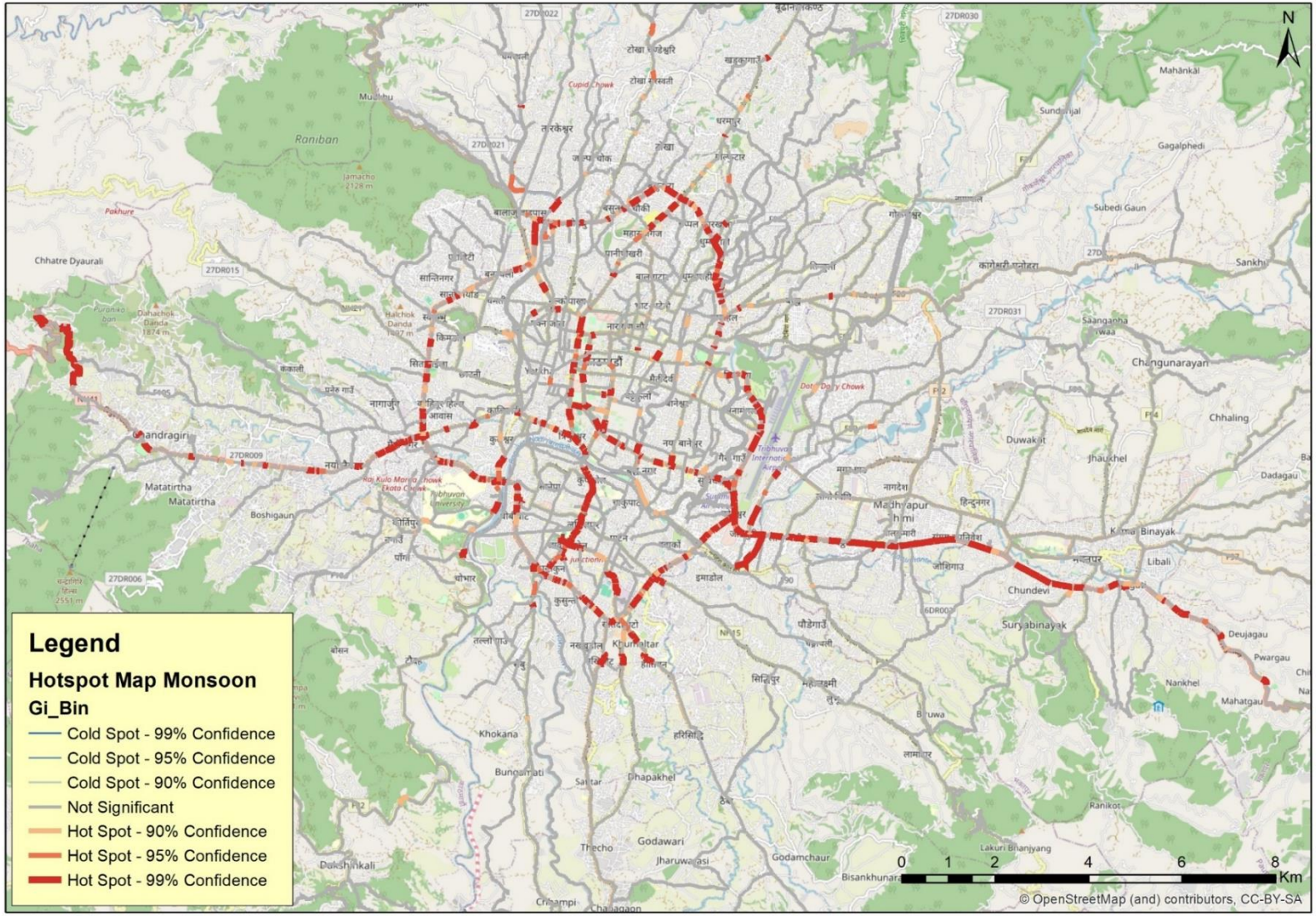
Legend
Hotspot Map Monsoon
Gi_Bin
Cold Spot - 99% Confidence
Cold Spot - 95% Confidence
Cold Spot - 90% Confidence
Not Significant
Hot Spot - 90% Confidence
Hot Spot - 95% Confidence
Hot Spot - 99% Confidence
N
0 1 2 4 6 8
Km
© OpenStreetMap (and) contributors, CC-BY-SA

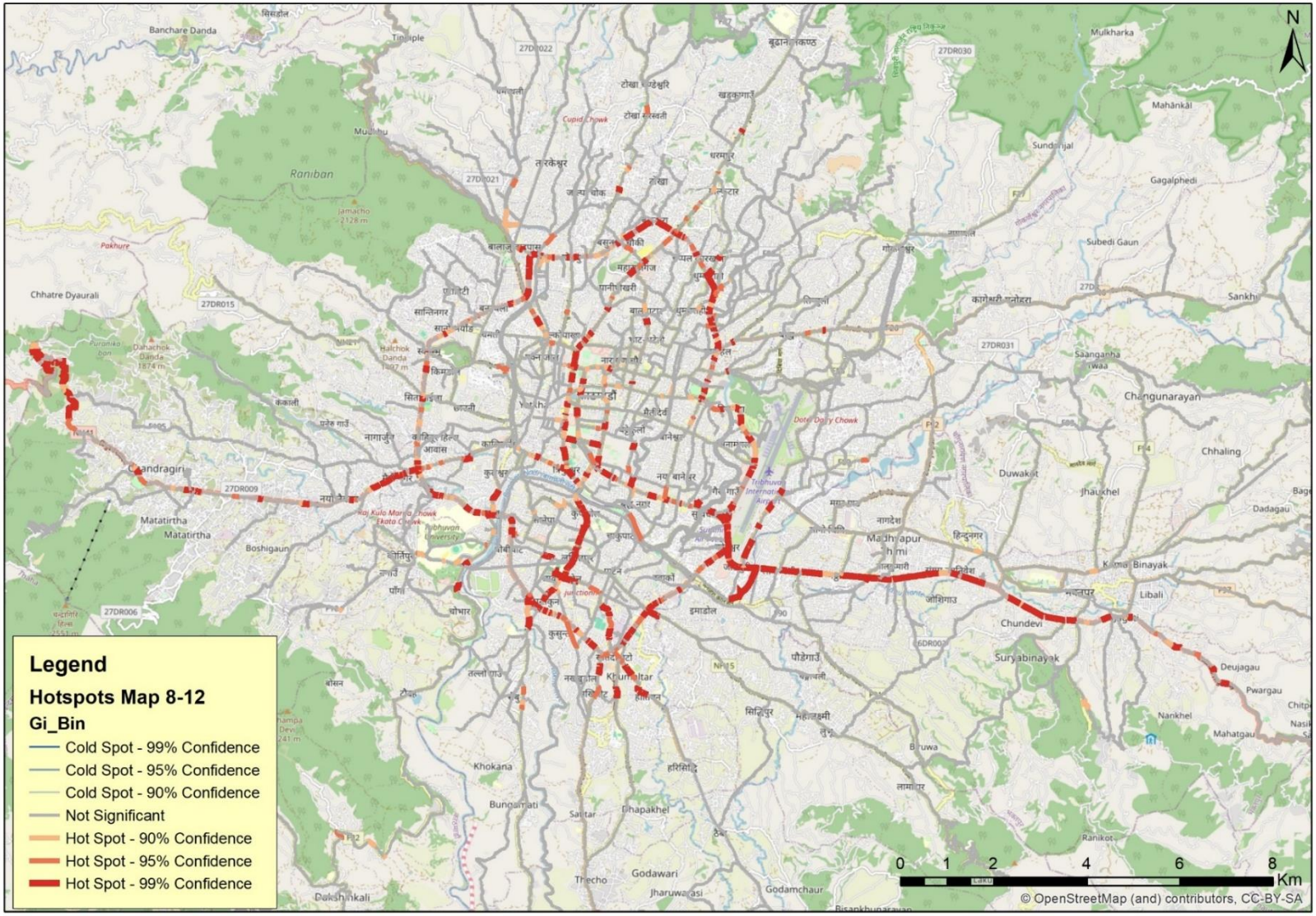
Legend
Hotspots Map 8-12
Gi_Bin
Cold Spot - 99% Confidence
Cold Spot - 95% Confidence
Cold Spot - 90% Confidence
Not Significant
Hot Spot - 90% Confidence
Hot Spot - 95% Confidence
Hot Spot - 99% Confidence
N
0 1 2 4 6 8
Km
© OpenStreetMap (and) contributors, CC-BY-SA

APPENDIX B: KDE Maps

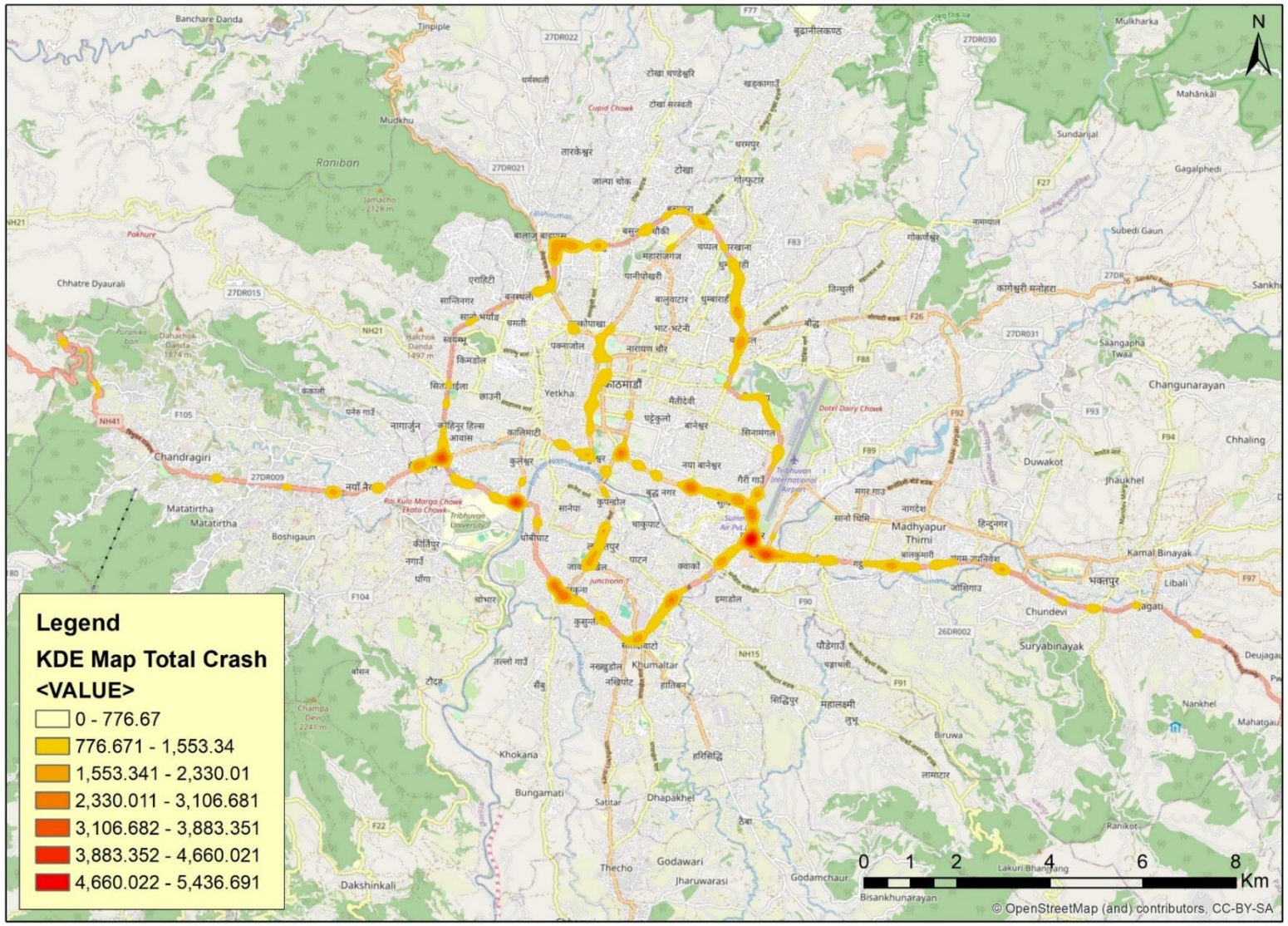
Legend
KDE Map Total Crash
<VALUE>
0 - 776.67
776.671 - 1,553.34
1,553.341 - 2,330.01
2,330.011 - 3,106.681
3,106.682 - 3,883.351
3,883.352 - 4,660.021
4,660.022 - 5,436.691
N
0 1 2 4 6 8
Km
© OpenStreetMap (and) contributors, CC-BY-SA

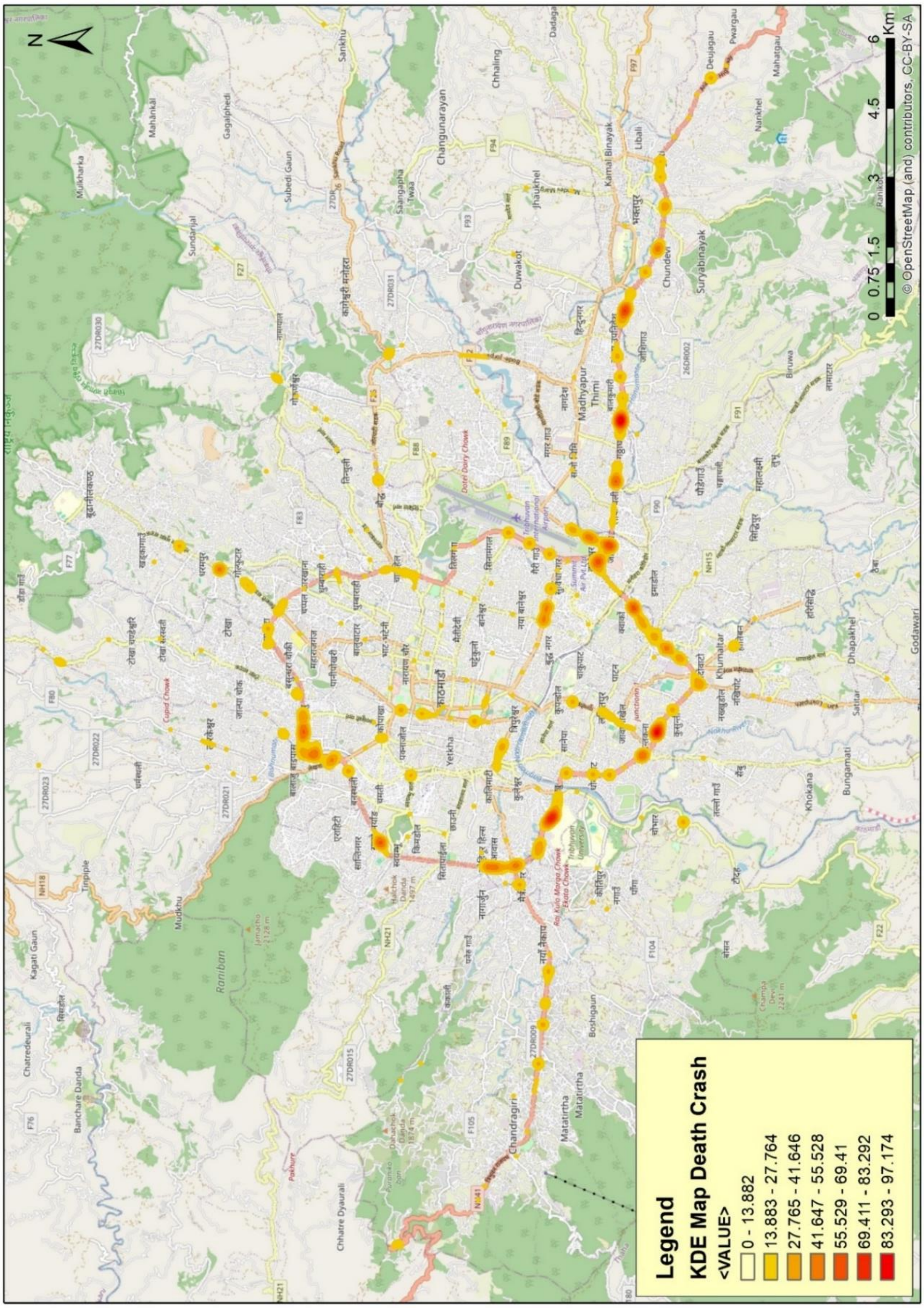
Legend
KDE Map Death Crash
<VALUE>
0 - 13.882
13.883 - 27.764
27.765 - 41.646
41.647 - 55.528
55.529 - 69.41
69.411 - 83.292
83.293 - 97.174
0 0.75 1.5 3 4.5 6 Km
© OpenStreetMap (and) contributors, CC-BY-SA

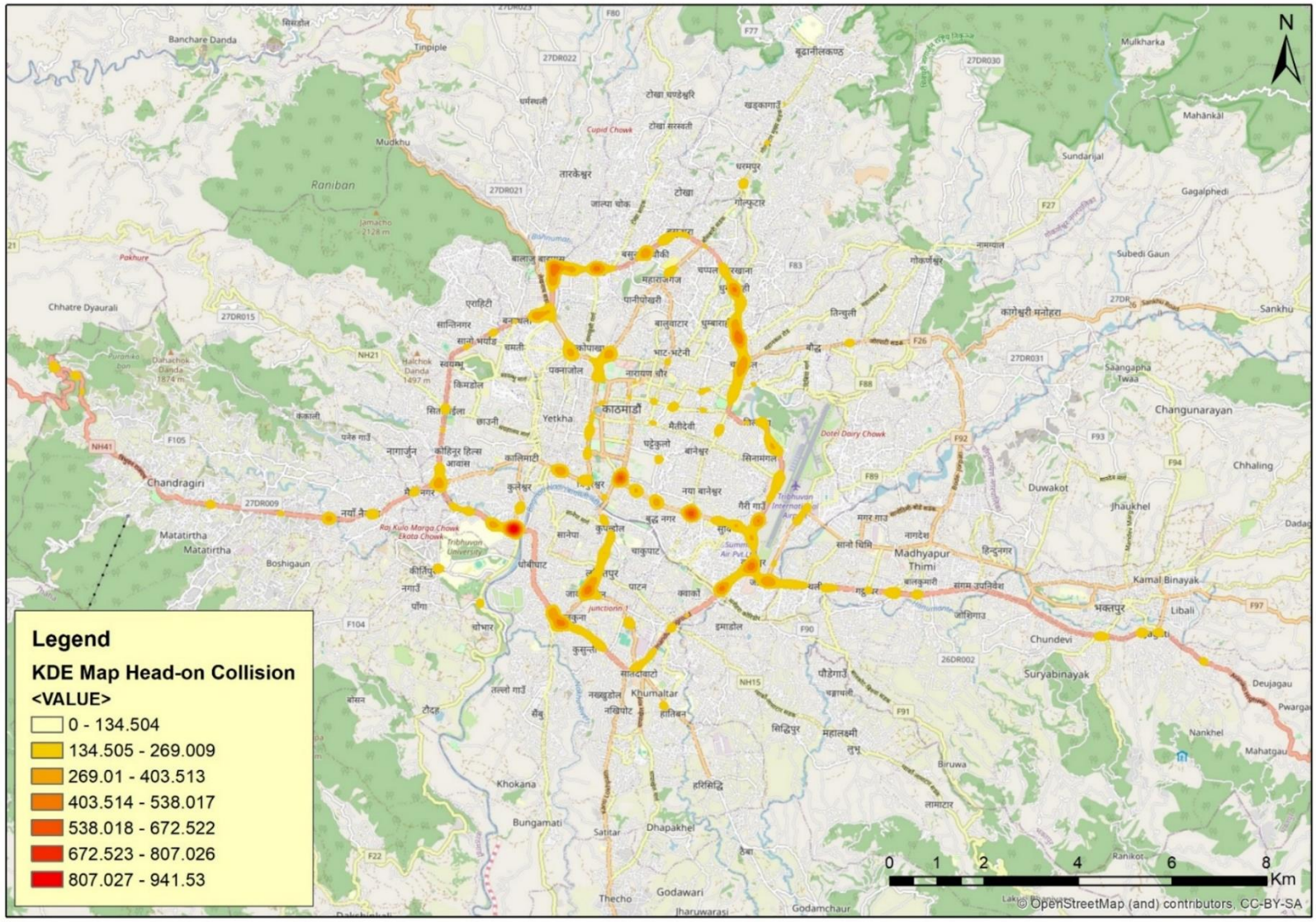
Legend
KDE Map Head-on Collision
<VALUE>
0 - 134.504
134.505 - 269.009
269.01 - 403.513
403.514 - 538.017
538.018 - 672.522
672.523 - 807.026
807.027 - 941.53
N
0 1 2 4 6 8
Km
© OpenStreetMap (and) contributors, CC-BY-SA
Banchare Danda
Tinpiple
Mudkhu
Raniban
Chhatre Dyaurali
Chandragiri
Matatirtha
Boshigaun
Khokana
Bungamati
Satitar
Dhapakhel
Thecho
Godawari
Jharuwarasi
Godamchaur
Yetkha
काठमाडौं
Khumaltar
Mulkharka
Mahankal
Sundarijal
Gagalphedi
Subedi Gaun
Sankhu
Changunarayan
Chhaling
Duwakot
Jhaukhel
Madhyapur Thimi
Kamal Binayak
Bhaktapur
Libali
Chundevi
Suryabinayak
Deujagau
Nankhel
Mahatgau
Biruwa
Ranikot

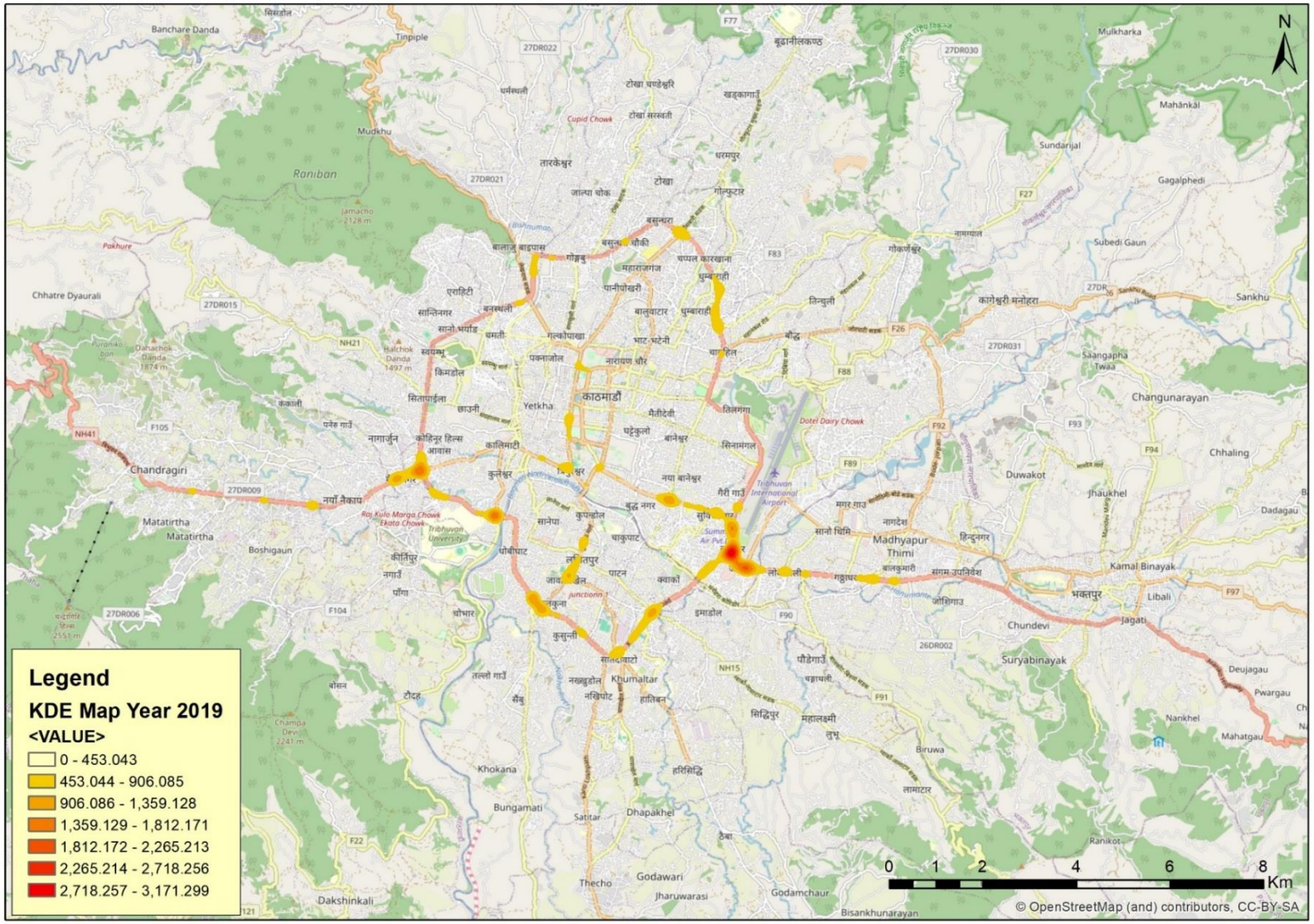
Legend
KDE Map Year 2019
<VALUE>
0 - 453.043
453.044 - 906.085
906.086 - 1,359.128
1,359.129 - 1,812.171
1,812.172 - 2,265.213
2,265.214 - 2,718.256
2,718.257 - 3,171.299
N
0 1 2 4 6 8
Km
© OpenStreetMap (and) contributors, CC-BY-SA

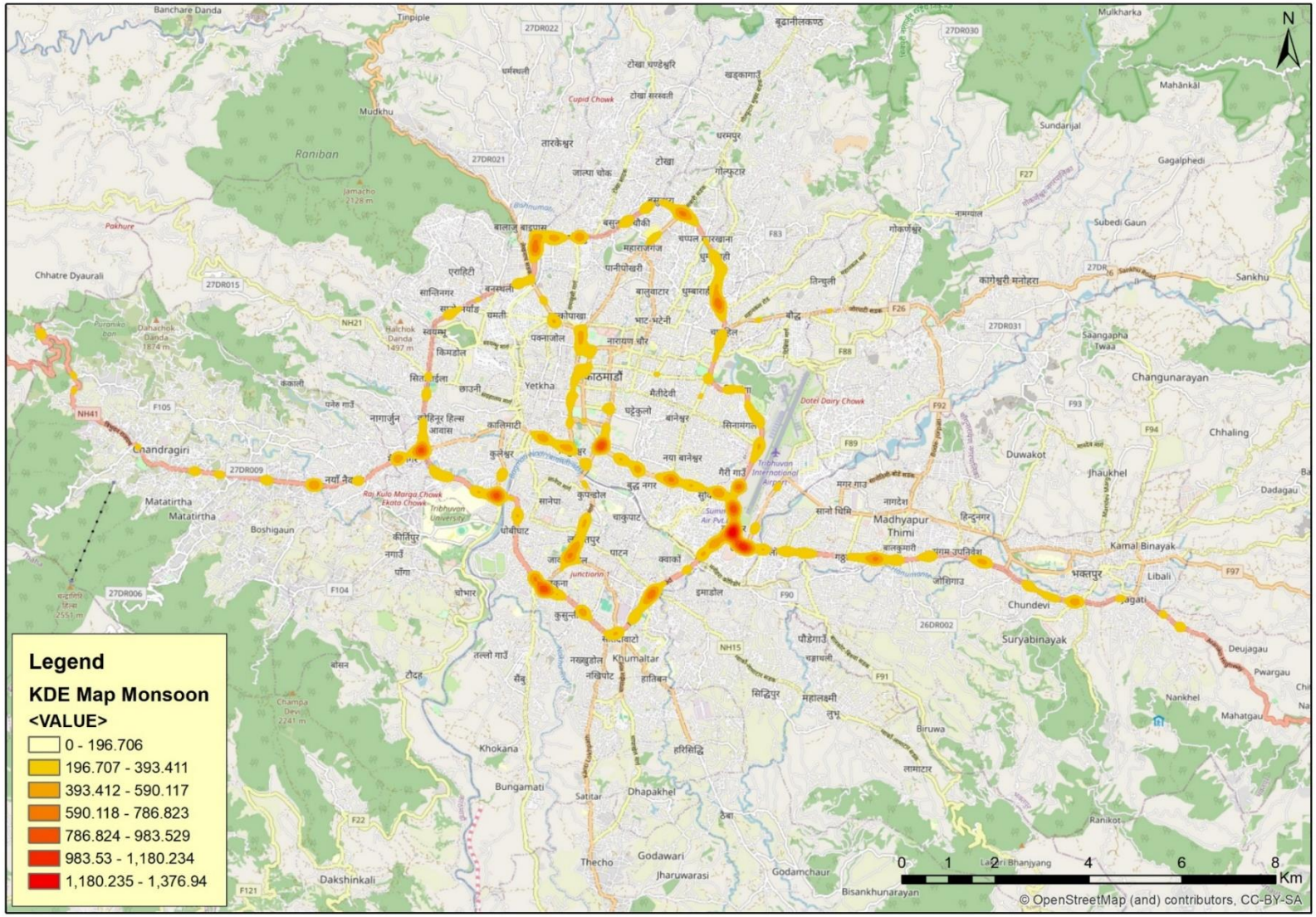
Legend
KDE Map Monsoon
<VALUE>
0 - 196.706
196.707 - 393.411
393.412 - 590.117
590.118 - 786.823
786.824 - 983.529
983.53 - 1,180.234
1,180.235 - 1,376.94
N
0 1 2 4 6 8
Km
© OpenStreetMap (and) contributors, CC-BY-SA

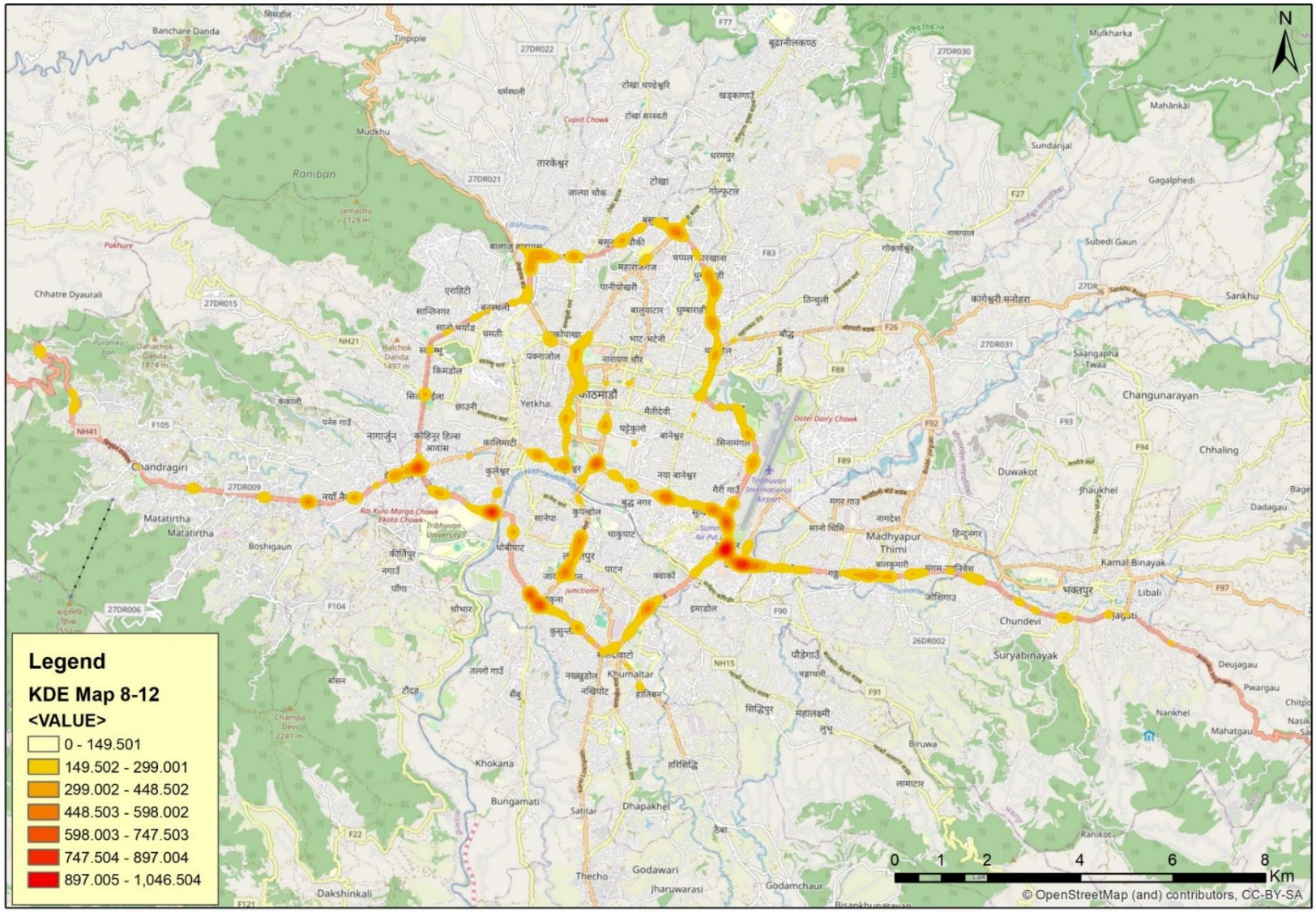
Legend
KDE Map 8-12
<VALUE>
0 - 149.501
149.502 - 299.001
299.002 - 448.502
448.503 - 598.002
598.003 - 747.503
747.504 - 897.004
897.005 - 1,046.504
N
0 1 2 4 6 8
Km
© OpenStreetMap (and) contributors, CC-BY-SA

APPENDIX C: List of Hotspot Locations by Road Links

S.N.	Link Name	Hotspot Location and Length
1.	Manohara-Sallaghari-Hanumante Culvert	Manohara Bridge (151.21 m), Lokanthali (500.01 m), Kaushaltar-Gatthaghar (1003.21 m), Gatthaghar Chowk- Chardobato-New Thimi (827.312 m), New Thimi-SS Chowk (504.74 m), Radhe Radhe-Old Hanumante Bridge (825.41 m), Old Hanumante Bridge-Srijananagar Chowk (379.95 m), Sallaghari Bus stop-Surbarna Chowk (285.84 m), Subarna Chowk-Chundevi-Ghalate Chowk-Pandu Bazar (947.91 m), Suryabinayak/ Doleshwor Busstop (219.54 m), Aadarsha Chowk (340.12 m), Jagate Chowk (197.47 m)
2.	Thapathali-Tikabhairab(KVRR)	Kupondole Bus Stop-Jawlakhel Chowk (1884.08 m), Embassy of Switzerland Junction-Muncha Group (203.87 m), Ekantakuna Chowk (110.66 m)
3.	Nagdhunga-Kalanki (Ring road)	Nagdhuga Check Post-Bhadbhanjyang (659.46 m), Tribhuwan Park (202.18 m), Matatirtha Drinking Water Project (211.42 m), Gurjudhara Busstop (156.89 m), CG Digital Park/Satungal (109.71 m), Sipradi Trading-Ambrosia Ideal Secondary School (254.33 m), Tinthana/Naikap (136.23 m), Kalankisthan (Sitara Carriers-Kurdan Football Academy) (205.02 m), Dhungeadda/Maitrinagar (544.25 m), Baba Oil Store (88.02 m) and Kalanki (175.64 m)
4.	Maitighar-Tinkune	Maitighar (106.33 m), Babarmahal (362.94 m), Bijulibajar Bridge (149.46 m), NMB Bank-AlphaBeta (199.23 m), Naya Baneshwor Chowk (BICC) (325.18 m), DOS-Civil Hospital (267.55 m), Subidhanagar (167.13 m), Maitighar Chowk (400.32 m)
5.	Koteshwar-Manohara bridge	Koteshwor Chowk (223.418 m), Nepal Army Ground-Kamakhya Gas Station (173.33 m), Jadibuti Chowk-Manohara (376.83 m)
6.	Tinkune - Sinamangal - Gaushala (KTM Ringroad)	Tinkune Chowk-Gairigaon Petrol Pump (355.19 m), Shakti Binayak Marg Chowk-Sinamangal Busstop (641.33 m), Airport Park (Peace Stupa)-Summit Residency Hotel (401.43 m), Airport Gate-Shambhu Marg Chowk (219.84 m), Airport Road Chowk-Sherpa Memorial Park (212.09 m), Bagmati Bridge-Tilganga Hospital (208.43 m), Bagmati Bridge-Pashupatinath South

S.N.	Link Name	Hotspot Location and Length
		Gate/Pinglasthan (124.33 m), Pashupati Parking (139.53 m)
7.	Maharajganj - Balaju Bypass Junction (KTM Ringroad)	NarayanGopal Chowk-Sanjha Bus stop (452.28 m), Basundhara Bus stop-Basundhara Big Mart(346.12 m), Multi-Agro National (Head Office)-Tilingatar Police Station (234.63 m), Basundhara Police Station Bus stop (100.22 m), Gongabu Aawas (100.34 m), Gongabu Bus stop/Samakhusi (116.02 m), BG Mall-Mitranagar Marg Junction (164.90 m), New Buspark-Byass Junction (290.82 m)
8.	Kalanki - Balkhu (KTM Ringroad)	Kalanki Underpass (100.32 m), Bhatbhateni-Sita Petrol Pump (417.67 m), Madannaga-TU Examination Controller office (381.26 m), Balkhu Chowk-Balkhu Bridge (240.23 m)
9.	Chabahil - Sankhapark (KTM Ringroad)	Chabahil Chowk (212.79 m), Hospital Marg-Substation (100.52 m), Gopikrishna bus stop-Dhobikhola Bridge (122.42 m), Dhobikhola Bridge-Sukedhara-Dhumbarahi chowk (1121.25 m)
10.	Manohara River - Koteshwor (H03) KTM Ringroad)	Whole section from Balkumari Bridge-Koteshwor (910.05 m)
11.	Tripureshwar-Balaju Ring road	Nepal Telecom (Provincial Office)-China Town/KMC Road junction (298.43 m), Sundhara-New Road junction (366.14 m), Mahaankaal Temple (100.35 m), Bir Hospital Bus stop-Bhotahiti Overhead Bridge (141 m), Jyatha Junction-Election Commission (221.31 m), Kesar Mahal Junction-Lainchaur (400 m), Sorakhutte (220.16 m), Nayabazaar (217.94 m)
12.	Satdobato- Gwarko (KTM Ringroad)	Satdobato Chowk (166.67 m), Satdobato Swimming pool-ANFA (426.54 m), B&B Hospital Bus stop (101.64 m), Gwarko Chowk (124.62 m)
13.	Ekantakuna- Kusanti - Satdobato (KTMRingroad)	Ekantakuna Chowk (100 m), Trasport Management Office (126.2 m), Kusunti Height Bus stop (120 m), Damodar Marg Junction- Thasikhel- Mahalaxmisthan Chowk (479.85 m), JRC Chowk-Talchikhel Chowk (182.31 m), Chapagaon Dobato Chowk-Overhead Bridge (155.26 m)
14.	Ring road-Balaju Bypass	Bypass Junction- Lumbini Auto Diesel (504.39 m), Balaju Chowk (151.32 m)
15.	Kalanki (Ring road)-Tripureswor	Kalanki Chowk (116.80 m), Ganeshan Singh Road/Mega Banquet (100.26 m), Rabibhawan (168.16 m), Kanak Oil Traders-

S.N.	Link Name	Hotspot Location and Length
		Himalayan Bank (114.22 m), Teku Bus stop-Sungabha Marg Junction (150.17 m), Tripuresvara bus park-Baithak Event (107.12 m), Department of Industry-Tripureshwor Chowk (223.19 m)
16.	Swoyambhu - Kalanki (KTM Ringroad)	Hotel Mystic Budhha-Fatafat Sewa Pvt. (175.28 m) Sitapaila Chowk (125.58 m) Soltee Dobatoo Chowk (107.30 m), Bafal (168.18 m), Syuchatar Bridge (200.31 m), Gyanodaya Marg Junction (Makalu Oil Store)-Kalanki (289.8 m)
17.	Balkhu - Ekantakuna (KTMRingroad)	Balkhu Busstop-Sajha Petrol Pump/Sanepa (174.85 m), Jhamsikhel-Star Hospital (156.67 m), Nakkhu Dobato-Ekantakuna Chowk (394.08 m)
18.	Tinkune-Koteshwor	Whole section from Tinkune-Koteshwor (434.57 m)
19.	Peepalmod-Nagdhunga	Nagdhunga-Chissapani Road Junction (841.35 m), Pipalmod-Chhatre Deurali (839.46 m)
20.	Jadibuti (ARM)-Sinamangal	Thapagaon (173.34 m), Bandana Oil Store-Majestic Events (119.13 m), Hamro Sahayatri Hospital-Near KMC 32 Ward Office (441.29 m)
21.	Balaju Junction - Banasthali - Swoyambhu (KTM Ringroad)	Bhatbhateni Balaju (170.86 m), Sano Bharyang Chowk/Bus stop (117.75 m), Thulo Bharyang Chowk/ Bus stop (132.24 m)
22.	Lainchaur-Lazimpat-Maharajgunj	Lazimpat/Hotel ambassador (112.85 m), National Police Academy (216.80 m), Kanti Hospital Mod (122.95 m), Teaching Hospital (196.22 m), US Embassy (222.09 m)
23.	Nakhudobato-Nakhu Chowk	Whole section from Nakkhu Dobato Chowk-Nakkhu Bridge (681.63 m)
24.	Sankhapark - Maharajganj (KTM Ringroad)	Sankha park-Chapal Karkhana Bus stop (216.097 m), Chapal Karkhana Bus stop - Everest Bank (108.78 m), Bhatbhateni-Narayan Gopal Chowk (195.38 m)
25.	Balkhu-Kuleswor-Kalimati	Balkhu Chowk (166.15 m), Siddhi Poly Path Lab- Kuleshwor Ganesthan(151.21 m)
26.	Gwarko-Manohara River (Balkumari) (KTMRingroad)	Gwarko Chowk-Workshop behind Prabhu Bank Limited (291.71 m), Kharibot Overhead Bridge (148.64 m), Balkumari Bridge (177.16 m)
27.	Narayanhiti palace southgate-Durbarmarg-Ghantaghar-Bhadrakali	Durbarmarg (117.53 m), Mahendra Statue-Randeep Bridge (389.21 m), Ratna Park (193.61 m)

S.N.	Link Name	Hotspot Location and Length
28.	Hanumante Culvert-Sanga	Nangkhel (122 m), Bhattedhikoor Bus stop (370 m), Nalinchowk Bus stop (247 m)
29.	Mitrapark - Chabahil (KTM Ringroad)	Stupa-Chabahil Chowk (220 m)
30.	Jayanepal-Thapathali (KVRR)	Adwait Marg Chowk-Padmodaya mod (166.32 m), Agricultural Development Bank- Maitighar Chowk (239 m)
31.	Thapathali-Tripureswor	Thapathali Chowk-Ichu Culvert (204.40 m), International Patho Scientific-Tripureshwor Chowk (224.6 m)
32.	Satdobato-Karmanas bridge	NARC-Renewable Energy Test Station (266.27 m), Hattiban (Tranquility Hospital-City Scape Housing) (313.34 m)
33.	Kalopul-Nagpokhari-Kesharmahal-Tridevimarg (Sanchayakosh)	Narayanhiti South Gate Junction (100.76 m), Parking-Kesar Mahal Chowk-Tridevi Temple (231.28 m)
34.	Chabahil (Ktm Ring Road)-Pipalbot	Chabahil Chowk (110.17 m), Chucchepati (111.07 m)
35.	Satdobato-Jawalakhel	Ashok Stupa-Patan Hospital (321.36 m), Manbhawan Bus stop-Jawlakhel Bus stop (250.64 m)
36.	Balkhu-Chovar	Balkhu Chowk (101.19 m), Chovar Gate (204.98 m)
37.	Gaushala-Mitra Park (KTM Ringroad)	Bhandarkhal (131.6 m), Jay Bageshwori/near Pushpanjali Gas Station (100.9 m)
38.	Jawlakhel-St.Mary's West	Jawlakhel Chowk-St. Xavier’s Gate (262.58 m)
39.	Purano Baneswor-Naya Baneswor (BICC)	BICC-New Baneshwor Chowk (293.90 m)
40.	Gwarko-Lubhu-Lankuri Bhanjyang	Gwarko Chowk-Imadol (283.66 m)
41.	Golphutar-Pipalbot-Sankhapark	Dhumbarahi Chowk-Little More Studio (177.24 m)
42.	Shantinagar - Bhimsengola	Harisidhi Oil Store-Shantinagar (191.95 m)
43.	Bijulibazar-Anamnagar	Bijulibazar Bridge-Dhobikhola Bridge (224.46 m)
44.	Chardobato-Balkot	Chardibato Chowk (105.56 m)
45.	Jadibuti-Narephant	ENT Hospital (193.17 m)
46.	Satdobato (Ring Road)-Dhapakhel -Thecho(KVRR)	National Biotechnology Research Centre-Shital Marg (255.34 m)
47.	Sundhara-Singhadarbar (Prithivi path)	Sundhara-Bhadrakali (231.50 m)
48.	Samakhushi Chok-Tokhagaun-Chandeshwarigaun(KVRR)	Saibaba Chowk-Bhutkhel Park (206.59 m)
49.	New Buspark Road (Inside)	Internal Road of New Buspark (301.62 m)
50.	Satdobato-Sunakothi	Chapagaon Dobato Chowk (100 m)

S.N.	Link Name	Hotspot Location and Length
51.	Bansbari-Budhanilkantha	Shahid Gangalal National Heart Centre (116.45 m)
52.	New Buspark- Mahepi	Mitranagar (124.85 m)
53.	Pipal Bot-Sankhu	Bajra International College-Chusang Tazan Junction (102.3 m)
54.	Darbarmarg-Jamal	Jamal Bus stop-Overhead Bridge (138.12 m)
55.	Tinkune north	Heli Everest- Gairigaon Pump (115.4 m)
56.	Maharajgunj-Bansbari	Naryangopal Chowk (100.3)

APPENDIX D: Site Visit Checklist

Site Observation Checklist

Date: 2024/06/11 (4:30PM). Weather: Cloudy.

Road/Link Name: Kalanki-Nagdhunga. Site Name: Dhungadda.

Start Coordinates: 27° 41' 31"N, 85° 16' 36"E End Coordinates: 27°41'25"N, 85°16'26"E

S.N.	Aspect	Category	Description	Observation/Remarks
1.	Road Design	Speed Limit		not on road (At Minor Intersection)
		Junction	Type/Layout (Y/T/Right Angle)	Y
			Conflicts (Crossing/Merging/ Diverging)	Merge / Diverge
			Visibility (Sight lines clear of vegetation/structures)	Yes.
			Turning lanes/tapers (Adequacy of lane width & taper length)	No.
			Presence of Signal	No.
			Pedestrian Crossing (Position, Marking, Refuge Island, Signalization)	No.
			Stop line & Markings	No.
		Cross-Section	Adequacy of lane & shoulder width	Yes.
			Separation of traffic (Pedestrian sidewalks, overhead bridge, bicycle lanes, median)	Median present but not on whole road. Sidewalks present. No cycle lanes, No overhead bridge.
			Sight distance	O.K.

			Surface defect	No.
			Drainage condition	O.K.
			Merging/Diverging to side roads	Yes to access road. (But no proper sign)
			Bridge Approach	–
			Traffic island	Median present; not end treated.
		Alignment	Sharp Curve	Not sharp.
			Visibility at Curve	Yes visible
			Gradient	O.K.
		Midblock Crossings	Location, Marking, Refuge Island, Signalization, Signs	No.
		Road Marking	Type	Lane, centre (No crossing & crossing allowed)
			Clarity	Faded.
		Traffic Signals	Recognizable	Not Present.
			Turning movement included	
			Pedestrian phase/signal	
			Placement	
			Operation	
		Traffic Signs	Clarity	No (Faded?)
			Visibility	No

			Placement as per Standard	No
		Other Safety Features	Safety barrier, guardrails, etc. (Obstacle, end treatment, delineation etc.)	No guardrails along footpath but present on slope end only at bus
			Traffic calming measures	NO.
		Road Lighting	Presence of streetlights	Yes
			Lighting condition at night	Good.
2.	Road Users	Drivers	Response/compliance to traffic signals/signs/control devices	
			Use of Seatbelt	Except bus & truck drivers.
			Wearing of Helmet	Yes (some Pillion rides seen wearing)
			Excessive Vehicle Speed	Yes
			Turning Movements (Left, Right & U-turn)	Yes.
			Overtaking	Yes . (From left & wrong lane)
			Parking on street	~~No~~ Yes
			Yielding to Pedestrian	~~Yes~~ No
			Picking/dropping on carriageway	Yes.
		Pedestrians	Safe walking behavior	Some walk outside footpath.
			Usage of designated crossing	No crossing present.
			Usage of designated bus stops	Yes .

3.	Environment	Landuse	Surrounding landuse type	residential, commercial.
		Access	Access to properties clear	clear
		Right of Way	Width minimized due to encroachment	encroached.
		Roadside Hazard	Trees/Poles/Buildings/Structures	poles on shoulders.
		Services	Bus stops	Yes. (with pick n drop sign) Turning present near it.
			Fuel pump	Yes. (cctv installed)
			On-road/ Off-road Parking Provisions	no onstreet parking no offstreet parking
		Street vendors	Occupy footpaths/shoulders	Occupy footpath.
4.	Others	Police deployed to control night bus parking. CC camera installed (2 days before)		

APPENDIX E: Site Visit Photographs

No physical separation at Dhungeadda

No crosswalks marking & sign, school-zone sign or speed limit sign at Chundevi

No central dividers & pedestrian crossing marking at Thasikhel

Outer divider openings & no central dividers at Balkhu

Rear end collision observed at Kaushaltar

No proper intersection layout at Kaushaltar

Spatio-Temporal Analysis of Road Traffic Crash Hotspots in Kathmandu Valley, Nepal

ORIGINALITY REPORT

5%
SIMILARITY INDEX

PRIMARY SOURCES

1	www.mdpi.com Internet	135 words — < 1%
2	savoirs.usherbrooke.ca Internet	84 words — < 1%
3	eprints.soton.ac.uk Internet	59 words — < 1%
4	elibrary.tucl.edu.np Internet	56 words — < 1%
5	eprints.staffs.ac.uk Internet	41 words — < 1%
6	www.hindawi.com Internet	41 words — < 1%
7	bmcvetres.biomedcentral.com Internet	40 words — < 1%
8	www2.mdpi.com Internet	37 words — < 1%
9	hrmars.com Internet	35 words — < 1%

त्रिभुवन विश्वविद्यालय
Tribhuvan University
इन्जिनियरिङ अध्ययन संस्थान
Institute of Engineering
डीनको कार्यालय
OFFICE OF THE DEAN

GPO box- 1915, Pulchowk, Lalitpur
Tel: 977-5-521531, Fax: 977-5-525830
dean@ioe.edu.np, www.ioe.edu.np
गोश्वारा पो.ब. न- १९१५, पुल्चोक, ललितपुर
फोन- ५५२१५३१, फ्याक्स- ५५२५८३०

Date: July 7, 2024

To Whom It May Concern:

This is to certify that the paper titled "***Spatial Analysis of Road Traffic Crash Hotspots in Kathmandu Valley, Nepal***" (Submission# **59**) submitted by **Anuradha K.C.** as the first author, which had been accepted for presentation after the peer-review process, has successfully been presented at the 15th IOE Graduate Conference held during May 17 & 18, 2024. Kindly note that the final revision of the papers and publication process of the conference proceedings is still underway and hence inclusion of the accepted manuscript in the conference proceedings is contingent upon timely response to further edits during the publication process.

Bhim Kumar Dahal, PhD
Convener,
15th IOE Graduate Conference